

COMBUSTION CHARACTERISTICS OF HYDROGEN IN CONSTANT  
VOLUME COMBUSTION CHAMBER

PATTANIT NOMTHONGTHAI

A THESIS SUBMITTED IN PARTIAL FULFILLMENT  
OF THE REQUIREMENT FOR THE DEGREE OF  
MASTER OF ENGINEERING IN AUTOMOTIVE ENGINEERING  
(INTERNATIONAL PROGRAM)  
INTERNATIONAL COLLEGE  
KING MONGKUT'S INSTITUTE OF TECHNOLOGY LADKRABANG

2014

KMITL-2014-IC-M-004-012

COMBUSTION CHARACTERISTICS OF HYDROGEN IN CONSTANT  
VOLUME COMBUSTION CHAMBER

PATTANIT NOMTHONGTHAI

A THESIS SUBMITTED IN PARTIAL FULFILLMENT  
OF THE REQUIREMENT FOR THE DEGREE OF  
MASTER OF ENGINEERING IN AUTOMOTIVE ENGINEERING  
(INTERNATIONAL PROGRAM)  
INTERNATIONAL COLLEGE  
KING MONGKUT'S INSTITUTE OF TECHNOLOGY LADKRABANG  
2014

KMITL – 2014 – IC – M – 004 – 012

COPYRIGHT 2014

INTERNATIONAL COLLEGE

KING MONGKUT'S INSTITUTE OF TECHNOLOGY LADKRABANG

NATIONAL SCIENCE AND TECHNOLOGY DEVELOPMENT AGENCY

<b>Thesis</b>	Combustion characteristics of hydrogen in constant volume combustion chamber
<b>Student</b>	Mr. Pattanit Nomthongthai
<b>Student ID</b>	53600904
<b>Degree</b>	Master of Engineering
<b>Program</b>	Automotive Engineering ( International Program )
<b>Year</b>	2014
<b>Thesis Advisor</b>	Asst. Prof. Dr. Chinda Charoenphonphanich Dr. Manida Tongroon Prof. Dr. Hidenori Kosaka

## ABSTRACT

The increasing of global energy demand and stringent pollution regulations have promoted research on alternative fuels. Hydrogen has played a big role in automobile and it is a clean energy that does not produce any pollution. Therefore, this research would like to study the combustion characteristics of dilute Hydrogen-Air mixture in constant volume combustion chamber (CVCC) in wide length of equivalence ratio, swirl intensity from difference initial pressures, chamber temperature and position of spark plug. The results of this study are maximum combustion pressure, mass fraction burn rate, combustion duration, combustion delay and lean burn limit. Schlieren technics and high speed video camera are used in order to take the video files of swirl intensity and combustion phenomena.

The combustion efficiency was increased by increasing initial temperature and swirl intensity. In lean burn limit condition, high swirl intensity is more efficient with center ignition conditions but sidewall ignition is suitable for low swirl intensity.

## ACKNOWLEDGEMENTS

Initially, I would like to express, first and foremost, to my supervisor Asst. Prof. Dr. Chinda Charoenphonphanich, Dr. Preechar Karin and Prof. Dr. Hidenori Kosaka for his extensive advice, guidance and encouragement throughout my thesis.

I am extremely grateful to thank Dr. Manida Tongroon, Dr. Nuwong Chollacoop and National Metal and Materials Technology Center (MTEC), THAILAND for the financial, measuring equipment and also intensive suggestion support that made my study meet well accomplishment.

I wish to express my gratitude to assistance from my senior at KMITL automotive laboratory, P'Piyaboot, P'Prathan, P'Pisan and P'Wittawat for their sincere advice and technical support such as equipment and controller program. I am pleased to have this opportunity to thank the many colleagues and bachelor subordinate who have helped me with this dissertation.

I am also wish to thank Pathumwan Institute of Technology for their support in pressure measuring device and data acquisition system,

Last but not least, I cannot thank enough to my family for their love, interests and supports throughout my life.

# CONTENTS

	Page
Abstract.....	I
Acknowledgements.....	II
Contents.....	III
List of tables.....	VII
List of figures.....	VIII
Chapter 1 : Introduction.....	1
1.1 Background.....	1
1.2 Objectives.....	5
Chapter 2 : Literature Reviews.....	6
2.1 Introduction.....	6
2.2 Combustion characteristics in constant volume combustion chamber.....	6
2.3 Effect of equivalence ratio on hydrogen combustion.....	8
2.4 Mass fraction burn rate and combustion duration.....	10
2.5 Lean flammability and ignition limit.....	11
2.6 Cyclic of variation (CoV).....	13
2.7 Schlieren photography technique.....	15
Chapter 3 : Experimental Apparatus and Procedure.....	19
3.1 Experimental apparatus.....	19

## CONTENTS (continued)

	Page
3.1.1 Hydrogen supply system.....	20
3.1.2 Air supply system.....	21
3.1.3 Temperature control system.....	22
3.1.4 Driver and controlled module.....	23
3.1.5 Data acquisition system.....	26
3.1.6 Schlieren photography setup.....	28
3.1.7 High speed video camera.....	31
3.1.8 Constant volume combustion chamber.....	33
3.1.9 Ignition system.....	37
3.2 Experimental Conditions.....	39
3.3 Experimental Procedure.....	40
3.3.1 Swirl setup.....	40
3.3.2 Equivalence ratio calibration.....	44
3.3.3 Timing sequence.....	49
3.3.4 Lean burn limit investigation.....	50
3.3.5 Mass fraction burn rate and combustion duration.....	51
3.3.6 Combustion delay.....	52
Chapter 4 : Results and Discussions.....	53
4.1 Effect of initial temperature.....	53

## CONTENTS (continued)

	Page
4.2 Effect of equivalence ratio.....	54
4.3 Effect of swirl intensity on combustion pressure.....	55
4.3.1 Equivalence ratio = 0.2.....	55
4.3.2 Equivalence ratio = 0.3.....	57
4.3.3 Equivalence ratio = 0.4.....	58
4.3.4 Equivalence ratio = 0.5.....	60
4.4 Effect of swirl intensity on mass fraction burn rate.....	61
4.4.1 Equivalence ratio = 0.2.....	61
4.4.2 Equivalence ratio = 0.3.....	62
4.4.3 Equivalence ratio = 0.4.....	63
4.4.4 Equivalence ratio = 0.5.....	64
4.5 Effect of swirl intensity on combustion duration.....	69
4.6 Effect of swirl intensity on combustion delay.....	71
4.7 Effect of swirl intensity on lean burn limit.....	73
Chapter 5 : Conclusions.....	77
References.....	80
Appendices.....	82
Appendix A : Material specification.....	83
Steel for constant volume combustion chamber.....	83

## CONTENTS (continued)

	Page
Quartz glass specification.....	84
Graphite gasket detail.....	85
Data acquisition system.....	86
Pressure sensor.....	87
Hydrogen quality.....	88
Flashback arrestor.....	89
Hydrogen pressure regulator.....	90
Electronic Opto-Isolate driver.....	91
Appendix B : Controller block diagram.....	92
Partial pressure calibration program.....	92
Experimentally sequential program.....	94
Appendix C : Publications.....	96
Author Biography.....	112

## LIST OF TABLES

	Page
Table 1 Hydrogen properties compared with CNG and gasoline [2].....	4
Table 2 Experimental conditions.....	39
Table 3 Swirl intensity to air velocity conversion.....	43
Table 4 Hydrogen partial pressure compared with equivalence ratio.....	46
Table 5 Hydrogen injection duration compared with equivalence ratio.....	48

## LIST OF FIGURES

	Page
Figure 1.1: World energy demand from Exxon Mobil Corporation.....	1
Figure 1.2: World energy demand from IEA.....	2
Figure 1.3: Announcement from Ministry of Energy, USA (a) Global temperature and (b) Amount of Carbon dioxide.....	3
Figure 2.1: Experimental setup of Constant volume combustion chamber (a) first time introduced by J.Song and D.Lee, 2002 (b) revised experiment by Kihyung Lee et al, 2004.....	7
Figure 2.2: Schematic diagram of hydrogen combustion in CVCC by Xinghua Liu, Zhiqiang Fan, Fushui Liu, Jiangang Jiu and Ruwei Wang.....	8
Figure 2.3: The results of flame propagation by varied equivalence ratio and compared it in unit of time after ignition.....	9
Figure 2.4: Definition of combustion duration and combustion delay.....	10
Figure 2.5: Lean limit investigation base on coefficient of variation (a) Lewis Flight propulsion Lab (1959) (b) Y.Li and H.Zhao “Development of fuel stratification spark ignition engine”(2005) and (c) Jinhua W. et al “Study of cyclic variations of direct injection combustion fueled with natural gas-hydrogen blend using a constant volume vessel”(2008).....	12
Figure 2.6: Deflagration wave structure.....	16
Figure 2.7: Flame region that recorded with different direct-photograph technique.....	17
Figure 3.1: Schematic diagram of experimental apparatus.....	19
Figure 3.2: Hydrogen supply system.....	20
Figure 3.3: Hydrogen flashback arrestor.....	20
Figure 3.4: Air supply system.....	21

## LIST OF FIGURES (continued)

	Page
Figure 3.5: Two band of heater attached to the combustion chamber.....	22
Figure 3.6: Temperature indicator and controller.....	22
Figure 3.7: Schematic diagram of driver and controlled module system.....	23
Figure 3.8: Computer controller program for hydrogen rich-lean calibration.....	24
Figure 3.9: Computer controller program for driver module.....	25
Figure 3.10: Driver module.....	26
Figure 3.11: Pressure sensor.....	26
Figure 3.12: DEWETRON DEWE-5000.....	27
Figure 3.13: Layout of Schlieren photography system.....	28
Figure 3.14: Real experimental layout of Schlieren photography.....	29
Figure 3.15: Real alignment of Schlieren photography system.....	30
Figure 3.16: The example image that reflected from spherical mirror.....	30
Figure 3.17: Photron SA3 high speed video camera.....	31
Figure 3.18: Real experiment image from high speed video camera.....	31
Figure 3.19: Photron FASTCAM software shows the camera setting and real time viewer.....	32
Figure 3.20: Real experimental equipment of CVCC.....	33
Figure 3.21: Air swirl and spark plug position.....	34
Figure 3.22: Dimension of CVCC.....	35
Figure 3.23: CAE simulation result of main chamber.....	36

## LIST OF FIGURES (continued)

	Page
Figure 3.24: CAE simulation result of chamber lid with quartz glass.....	36
Figure 3.25: directional Ignition coil and spark plug.....	37
Figure 3.26: Spark plug for center ignition.....	38
Figure 3.27: Two varying conditions of ignition point (center and side wall).....	38
Figure 3.28: Swirl setup definition.....	40
Figure 3.29: (a) Shadowgraph image of swirl intensity (b) grid pixel for air velocity measurement .....	41
Figure 3.30: Air velocity that was resulted by Photron FASTCAM Analysis program.....	43
Figure 3.31: Result of partial pressure calculated from chemical equation.....	45
Figure 3.32: Exact result of hydrogen partial pressure.....	46
Figure 3.33: Calibration program for hydrogen injection duration.....	47
Figure 3.34: Injection duration result from calibration program.....	48
Figure 3.35: Experimentally sequential signal.....	49
Figure 3.36: Sequential signal controller program.....	50
Figure 3.37: Example data of lean burn limit.....	51
Figure 3.38: Combustion duration was defined from 10% to 90% of mass fraction burnt.....	51
Figure 4.1: Effect of initial temperature to hydrogen combustion.....	53
Figure 4.2: Effect of equivalence ratio (a) center ignition and (b) sidewall ignition.....	54
Figure 4.3: Effect of swirl intensity on equivalence ratio = 0.2 (a) center ignition and (b) sidewall ignition.....	55

## LIST OF FIGURES (continued)

	Page
Figure 4.4: Effect of swirl intensity on equivalence ratio = 0.3 (a) center ignition and (b) sidewall ignition.....	57
Figure 4.5: Effect of swirl intensity on equivalence ratio = 0.4 (a) center ignition and (b) sidewall ignition.....	58
Figure 4.6: Effect of swirl intensity on equivalence ratio = 0.5 (a) center ignition and (b) sidewall ignition.....	60
Figure 4.7: Mass fraction burn rate of hydrogen combustion with equivalence ration = 0.2...	61
Figure 4.8: Mass fraction burn rate of hydrogen combustion with equivalence ration = 0.3...	62
Figure 4.9: Mass fraction burn rate of hydrogen combustion with equivalence ration = 0.4...	63
Figure 4.10: Mass fraction burn rate of hydrogen combustion with equivalence ration =0.5..	64
Figure 4.11: The comparison of flame propagation in conditions of equivalence ratio = 0.2 (a) center ignition and (b) sidewall ignition.....	65
Figure 4.12: The comparison of flame propagation in conditions of equivalence ratio = 0.3 (a) center ignition and (b) sidewall ignition.....	66
Figure 4.13: The comparison of flame propagation in conditions of equivalence ratio = 0.4 (a) center ignition and (b) sidewall ignition.....	67
Figure 4.14: The comparison of flame propagation in conditions of equivalence ratio = 0.5 (a) center ignition and (b) sidewall ignition.....	68
Figure 4.15: The results of combustion duration with variation of equivalence ratio, swirl intensity and (a) center ignition and (b) sidewall ignition.....	69

Figure 4.16: The results of combustion delay with variation of equivalence ratio, swirl intensity and (a) center ignition and (b) sidewall ignition.....	71
Figure 4.17: The combustion stability in lean burn conditions of center ignition.....	73
Figure 4.18: The combustion stability in lean burn conditions of sidewall ignition.....	74
Figure 4.19: The lean burn limit result of all conditions including swirl intensity and ignition position.....	75
Figure 4.20 Flame propagation of hydrogen lean burn limit combustion.....	76

# CHAPTER 1

## INTRODUCTION

### 1.1 Background

From Exxon Mobil Corporation and IEA (International Energy Agency) reports, World energy consumption has been increasing year by year continuously. In 2030, the energy demand rise significantly especially in transportation section. The problem that should be concerned is the fossil fuel will be empty in the near future because of the energy majority sources are come from crude oil and fossil fuel. Moreover, in the environmental issues, the ministry of energy, USA announces that the global temperature and also the intensity of carbon dioxide in the atmosphere have been glowing continuously. It difficult to said that the new technology of internal combustion engine can improve the aforementioned issues.

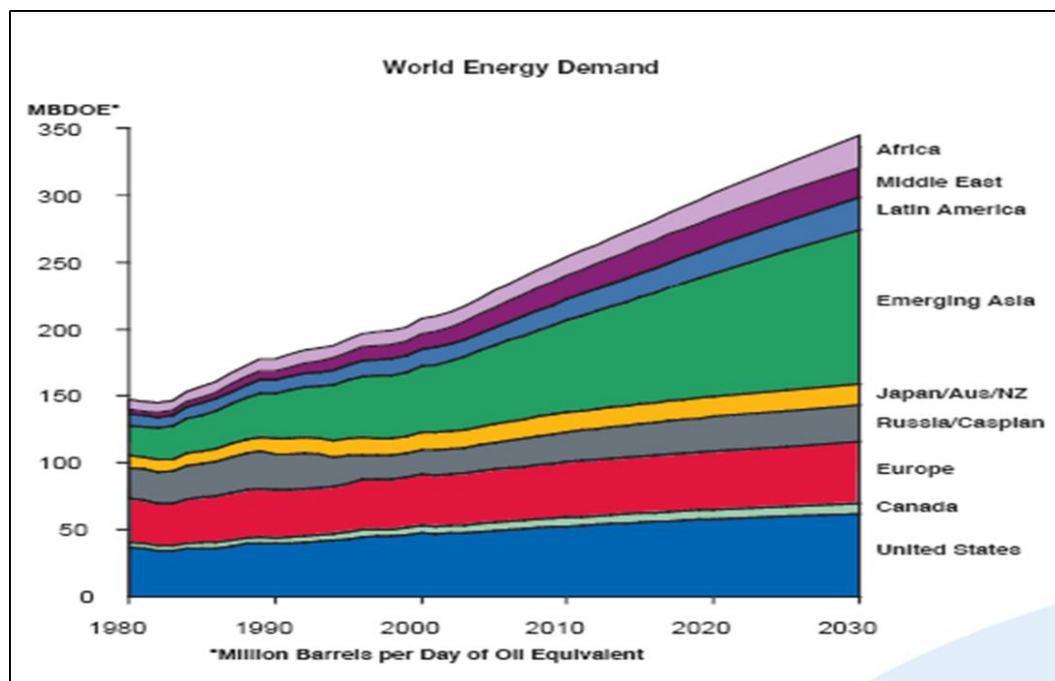


Figure 1.1: World energy demand from Exxon Mobil Corporation

## World Energy Demand to 2030

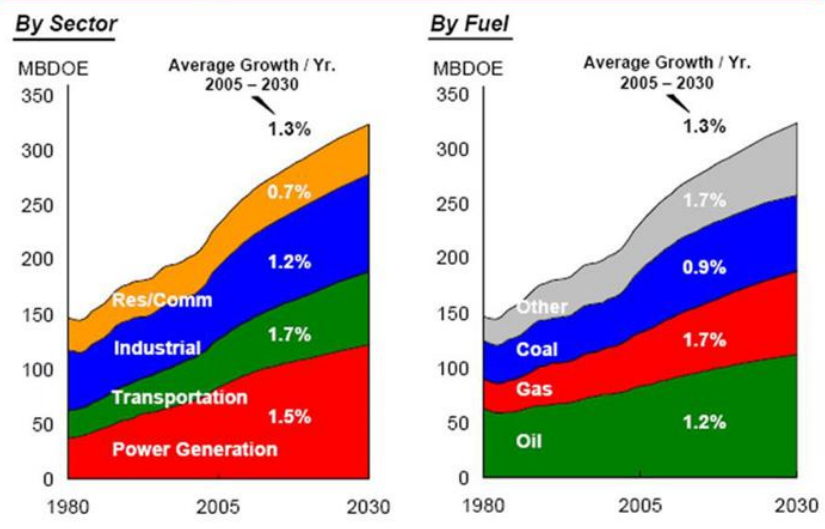
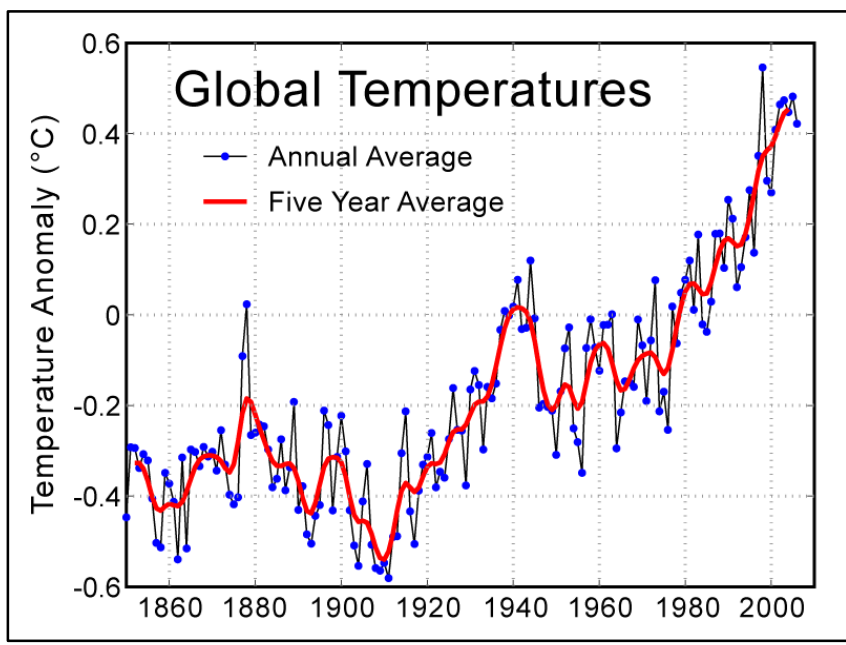
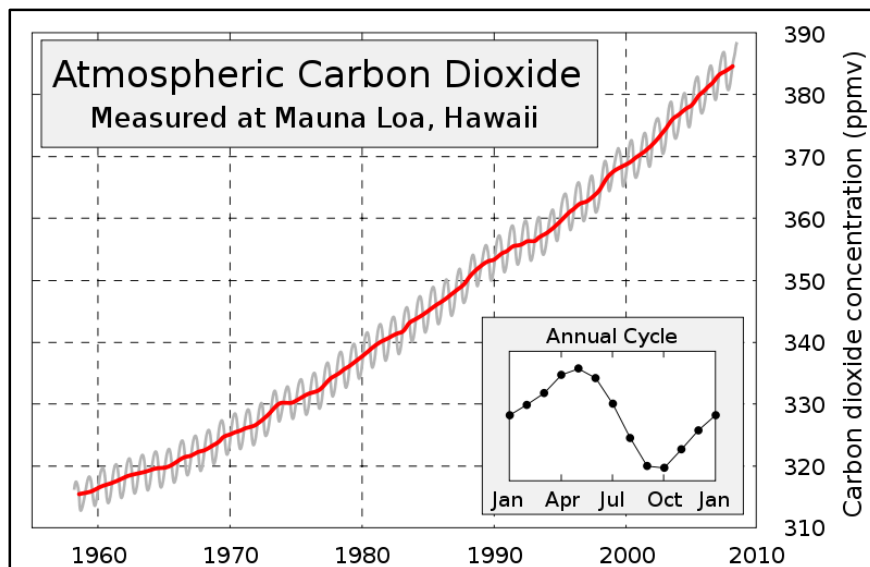


Figure 1.2: World energy demand from IEA



(a)



(b)

**Figure 1.3:** Announcement from Ministry of Energy, USA (a) Global temperature and (b) Amount of Carbon dioxide

One of solution to reduce fossil fuel consumption emissions is using the alternative fuel that can provide higher combustion efficiency than the conventional fossil fuel. Hydrogen ( $H_2$ ), one of challenging in alternative fuel that call “Clean energy” because it produce only steam ( $H_2O$ ) after combustion. It can be reduce the amount of greenhouse gases that release to environment[1]. Hence, in this research, Hydrogen was used to investigate to study the combustion phenomena and optimize main parameter that effect on the combustion efficiency.

Focusing on global impact, hydrogen can produce not only from water with water electrolysis process to separate  $H_2$  from  $H_2O$  but also steam reforming process from methane ( $CH_4$ ), bio-fermentation process from biomass and bio-photolysis process from algae.

**Table 1:** Hydrogen properties compared with CNG and gasoline [2]

<b>Properties</b>	<b>Hydrogen</b>	<b>CNG</b>	<b>Gasoline</b>
<b>Density (kg/m<sup>3</sup>)</b>	0.0824	0.72	730
<b>Flammability limits (volume % in air)</b>	4-75	4.3-15	1.4-7.6
<b>Flammability limits (<math>\phi</math>)</b>	0.1-7.1	0.4-1.6	0.7-4
<b>Autoignition temperature in air (K)</b>	858	723	550
<b>Flame velocity (m/s)</b>	1.85	0.38	0.42
<b>Adiabatic Flame temperature (K)</b>	2480	2214	2580
<b>Stoichiometric air/fuel mass ratio</b>	35.52	14.49	14.7
<b>Lower heating value (MJ/kg)</b>	119.7	45.8	44.79
<b>Heat of combustion (MJ/kg<sub>air</sub>)</b>	3.37	2.9	2.83

The technical review from Sandia National Laboratory shows that Hydrogen has lots of benefit properties compared with Compressed Natural Gas (CNG) and Gasoline such as Hi-speed flame velocity occurs in combustion phenomena to get high performance and combustion efficiency. It has highest heating value per unit of mass to provide the highest combustion performance and efficiency. Knocking can be avoided because of hydrogen has auto-ignition temperature higher than any fuels compared. And also, hydrogen has the widest length of equivalence ratio that means it can combust in ultra-lean condition to reduce the fuel consumption.

In this study, the effect of swirl intensity and position of spark plug was investigated in hydrogen combustion in constant volume combustion chamber which is the combustion simulator equipment. The structure is similar to the real engine combustion chamber in case of compression stroke but it does not have the piston movement [3] [4]. The pressure analysis data from pressure transducer can be collected. Combustion delay, combustion duration,

mass fraction burn rate and lean burn limit were analyzed. The high speed video camera with schlieren method was used to observe flame propagation during the combustion phenomena.

## 1.2 Objectives

- 1.2.1. To study and analyze the main parameter that has the effect for hydrogen combustion
- 1.2.2. To optimize parameters to get the highest efficiency
- 1.2.3. To provide technical combustion information

## CHAPTER 2

# LITERATURE REVIEWS

### 2.1 Introduction

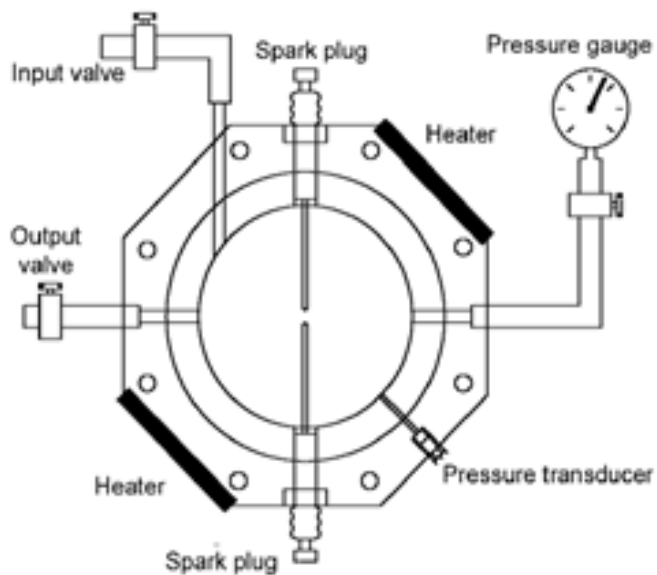
Hydrogen combustion has been recognized as a mean of both improving engine efficiency with no exhaust emissions. However, there are many factors that affect the combustion process, such as equivalence ratio, initial temperature, swirl intensity, ignition position, ambient temperature and pressure etc. Consequently, control combustion stability of this combustion has been challenging. In view of the wide range of investigation to improve combustion stability and efficiency, the literature reviews will be focused on influence of the equivalence ratio and the swirl intensities that effect on the combustion characteristics.

In this chapter, the reviewed papers will be presented the fundamental of hydrogen combustion and their strategies including definition of combustion characteristics in constant volume combustion chamber, parameters that cause to hydrogen combustion phenomena and visualized technique to support flame propagation analysis. Finally, In order to improve combustion stability, influenced parameters were considered.

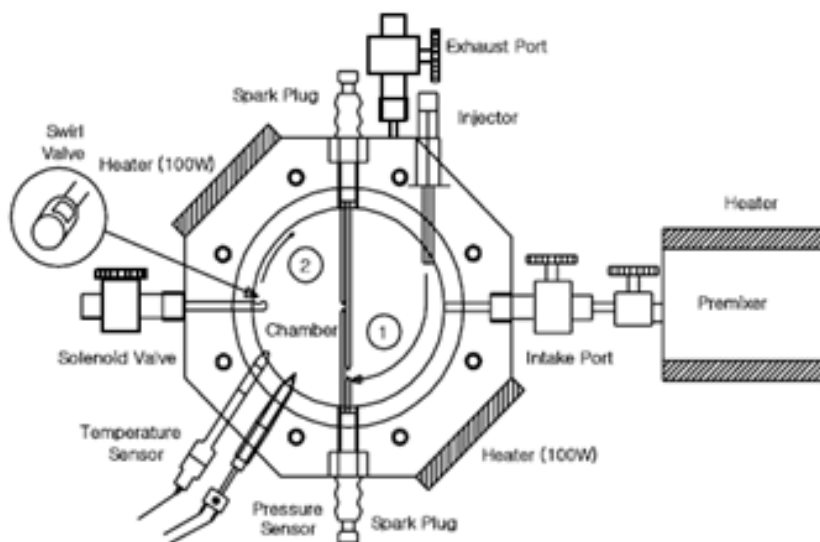
### 2.2 Combustion characteristics in constant volume combustion chamber

For combustion analysis, the real engine has many parameters that affect to the combustion characteristics such as manifold design, valve shape and duration, piston geometry, and etc. In the recent years, many researchers try to avoid that undesirable effects and concentrate on only the fuel and combustion within combustion chamber. Experimental studies which carry on the constant volume combustion chamber may easier control parameter than that the real engine. The word “Constant Volume Combustion Chamber” or “CVCC” was first introduced in 2002 by publication of Jeonghoon Song and Dae Hee Lee [5]. The experimental setup of their study was shown in Figure 2.1(a). In the year 2004, Kihyung Lee et al [6]. Study the effect of mixture stratification in a constant volume combustion

chamber. In this study, the experimental apparatus were more complicated than that the previous as shown in Figure 2.1(b).



(a)



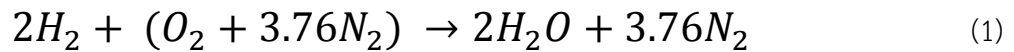
(b)

**Figure 2.1:** Experimental setup of Constant volume combustion chamber (a) first time introduced by J.Song and D.Lee, 2002 (b) revised experiment by Kihyung Lee et al, 2004

The majority components in the constant volume combustion chamber were pressure transducer or data acquisition system, it is useful tool for analyzing the combustion behavior and another was the quartz glasses for combustion flame visualization. Also, high speed video camera and temperature sensor may be demanded.

### 2.3 Effect of equivalence ratio on hydrogen combustion

The equivalence ratio is the relative ratio between actual air/fuel ratio and calculated air/fuel ratio. If the equivalence ratio equal to 1, it is stoichiometric ratio. The calculated air/fuel ratio can calculate by using chemical equation.



The effect of equivalence ratio on hydrogen combustion was introduced in 2012 by Xinghua Liu, Zhiqiang Fan, Fushui Liu, Jiangang Jiu and Ruwei Wang from China [7]. They studied hydrogen combustion in constant volume combustion chamber by investigated the effect of equivalence ratio and initial pressure.

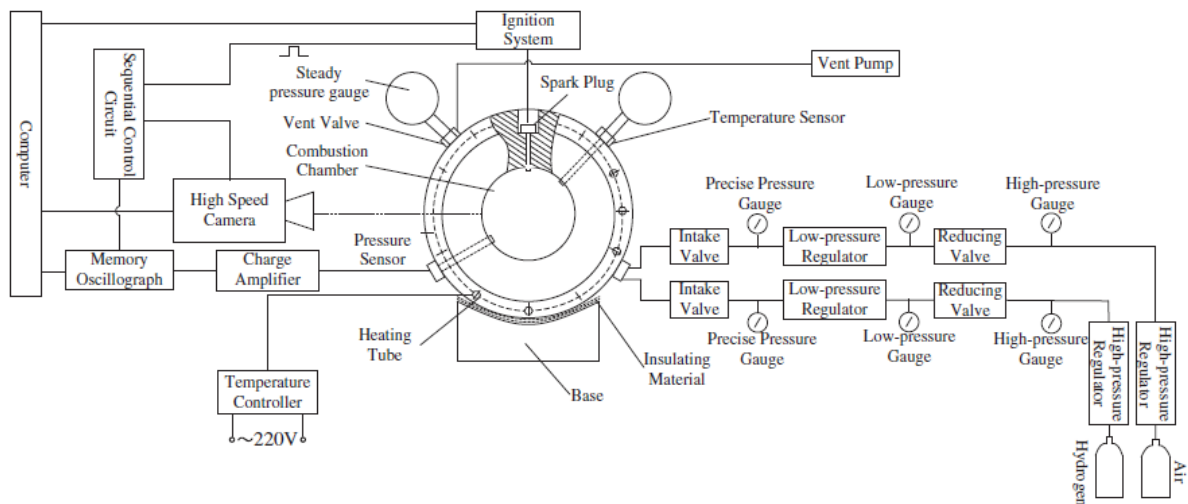


**Figure 2.2:** Schematic diagram of hydrogen combustion in CVCC by Xinghua Liu, Zhiqiang Fan, Fushui Liu, Jiangang Jiu and Ruwei Wang

Figure 2.2 shows the schematic diagram of researcher from Beijing Institute of technology in China. The researcher used CVCC to avoid the uncontrolled parameters. They designed the ignition point to locate in top of CVCC to make a condition that similar to real engine. The results of combustion characteristics in figure 2.3 were shown in type of flame propagation by using Schlieren technique with high speed video camera. When increasing the equivalence ratio the speed of combustion or combustion duration was higher than low equivalence ratio conditions.

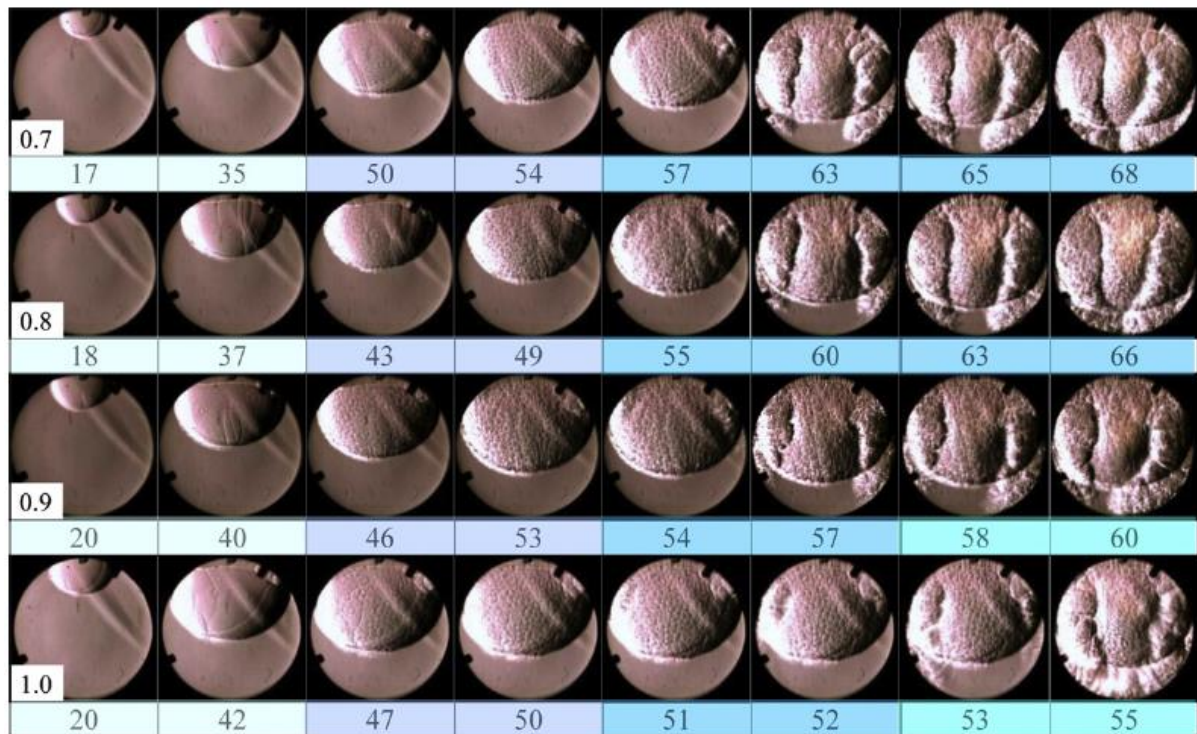


**Figure 2.3:** The results of flame propagation by varied equivalence ratio and compared it in unit of time after ignition.

The researcher explained that when increased the equivalence ratio, the combustion pressure increased. Also the flame propagation shown the difference combustion speed that higher equivalence ratio, higher flame speed.

## 2.4 Mass fraction burn rate and combustion duration

The mass fraction burn rate of fuel-air mixture was calculated from the measured combustion pressure profile under the assumption that the pressure in the combustion chamber corresponds to the mass fraction burnt [5],[8]

$$M_f(t) = \frac{P(t) - P_i}{P_{max} - P_i} \quad (2)$$

Where  $P_i$  and  $P_{max}$  are the initial pressure and maximum pressures respectively. The duration of flame-kernel development in other word, combustion delay ( $t_{0\%} - t_{10\%}$ ) was defined the period of time from ignition process to burning of 10% of mass [9] [10], and the combustion duration was defined as the time period beginning from after 10% burning of mass and ending after burning of 90%. The time  $t_{max}$  is the period from ignition to complete burning of the entire mixture (100%) in the combustion chamber.

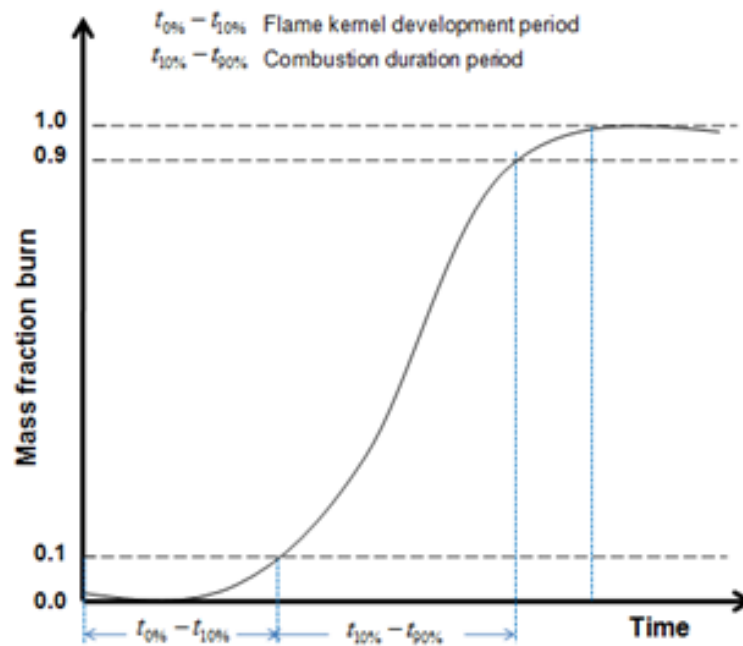


Figure 2.4: Definition of combustion duration and combustion delay

For clearly understand, the definition of combustion duration and combustion delay were shown in graph of measured pressure data in figure 2.4. Naoki Shiraishi et al.[11] and Kihyung Lee et al [6] give the definition of ignition-combustion interval as elapsed time from start of ignition to start of combustion can be defined as ignition delay.

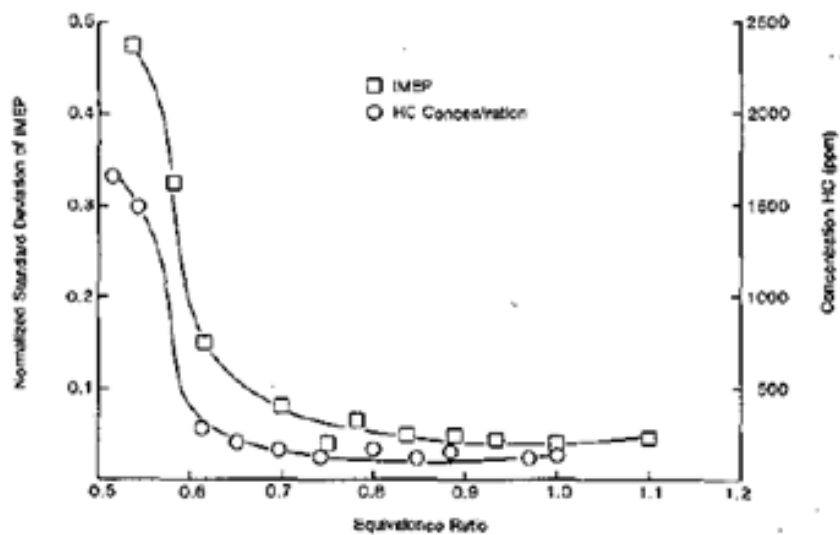
## 2.5 Lean flammability and ignition limit.

The combustion limit to be considered in spark ignition engine was separated into two types. First type is lean flammability limit and another is lean ignition limit [ Quad A. (1976) ]. In spark ignition engine, spark plug was discharged to emit the energy to initiate the chemical reaction between fuel and air to become burnt.

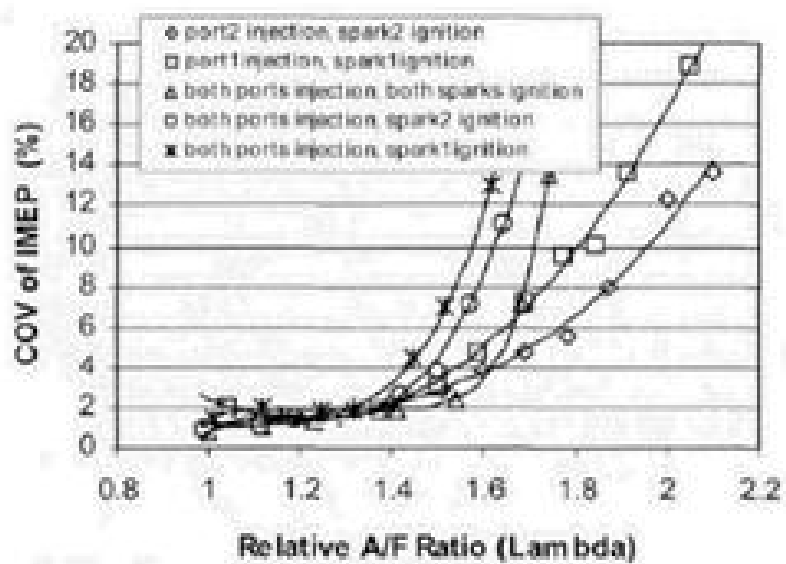
Lean flammability limit (LFL), is the leanest air-fuel mixture condition that can sustain flame propagation, and should be independent of ignition source and combustion vessel geometry [ Coward H. et al.(1952)]. In the spark ignition engine, lean limit commonly referred to as the lean misfire limit (LML) that means misfire results when the concentration of fuel is over lean in mixtures and it does not ignite, does not burn completely, or burns with such low flame speeds that blow down occurs before combustion is complete.

Lean ignition limit is defined by minimum external energy that must be supplied to critical volume to raise the mixture to its minimum ignition temperature [ Chigier N.(1981) ].

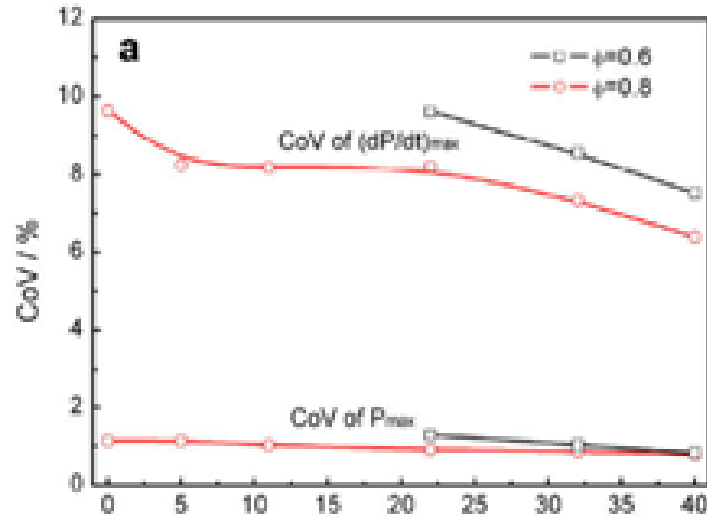
The exact definition of the lean misfire limit is difficult to explain because an engine can operate in a stable mode with temporary misfire at a certain air-fuel ratio. Since, there were variety of other methods to indirectly measure and define the lean misfire limit (LML). Selected definitions of LML found in the literature are specified amount of hydrocarbon or carbon monoxide content in exhaust gases [ Shimoto G. (1978) ] , the number of audible misfires counted over a time period [ Chaster K. (1977) ] or variation of mean effective pressure or indicated mean effective pressure [Winsor R. (1973)]. Because cylinder pressure and exhaust gas content are most easily measured, the majority of work relating to lean combustion has adopted definitions using either or both measurements. When relating air-fuel ratio to cylinder pressure or exhaust gas content as the air-fuel ratio increases from stoichiometric, a point is reach where variations increase sharply, which is approximately the lean misfire limit.



(a)



(b)



(c)

**Figure 2.5:** Lean limit investigation base on coefficient of variation (a) Lewis Flight propulsion Lab (1959) (b) Y.Li and H.Zhao “Development of fuel stratification spark ignition engine”(2005) and (c) Jinhua W. et al “Study of cyclic variations of direct injection combustion fueled with natural gas-hydrogen blend using a constant volume vessel”(2008).

Figure 2.5 show some of literature result for investigating the lean miss fire limit. From all of displayed result, the lean limit investigation, were based on coefficient of variation of indicated mean effective pressure but was not define the certain number of variation as the lean limit. However, In Jinhua Wang’s study [12] , the researcher had set the 20% variation as the lean limit point.

## 2.6 Cyclic of variation (CoV)

Cyclic variations in the combustion process are caused by variations in mixture motion within the cylinder at the time of spark cycle-by-cycle, variations in the amounts of air and fuel fed to the cylinder each cycle, and variations in the mixing of fresh mixture and residual

gases within the cylinder each cycle, especially in the vicinity of the spark plug. Variations between cylinders are caused by differences in these same phenomena, cylinder-to-cylinder

As the mixture becomes leaner with excess air or more dilute with a higher burned gas fraction from residual gases or exhaust gas recycle, the magnitude of cycle-by-cycle combustion variations increases.

Cycle-by-cycle combustion variations are evident from the beginning of the combustion process. Analysis of flame photographs from many engine cycles taken in special research engines with windows in the combustion chamber has shown that dispersion in the fraction of the combustion chamber volume inflamed is present from the start of combustion. Dispersion in burning rate is also evident throughout the combustion process. Three factors have been found to influence this dispersion

1. The variation in gas motion in the cylinder during combustion, cycle-by-cycle
2. The variation in the amounts of fuel, air, and recycled exhaust gas supplied to a given cylinder each cycle
3. Variations in mixture composition within the cylinder each cycle-especially, near the spark plug-due to variations in mixing between air-fuel, recycled exhaust gas, and residual gas

The useful statistics tool for lean limit investigation is coefficient of variation (CoV). These parameter can be calculated directly from pressure history data. The peak pressure and indicated mean effective pressure were counted and converted to CoV by follow formula.  
[ Heywood J.B. (1998) P.413-423]

$$\text{CoV}_x = \frac{\sigma_x}{\bar{x}} \times 100\% \quad (3)$$

Where,

$$\bar{x} = \frac{1}{N} \sum_{i=1}^N x_i \quad (4)$$

and the standard deviation

$$\sigma_x = \sqrt{\frac{\sum_{i=1}^N (x_i - \bar{x})^2}{N}} \quad (5)$$

## 2.7 Schlieren photography technique

There are many methods to derive and measure the flame velocity. The four famous method that apply in combustion research were

1. Bunsen-burner method
2. Transparent-tube method
3. Soap-bubble method
4. Constant-volume bomb method

For the first method, Flame will be stationary during combustion while three methods remaining were observed the propagation flame or non-stationary. In Soap-bubble method, high speed video camera was need. Thus, it's very complicated than two first method. The constant-volume bomb method was the most complicated method apply to flame propagation measurement due to this method have to know both rate of pressure rise and rate of flame area expansion in the same time. However, flame area expansion rate can be investigated by using direct-photograph or particle-tracking technique.

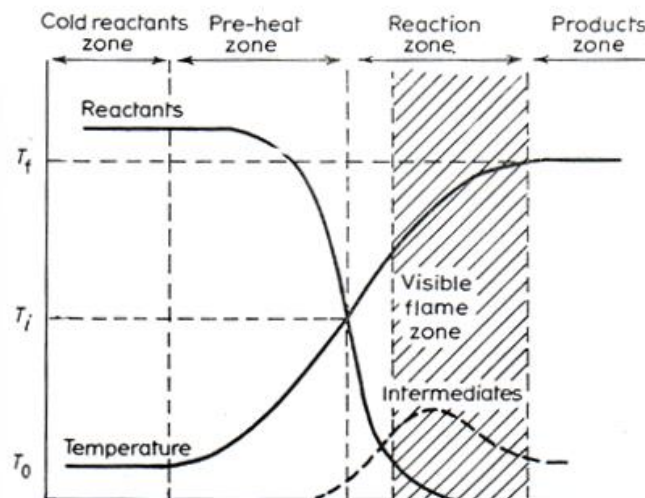
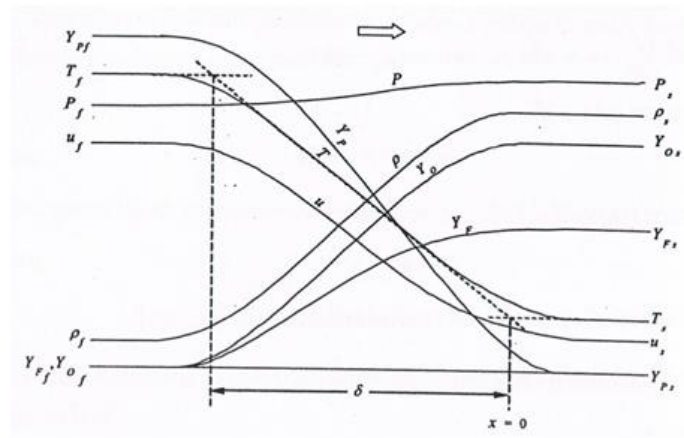


**Figure 2.6:** Deflagration wave structure

Even though the direct-photograph technique cannot get the high accuracy but it was the easiest technique to collect the flame shapes and also its sizes compare with another technique. This technique will observed the luminous region in luminous zone due to thermal radiation from hot gas from the combustion. However, the intensity of this luminous region was too much because it occurs toward to the post flame. Moreover, the luminous zone was too far from the unburned mixture region as shown in figure 2.7. This conflict to the burning velocity definition. Consider in deflagration wave in combustion process which is shown in

figure 2.6. Definition of burning velocity is relation velocity of flame expansion rate to the velocity unburned mixture. Thus, flame surface that use to measure the burning velocity should be the flame surface that occur close to the unburned mixture ( $x=0$ ) as shown in figure 2.6 and figure 2.7

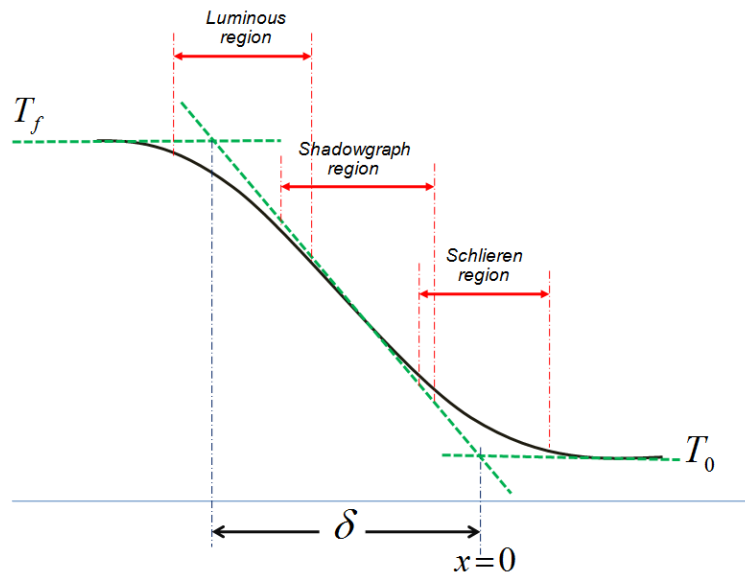


**Figure 2.7:** Flame region that recorded with different direct-photograph technique

For resolve that problem, special photography technique was developed. First is shadow graph technique, second is Schlieren technique and third is Interferograph technique. All of these technique were developed base on the two physical concept, Different of density within flame due to variation of temperature gradient and species, and different of reflexive index within reaction flame. Thus, when the light pass thought the flame, light from the light source will be reflex and this reflexive light will travel with longer distance compare with non-reflected light. Consequently, different time assume from different distance will be developed to principal operation of Interferograph technique. Schlieren technique will show the flame that be responded to the density gradient while the Shadowgraph technique will show the flame that be responded to the second derivative of density. Assume that the density of flame depend only on the temperature ( $\rho = 1/T$ ). So, Shadowgraph image will display the

flame edge that  $\frac{dT}{dx}$  is maximum or close to inflexion point while the Schlieren technique image will show the flame edge that  $\frac{d^2T}{dx^2}$  is maximum. These region were very close to the unburned region as shown in **Error! Reference source not found..** Therefore, flame surface that be observed from Schlieren photograph technique is the most appropriate method for using to flame speed calculation even its apparatus was more complicated than Shadowgraph or Interferograph technique.

## CHAPTER 3

## EXPERIMENTAL APPARATUS AND PROCEDURE

## 3.1 Experimental apparatus

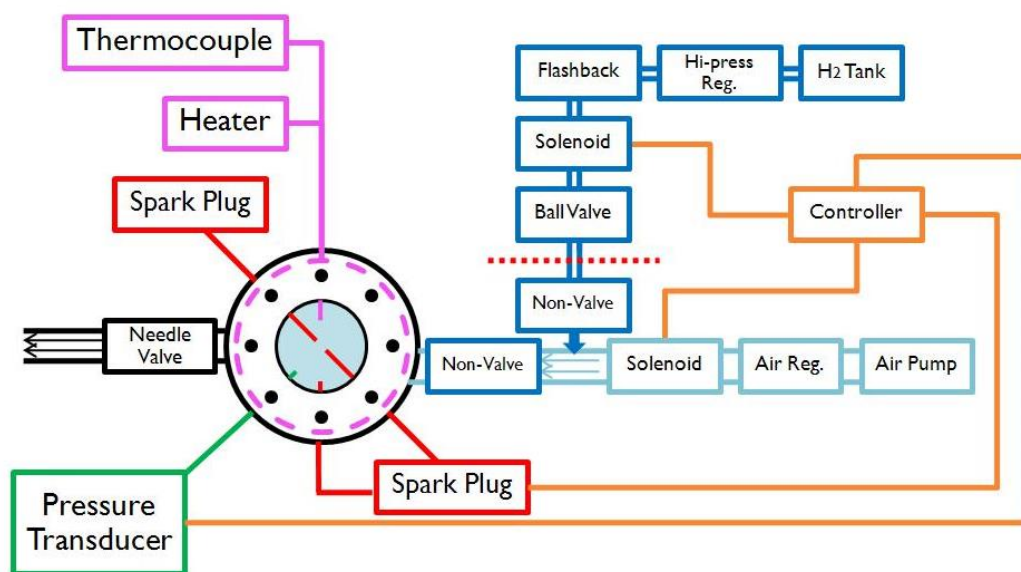


Figure 3.1: Schematic diagram of experimental apparatus

Figure 3.1 show the schematic diagram of experimental apparatus which used in this research. It has seven sections, the constant volume combustion chamber, hydrogen supply system, air supply system, ignition system, temperature control system, controller module and pressure transducer system.

### 3.1.1 Hydrogen supply system



**Figure 3.2:** Hydrogen supply system

The hydrogen supply system as shown in Figure 3.2 was fed from hydrogen tank with high ultra-purity 99.999%. Then passing through the hydrogen pressure regulator. To avoid the accident, hydrogen pressure should set as low as possible and it was set at 1.0 bar. Also hydrogen flashback arrestor was used to reduce the risk of causing harm. Electric solenoid valve which work by electrical signal from controller used to open or close amount of hydrogen from calculation. The coupling connector was used to cut off the hydrogen supplying line before the combustion process.



**Figure 3.3:** Hydrogen flashback arrestor

Flashback arrestor from WITT model RF 53 N/H was used to protect single cylinders, outlet points or pipelines and can be used for almost all technical gases. By combination of established safety elements flashback arrestors provide protection against flashbacks and backfire. Flashback arrestors also prevent the formation of dangerous gas mixtures within the pipeline.

### 3.1.2. Air supply system

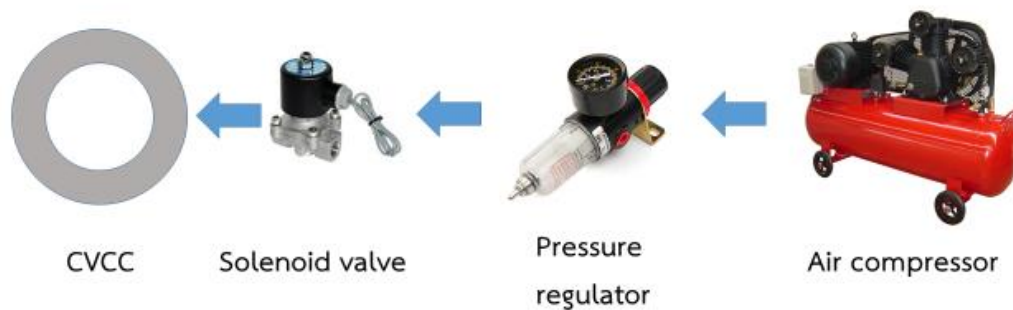


**Figure 3.4:** Air supply system

The air supply system as shown in Figure 3.4 consist of air compressor that can pressurized up to 10 bar. Second, pressure regulator included air dryer and air filter used to adjust the air pressure before charge to the constant volume combustion chamber and also used to vary the differential swirl intensity. Finally, High pressure solenoid valve which worked by electrical signal from controller. It used to open or close the air pressured from pressure regulator which passed through the check valve to avoid the incidental accident of back pressure from explosion gas in the constant volume combustion chamber.

### 3.1.3. Temperature control system

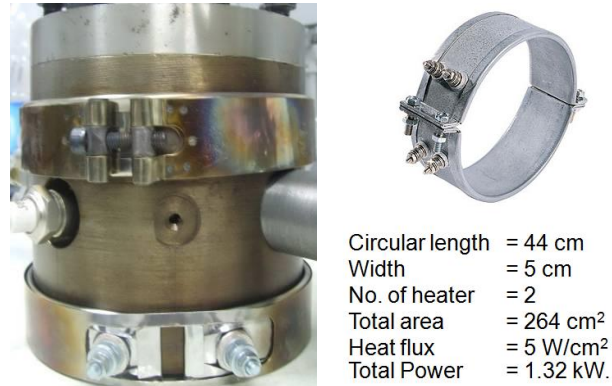


**Figure 3.5:** Two band of heater attached to the combustion chamber

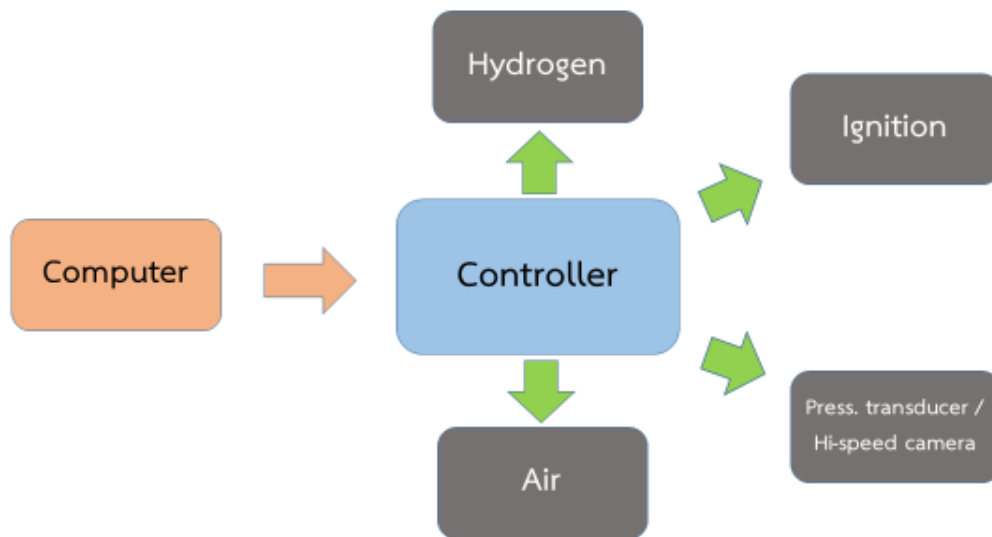
For study in hydrogen combustion in constant volume combustion chamber, the heater and temperature control system were used realize the initial temperature close to real engine [13]. Another thing is the combustion product, stream was attached to quartz glass, so it is difficult to capture photo and video via high speed video camera. The temperature controller was controlled the temperature over 100 degree Celsius to burn stream that overlay at the quartz glass.



**Figure 3.6:** Temperature indicator and controller

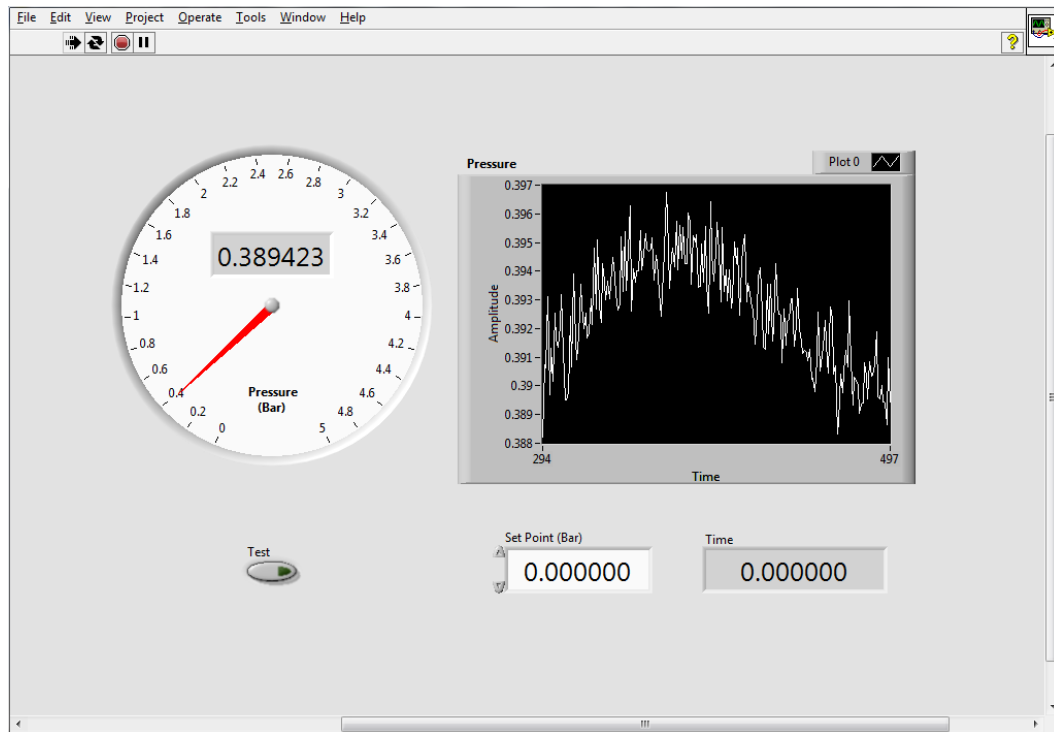
The position to measure air temperature for this study is inside of combustion chamber. The K type of thermocouple was equipped to this system. To avoid the effect of chamber temperature, this type of thermocouple was isolate with graphite along length. So it can measured temperature only at the tip that located inside of combustion chamber. Moreover, the temperature indicator was showed both target temperature and operation temperature.

#### 3.1.4. Driver and controlled module



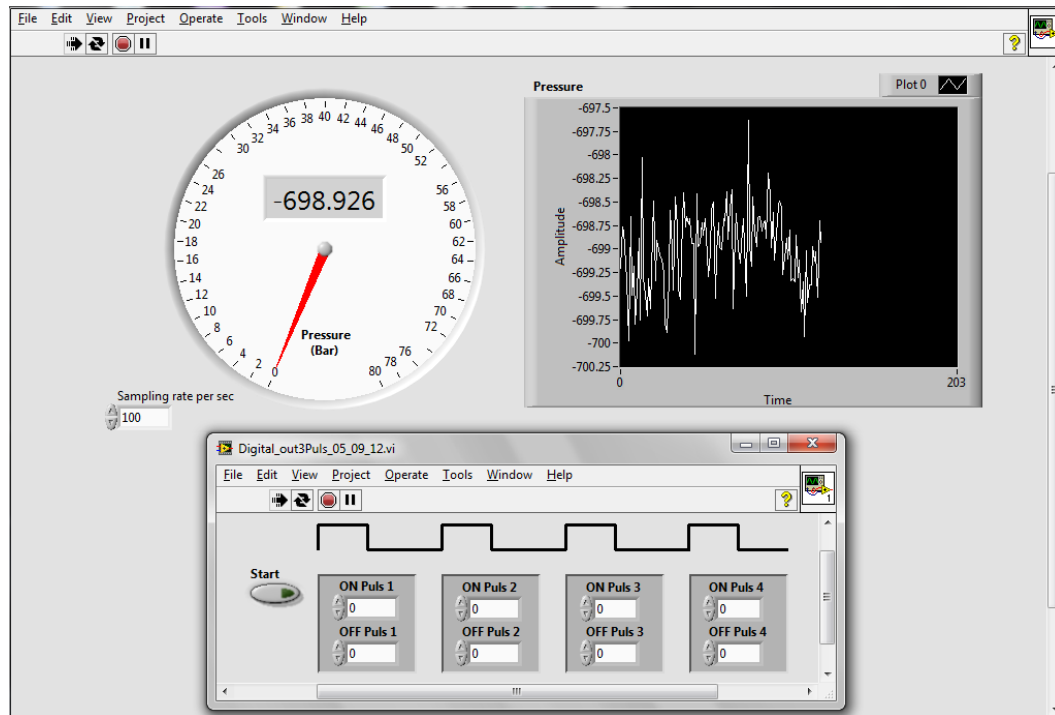
**Figure 3.7:** Schematic diagram of driver and controlled module system

Figure 3.7 show the schematic diagram of driver and controller module. The operation input power came from 2 sources separated that are 12V from battery and 5V from computer. The power from 12V battery was used to operate hydrogen solenoid, air solenoid, ignition system and also for high speed video camera. Shield cable was used to interface the command digital signal from computer to driver module.



**Figure 3.8:** Computer controller program for hydrogen rich-lean calibration

In this experiment, equivalence ratio was one of parameter for varied. So Equivalence was calculated by partial pressure from chemical equation. This program was use to convert partial pressure to injection duration. Initial pressure of hydrogen was fixed at 1 bar of gauge pressure then set target pressure to the calibration program. After that, injected hydrogen to combustion chamber, the gauge pressure inside combustion chamber was measured by pressure sensor. Finally, when pressure reached to target pressure, injection duration was resulted.



**Figure 3.9:** Computer controller program for driver module

This figure 3.9 shows computer program to control 4 devices (hydrogen solenoid, air solenoid, ignition system high speed video camera signal) in hydrogen combustion process. The program was designed to input the on/off duration time for each device individually. Hydrogen was injected to combustion chamber first then air was injected. Ignition signal and high speed video camera signal were commanded in the same time to capture combustion phenomena when hydrogen-air combustion was started.

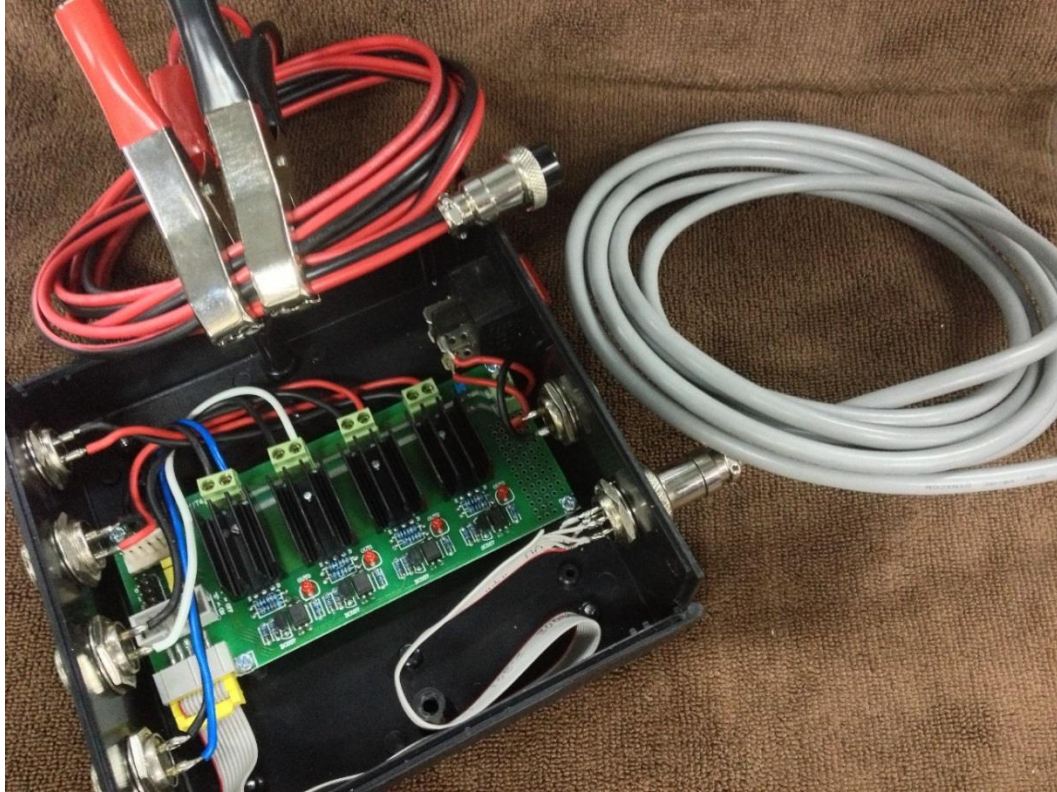


**Figure 3.10:** Driver module

For driver module in this experiment, Opto-isolator type was used because it is the fastest signal interfacing. It has back signal isolator, so the high voltage back from ignition coil can be avoided. This driver used to convert 5V signal from computer to 12V for 4 channel devices.

### 3.1.5. Data acquisition system



**Figure 3.11:** Pressure sensor

When analyzing the hydrogen combustion characteristics in constant volume combustion chamber, high quality of combustion pressure data was necessary to collect. In this study, the pressure transducer from KISTLER model 6057 ASP which can operate with high pressure up to 250 bar and can be resist temperature up to 300 degree Celsius was chosen. Sampling rate that set through this experiment was set at 10,000 data/second.

DEWETRON DEWE-5000 in figure 3.12 is a charge amplifier which was used to collect the signal data from pressure sensor in unit of coulomb and convert to voltage. The data can be exploded in form of Microsoft Excel that can be processed to figure and chart via computer.



**Figure 3.12:** DEWETRON DEWE-5000

### 3.1.6. Schlieren photography setup

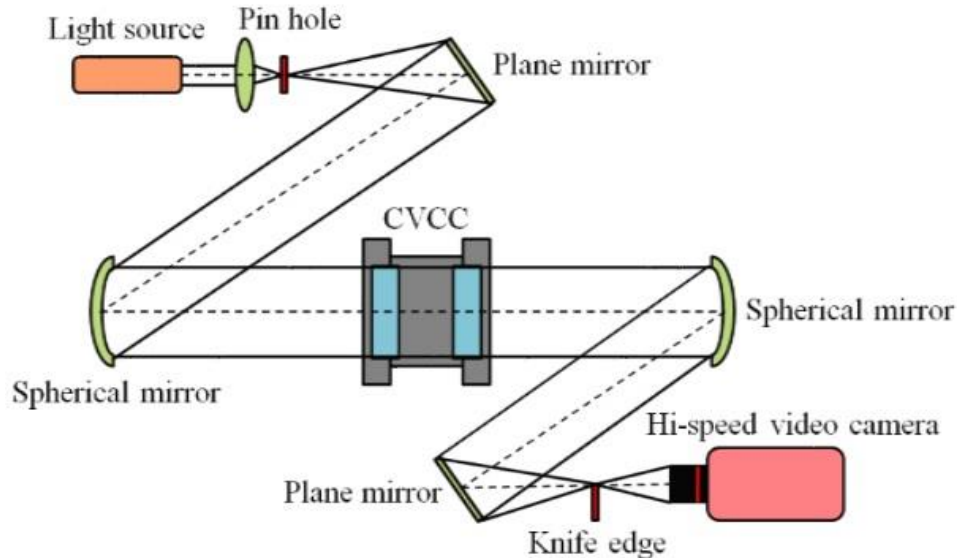


**Figure 3.13:** Layout of Schlieren photography system

The Schlieren photography was very useful device for combustion phenomena and flame propagation analysis. The gradient density of burnt and unburnt mixture in combustion chamber were measured by high speed video camera directly. The combustion density was respond to combustion pressure, combustion temperature and boundary of reaction zone. Therefore, Schlieren photography technique which closely related to gradient density was chosen.

Schlieren photography system consist of three main equipment. First of all is light source which generate high intensity light pass through combustion chamber. Second, two spherical mirrors for reflected light direct to the object. Third, knife edge, used to focus only detail of density of an object.

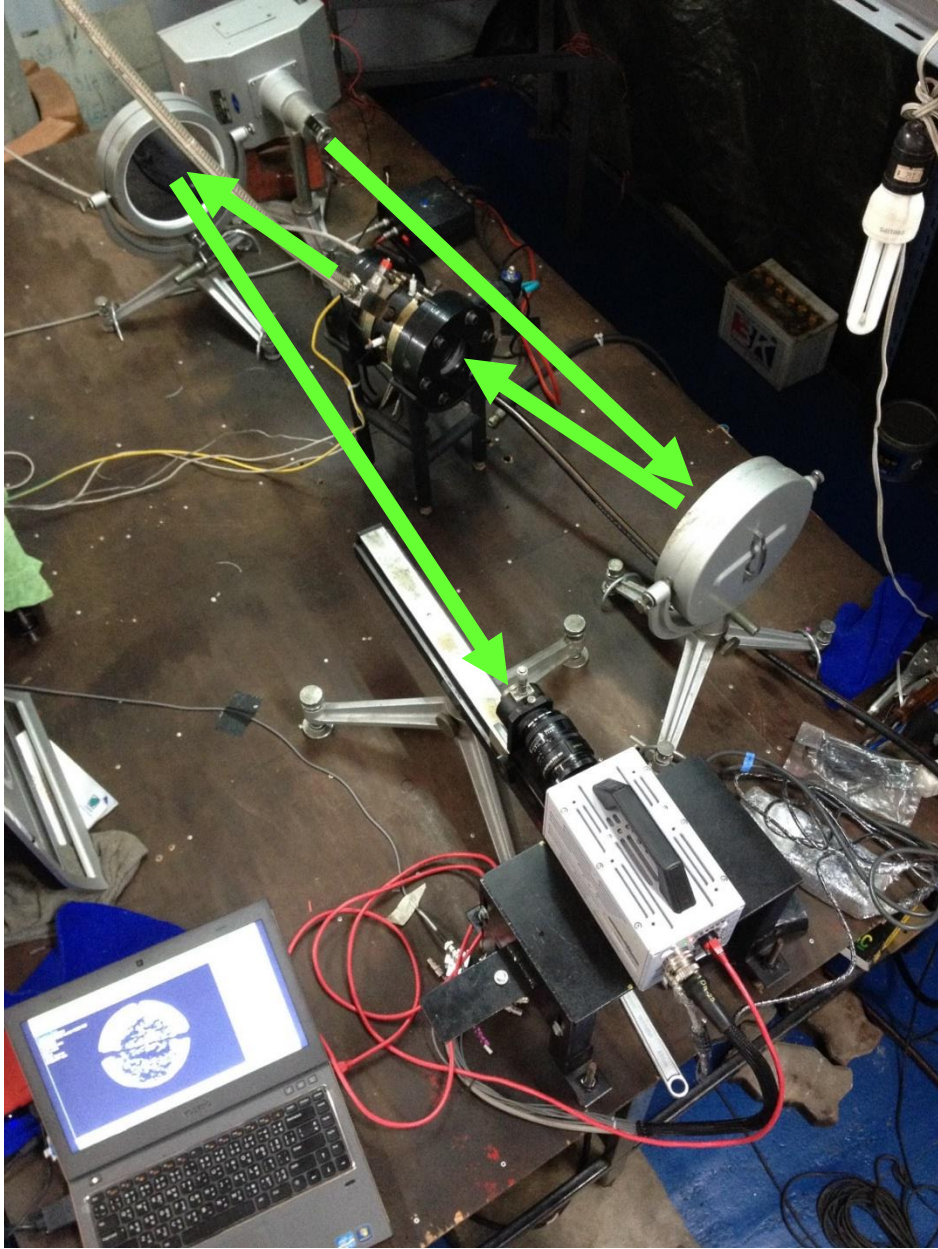


**Figure 3.14:** Real experimental layout of Schlieren photography

Figure 3.14 and 3.15 show Schlieren photography system with laser alignment to avoid distortion of image of this experiment.

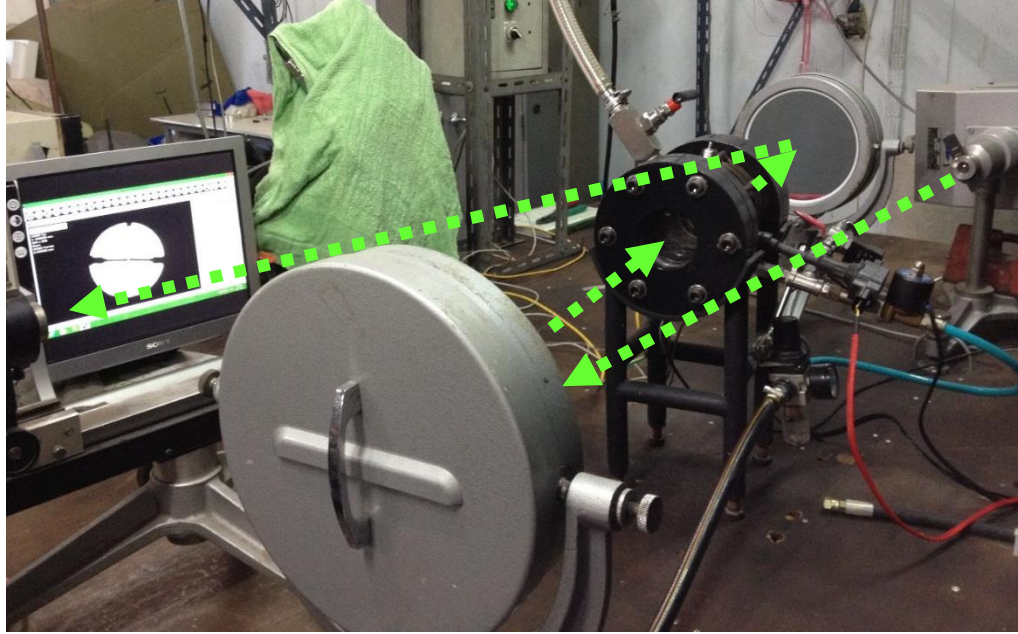


Figure 3.15: Real alignment of Schlieren photography system



Figure 3.16: The example image that reflected from spherical mirror

### 3.1.7. High speed video camera

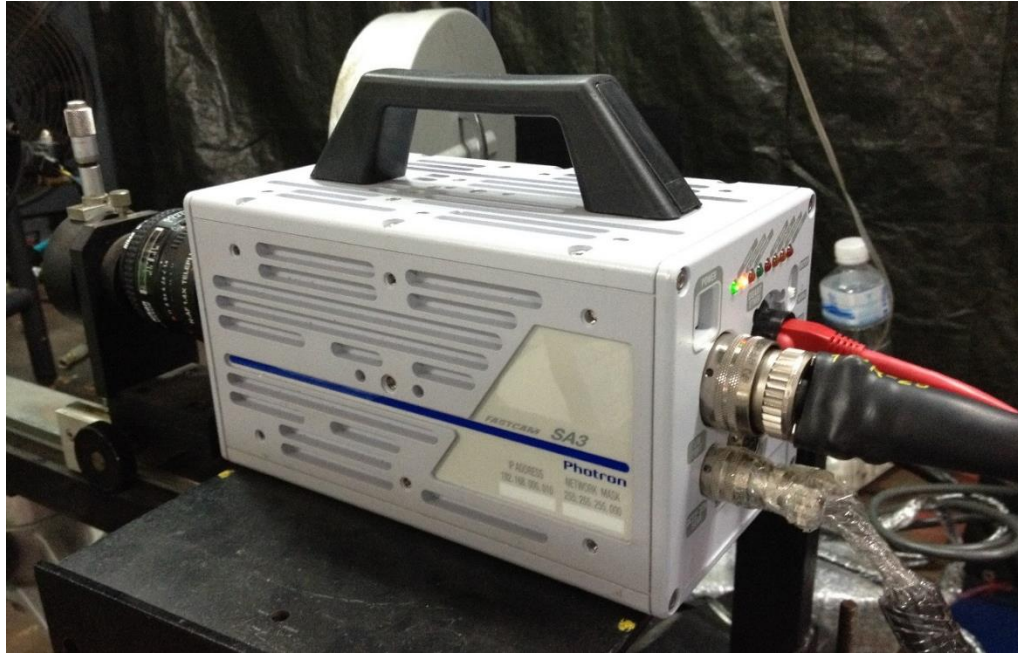


Figure 3.17: Photron SA3 high speed video camera

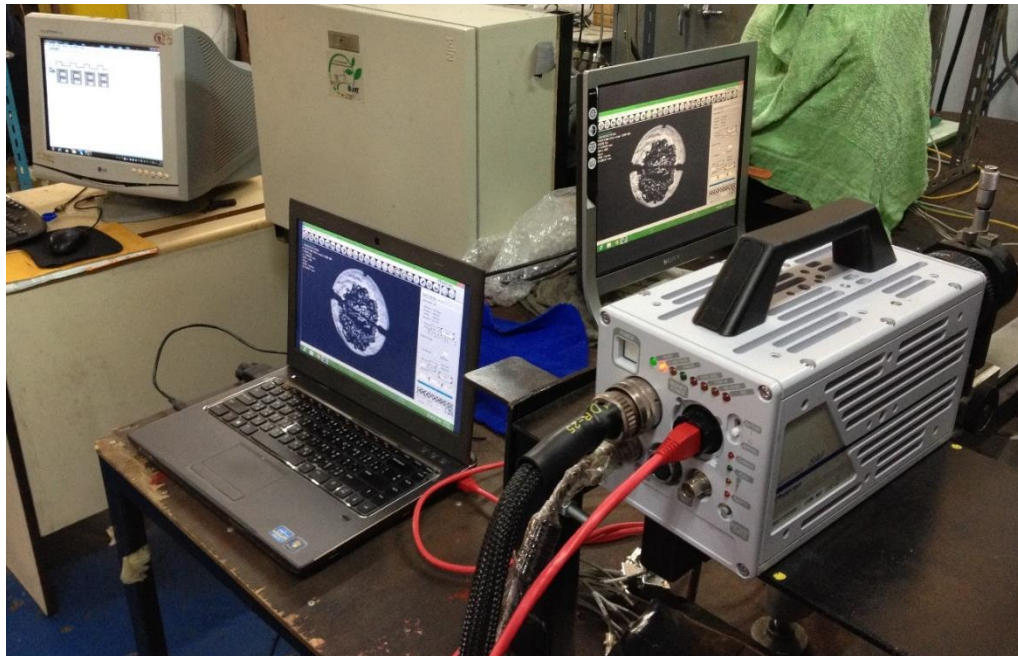


Figure 3.18: Real experiment image from high speed video camera

The model of high speed video camera, Photron FASTCAM SA3 with fix focal length lens (50 mm. and  $f=1.4$ ) and 1.4x adapter ring were used in this study. It is a monochrome video camera which can record 12,000 fps at 384 x 288 pixels resolution. Triggering mode in this experiment was set at 3 msec before start of combustion in all condition. Figure 3.18 shows the example display on laptop that was used to observe and operate the high speed video camera separately because it has to use much of transfer rate and avoid the interference to the command program. The software program of Photron FASTCAM camera was shown in figure 3.19 that shows the camera setting and user viewer.

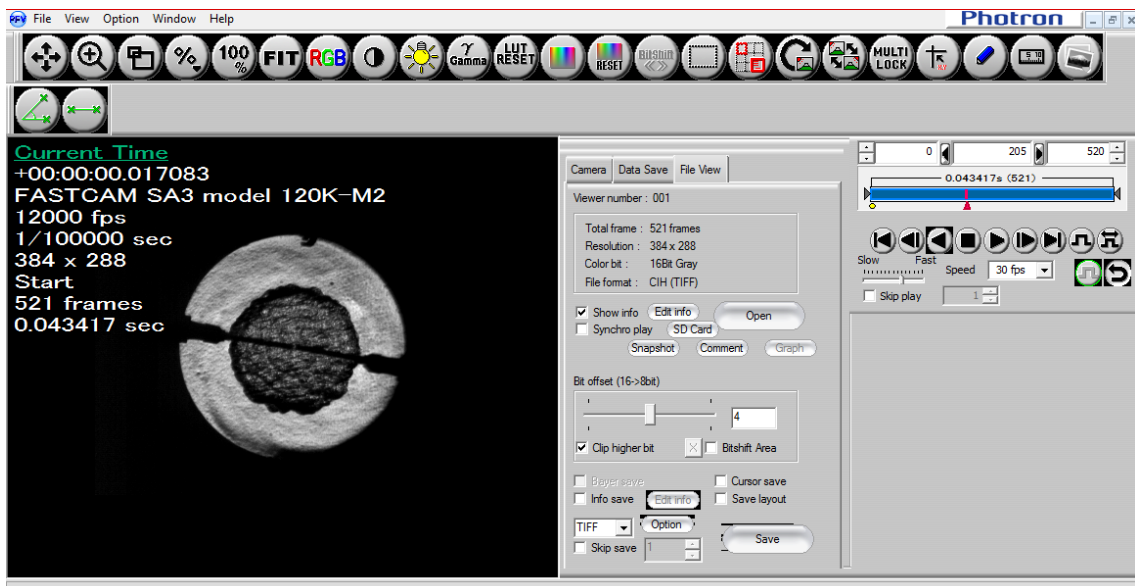


Figure 3.19: Photron FASTCAM software shows the camera setting and real time viewer

### 3.1.8. Constant Volume Combustion Chamber (CVCC)



**Figure 3.20:** Real experimental equipment of CVCC

In this study, the experiment was used a Constant Volume Combustion Chamber (CVCC) instead of real engine. The main reason is CVCC can control and fix many parameters. The real engine can make many fluctuation error to disturb the combustion characteristics. Figure 3.20 shows Constant Volume Combustion Chamber with measuring devices in this study. In hydrogen supply line, electrical solenoid valve was used to open or close by digital signal from computer program. Mechanical ball valve and quick coupling was used to close and release the hydrogen line before combustion to avoid the accident that back combustion pressure cause explosion to hydrogen tank. Air supply line, this experiment was fixed initial pressure of air at 5 bar thus, 6 bar pressure gauge was used to measure the real pressure of air before injected to CVCC. Air injection was controlled by electrical solenoid valve that commanded from computer program. Both hydrogen and air supply line can avoid the

explosion gas from CVCC by using mechanical check valve. Furthermore, spark plug, exhaust valve were necessary for this study.

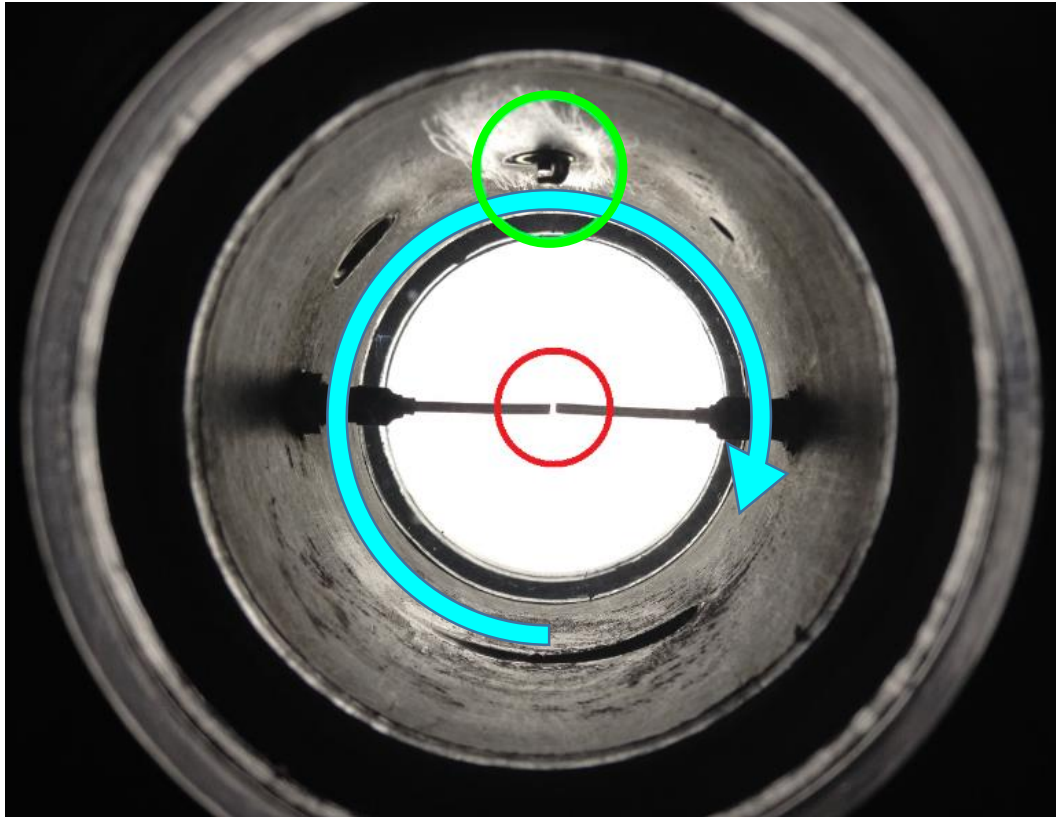


**Figure 3.21:** Air swirl and spark plug position

Swirl intensity is one of parameters in this study. The swirl port tangential hole drilled from side surface of combustion chamber. It can injected air into CVCC with tangent direction to make swirl inside CVCC. Another device is spark plug. In this study, two positions of spark plug (center/side) were one of varying parameters.

The dimension of CVCC as shown in figure 3.22 has 70 mm. of inner diameter and 100 mm. of length. So, the volume of CVCC is 384.84 cc. that similar to one cylinder of small conventional engine [14].

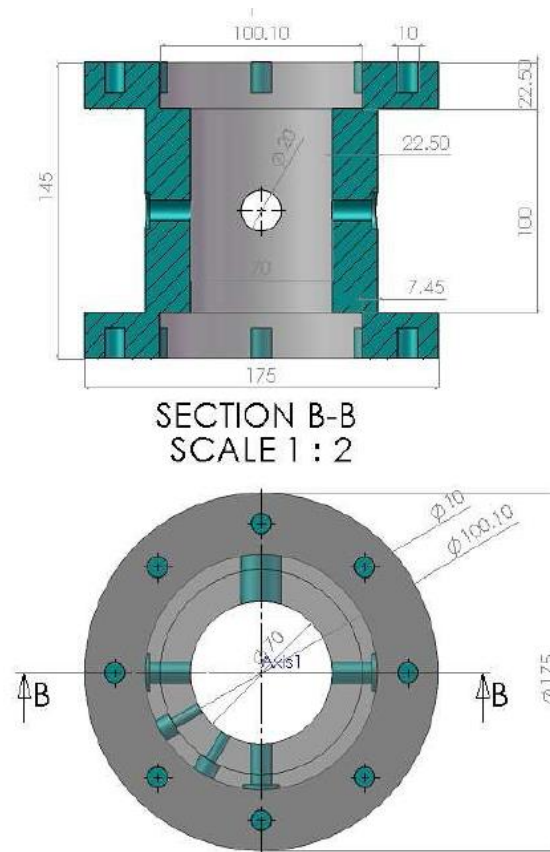


**Figure 3.22:** Dimension of CVCC

When designing CVCC, it have to ensure that CVCC can bear to the maximum combustion pressure to avoid damage and dangerous to people. The simulation process must use to guarantee. From maximum pressure calculation at equivalence ratio equal to 1 [15] [16], 69 bar is a result. But for more safety, 80 bar was used to simulate with CAE simulation program.

CVCC was separated into two parts, main chamber and chamber lid with quartz glass. Main chamber and chamber lid were material designed with ASTM A283 steel grade D or steel SS400 which has a yield strength at 230 MPa. The results were shown in Figure 3.23 and 3.24 that show the maximum stress of main chamber equal to 26.9 MPa and 47.2 MPa for chamber lid with quartz glass. So, the safety factor were 8.55 and 4.87 for main chamber and chamber lid with quartz glass respectively.

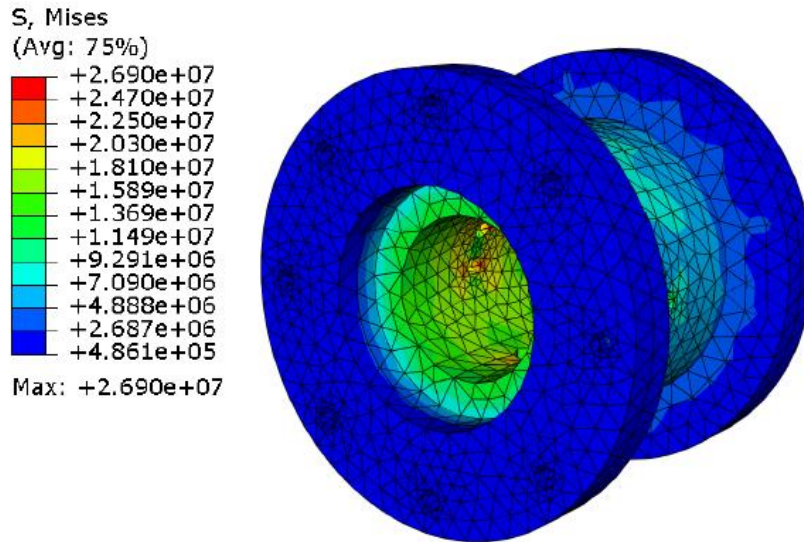


Figure 3.23: CAE simulation result of main chamber

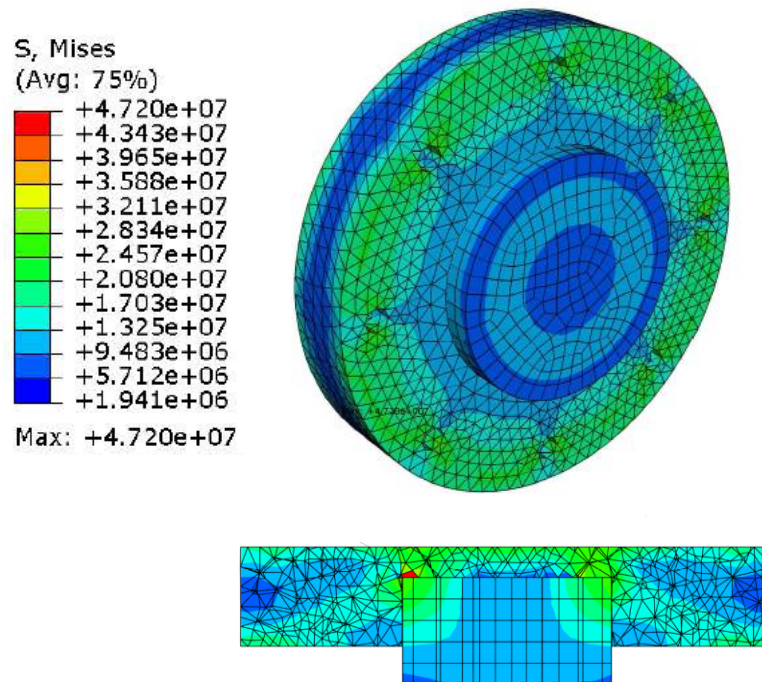
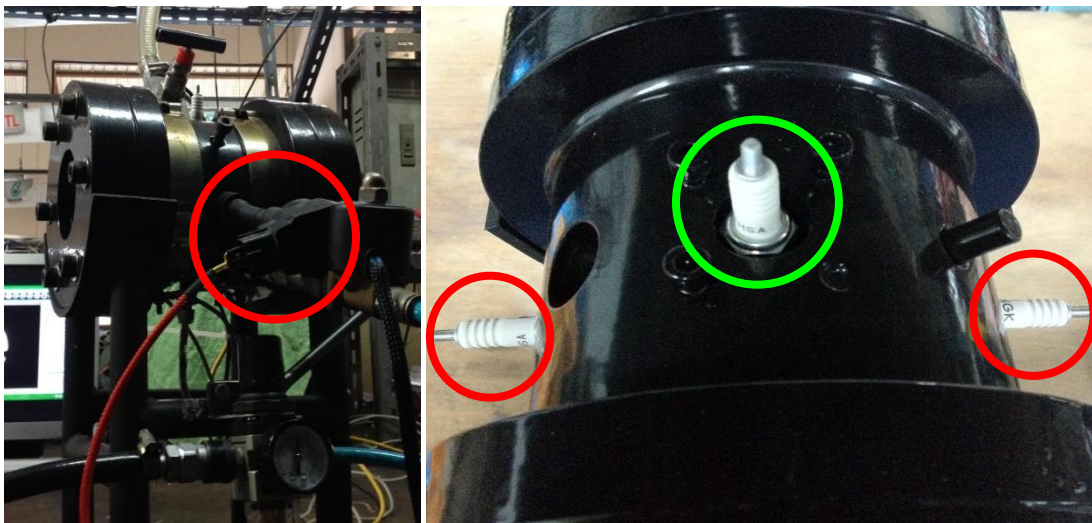


Figure 3.24: CAE simulation result of chamber lid with quartz glass

In order to observe flame propagation, quartz glass is transparent material that was chosen in this study. For safety to the quartz glass, graphite gasket was used to attach between quartz and steel devices (main chamber and chamber lid) in order to support the explosion impact of two side of CVCC. Moreover, graphite gasket acted like sealer to prevent combustion leakage and can resist high temperature up to 1650 degree Celsius.

### 3.1.9. Ignition system



**Figure 3.25:** directional Ignition coil and spark plug

Hydrogen-Air combustion in this study have to ignite mixture by spark ignition process like Spark Ignition engine (SI engine). So, the conventional ignition coil from Denso and spark plug from NGK CR8E were chosen for this study as shown in figure 3.25. The ignition system is one of varying parameters that has two position of ignition points (center and side wall ignition) as shown in figure 3.26 and 3.27. For center ignition condition, two of spark plug were electrode extended to the center of CVCC. One side spark plug was used as anode while another one was cathode. Another condition is side wall ignition that spark plug located at top of CVCC and has both anode and cathode by itself.



Figure 3.26: Spark plug for center ignition

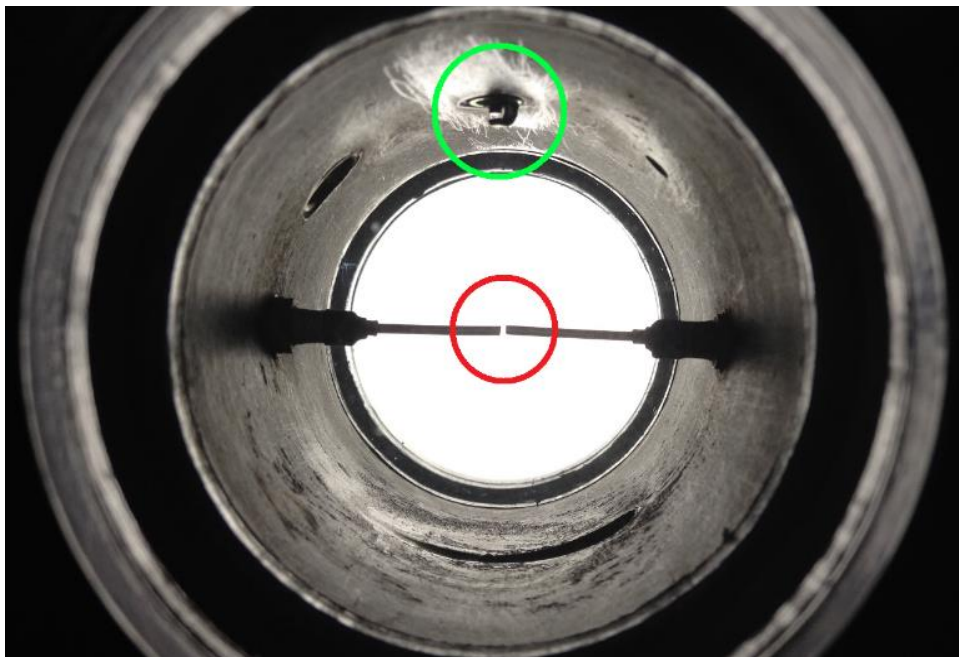


Figure 3.27: Two varying conditions of ignition point (center and side wall)

### 3.2 Experimental conditions

In hydrogen combustion, it has many parameter that affected to the combustion behaviors. The author need to fix and control many parameters and observe only in equivalence ratio, initial temperature, swirl intensity and position of spark plug that effected to hydrogen combustion characteristics. The fixed and variable parameters were shown in table 2.

**Table 2:** Experimental conditions

Experimental parameters	Conditions
Initial pressure (bar)	5
Hydrogen supply pressure (bar)	1
Ignition coil charge time (msec)	3
Hydrogen – Air interval (sec)	5
Air – ignition interval (msec)	35
Air injection duration (sec)	1.8
Initial temperature (Celsius)	85, 95, 105
Equivalence ratio	0.2, 0.3, 0.4, 0.5
Hydrogen injection duration (msec)	266, 612, 1278, 5814
Swirl intensity in $\Delta P$ (bar)	1, 2, 3, 4
Swirl intensity in velocity (m/s)	5.73, 6.50, 7.54, 8.10
Position of spark plug	Center and Side wall

From the experimental condition in table 2, initial temperature were varied by 85, 95 and 105 degree Celsius to investigate the effect of pre-ignition temperature on hydrogen combustion behavior. Equivalence ratio is one of parameters to study its effect to the combustion characteristics. Because of the properties of hydrogen, it can be combusted with ultra-lean condition. So, the lean condition with 0.2, 0.3, 0.4 and 0.5 of equivalence ratio were chosen. Four conditions of Turbulence flow inside CVCC was assumed as swirl intensity by varying the differential pressure between air injected and inner chamber pressure. Another variable parameter is the spark plug position. Density of hydrogen and air are very different, the mixture may discriminate as layer. Thus, changing the ignition point was an investigated parameter.

### 3.3 Experimental procedure

#### 3.3.1 Swirl setup

Swirl intensity in this study was varied by adjusting the differential pressure between air input pressure and inner chamber pressure. The definition of this parameter was shown in figure 3.28

#### 4 Conditions :

0.4MPa	$\Delta P=0.1MPa$	→ 0.5MPa
0.3MPa	$\Delta P=0.2MPa$	→ 0.5MPa
0.2MPa	$\Delta P=0.3MPa$	→ 0.5MPa
0.1MPa	$\Delta P=0.4MPa$	→ 0.5MPa

\* Gauge pressure

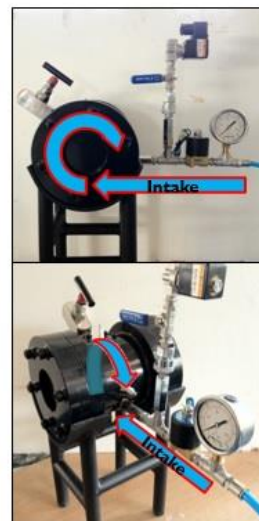
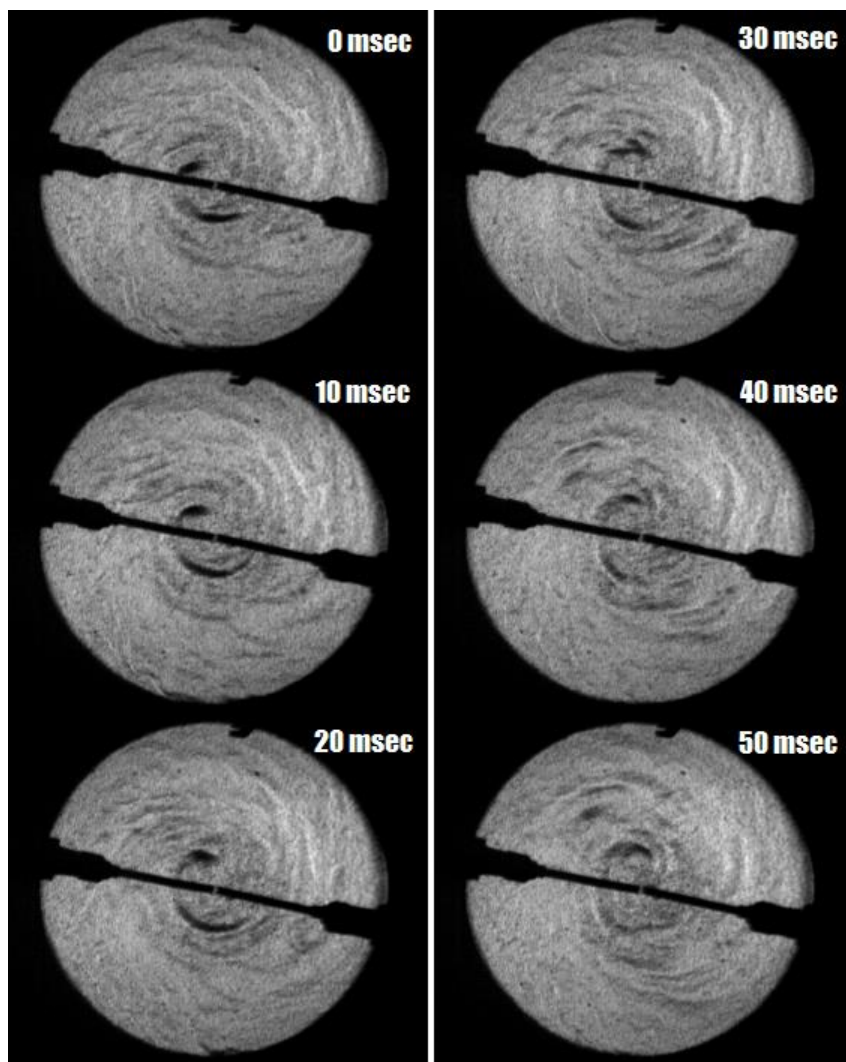


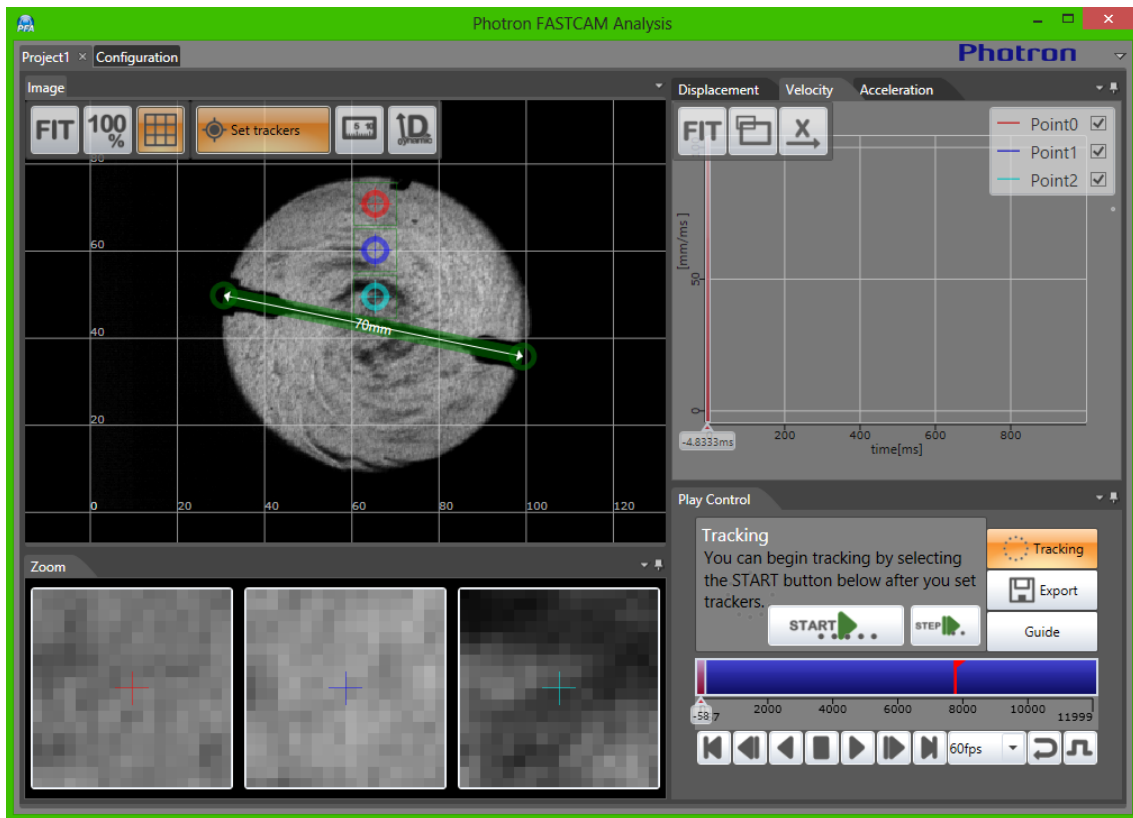
Figure 3.28: Swirl setup definition

For swirl intensity condition, this testing was separated into two stages. First stage, after hydrogen was injected to CVCC, air was input to make a pre-stage of pressure. Last stage, air pressure at 5 bar was follow to CVCC for 1.8 second for ensure that CVCC was filled with air at 5 bar.

With utilizing of Schlieren photography and high speed video camera, air motion image can be to investigate the air velocity in all of swirl intensity conditions. In this experiment, air velocity was measured by putting the powder particle into CVCC and using computer program to track the motion speed of shadowgraph video.



(a)



(b)

**Figure 3.29:** (a) Shadowgraph image of swirl intensity (b) grid pixel for air velocity measurement

Figure 3.29 show the air motion image that was taken by Photron FASTCAM SA3 high speed camera with Schlieren photography technique. Photron FASTCAM Analysis was used to investigate the air velocity by locking the three points of powder particle and tracking the motion of it that rotated inside CVCC. The results of air velocity were averaged from three tracking point as an average air velocity in unit of m/s as shown in figure 3.30

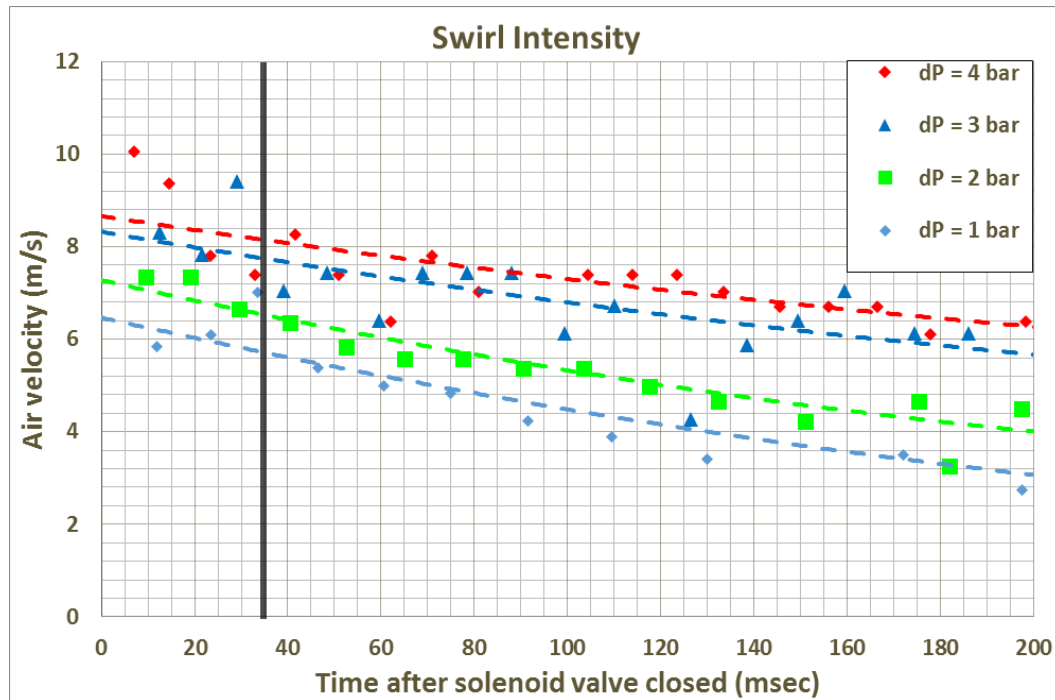


Figure 3.30: Air velocity that was resulted by Photron FASTCAM Analysis program

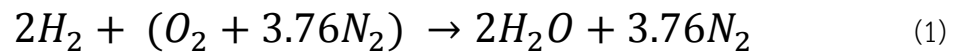
The result as shown in figure 3.30, it can be make a trend line to make an average velocity while the time still continue. The swirl velocity was deteriorated but the air velocity in real engine still high. Thus, this study have to select the time after solenoid valve closed as fast as possible [18]. Therefore, the timing at 35 msec after solenoid valve closed was chosen. Because of before 35 msec, the raw data so scattered [13].

Table 3: Swirl intensity to air velocity conversion

Swirl intensity by differential pressure (bar)	Air velocity (m/s)
1	5.73
2	6.50
3	7.54
4	8.10

### 3.3.2 Equivalence ratio calibration

This experiment was tested in constant volume combustion chamber. The initial air pressure was fixed. Thus, the amount of hydrogen was controlled by partial pressure calculation with balanced chemical equation because density of hydrogen is too low to measure in unit of mass.



$$P = P_1 + P_2 \quad (2)$$

$$x_i = \frac{P_i}{P} = \frac{n_i}{n} \quad (3)$$

$$P_i = x_i \cdot P \quad (4)$$

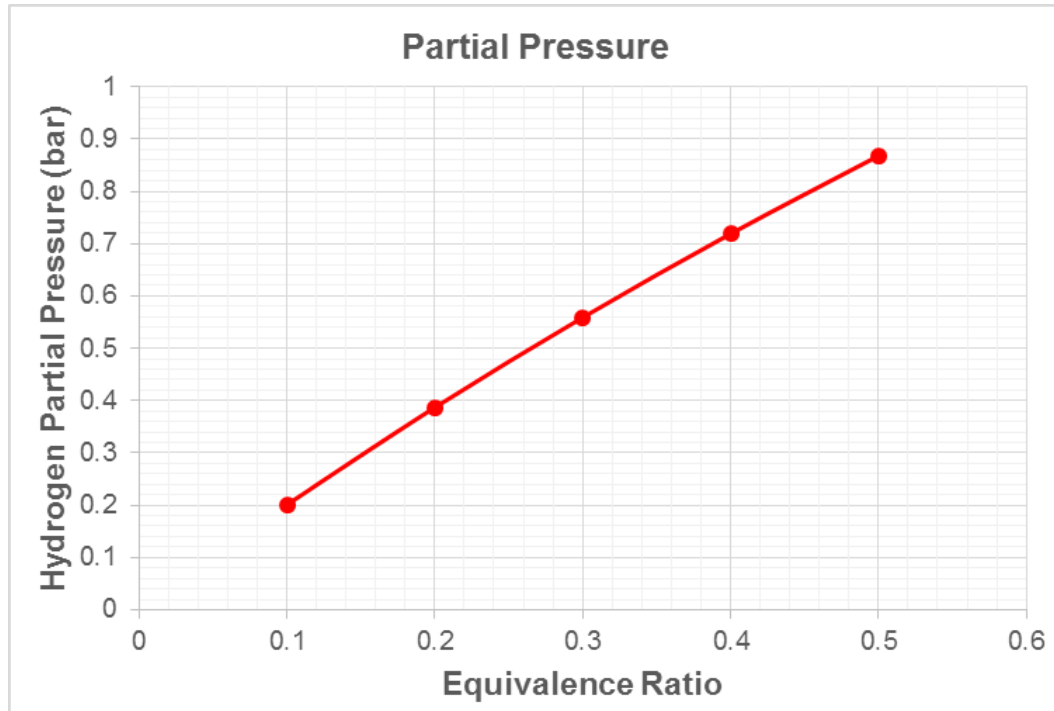


Figure 3.31: Result of partial pressure calculated from chemical equation

The result of partial pressure was shown in figure 3.31. But actually, hydrogen and air have another parameter that call compressibility factor ( $Z$ ) in the real gas equation.

$$PV = ZnRT \quad (5)$$

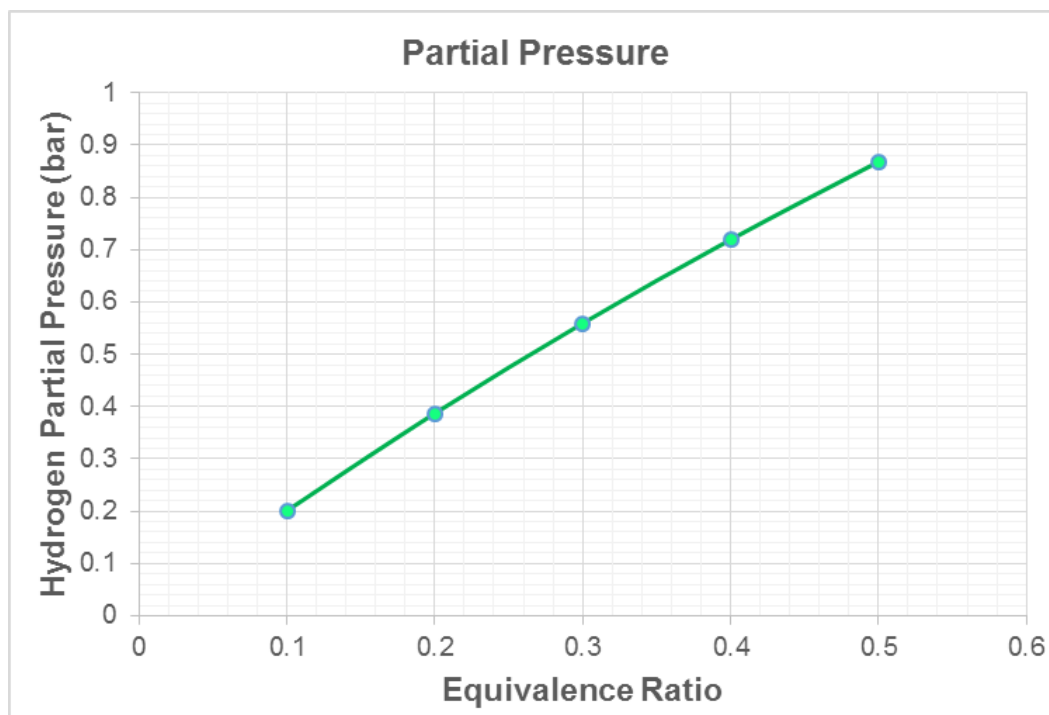


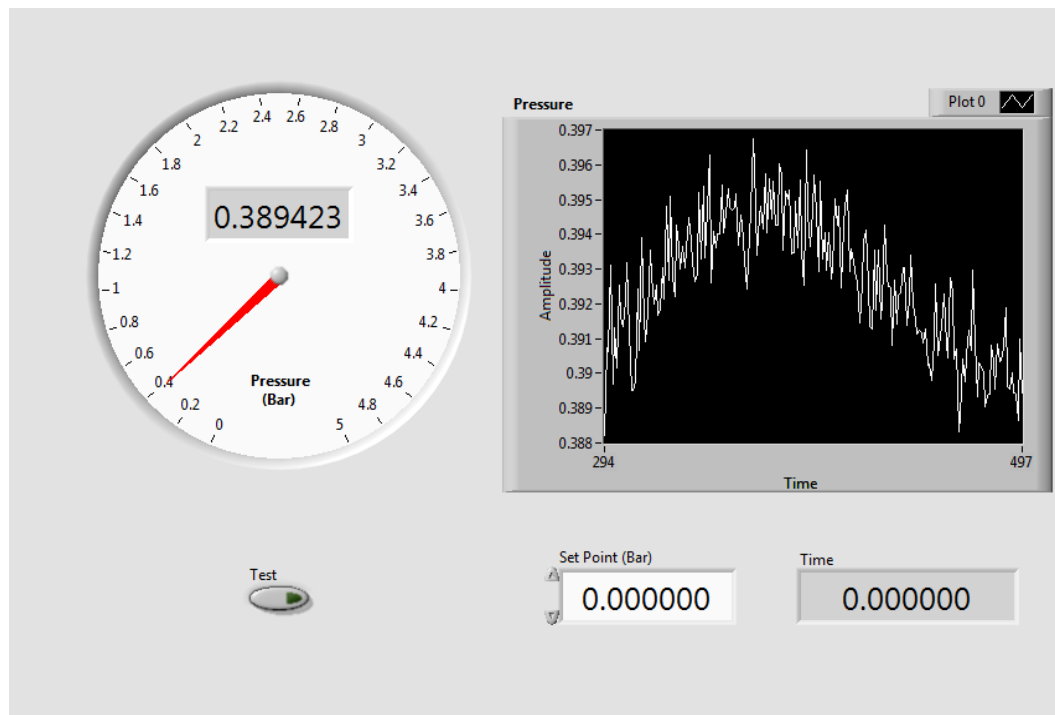
Figure 3.32: Exact result of hydrogen partial pressure

Table 4: Hydrogen partial pressure compared with equivalence ratio

Equivalence ratio	Partial pressure (bar)
0.1	0.20110
0.2	0.38720
0.3	0.55931
0.4	0.71941
0.5	0.86817

The exact result after calculated with real gas equation were shown in figure 3.32 and explained in detail in table 4.

For easier for testing in this experiment, equivalence ratio was investigated by controlled the injection duration. Thus, hydrogen partial pressure was calibrated into injection duration time by using computer program.



**Figure 3.33:** Calibration program for hydrogen injection duration

Figure 3.33 shows the computer program that was used to investigate injection duration. By input the target pressure that comes from calculation, program would opened the injection valve then counting duration time that hydrogen pressure rising reached to the target pressure.

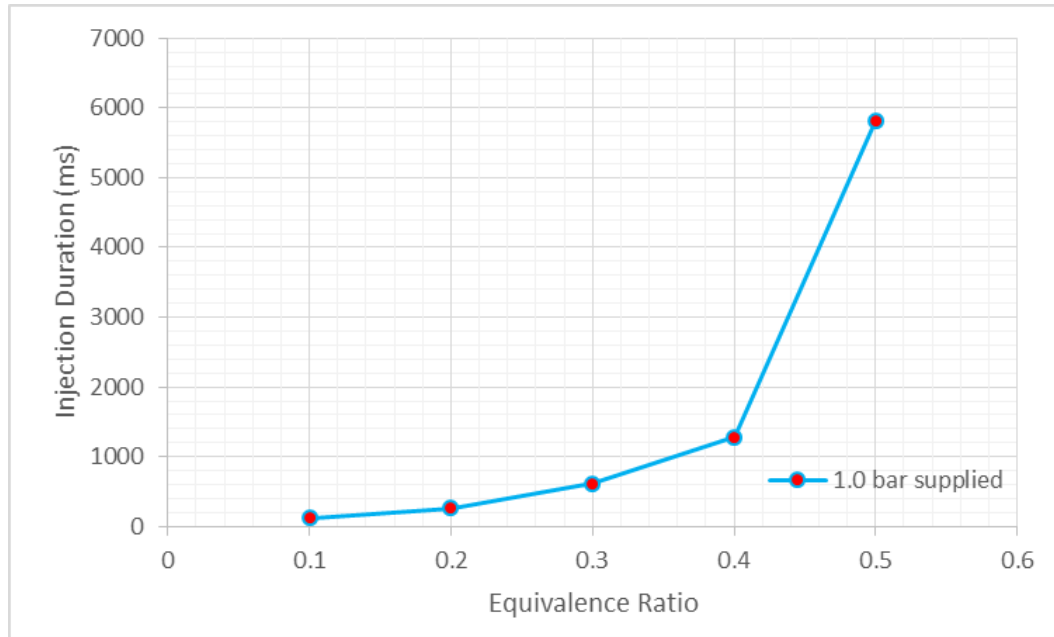


**Figure 3.34:** Injection duration result from calibration program

**Table 5:** Hydrogen injection duration compared with equivalence ratio

Equivalence ratio	Injection duration (msec)
0.1	118
0.2	266
0.3	612
0.4	1278
0.5	5814

Figure 3.34 and table 5 were shown the calibration result that came from computer program.

### 3.3.3 Timing sequence

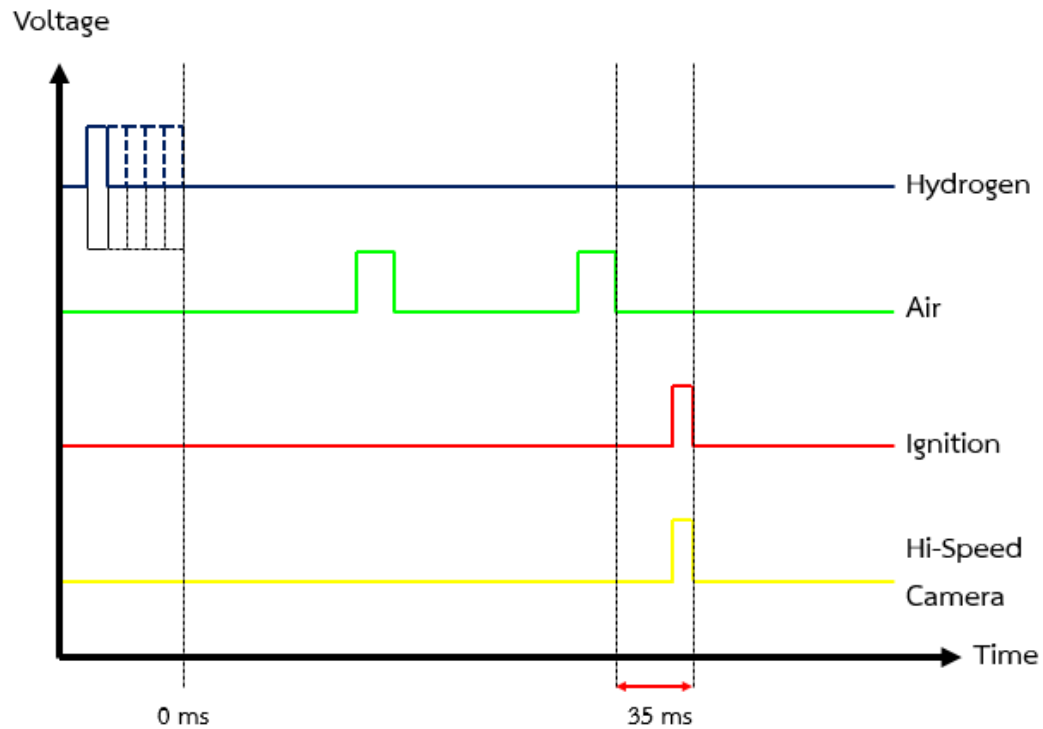
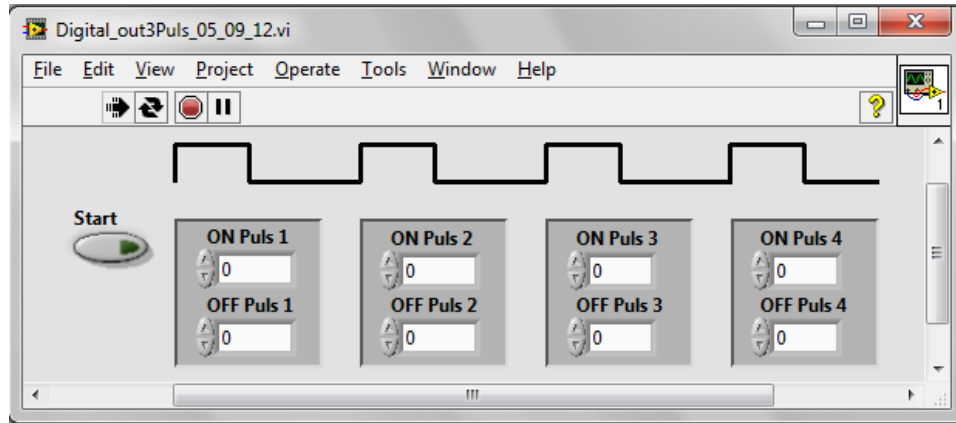


Figure 3.35: Experimentally sequential signal

All of sequential signal were controlled by computer program. Hydrogen was injected in the first stage then low pressure air was injected to make a pre-stage after that high pressure air at 5 bar was injected to make swirl intensity. From the swirl investigation, combustion should start at 35 msec after high pressure air injected but the ignition coil used charge time for 3 msec. so the ignition signal was commanded at 32 msec after the air-solenoid closed and also the signal for high speed video camera was commanded together.



**Figure 3.36:** Sequential signal controller program

The controller program was designed to control 4 channels and 5 stages (hydrogen, low pressure air, high pressure air, ignition coil and high speed video camera). The interval input was added to this program in every stage of testing sequent.

### 3.3.4 Lean burn limit investigation

The important thing of fuel-air combustion is stability and low consumption. Lean burn limit is leanest fuel-air mixture that can sustain the flame stability. This experiment was investigated the minimum equivalence ratio that can be ignited at certain pressure and temperature. Lean burn limit was defined by reaching the maximum acceptable the value of coefficient of variation on maximum combustion pressure. Figure 3.37 shows the definition of lean burn limit used in this study. The condition were collected the lean burn limit and maximum result of CoV at 20% of maximum combustion pressure.

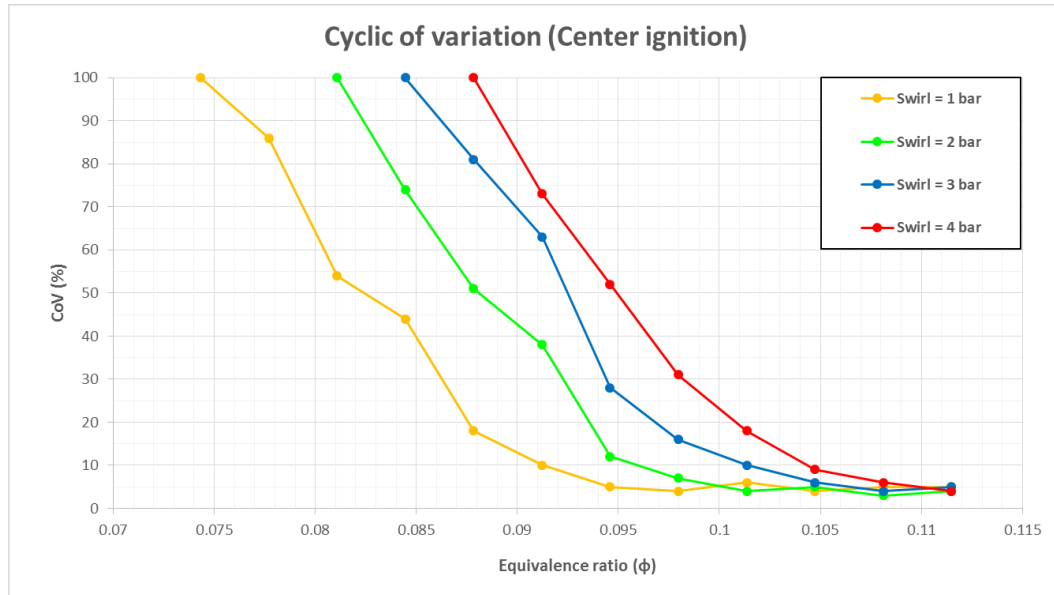


Figure 3.37: Example data of lean burn limit

### 3.3.5 Mass fraction burn rate and combustion duration

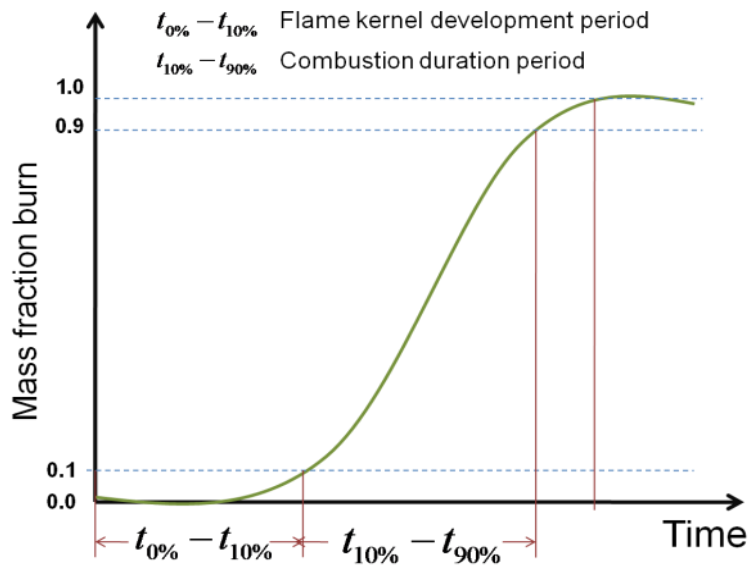


Figure 3.38: Combustion duration was defined from 10% to 90% of mass fraction burnt

Mass fraction burn rate was calculated from real combustion pressure compared with maximum combustion pressure as shown in equation 6

$$M_f(t) = \frac{P(t) - P_i}{P_{max} - P_i} \quad (6)$$

Where  $P(t)$  is the combustion pressure at interested time,  $P_i$  is the initial pressure and  $P_{max}$  is the maximum combustion pressure.

### 3.3.6 Combustion delay

In this experiment, combustion delay is one of the main result that was investigated. To find that which parameters was effected to the speed of start of combustion, the result of mass fraction burn rate in the figure 3.38 also used to define from start of ignition to 10% of combustion pressure [10].



## 4.2 Effect of equivalence ratio

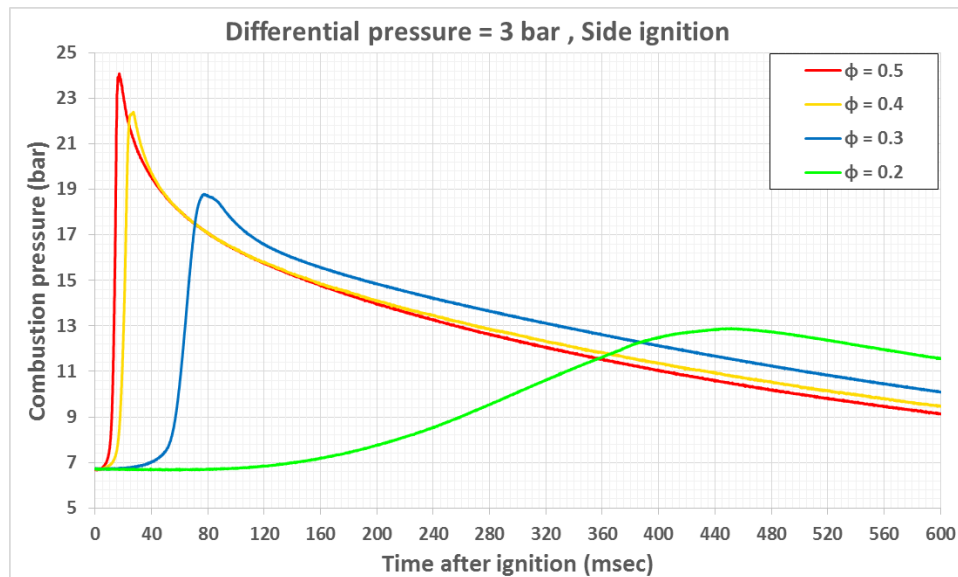
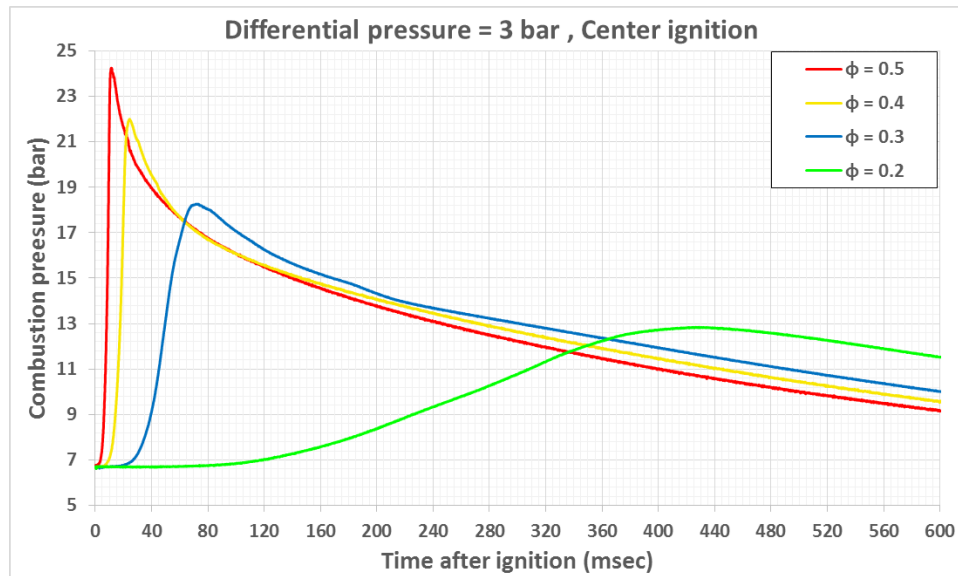


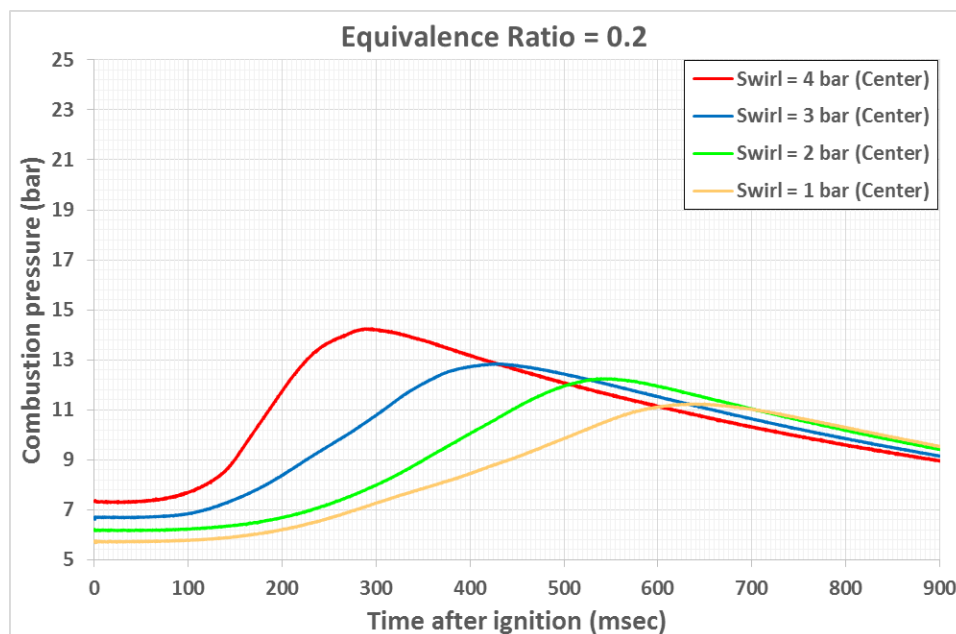
**Figure 4.2:** Effect of equivalence ratio (a) center ignition and (b) sidewall ignition

Equivalence ratio is the ratio between actual air/hydrogen ratio divided by stoichiometric air/hydrogen ratio. If increase equivalence ratio, amount of hydrogen will be increase. Thus when increasing the equivalence ratio means increasing input energy. The results as shown in figure 4.2 (a) and (b) show the conditions of fixed 3 bar of swirl intensity, varied equivalence ratio and changed the position of spark plug. Maximum combustion pressure increased and combustion delay decreased while increasing equivalence ratio.

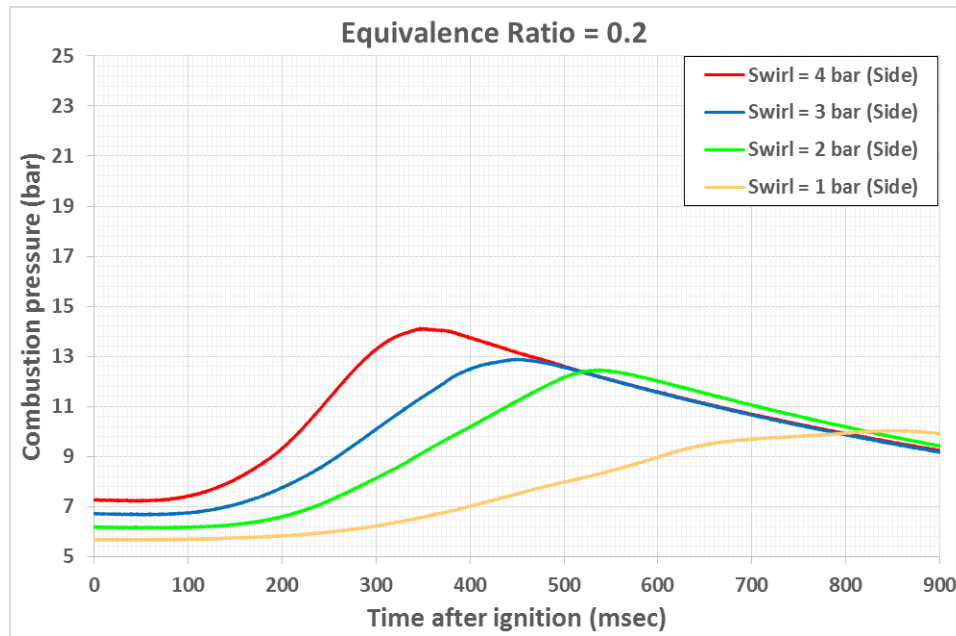
### 4.3 Effect of swirl intensity on combustion pressure

The definition of swirl intensity in this experiment was mentioned in the previous chapter. Differential pressure was investigated to define the intensity of swirl as tangential velocity. For variation of swirl intensity, differential intake pressure were varied from 1 bar to 4 bar while results of tangential velocity were 5.73, 6.50, 7.54 and 8.10 m/s respectively.

#### 4.3.1 Equivalence ratio = 0.2



(a)

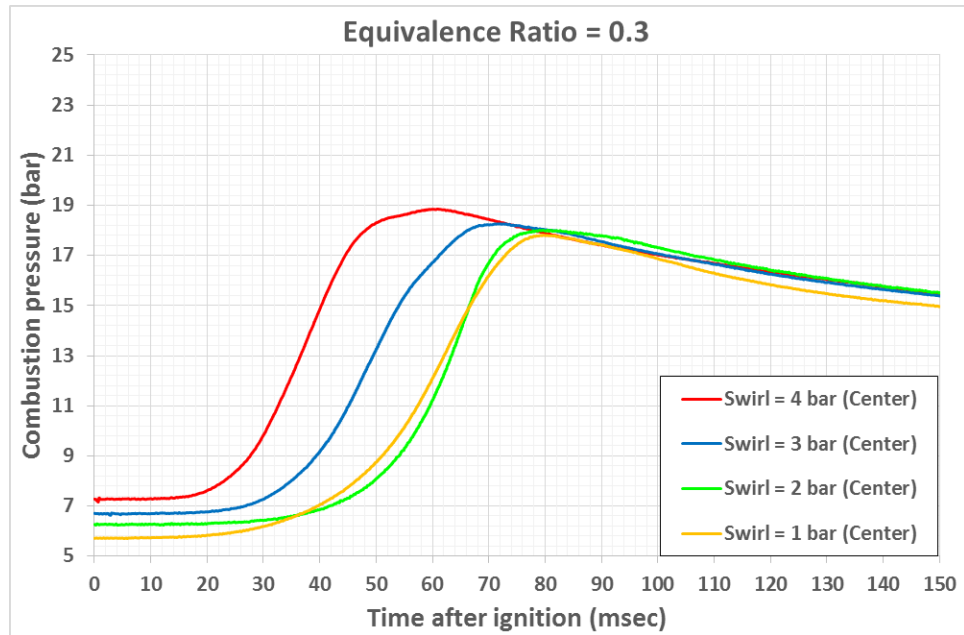


(b)

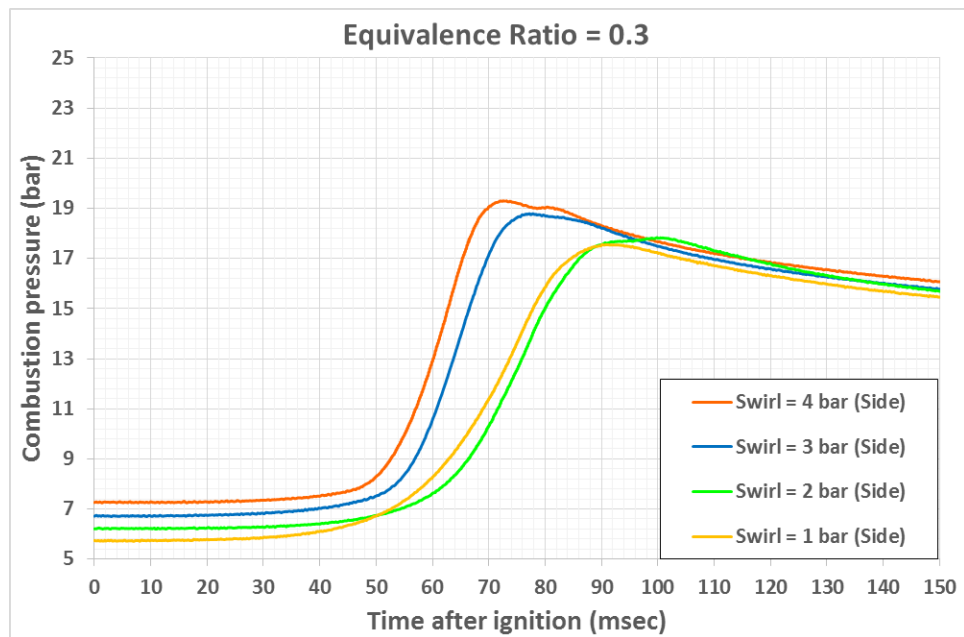
**Figure 4.3:** Effect of swirl intensity on equivalence ratio = 0.2 (a) center ignition and (b) sidewall ignition

Figure 4.3 show the combustion pressure of hydrogen (a) center ignition and (b) sidewall ignition in the conditions of equivalence ratio equal to 0.2 and varied swirl intensity from differential pressure equal to 1 bar to 4 bar. The results explained that at the same equivalence ratio but increased swirl intensity, the maximum combustion pressure were increased and the combustion delay were decreased. In the case of center ignition, the maximum combustion pressure were 11.33, 12.25, 12.84 and 14.25 bar while the maximum combustion pressure of sidewall ignition were 10.05, 12.46, 12.89 and 14.12 bar during the variation of swirl intensity of 1, 2, 3 and 4 bar respectively.

## 4.3.2 Equivalence ratio = 0.3



(a)

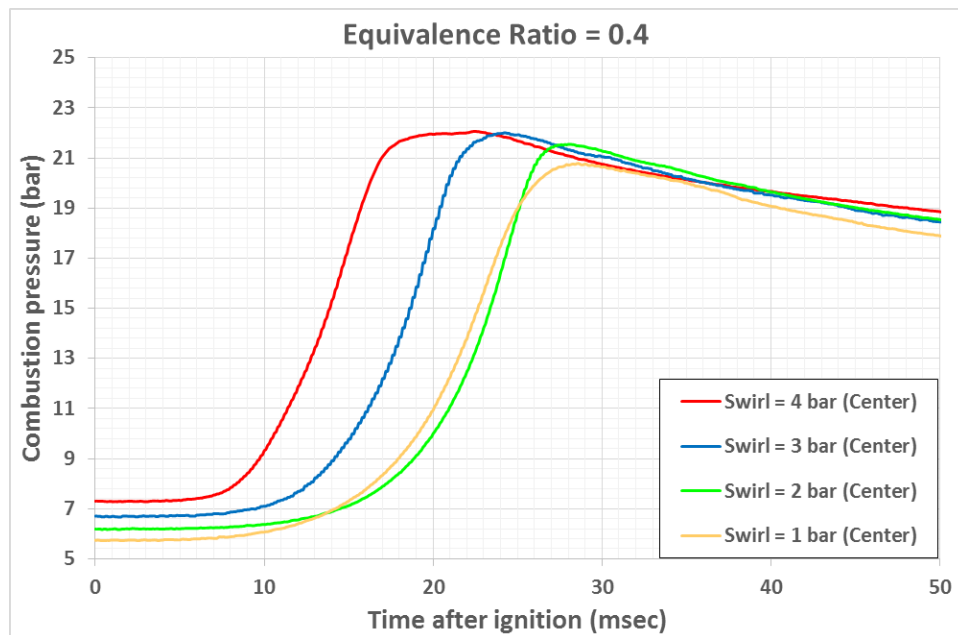


(b)

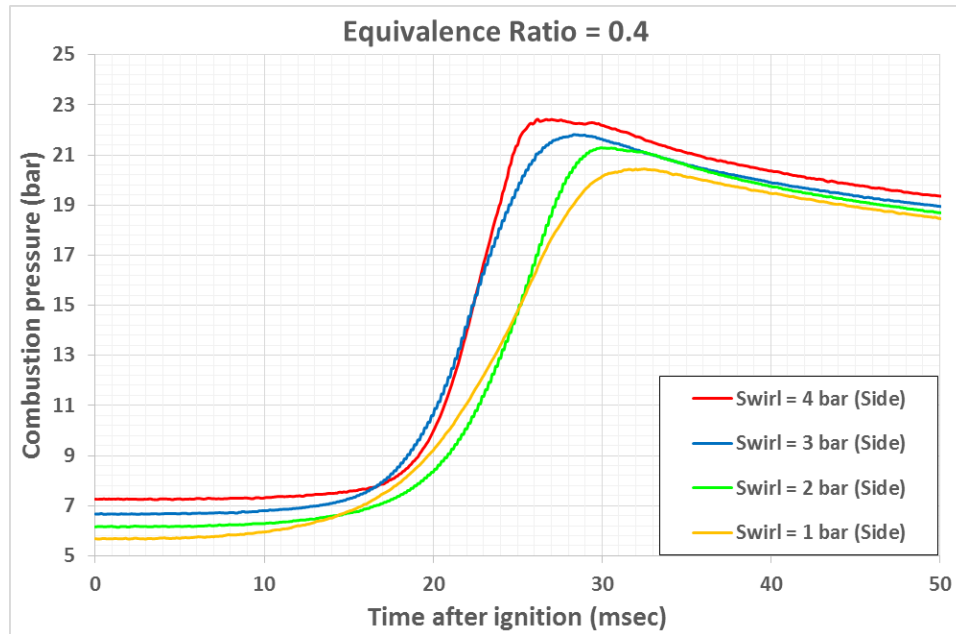
**Figure 4.4:** Effect of swirl intensity on equivalence ratio = 0.3 (a) center ignition and (b) sidewall ignition

Figure 4.4 show the combustion pressure of hydrogen (a) center ignition and (b) sidewall ignition in the conditions of equivalence ratio equal to 0.3 and varied swirl intensity from differential pressure equal to 1 bar to 4 bar. The results explained that at the same equivalence ratio but increased swirl intensity, the maximum combustion pressure were increased and the combustion delay were decreased. In the case of center ignition, the maximum combustion pressure were 17.92, 18.01, 18.26 and 18.85 bar while the maximum combustion pressure of sidewall ignition were 17.55, 17.83, 18.79 and 19.30 bar during the variation of swirl intensity of 1, 2, 3 and 4 bar respectively.

#### 4.3.3 Equivalence ratio = 0.4



(a)



(b)

**Figure 4.5:** Effect of swirl intensity on equivalence ratio = 0.4 (a) center ignition and (b) sidewall ignition

Figure 4.5 show the combustion pressure of hydrogen (a) center ignition and (b) sidewall ignition in the conditions of equivalence ratio equal to 0.4 and varied swirl intensity from differential pressure equal to 1 bar to 4 bar. The results explained that at the same equivalence ratio but increased swirl intensity, the maximum combustion pressure were increased and the combustion delay were decreased. In the case of center ignition, the maximum combustion pressure were 20.78, 21.54, 22.00 and 22.07 bar while the maximum combustion pressure of sidewall ignition were 20.44, 21.28, 21.81 and 22.42 bar during the variation of swirl intensity of 1, 2, 3 and 4 bar respectively.

## 4.3.3 Equivalence ratio = 0.5

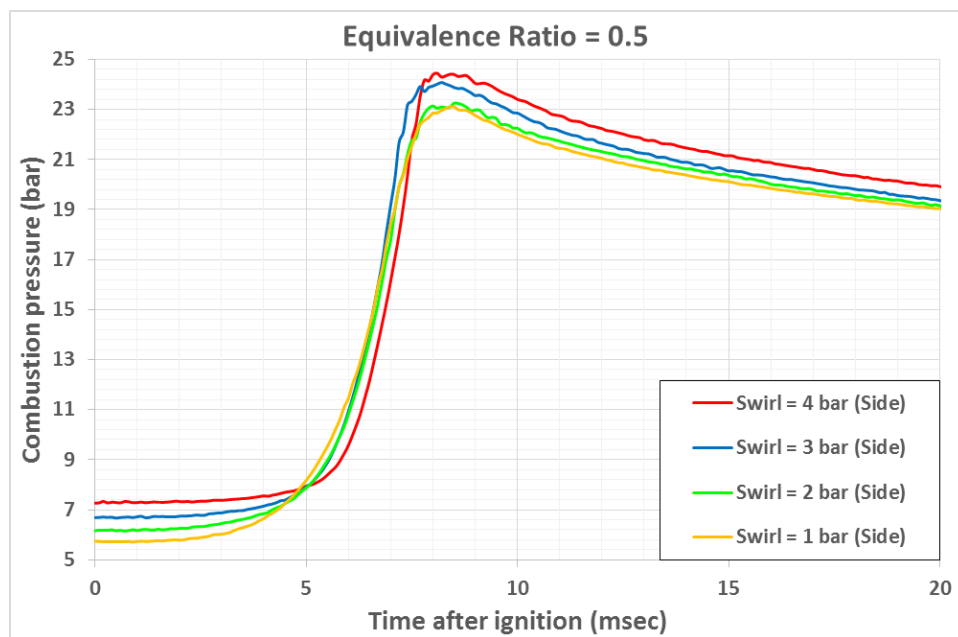
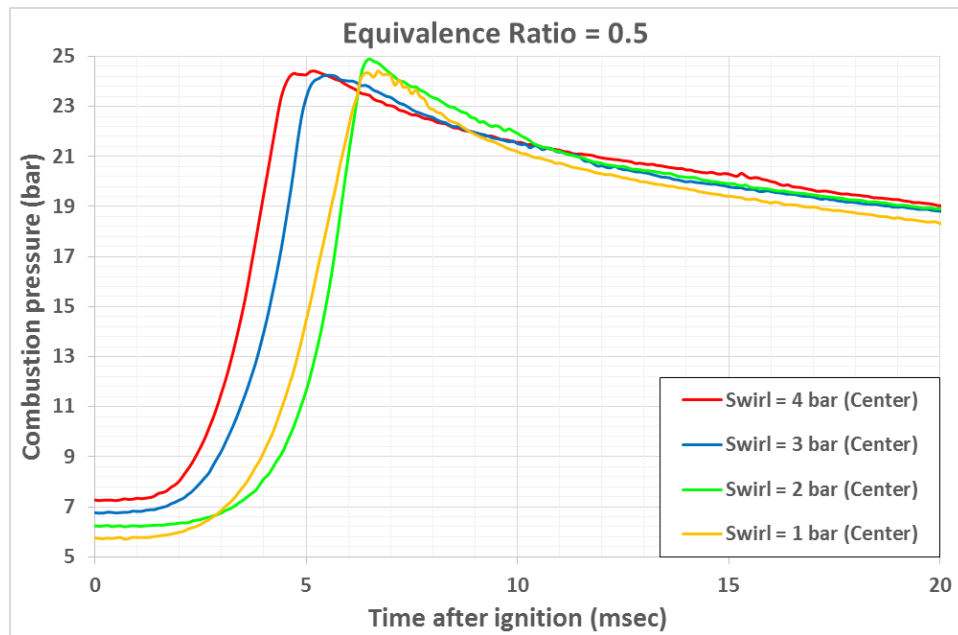


**Figure 4.6:** Effect of swirl intensity on equivalence ratio = 0.5 (a) center ignition and (b) sidewall ignition

Figure 4.6 show the combustion pressure of hydrogen (a) center ignition and (b) sidewall ignition in the conditions of equivalence ratio equal to 0.5 and varied swirl intensity from differential pressure equal to 1 bar to 4 bar. The results explained that at the same equivalence ratio but increased swirl intensity, the maximum combustion pressure were increased and the combustion delay were decreased. In the case of center ignition, the maximum combustion pressure were 24.42, 24.89, 24.25 and 24.41 bar while the maximum combustion pressure of sidewall ignition were 23.11, 23.25, 24.08 and 24.45 bar during the variation of swirl intensity of 1, 2, 3 and 4 bar respectively.

#### 4.4 Effect of swirl intensity on mass fraction burn rate

Mass fraction burn rate can explain in easy knowledge that it is rate of pressure rise from start of ignition to the maximum combustion pressure. If the mass fraction burn rate become faster, combustion efficiency and performance will be increased.

##### 4.4.1 Equivalence ratio = 0.2

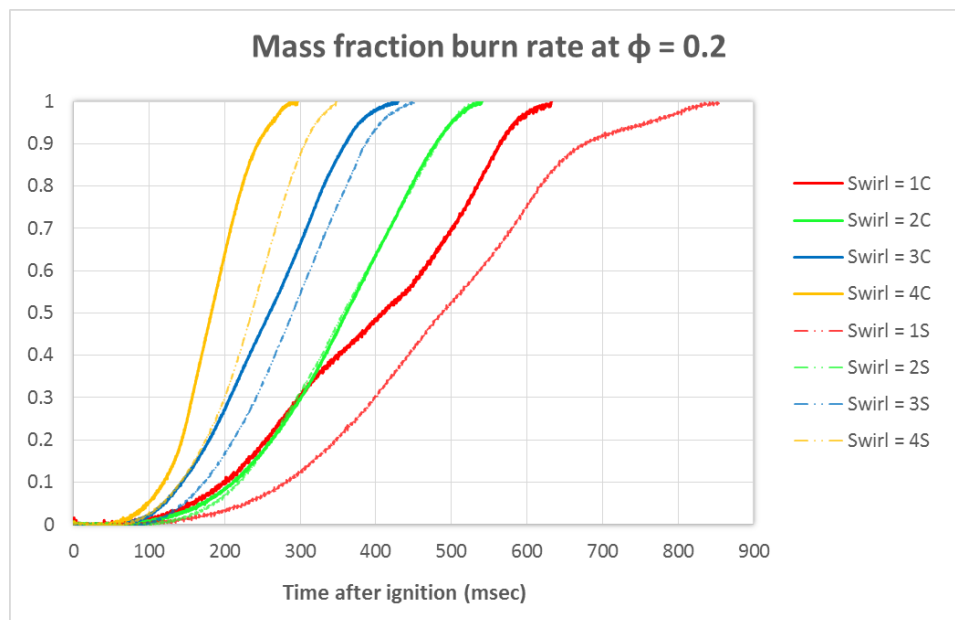
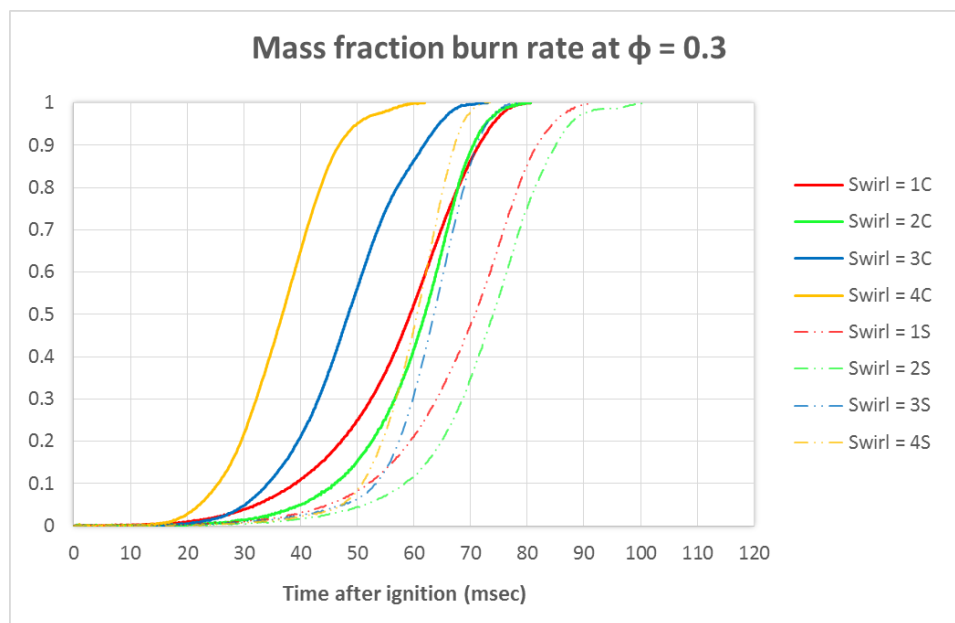


Figure 4.7: Mass fraction burn rate of hydrogen combustion with equivalence ratio = 0.2

The results of mass fraction burn rate was shown in figure 4.7. This conditions were tested with equivalence ratio equal to 0.2 and the various parameters were swirl intensity and position of spark plug.

The results show that when increased swirl intensity, mass fraction burn rate increased. But when change the position of spark plug from center ignition to sidewall ignition, mass fraction burn a little bit decreased. The results in condition of center ignition were 632, 540, 429 and 296 msec while sidewall were 854, 537, 452 and 347 msec by varied swirl intensity from 1 bar to 4 bar respectively.

#### 4.4.2 Equivalence ratio = 0.3



**Figure 4.8:** Mass fraction burn rate of hydrogen combustion with equivalence ration = 0.3

The results of mass fraction burn rate was shown in figure 4.8. This conditions were tested with equivalence ratio equal to 0.3 and the various parameters were swirl intensity and position of spark plug.

The results show that when increased swirl intensity, mass fraction burn rate increased. But when change the position of spark plug from center ignition to sidewall ignition, mass fraction burn a little bit decreased. The results in condition of center ignition were 81, 79, 72 and 61 msec while sidewall were 91, 99, 77 and 73 msec by varied swirl intensity from 1 bar to 4 bar respectively.

#### 4.4.3 Equivalence ratio = 0.4

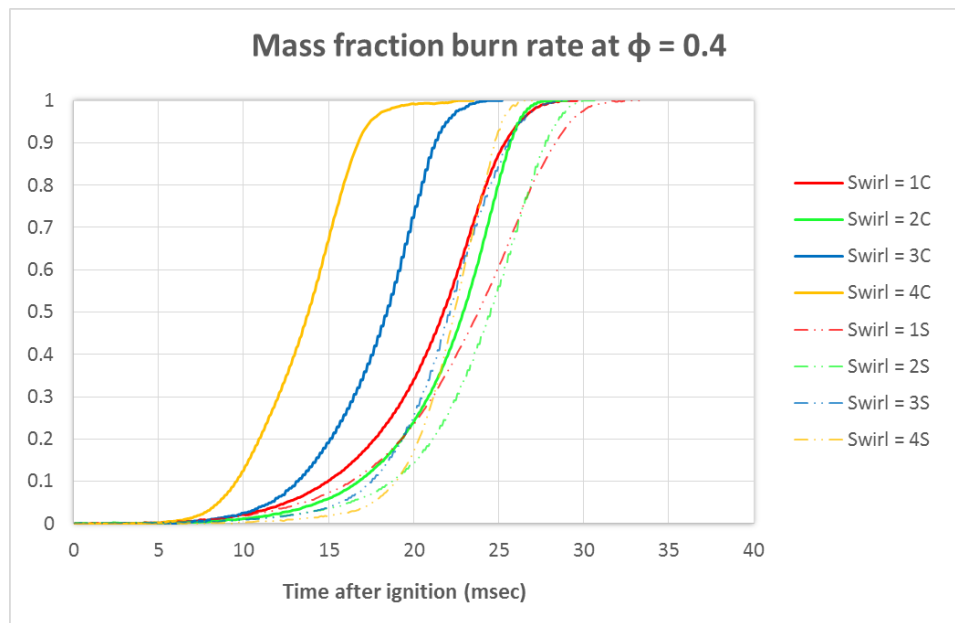


**Figure 4.9:** Mass fraction burn rate of hydrogen combustion with equivalence ration = 0.4

The results of mass fraction burn rate was shown in figure 4.9. This conditions were tested with equivalence ratio equal to 0.4 and the various parameters were swirl intensity and position of spark plug.

The results show that when increased swirl intensity, mass fraction burn rate a little bit increased. But when change the position of spark plug from center ignition to sidewall ignition, mass fraction burn a little bit decreased. The results in condition of center ignition

were 29, 28, 24 and 22 msec while sidewall were 33, 30, 28 and 26 msec by varied swirl intensity from 1 bar to 4 bar respectively.

#### 4.4.4 Equivalence ratio = 0.5

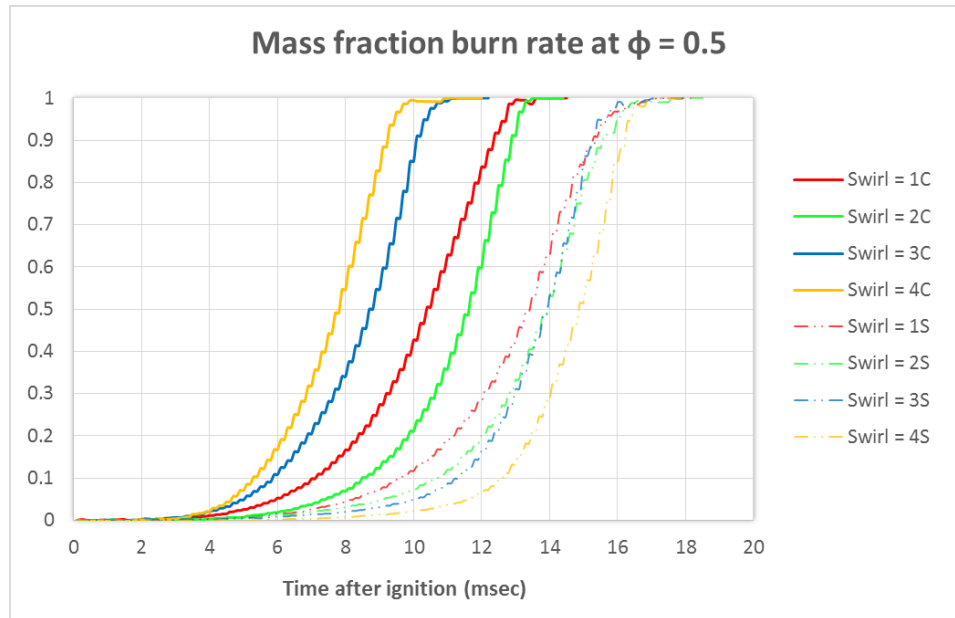
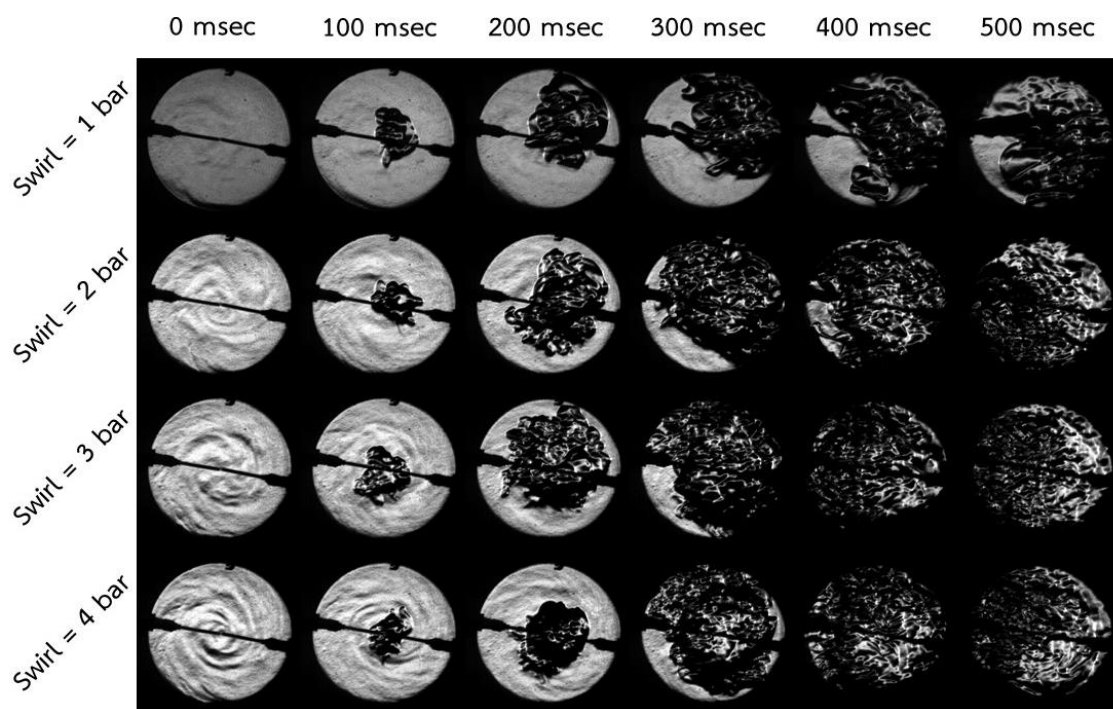


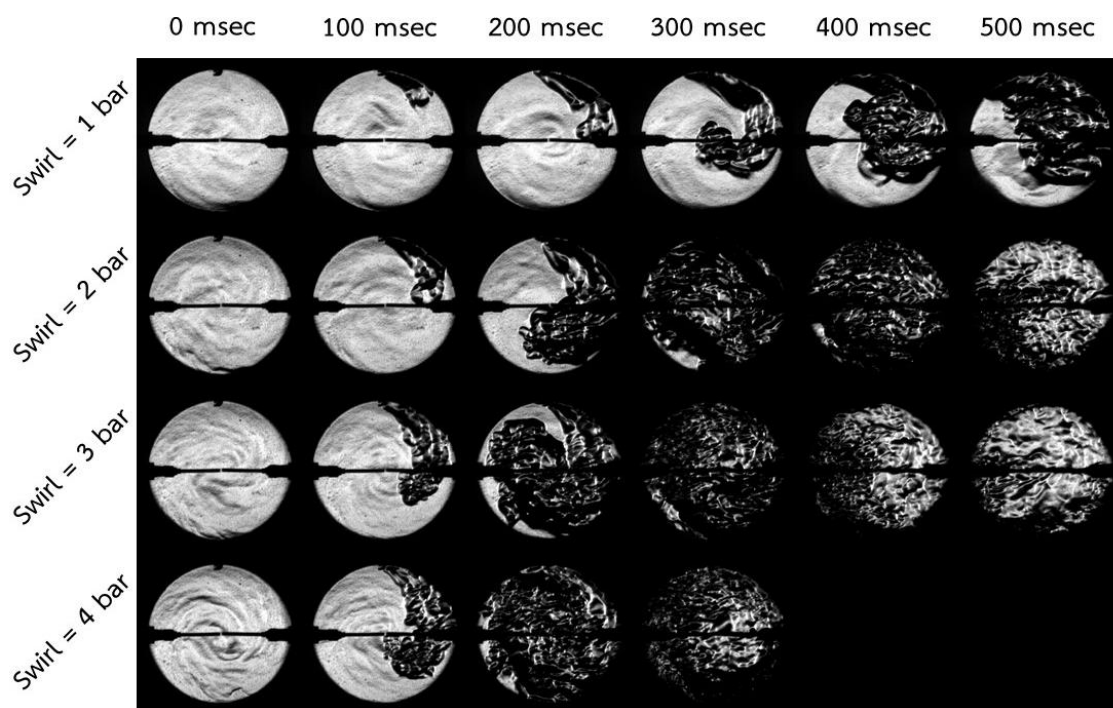
**Figure 4.10:** Mass fraction burn rate of hydrogen combustion with equivalence ratio = 0.5

The results of mass fraction burn rate was shown in figure 4.10. This conditions were tested with equivalence ratio equal to 0.5 and the various parameters were swirl intensity and position of spark plug.

The results show that when increased swirl intensity, mass fraction burn rate not be significant increased. But when change the position of spark plug from center ignition to sidewall ignition, mass fraction burn a little bit decreased. The results in condition of center ignition were 14, 13, 11 and 11 msec while sidewall were 17, 17, 17 and 17 msec by varied swirl intensity from 1 bar to 4 bar respectively.



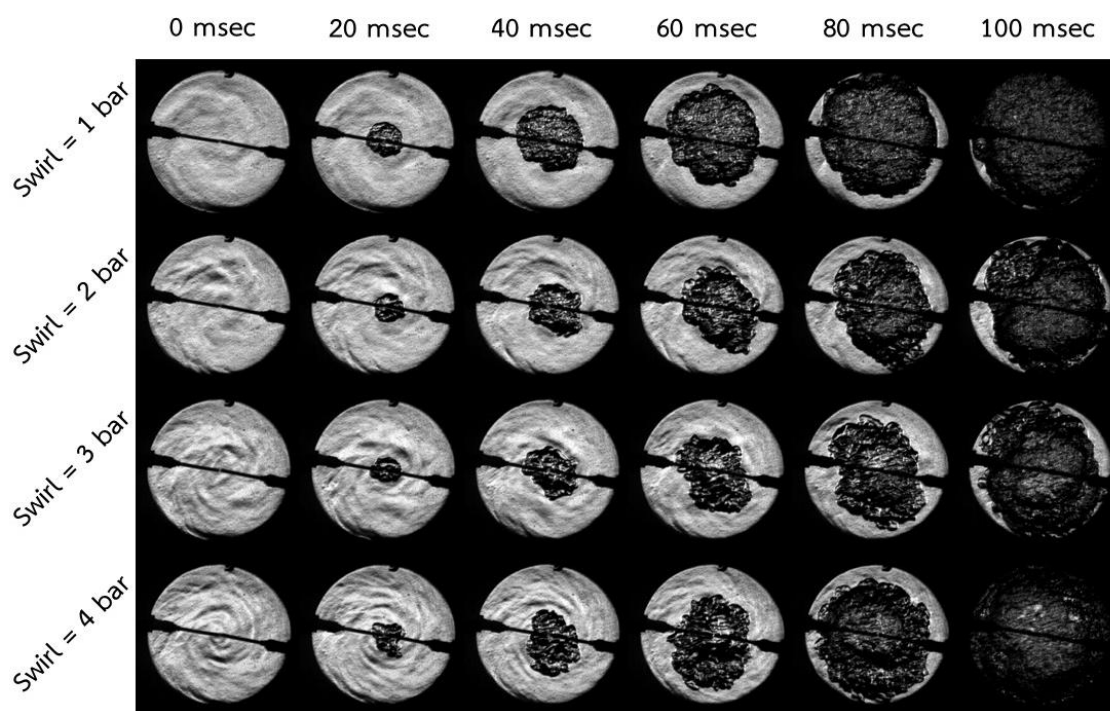
(a)



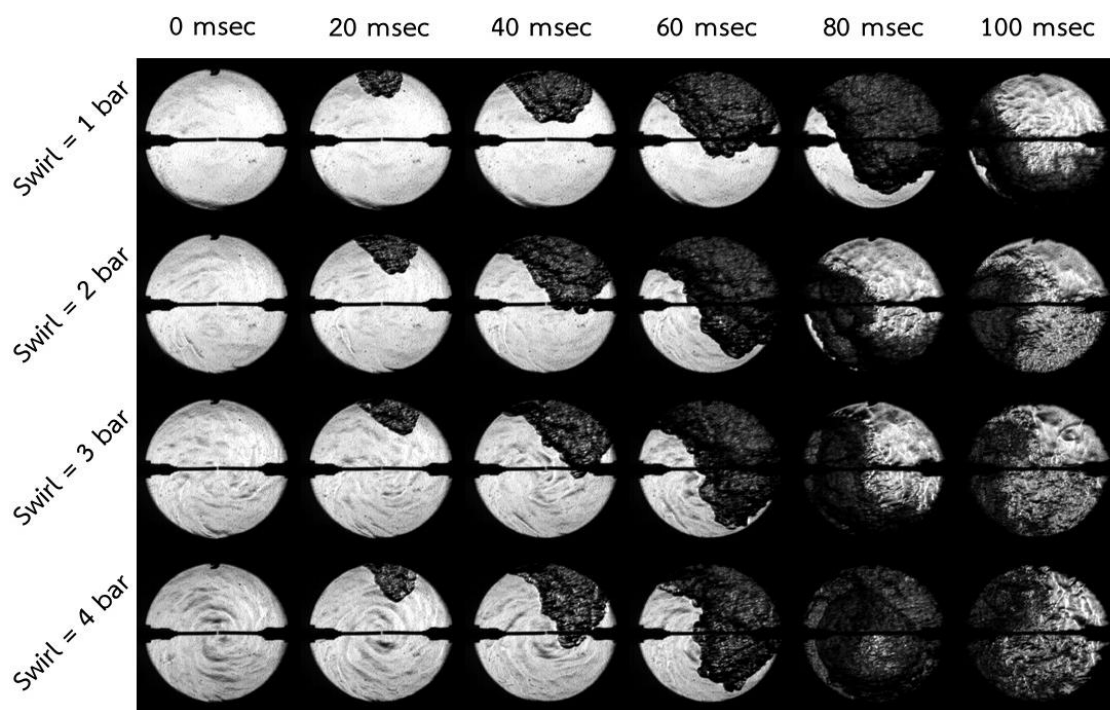
(b)

Figure 4.11: The comparison of flame propagation in conditions of equivalence ratio = 0.2

(a) center ignition and (b) sidewall ignition

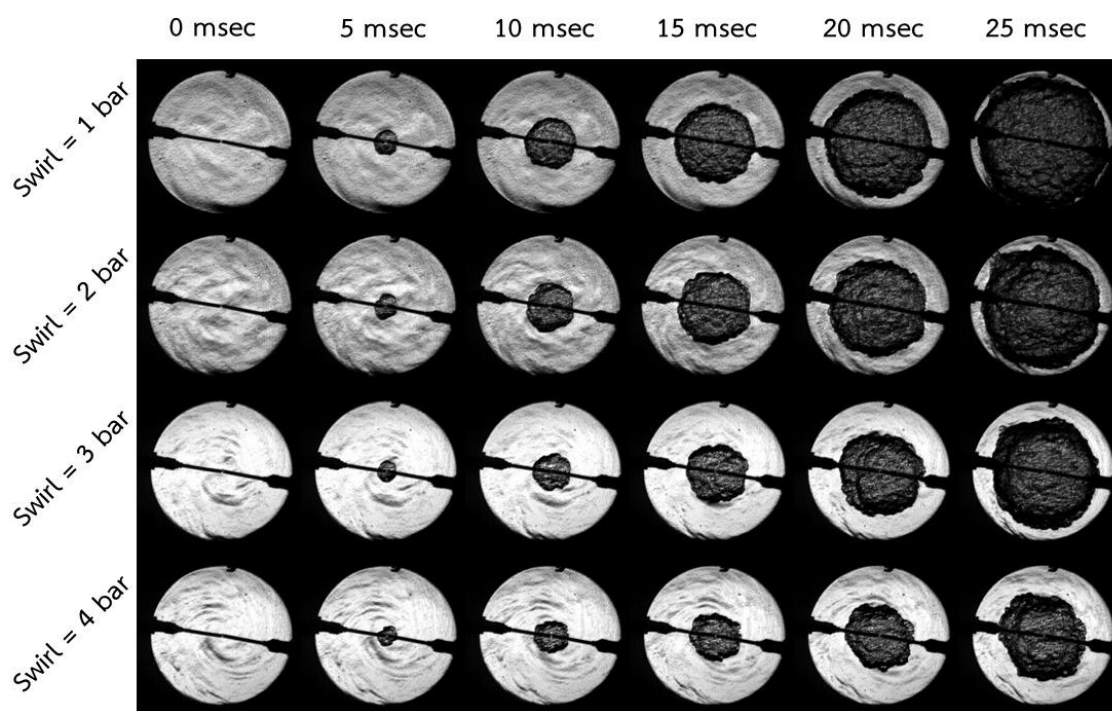


(a)

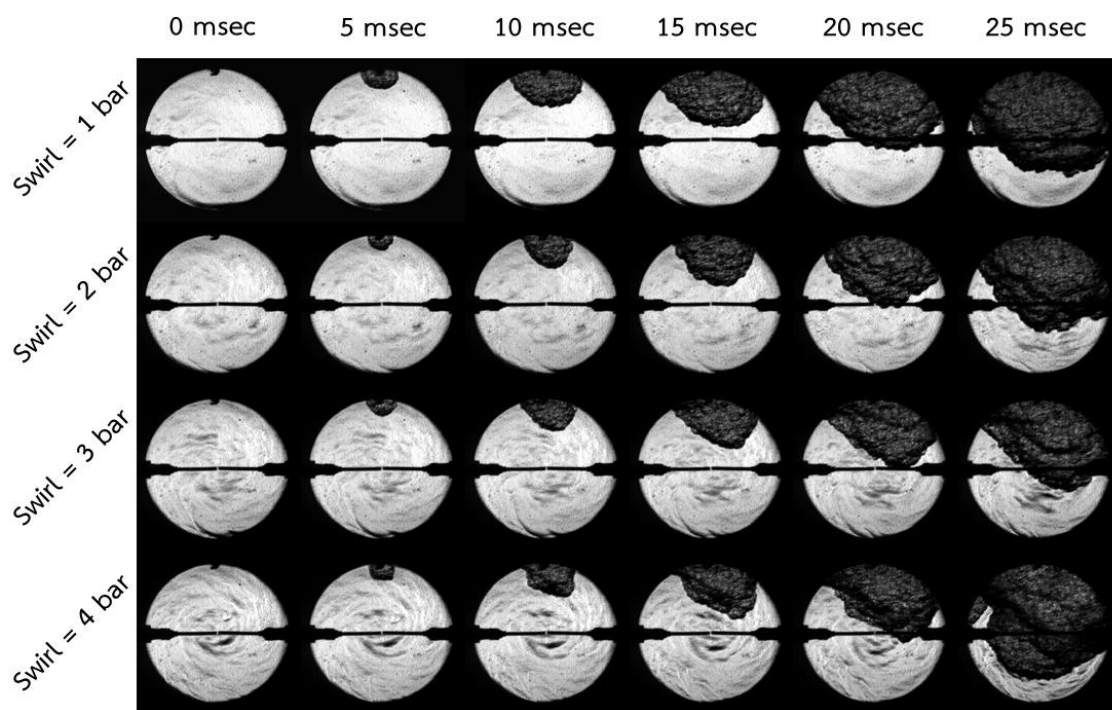


(b)

Figure 4.12: The comparison of flame propagation in conditions of equivalence ratio = 0.3  
(a) center ignition and (b) sidewall ignition



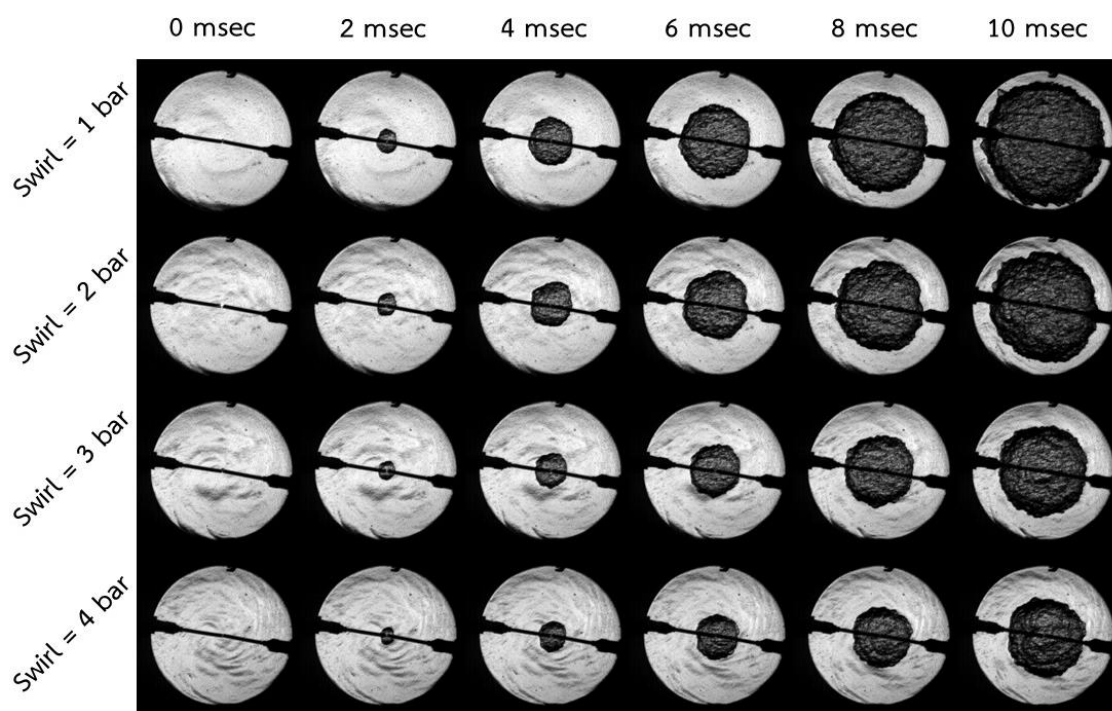
(a)



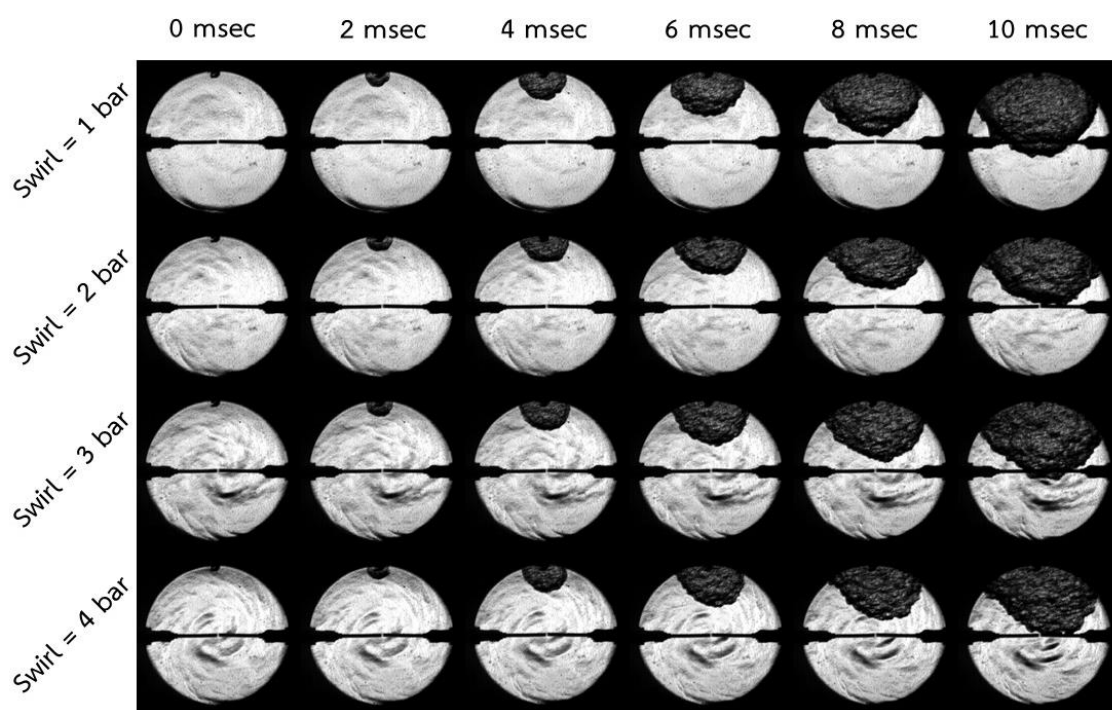
(b)

Figure 4.13: The comparison of flame propagation in conditions of equivalence ratio = 0.4

(a) center ignition and (b) sidewall ignition



(a)

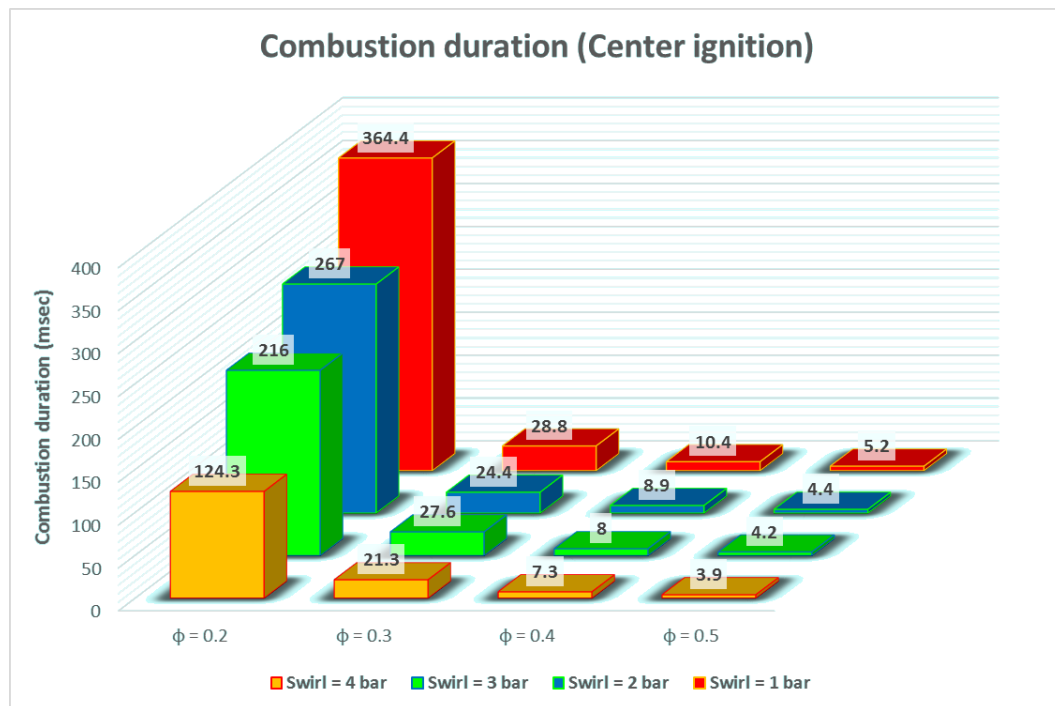


(b)

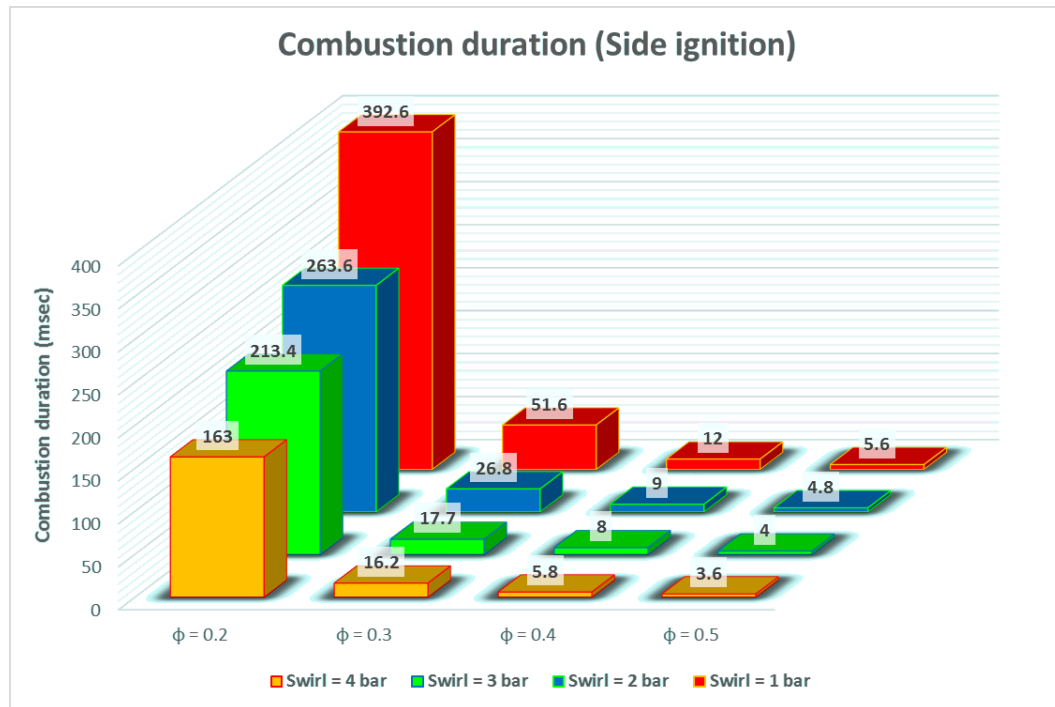
Figure 4.14: The comparison of flame propagation in conditions of equivalence ratio = 0.5  
(a) center ignition and (b) sidewall ignition

#### 4.5 Effect of swirl intensity on combustion duration

From quantitative analysis, combustion duration may be taken into account by using mass fraction burn rate data. From the mass fraction burned, flame development period and combustion duration are defined as the duration period of 10% and 90 % mass fraction burned respectively.



(a)



(b)

**Figure 4.15:** The results of combustion duration with variation of equivalence ratio, swirl intensity and (a) center ignition and (b) sidewall ignition

Figure 4.15 show the results of combustion duration of hydrogen in condition of equivalence ratio, swirl intensity and position of spark plug variation. The trend of graph can show that when increase the swirl intensity, it can be reduced the combustion duration in all of equivalence ratio variation. Especially in lean conditions, swirl intensity has more effected to improve combustion efficiency.

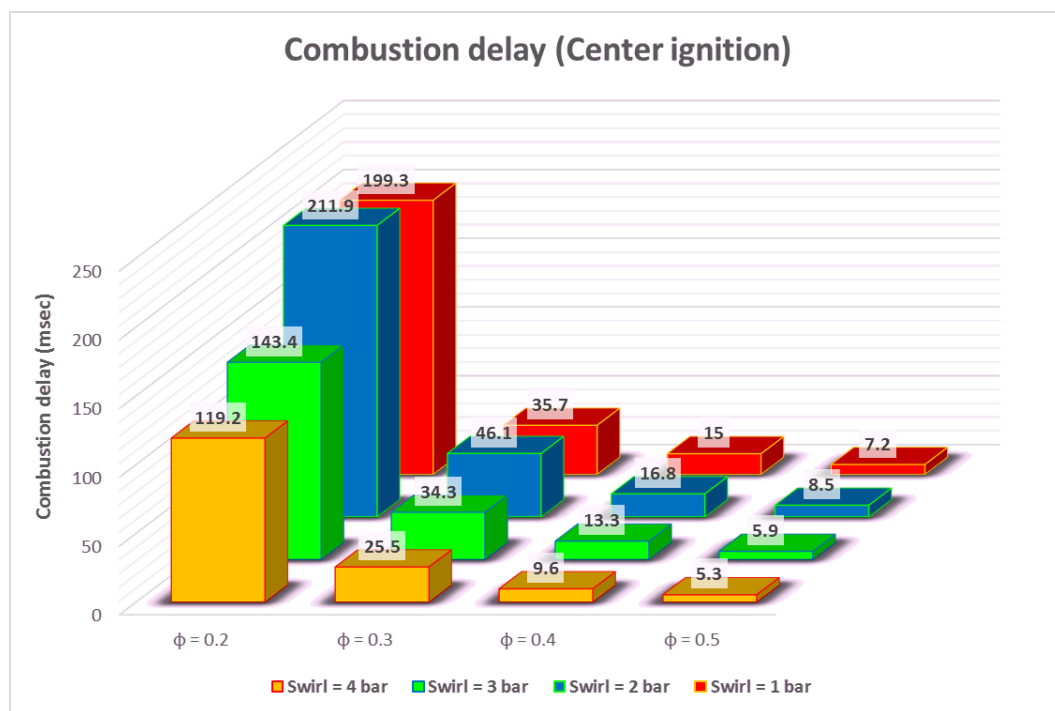
For center ignition, the most effect occurs in lean burn condition at 0.2 of equivalence ratio. When increasing swirl intensity, combustion duration was decreased up to 65.89% that from 364.4 msec to 124.3 msec. For sidewall ignition, the most effect also occurs in lean burn condition at 0.2 of equivalence ratio. The result of reduction of combustion duration was up to 58.48% that from 392.6 msec to 163 msec.

The reason of swirl intensity that caused to combustion duration is the mixture formation. In low speed of air velocity, the mixture of hydrogen-air cannot be a homogeneous

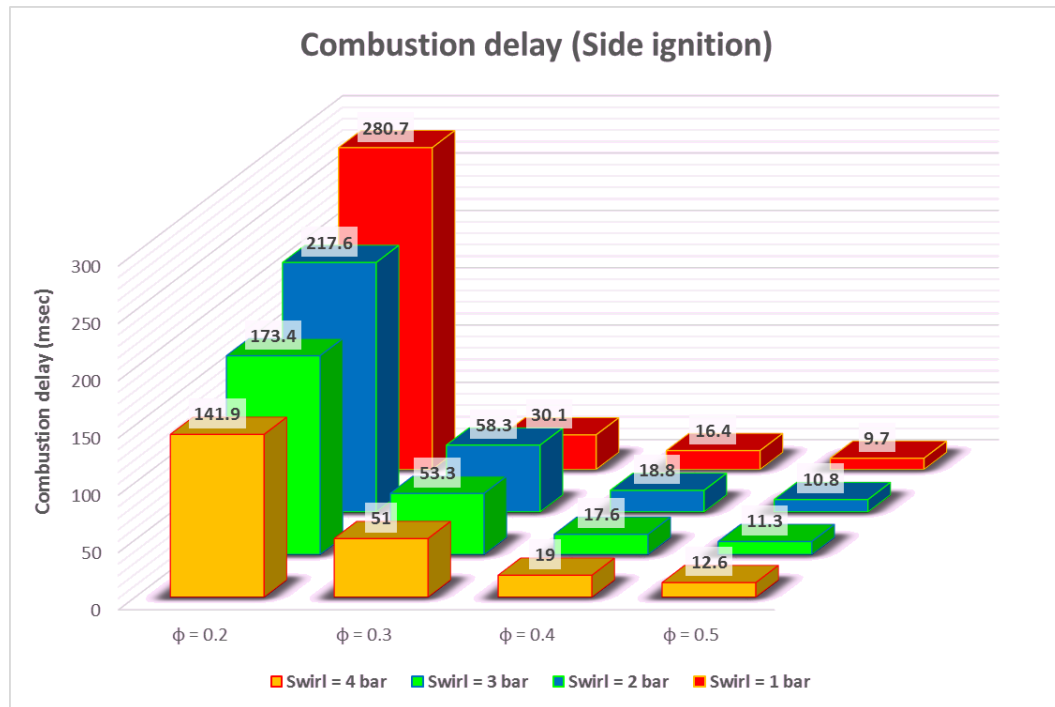
so rich-lean layer can be appears inside CVCC. Thus the combustion efficiency was lower than high speed of air velocity that increasing chance to interact between hydrogen and air.

#### 4.6 Effect of swirl intensity on combustion delay

Combustion delay means the responsibility or activated time after spark plug was sparked. In this study, combustion delay was measured from start of ignition to 10% of mass fraction burn rate.



(a)



(b)

**Figure 4.16:** The results of combustion delay with variation of equivalence ratio, swirl intensity and (a) center ignition and (b) sidewall ignition

Figure 4.16 show the results of combustion Delay of hydrogen in condition of equivalence ratio, swirl intensity and position of spark plug variation. Almost results of combustion delay did not change much while varied the swirl intensity except in lean burn conditions.

The important results were presented in lean condition at 0.2 of equivalence ratio with ignition position both center ignition and sidewall ignition as well. In center ignition conditions, the combustion delay was decreased of 43.75% that from 211.9 msec to 119.2 msec. And also, the results of sidewall ignition was decreased of 49.45% that from 280.7 msec to 141.9 msec.

The possibility to be ignite faster is the interaction chance between fuel and oxygen in air. When increase swirl intensity means increase the opportunity of reaction of hydrogen

to be burnt. Whereas in middle and high of equivalence ratio, the density of hydrogen is much enough. Therefore, the delay time of start of ignition just was a little bit difference.

#### 4.7 Effect of swirl intensity on lean burn limit

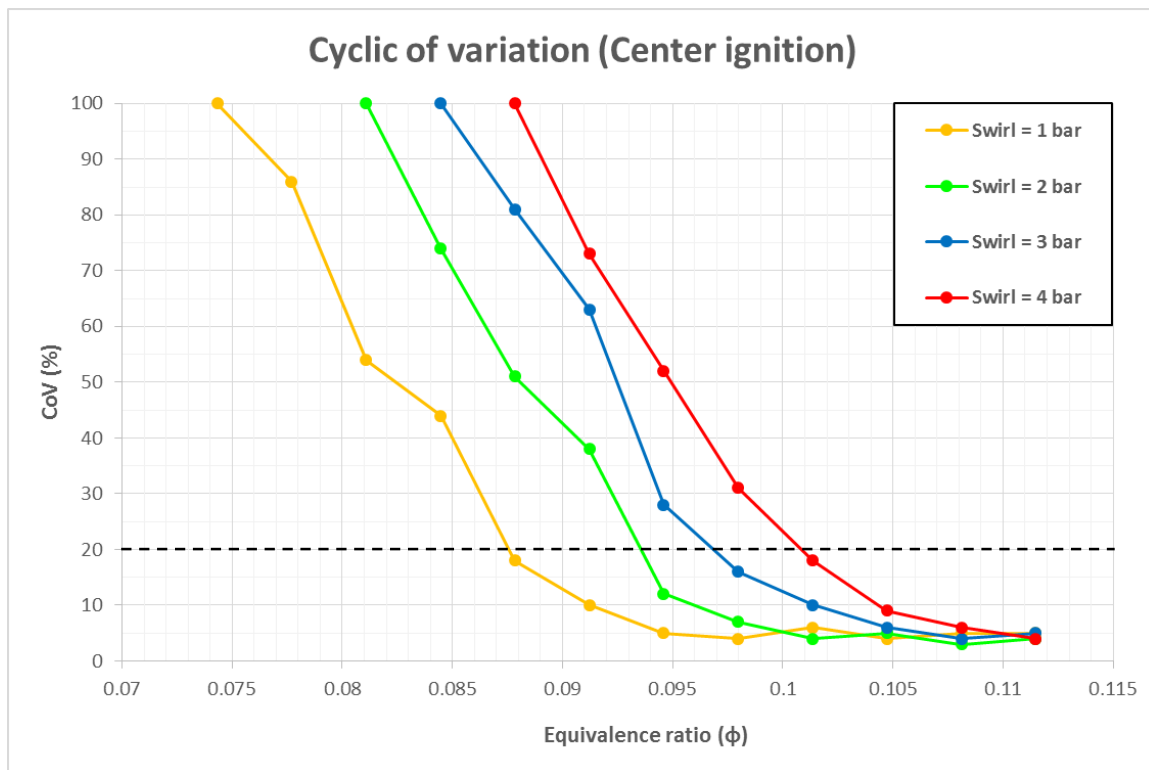
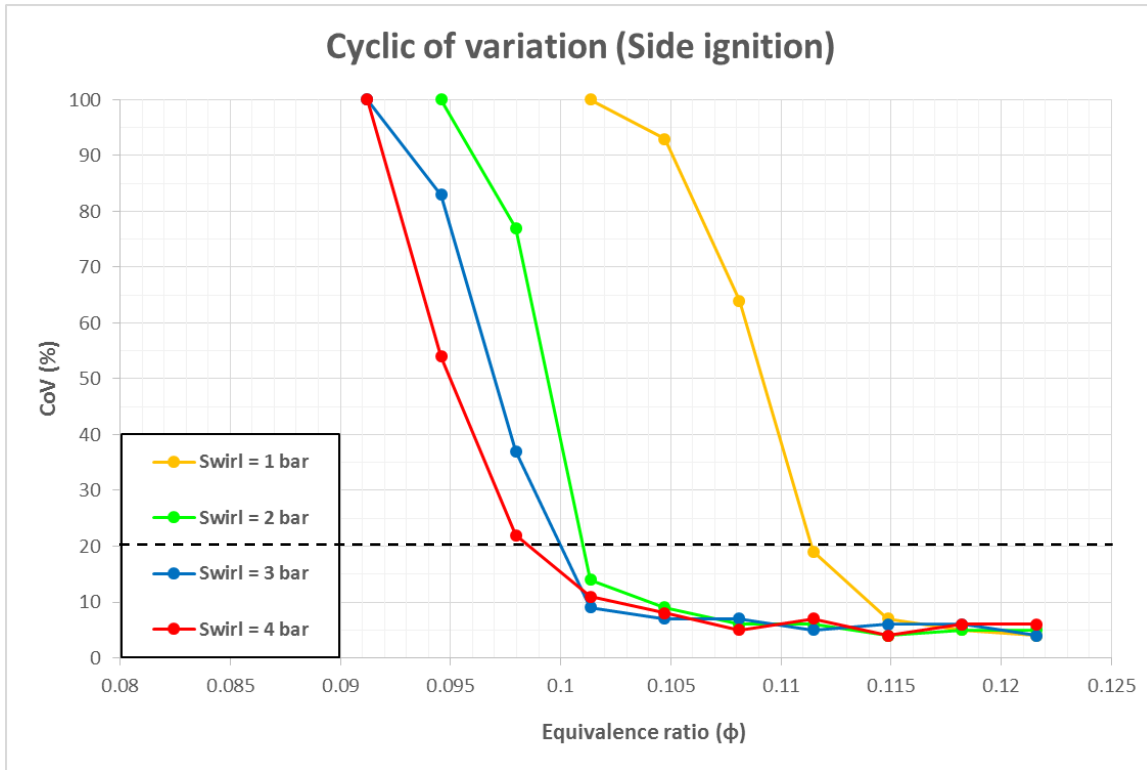


Figure 4.17: The combustion stability in lean burn conditions of center ignition



**Figure 4.18:** The combustion stability in lean burn conditions of sidewall ignition

Lean burn limit was measured by stability of maximum combustion pressure. Figure 4.17 and 4.18 show the variation of peak pressure that were analyzed by data acquisition in both center ignition and sidewall ignition as well. In this study, author focused on the variation of maximum combustion pressure that not over 20%.



**Figure 4.19:** The lean burn limit result of all conditions including swirl intensity and ignition position

The results of lean burn limit were shown in figure 4.19 that the author separated into two conditions. Firstly, the results of lean burn limit of center ignition, which were increased while increased the swirl intensity. In contrast, the second results of lean burn limit of sidewall ignition were decreased while increased the swirl intensity.

Lean burn limit of center ignition condition were 0.087, 0.093, 0.096 and 0.100 but in the sidewall ignition condition were 0.111, 0.101, 0.100 and 0.098 while the differential pressure of swirl intensity were 1, 2, 3 and 4 bar respectively.

The results show the inversion of lean burn limit between center ignition and sidewall ignition. Hydrogen and air have different density. Therefore, when increasing swirl intensity, the tangential force was took the higher density of mixture went to center of combustion chamber means that the amount of air was appeared around the center spark plug. Thus, the possibility of hydrogen combustion was decreased. In the other hand, amount of hydrogen was appeared around ring side of CVCC. Therefore, the hydrogen combustion with sidewall ignition had opportunity to ignite more than center ignition while the swirl intensity increasing.

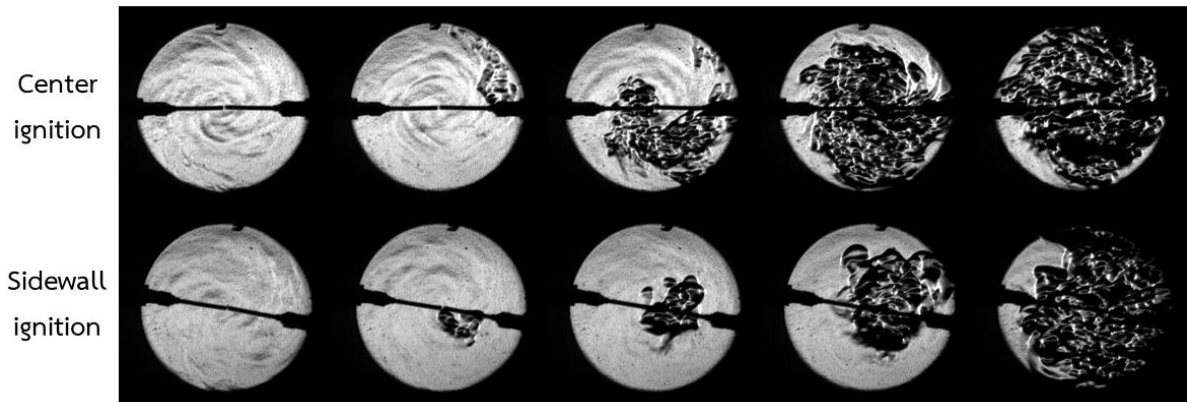


**Figure 4.20** Flame propagation of hydrogen lean burn limit combustion

As the results, it can confirm that swirl intensity hardly affect to hydrogen combustion behaviors to improve the combustion efficiency and also the combustion stability as well included maximum combustion pressure, mass fraction burn rate, combustion duration, combustion delay and also especially in lean burn limit conditions that effected to both behaviors increase and decrease the lean limit of hydrogen combustion.

## CHAPTER 5

# CONCLUSIONS

The combustion characteristics of hydrogen were investigated by using constant volume combustion chamber. Following conclusions can be drawn.

- 5.1. From the result of hydrogen combustion while increasing the initial temperature, the combustion efficiency such as maximum combustion pressure, combustion duration and etc. were improved to be high. The combustion process has to use the activation energy to react between hydrogen and oxygen. Therefore, when increased the initial temperature, mixture does not need activation energy so much to be burnt. Thus, peak pressure and combustion speed were improved.
- 5.2. In the variation of equivalence ratio conditions, as basic knowledge of combustion, the hydrogen combustion characteristics was increased in both performance and efficiency when increasing amount of hydrogen. Figure 4.2 show the maximum combustion pressure increased 89.84% and 86.04% in case of center and sidewall ignition respectively. Moreover, combustion duration were shorten up to 98.06% while increasing equivalence ratio from 0.2 to 0.5. The reason of this phenomenon came from the power input of hydrogen. When increasing equivalence ratio, the power input also increased. Therefore, the combustion result were mentioned.
- 5.3. From these results of mass fraction burn rate, it demonstrates that high swirl intensity may accelerate the beginning of combustion period and reduce time of heat loss in early stage of the combustion.
- 5.4. From CoV of lean burn limit investigation results, it found that appropriate equivalence ratio that the mixture can be make the stable combustion (low CoV) even the swirl intensities were changed can be found at  $\phi > 0.087$  for center ignition and  $\phi > 0.098$  for sidewall ignition
- 5.5. Because of swirl intensity can improve the mixture distribution performance. These phenomena may be discussed that atomization of hydrogen was accelerated by

the increase of the turbulence intensity. Under low swirl condition, hydrogen formed layer on the top of cylinder wall surface because of hydrogen density that so different compared with air. In other word, swirl intensity can directly affects to the lean burn limit by diffusing amount of hydrogen and air to increase the degree of homogeneous mixture formation.

- 5.6. In very lean conditions such as  $\phi$  0.2 and 0.3, swirl intensity also affected to the hydrogen combustion characteristics. Figure 4.3 and 4.4 show the different results that turbulent flow can increase chance of reaction between hydrogen and air. Thus the combustion efficiency (maximum combustion pressure, combustion duration and combustion delay) was increased.
- 5.7. Increasing of rate of turbulence flow can improve the delay time to start of combustion but in the condition of swirl intensity = 2 bar, the result is divergent that affected from characteristics of aerodynamics of turbulence flow inside CVCC.
- 5.8. Flame propagation that were shown in figure 4.11 can confirm that the burning speed in each case of swirl flow were different. High turbulent affected to combustion speed that combustion flame can fulfill combustion chamber faster than low turbulent intensity.
- 5.9. Position of spark plug compared between center position and sidewall position, this parameter cannot affect to the hydrogen combustion phenomena so much. Although the combustion delay of sidewall conditions were a little bit longer because the thermal radiation to the atmosphere but the maximum combustion pressure were similar since the amount of mixture that enough for ignite in everywhere inside CVCC.
- 5.10. Another result that directly related to the ignition position is lean burn limit of hydrogen. The result of lean burn limit show the inversion of combustion stability when changed swirl intensity conditions. Amount of air was went to center of combustion chamber by tangential force but hydrogen was went to the outside that because of the density of itself. Therefore center ignition was suitable for low turbulent flow but sidewall ignition with high swirl intensity is become more effective combustion.

For better understanding of hydrogen combustion phenomena, further studies should include advanced method to identify the consistency of the swirl intensities and mixture formation distribution and consider the relationship between burning rate and swirl strength. Also should use some advanced technique to confirm the equivalence ratio that came from calculation.

## REFERENCES

- [1] Bohacik T., De Maria S., and Saman W.Y. 1996. "Constant-Volume Adiabatic Combustion of Stoichiometric Hydrogen-Oxygen Mixtures." **WREC 1996**. University of South Australia.
- [2] **Technical Review of Hydrogen-fueled Internal Combustion Engines**. Sandia National Laboratory.
- [3] Tinaut F.V., Melgar A., Giménez B., and Reyes M. 2010. "Characterization of The Combustion of Biomass Producer Gas in a Constant Volume Combustion Bomb." **Fuel 89**. 724-731.
- [4] Dhananjay Kumar Srivastava, Kewal Dharamshi and Avinash Kumar Agarwal. 2011. "Flame kernel characterization of laser ignition of natural gas-air mixture in a constant volume combustion chamber." **Optic and Lasers in Engineering 49**. 1201-1209.
- [5] Jeonghoon Song, D.H.L. 2003. "Experimental Study of Ignition of a Gasoline-Air Mixture in a Constant-Volume Combustion Chamber." **Combustion, Explosion, and Shock Waves**. Vol. 39, No. 5.
- [6] Kihyung Lee C.L., and Haeyoung Jeoung. 2009. "A Study on the Effect of Stratified Mixture Formation on Combustion Characteristics in a Constant Volume Combustion Chamber." **JSME International Journal**. Series B, Vol.48.
- [7] Xinghua Liu, Zhiqiang Fan, Fushui Liu, Jiangang Jiu, and Ruwei Wang. 2012. "An Experimental Study of Combustion Characteristics of Hydrogen-Air Pre-Mixture on the Wall Boundary Condition." **International Journal of Hydrogen Energy 37**. 2655-2660.
- [8] Masahiko Fujimoto, M.T. 1993. "Effect of Swirl Rate on Mixture Formation in a Spark Ignition Engine Based on Laser 2-D Visualization Techniques." **SAE paper No.931905**.

## REFERENCES (continued)

- [9] Shahabuddin M., Liaquat A.M., Masjuki H.H., Kalam M.A., et al. 2013. "Ignition Delay, Combustion and Emission Characteristics of Diesel Engine Fueled with Biodiesel." **Renewable and Sustainable Energy Reviews** **21**. 623-632.
- [10] Lee K., Lee C., and Jeoung H. 2009. "A Study on the Effect of Stratified Mixture Formation on Combustion Characteristics in a Constant Volume Combustion Chamber." **JSME International Journal**. Series B, Vol. 48.
- [11] Naoki Shiraishi K.S., Syoji Nagasaka, Takayoshi Takano, and Hiroshi Sami. 2001. "A Study on Direct Injection Gasoline Combustion using Constant Volume Combustion Vessel." **The Fifth International Symposium on Diagnostics and Modeling of Combustion in Internal Combustion Engines (COMODIA 2001)**.
- [12] Jinhua Wang Z.H., Haiyan Miao, Xibin Wang, and Deming Jiang. 2008. "Characteristics of direct injection combustion fuelled by natural gas-hydrogen mixtures using a constant volume vessel." **International journal of hydrogen Energy** **33**.
- [13] Nomthongthai P., Tongroon M., Charoenphonphanich C., Kosaka H., and et al. 2012. "Design of Hydrogen Constant Volume Combustion Chamber." **TSME International Conference on Mechanical Engineering**.
- [14] Dugkhuntod T., Nomthongthai P. and Songsaengchan Y. 2009. **Ethanol Combustion Characteristics in a Constant-Volume Combustion Chamber (in Thai)**. Department of Mechanical Engineering, KMITL, Thailand.
- [15] Pulkrabek Willard W. **Engineering Fundamentals of the Internal Combustion Engine**. Prentice Hall, New Jersey.
- [16] Turns Stephen R. **An Introduction to Combustion: Concepts and Applications, 2<sup>nd</sup> edition**. ISBN 0-70-230096-5, McGraw-Hill Series in Mechanical Engineering.
- [17] Ornman P., Charoenphonphanich C., Chollacoop N., and Kosaka, H. 2011. **Effect of Ethanol Concentration of Gasohol on Lean Flammability Limit in Direct-Injection Stratified**. International College, KMITL, Thailand.

## APPENDICES

## Appendix A: Material specification

### Steel for constant volume combustion chamber

#### ASTM A284 Steel, grade D

Categories: [Metal](#); [Ferrous Metal](#); [ASTM Steel](#); [Carbon Steel](#); [Low Carbon Steel](#)

**Material Notes:** Carbon content increases with the thickness of the plate. Maximum thickness is 305 mm. Plates wider than 610 mm are tested in the transverse direction and the elongation requirement is reduced 2.0%

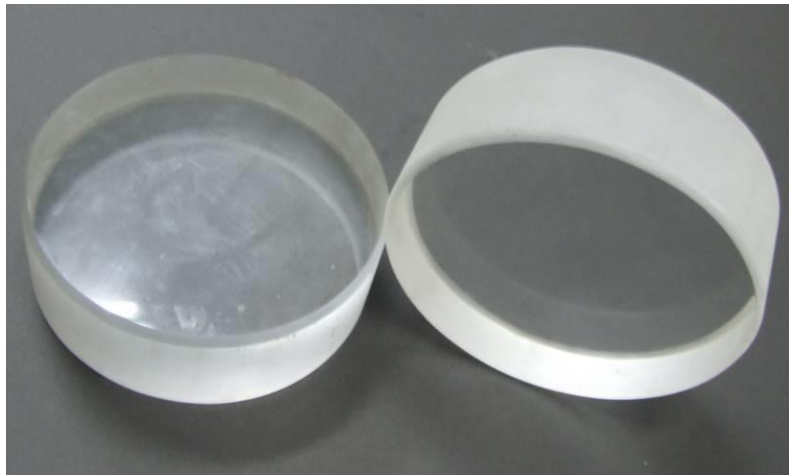
**Key Words:** AFNOR 35-501 E24-2, AFNOR 35-501 E24-3, BS4360 40(A)B, BS4360 40C, CSAG40-21230 G, DIN 17100 RSt 37-2, DIN 17100 St37-3U, EN10025(90) Fe E360B(FN), EN10025(90) Fe E 360 C, EN10025(93) S235JR(G2), EN10025(93) S235 J0, IS 226, IS Fe 410-S, JIS 3101 SS 400, JIS 3106 SM 400A, JIS 3106 SM 400B, ISO 630 Fe 360 B, ISO 630 Fe 360 C, MNC810E SS 13.11.00, MNC810E SS 13.12.00, NBN21-101 AE235B, NBN21-101 AE235 C, UNI 7070 Fe 360 B, UNI 7070 Fe 360 C

**Vendors:** No vendors are listed for this material. Please [click here](#) if you are a supplier and would like information on how to add your listing to this material.

Physical Properties	Metric	English	Comments
Density	7.85 g/cc	0.284 lb/in <sup>3</sup>	Typical of ASTM Steel
Mechanical Properties	Metric	English	Comments
Tensile Strength, Ultimate	415 MPa	60200 psi	
Tensile Strength, Yield	230 MPa	33400 psi	
Elongation at Break	21.0 %	21.0 %	in 200 mm
	24.0 %	24.0 %	In 50 mm.
Bulk Modulus	140 GPa	20300 ksi	Typical for steel
Shear Modulus	80.0 GPa	11600 ksi	Typical for steel
Component Elements Properties	Metric	English	Comments
Carbon, C	0.270 - 0.35 %	0.270 - 0.35 %	
Iron, Fe	98.0 %	98.0 %	
Manganese, Mn	<= 0.90 %	<= 0.90 %	
Phosphorous, P	<= 0.040 %	<= 0.040 %	
Silicon, Si	0.280 %	0.280 %	
Sulfur, S	<= 0.050 %	<= 0.050 %	

<http://www.matweb.com>

## Quartz glass specification



Specifications	Unit	Value
Specific gravity	g/cm <sup>2</sup>	2.21
Hardness	Mhos scale	5-7
Rapture strength	Mpa	800-1000
Compressive stress	Mpa	60-700
Young's Modulus 20 °C	Gpa	77.8
Young's Modulus 50 °C	Gpa	82
Young's Modulus 900 °C	Gpa	85
Possion ratio		0.17
Rigid index 900 C	Gpa	36.9
Speed of longinal wave	m/s	5.72x10 <sup>-3</sup>

## Graphite gasket detail



### ***SealPack Style 300R***

#### FLEXIBLE GRAPHITE ROLLS

Temperature Limits :

-200°C to + 1650°C

-200°C to + 850°C Non-Oxidizing atm.

+932°F (500°C) Oxidizing atm.

Chemical Resistance :

pH 0-14 except oleum, fuming nitric acid & aqua regia

Thickness (mm) 0.2, 0.35, 0.40, 0.50, 0.8, 1.0, 1.5

Width : 1000 - 1500 mm

Length : 50 - 100 m.

## Data acquisition system

### Instrument facts:

- AC or DC powered
- High accuracy, 16, 22 or 24 bit resolution
- Fast sampling, 100 kS/s up to 1 MS/s per channel
- Transient recording up to 1 GS/s
- Powerful Intel® Core™2 Duo PC inside
- 80 MB/s stream-to-disk rate
- Bright 17" display
- Spare panel for customization
- 5 available PCI slots



DEWE-5000 series		
Input specifications	DEWE-5000	DEWE-5001
Slots for DAQ or PAD modules	16	-
MDAQ input channels	-	Up to 32
<b>Main system <sup>1)</sup></b>		
Total PCI slots	5	5
Hard disk	1000 GB	
Data throughput	Typ. 70 MB/s <sup>2)</sup>	
Power supply	95 to 260 V <sub>AC</sub>	
Display	17" TFT display, 1280 x 1024 pixel	
Processor	Intel® Core™2 Duo 2 GHz	
RAM	2 GB	
Ethernet	10/100/1000 BaseT	
USB interfaces	4	
RS-232 interface	1	
Storage drive	Internal DVD +/-RW burner	
Operating system	Microsoft® WINDOWS® 7	
Dimensions (W x D x H)	460 x 351 x 192 mm (18.1 x 13.8 x 7.7 in.)	
Weight	Typ. 17 kg (37 lb.)	Typ. 16.5 kg (36 lb.)
<b>Environmental specifications</b>		
Operating temperature	0 to +50 °C, down to -20 °C with prewarmed unit	
Storage temperature	-20 to +70 °C	
Humidity	10 to 80 % non cond., 5 to 95 % rel. humidity	
Vibration <sup>3)</sup>	MIL-STD 810F 514.5, procedure I	
Shock <sup>3)</sup>	MIL-STD 810F 516.5, procedure I	

Pressure sensor

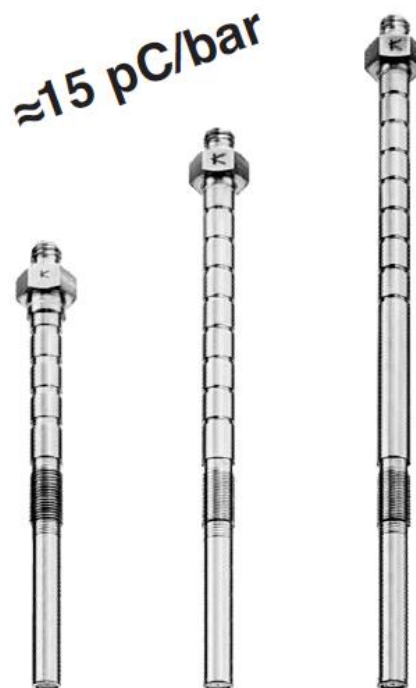
# KISTLER

1 ... 2

## 6057A80, 6057 Asp...

Miniature measuring probe for direct mounting or mounting in a glow plug adapter, resulting in an extremely short gas duct.

It can also be used in multivalve engines with small displacement. For the front diameter of only 4 mm, a measuring bore of 5 mm is sufficient. The probe mounts easily, after only slight modifications of the cylinder head, even across cooling water ducts, whereby sealing is assured by O-rings.



Type 6057A...

### Technical Data\*

<b>Range</b>	bar	0 ... 250
<b>Calibrated partial range</b>	bar	0 ... 50
<b>Overload</b>	bar	300
<b>Sensitivity</b>	pC / bar	≈-15
<b>Natural frequency</b> (Force link)	kHz	≈130
<b>Linearity</b> , all ranges at RT	% FSO	≤±0,6
<b>Acceleration sensitivity</b> (higher with long sensors)	bar / g	≤0,001
<b>Operating temperature range</b>	°C	-50 ... 350
<b>Sensitivity shift</b> 200 ... ±50 °C	%	≤±1,5
<b>Thermo shock error</b> (at 1500 r/min, 9 bar IMEP)		
Δ p (short-time drift)	bar	<±0,8
Δ IMEP	%	≤±4
Δ p <sub>max.</sub>	%	≤±2
<b>Insulation resistance</b> at 20 °C	TΩ	≥10
<b>Shock resistance</b>	g	2000
<b>Tightening torque</b>	Nm	1,2
<b>Capacitance</b> (6057A80)	pF	25
<b>Weight</b> (6057A80)	g	10
<b>Plug</b> , teflon insulator	Type	10-32 UNF

## Hydrogen quality



<b>Item</b>	<b>Product Description</b>															
1	<p><b>Hydrogen Ultra High Purity</b>            Purity 99.999%</p> <table data-bbox="678 1098 1065 1318"> <tr> <td>O2</td> <td>&lt;</td> <td>3 ppm</td> </tr> <tr> <td>H2O</td> <td>&lt;</td> <td>3 ppm</td> </tr> <tr> <td>CO</td> <td>&lt;</td> <td>1 ppm</td> </tr> <tr> <td>CO2</td> <td>&lt;</td> <td>1 ppm</td> </tr> <tr> <td>THC</td> <td>&lt;</td> <td>1 ppm</td> </tr> </table> <p>Gas content : 1.5 m<sup>3</sup>/cylinder            Cylinder Outlet valve : CGA 350            Filling Pressure : 2,000 psig at 27 °C</p>	O2	<	3 ppm	H2O	<	3 ppm	CO	<	1 ppm	CO2	<	1 ppm	THC	<	1 ppm
O2	<	3 ppm														
H2O	<	3 ppm														
CO	<	1 ppm														
CO2	<	1 ppm														
THC	<	1 ppm														

## Flashback arrestor



Safety device	Model ...-ES			
	F53N*	F53N/H*	RF53N	RF53N/H
Flame arrestor <b>[FA]</b>	X		X	
Non-return valve <b>[NV]</b>	-		X	
Temperature sensitive cut-off valve <b>[TV]</b>	X		X	
Weight [g]	181		195	
Certification BAM	BAM/ZBA/003/04			
Material	Housing – Stainless steel; Flame arrestor – Stainless steel; Seal – Elastomer			
Gases	max. working pressure [bar]			
Acetylene (A)	1,5	-	1,5	-
Natural gas (M)	5,0	12,0	5,0	12,0*
LPG (P)	5,0	8,0	5,0	8,0
Hydrogen (H)	3,0	10,0	3,0	9,0
Ethylene (E)	-	9,0	-	5,0
Oxygen (O)	30,0	-	30,0	-
Compressed air (D)	30,0	-	30,0	-
Connections	Order-No.			
1/4" NPT F	145-227	145-106	145-262	145-107
3/8" NPT F	-	-	145-024	145-121

## Hydrogen pressure regulator

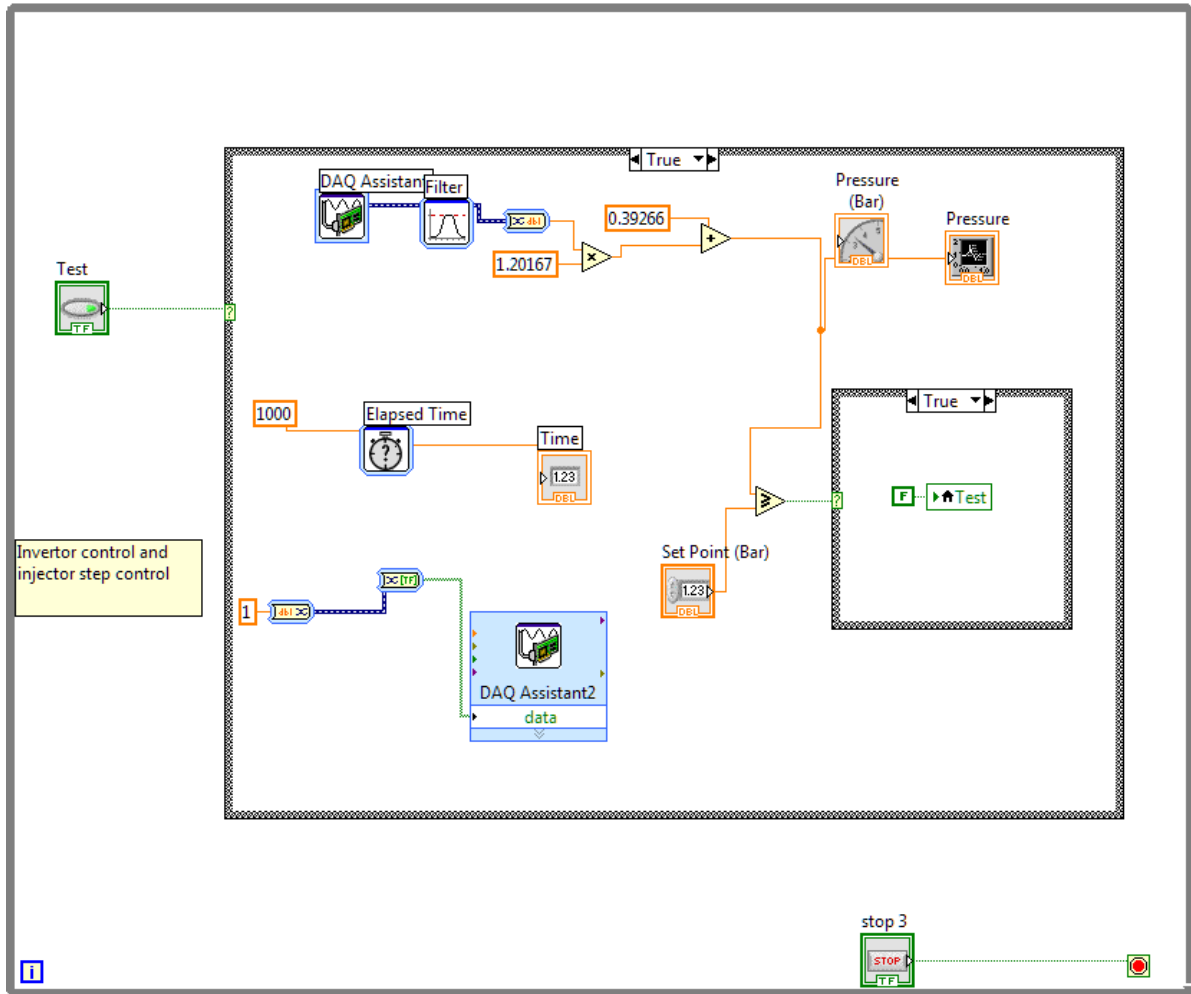


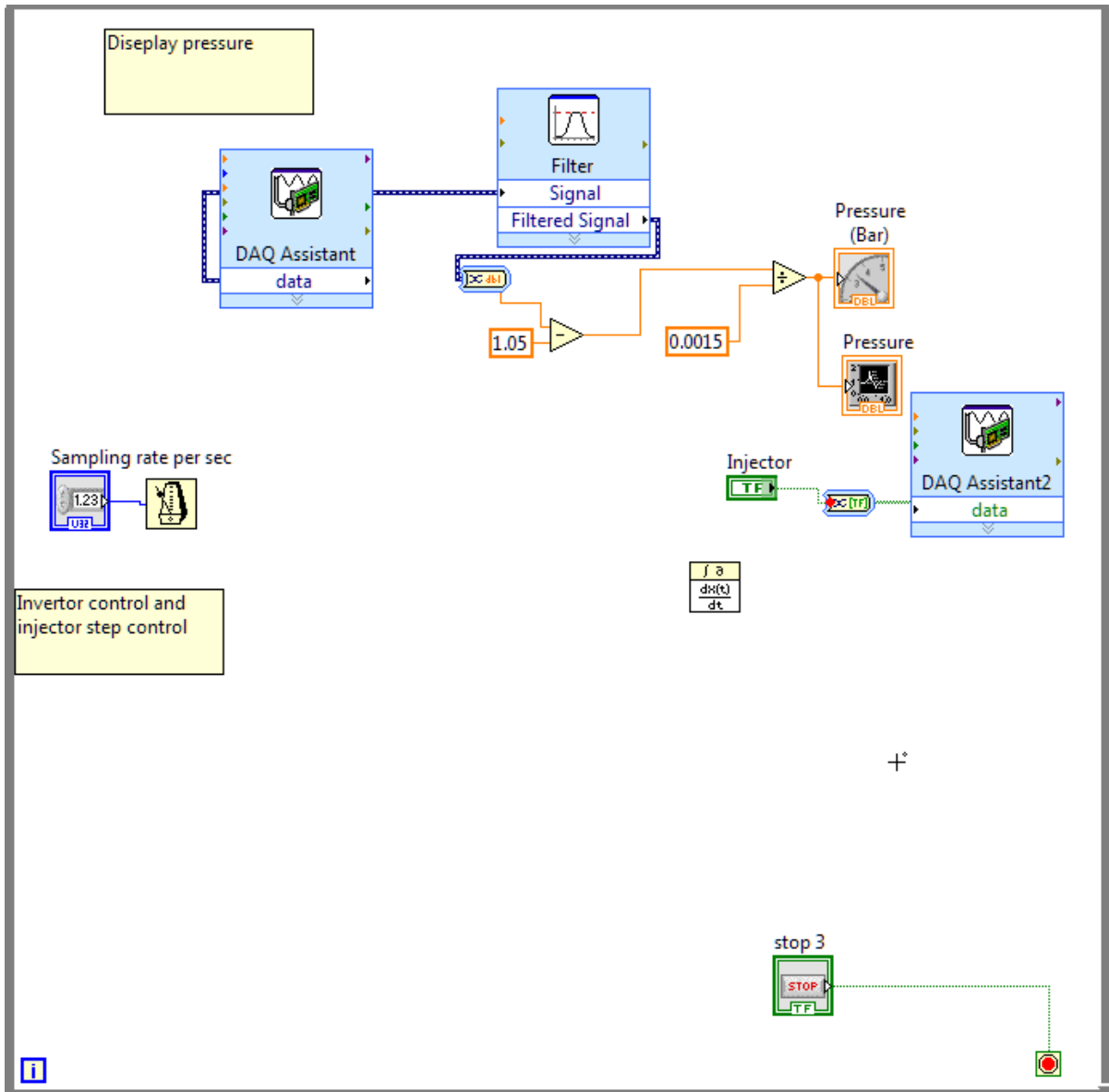
<b>MODEL TANAKA SS -150 SINGLE STAGE,FIVE-PORT,</b>	
<b>BODY</b>	NICKEL-PLATE BRASS BODY
<b>DIAPHRAGM</b>	316L STAINLESS STEEL DIAPHRAGM
<b>INLET PRESSURE</b>	0-3,000 PSIG (210 Bar)
<b>INLET GAUGE</b>	0-4,000 PSIG (280 Bar)
<b>OUTLET PRESSURE</b>	0 - 150 PSIG (10.5 bar)
<b>OUTLET GAUGE</b>	-.30inHg -0-150 PSIG
<b>GAUGE SCALE</b>	STANDARD BAR/PSIG
<b>GAS</b>	HYDROGEN (CGA-350)
<b>CGA INLET FITTING</b>	NICKEL-PLATE BRASS BODY
	NUT,NICKEL-PLATE BRASS BODY
<b>OUTLET FITTING</b>	1/4" TUBE,NICKEL-PLATE BRASS BODY
	1/8" TUBE,SS316L
<b>MANUFACTURED BY</b>	NIPPON CUTTING & WELDING EQUIPMENT CO.



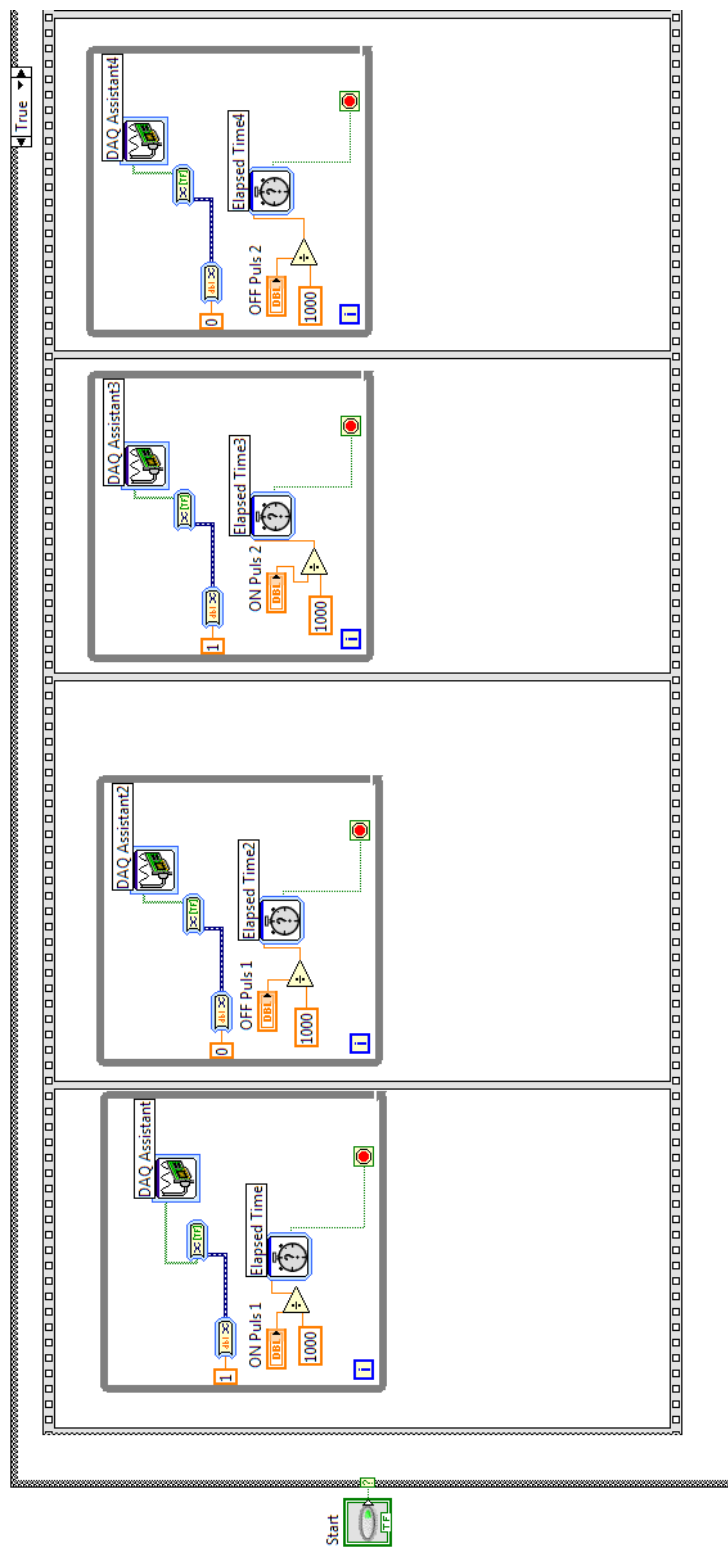
### Appendix B: Controller block diagram

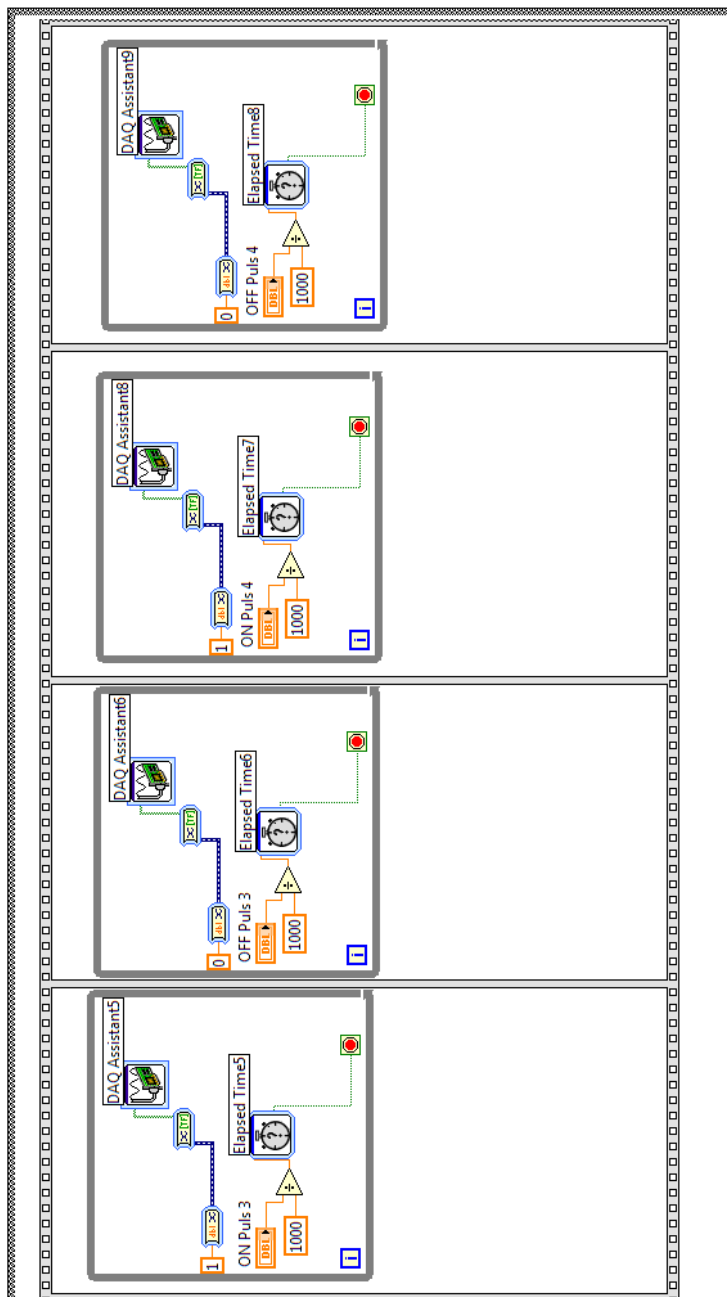
#### Partial pressure calibration program





## Experimentally sequential program





## Appendix C: Publications

# ME-NETT & TSME-ICoME 2012

**KMUTT**  24-27 October 2012  
Dusit Island Resort hotel, Chiang Rai

**The 26<sup>th</sup> Conference of the  
Mechanical Engineering Network of Thailand  
&  
The 3<sup>rd</sup> TSME-International Conference  
on Mechanical Engineering**

## Related Topics

- Aerospace and Marine Engineering
- Alternative Energy and Combustion
- Applied Mechanics, Materials and Manufacturing
- Biomechanics
- Computation and Simulation Techniques
- Dynamic System, Robotics and Control
- Energy Technology and Management
- Thermal System and Fluid Mechanics  
and Fields Related to Mechanical Engineering

## Important Dates

Abstract submission 1 - 31 March 2012  
Notification of abstract acceptance 30 April 2012  
Full manuscript submission deadline 15 June 2012  
Notification of full manuscript acceptance 31 July 2012  
Camera ready final manuscript submission deadline 31 August 2012

## Contact Us

Department of Mechanical Engineering, Faculty of Engineering  
King Mongkut's University of Technology Thonburi  
126 Pracha Uthit Rd., Bang Mod, Thung Khru, Bangkok 10140, THAILAND  
Tel : 02 470 9122-4 Fax : 02 470 9111 e-mail : [icome2012@kmutt.ac.th](mailto:icome2012@kmutt.ac.th)

[www.menett-icome2012.com](http://www.menett-icome2012.com) , [www.icome2012.kmutt.ac.th](http://www.icome2012.kmutt.ac.th)



## Design of Hydrogen Constant Volume Combustion Chamber

P. Nomthongthai<sup>1,\*</sup>, P. Ornman<sup>1</sup>, M. Tongroon<sup>2</sup>, P. Karin<sup>1</sup>, N. Chollacoop<sup>2</sup>  
C. Charoenphonphanich<sup>3</sup> and H. Kosaka<sup>4</sup>

<sup>1</sup> International College, King Mongkut's Institute of Technology Ladkrabang,  
Bangkok, Thailand, 10520

<sup>2</sup> National Metal and Materials Technology Center (MTEC),  
Pathumthani, Thailand 12120

<sup>3</sup> Faculty of Engineering, King Mongkut's Institute of Technology Ladkrabang,  
Bangkok, Thailand, 10520

<sup>4</sup> Department of Mechanical and Control Engineering, Tokyo Institute of Technology, Japan

\* Corresponding Author: Tel: 02 329 8261-2, Fax: 02 737 2580,  
E-mail: nongnot\_p@hotmail.com

### Abstract

This research is divided into two parts. First part is a design and simulation of Constant Volume Combustion Chamber (CVCC) and the second part is calibration of swirl intensity. Both parts are fundamental for investigation of combustion characteristic of hydrogen. For the first part, CATIA program was used for CAD design. The design was under the maximum combustion pressure condition which is calculated from thermodynamic analysis of otto cycle method. The result of simulation from ABAQUS program reveals maximum pressure of 8.0 MPa, with Safety Factor in main chamber and chamber cover equal to 12.75 and 7.26, respectively. For the second part, air velocity of swirl intensity was controlled by pressured difference between outside and inside the chamber, which was measured by Photron FASTCAM program, schlieren technique and hi-speed video camera in order to estimate the velocity of air. The velocities of air motion inside the chamber were 5.73, 6.50, 7.54, 8.10 and 9.32 m/s at difference pressure equal to 0.1, 0.2, 0.3, 0.4 and 0.5 MPa, respectively.

**Keywords:** Constant Volume Combustion Chamber, Hydrogen, Swirl intensity, Schlieren technique

### 1. Introduction

Nowadays, fuel prices are very high so the automotive society wants to improve fuel consumption and thermal efficiency of the engine, as well as searching for the clean alternative fuel. The clean alternative fuel means the fuel that results less emission, air pollution, and global warming effects. One of the new alternative fuels considered is hydrogen.

Hydrogen can be produced from water via electrolysis, which is considered abundant because 3/4 of the world is covered by water.

For the combustion process, if hydrogen is used in the internal combustion engine, the product after combustion is only water. Hence, air emissions will be decreased (zero emissions) [1]. The characteristics of hydrogen are high flammability, high heating value, and high octane number, which could give rise to increased thermal efficiency. The properties of hydrogen compared with CNG and gasoline were shown in Table. 1.

The Constant Volume Combustion Chamber (CVCC) is the combustion simulator. The structure is similar the real engine combustion

chamber in the case of compression stroke but it does not have the piston movement [2, 3]. Thus, the volume of the CVCC is constant. Many researchers have investigated in the real engine but it has a lot of parameters that could influence the combustion characteristic. On the other hand, CVCC can be installed with various sensors and equipment such as temperature control, ignition, intake and exhaust system that could better control the parameter. Hence, the results of the experiment are more reliable.

Principle of operating of hydrogen CVCC is to effort the conditions that resemble to real engine combustion chamber, such as temperature and pressure before combustion. Hence, the maximum combustion pressure is the main parameter that governs CVCC designing and simulation.

The present study is divided into two parts. First is a design and simulation of CVCC under condition of maximum calculated combustion pressure. Second is a measurement of air velocity in swirl intensity condition. Both parts are the conditions for study in combustion characteristics of hydrogen.

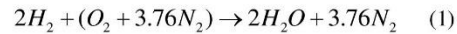
Table. 1 Properties of hydrogen compared with CNG and gasoline [4]

Property	Hydrogen	CNG	Gasoline
Density (kg/m <sup>3</sup> )	0.0824	0.72	730
Flammability limits (volume % in air)	4-75	4.3-15	1.4-7.6
Flammability limits (Ø)	0.1-7.1	0.4-1.6	0.7-4
Autoignition temperature in air (K)	858	723	550
Flame velocity (m/s)	1.85	0.38	0.42
Adiabatic Flame temperature (K)	2480	2214	2580
Stoichiometric air/fuel mass ratio	34.48	14.49	14.7
Lower heating value (MJ/kg)	119.7	45.8	44.79
Heat of combustion (MJ/kg <sub>air</sub> )	3.37	2.9	2.83

## 2. Experimental Procedure

### 2.1 Combustion pressure calculation

The chemical equation between hydrogen and air are shown in Eq. (1).



The combustion pressure can be calculated by using ideal gas equation Eq. (2) and thermodynamic analysis of otto cycle method [5, 6].

$$PV = m_m RT_1 \quad (2)$$

Where:

- P : Pressure of mixture
- V : Volume of combustion chamber
- m<sub>m</sub> : Overall mass of mixture
- R : Gas constant
- T<sub>1</sub> : Mixture temperature

Mass of hydrogen and air in combustion chamber can be calculated by using stoichiometric air/fuel mass ratio as shown in Eqs. (3), (4) respectively.

$$m_f = (1/35.48)(m_m) \quad (3)$$

$$m_{air} = (34.48/35.48)(m_m) \quad (4)$$

Combustion temperature is calculated by using Constant volume heat input equation Eq. (5).

$$m_f Q_{HV} \eta_c = m_m c_v (T_2 - T_1) \quad (5)$$

Where:

- m<sub>f</sub> : Mass of fuel (Hydrogen)
- Q<sub>HV</sub> : Heating value of fuel (Hydrogen)
- η<sub>c</sub> : Combustion efficiency
- c<sub>v</sub> : Constant volume specific heat capacity
- T<sub>2</sub> : Combustion temperature
- T<sub>1</sub> : Mixture temperature

Combustion temperature from Eq. (5) can calculate the combustion pressure (P<sub>2</sub>) by using Gay-Lussac's law Eq. (6).

$$P_1/T_1 = P_2/T_2 \quad (6)$$

Where:

- P<sub>1</sub> : Mixture pressure
- P<sub>2</sub> : Combustion pressure
- T<sub>1</sub> : Mixture temperature
- T<sub>2</sub> : Combustion pressure

### 2.2 CVCC Simulation

JIS S45C steel was chosen in order to make constant volume combustion chamber [7] as shown in Fig. 1 and the properties of this steel from JIS standard was shown in Table. 2.



Fig. 1 JIS S45C steel



Table. 2 Properties of JIS S45C steel

JIS S45C Steel, Normalized	
Properties	Metric
Density	7.85 g/cc
Hardness, Brinell	167 - 229
Tensile Strength, Ultimate	569 MPa
Tensile Strength, Yield	343 MPa
Elongation at Break	20.00 %
Modulus of Elasticity	205 GPa
Poisson Ratio	0.29
Machinability	55 %
Shear Modulus	80.0 GPa

Quartz glasses were used for covers both sides of CVCC because it was easy to visualize the combustion phenomena (Fig. 2). The properties of quartz glasses were shown in Table. 3.

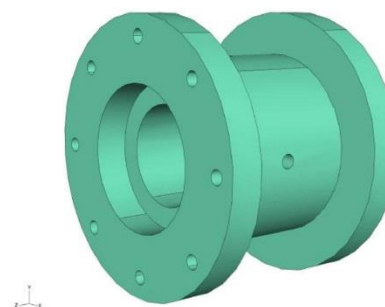


Fig. 2 Quartz glass

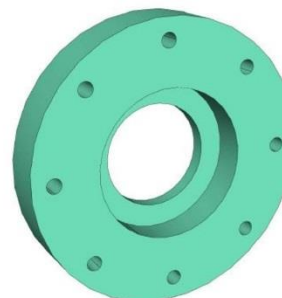
Table. 3 Properties of quartz glass

Properties	Metric
Specific	2.21 g/cc
Hardness	5-7 Mhos Scale
Rapture Strength	800-1000 MPa
Compressive Stress	60-700 MPa
Young's Modulus 20 °C	77.8 GPa
Young's Modulus 50 °C	82 GPa
Young's Modulus 900 °C	85 GPa
Poisson Ratio	0.17
Rigid Index 900 C	36.9 GPa
Speed of Longitudinal Wave	$5.72 \times 10^{-3}$ m/s

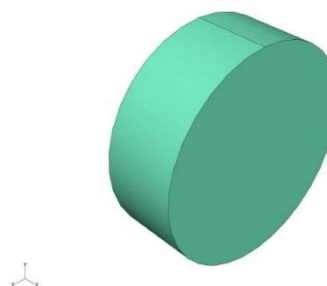
From combustion pressure calculated, CATIA and ABAQUS program were used for designing and simulation. Properties of material were set to simulation program, as shown in Fig. 3.



(a) Main chamber



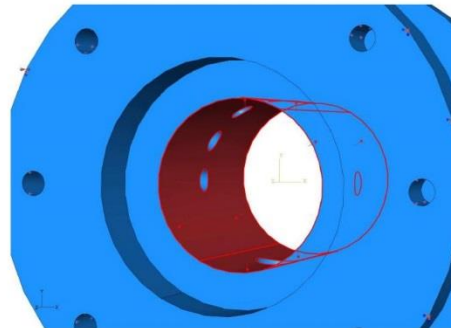
(b) Chamber cap



(c) Quartz glass

Fig. 3 Material setting

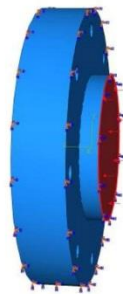
The over pressure (8.0 MPa) was used for simulation condition to assure that accident will not occur as shown in Fig. 4.



(a) Main chamber



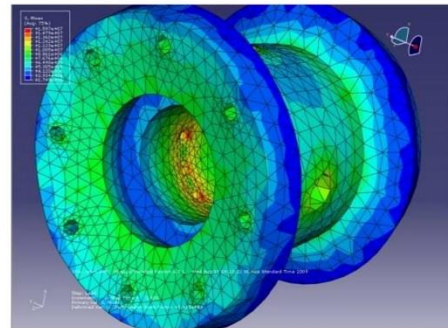
(b) Chamber cap



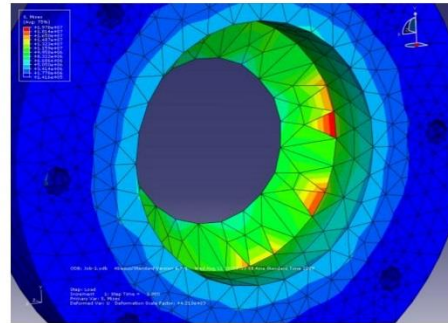
(c) Quartz glass

Fig. 4 Load setting at 8.0 MPa

From previous research [7, 8], this combustion chamber was used in order to study in gasoline and ethanol blended combustion. The result of maximum combustion pressure from the calculation is 4.2 MPa, and Fig. 5 shows the simulation result of 5.0 MPa. The safety factor of main chamber and chamber cap from simulation result are 21.47 and 17.34 respectively.



(a) Main chamber



(b) Chamber cap

Fig. 5 Simulation result of ethanol combustion

The results of real combustion pressure, as shown in Fig. 6, are not over in order to compare with the calculation result.

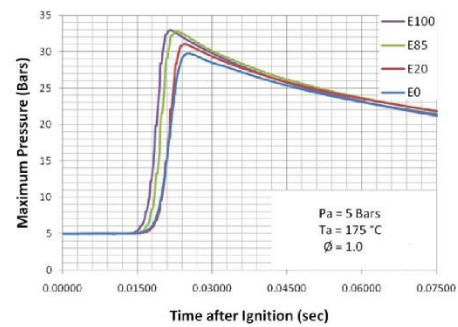


Fig. 6 Real combustion pressure from gasoline and ethanol blended

### 2.3 Swirl Intensity calibration

In this study, Swirl intensity is one of parameters that affects to combustion phenomena [9, 10] (Fig. 7).

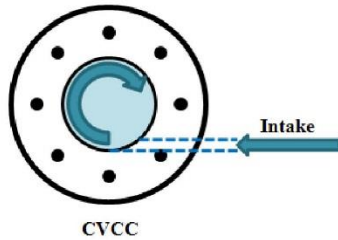


Fig. 7 Swirl intensity in CVCC

Thus, swirl intensity must be calibrated. The differential intake pressure was used in order to calibrate. The unit of swirl intensity is m/s and the initial pressure before combustion was fixed at 0.5 MPa so the differential pressure that set are 0.1, 0.2, 0.3, 0.4 and 0.5 MPa.

High speed video camera (Photron FASTCAM SA3 at 6,000 fps, 1/10,000 sec of shutter speed and monochrome color) and schlieren technique (light source from xenon lamp 6,000 K) was used in order to capture the motion of air in CVCC by using the various air densities, as shown in Figs. 8, 9.

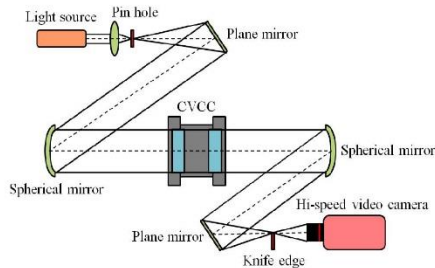


Fig. 8 Schlieren technique and high speed video camera diagram

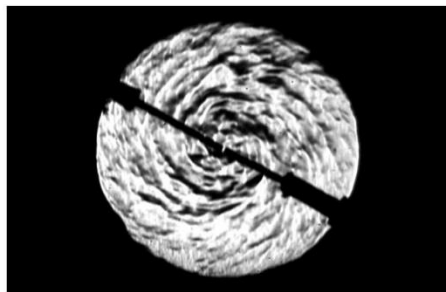
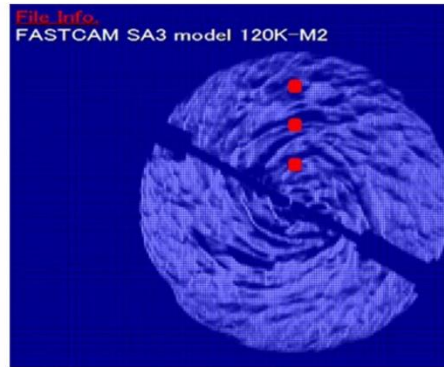
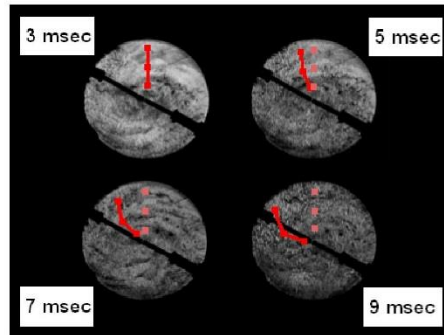


Fig. 9 Swirl intensity phenomena from schlieren technique and high speed video camera

In the measurement process, Photron FASTCAM program was used to measure the velocity of air elements by tracking 3 moving points (center, middle and side). In the given period of time, the air elements get the distance so air velocity can be determined, as shown in Fig. 10.



(a) Measured by using FASTCAM program



(b) Example of movement of air elements  
Fig. 10 Air velocity measurement

### 3. Results and Discussion

#### 3.1 Designing Result

The suitable design of CVCC is shown in Fig. 11. The main parameters that affected the design process are the area for installing testing equipments and safety factor from highest combustion pressure.

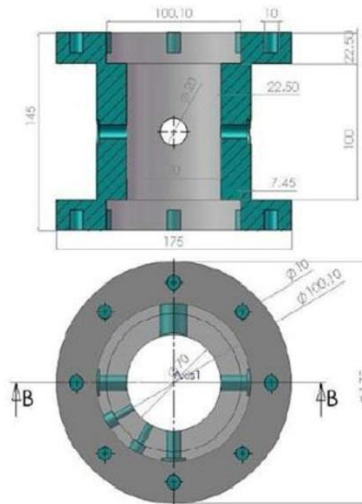
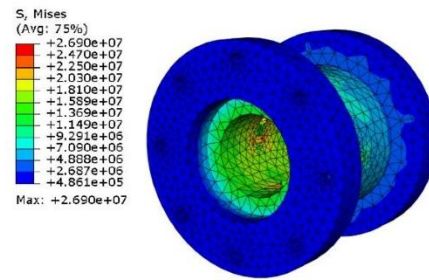


Fig. 11 The dimension of combustion chamber

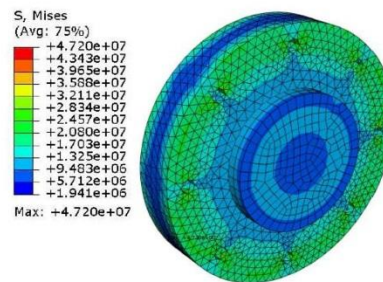
Dimension of quartz glass is 100 mm. with 35 mm. thickness. The diameter of combustion chamber is 70 mm. while length is 100 mm. Hence, volume of CVCC is 385 cc., which is similar to the volume of conventional small gasoline engine. All equipment, such as intake port, exhaust port, heater, spark plugs and sensors, can be installed on 115 mm. of outer diameter. Nonetheless, all of equipment are not necessary to simulate explicitly because the standard can be used in high pressure that is over the maximum combustion pressure. Hence, it can ensure that all of equipment parts, attached to combustion chamber, are not damaged.

### 3.2 Simulation Result

The result of maximum combustion pressure from the calculation is 6.9 MPa. In term of safety, over pressure was set in the simulation program at 8.0 MPa. The result is shown in Fig. 12, where von mises stress of main chamber is 26.9 MPa at edge of spark plugs hole, and von mises stress of chamber cap is 47.2 MPa at edge of bolt mounting. Therefore the safety factors are 12.75 and 7.26, respectively. The finding can guarantee that this CVCC will be adequate in term of safety.



(a) Main chamber



(b) Chamber cap with quartz glass

Fig. 12 Simulation result

According to the simulation result, hydrogen combusts with safety condition so the real combustion chamber is fabricated by such design, as shown in Fig. 13, 14.



Fig. 13 Real main chamber, chamber cap and quartz glass



Fig. 14 Real combustion chamber including equipment

### 3.3 Swirl intensity calibration result

Results of swirl intensity calibration were plotted as scattering graph and trend line. The example at pressure difference of 0.5 MPa is shown in Fig. 15.

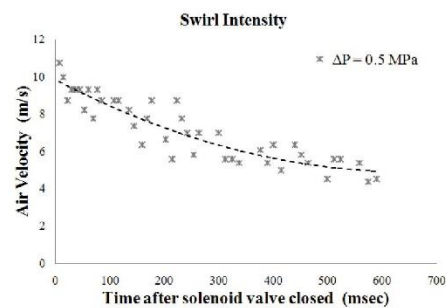


Fig. 15 Air velocity in condition of  $\Delta P = 0.5$  MPa

At the beginning, the results are disrupted values but become more stable closed to trend line when 35 msec after solenoid valve close. Therefore, the result at 35 msec was chosen for this study, as shown in Fig. 15. The air velocities are 5.73, 6.50, 7.54, 8.10 and 9.32 m/s for differential pressures of 0.1, 0.2, 0.3, 0.4 and 0.5 MPa respectively (Fig. 16). From this study, the differential intake pressure clearly had more effect for swirl intensity. If the pressure difference increases, the air velocity also increases.

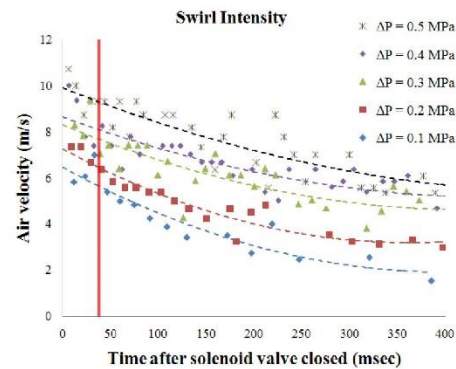


Fig. 16 Air velocity in 5 conditions

### 4. Conclusions

1. The designing of CVCC is accomplished for the study of hydrogen combustion with 3 important issues,

- 1.1 Similarity with real engine
- 1.2 Combustion pressure
- 1.3 Enough area around CVCC in order to install any equipment

All of issues can be designed and produced successfully by recourse to internal combustion theory and comparison with ethanol-gasoline blended study.

2. The real CVCC (main chamber, chamber caps and quartz glass) was also produced by design successfully.

3. When pressure difference between inside and outside of CVCC is increased, the diffusion of air will increase. Thus, air velocity of swirl intensity will increase as well. The best air velocity is that after the intake valve closed immediately but at that time, values obtained are also very scattered. Thus, 35 msec after intake valve closed is the most appropriate time since it does not spread much and close to the trend line.

4. From the experiment results, it is obvious that the way to find swirl intensity by using schlieren technique, high speed video camera and computer program is not too difficult. Next study, Hydrogen-air mixed will be calibrated.

### 5. Acknowledgement

The authors are grateful to scholarship support from TAIST Tokyo Tech Program, with special acknowledgement for Automotive Laboratory, KMITL and Bioenergy Laboratory, NSTDA/AMTEC, Thailand. The authors also thank Hi-Tech resource (Thailand) for their helps and supports in high speed video camera.



### 6. References

- [1] T. Bohacik, S. De Maria and W.Y. Saman. (1996). Constant-Volume Adiabatic Combustion of Stoichiometric Hydrogen-Oxygen Mixtures, *WREC 1996*, University of South Australia.
- [2] F.V. Tinaut, A. Melgar, B. Giménez and M.Reyes. Characterization of The Combustion of Biomass Producer Gas in a Constant Volume Combustion Bomb, *Fuel* 89, (2010) 724-731.
- [3] Dhananjay Kumar Srivastava, Kewal Dharamshi and Avinash Kumar Agarwal. Flame kernel characterization of laser ignition of natural gas-air mixture in a constant volume combustion chamber, *Optic and Lasers in Engineering* 49, (2011) 1201-1209.
- [4] Technical Review of Hydrogen-fueled Internal Combustion Engines, Sandia National Laboratory.
- [5] Willard W. Pulkrabek. Engineering Fundamentals of the Internal Combustion Engine, Prentice Hall, New Jersey.
- [6] Stephen R. Turns. An Introduction to Combustion: Concepts and Applications, 2<sup>nd</sup> edition, ISBN 0-70-230096-5, McGraw-Hill Series in Mechanical Engineering.
- [7] T. Dugkhuntod, P. Nomthongthai and Y. Songsaengchan. Ethanol Combustion Characteristics in a Constant-Volume Combustion Chamber (in Thai), Department of Mechanical Engineering, KMUTL (2009).
- [8] P. Ornman, H. Kosaka, N Chollacoop and C. Charoenphonphanich. Study on Combustion Characteristics of Direct Injection Stratified Charge in Ethanol/Gasoline Blends, *The First TSME International Conference on Mechanical Engineering*, (2010).
- [9] Jinhua Wang, Zuohua Huang, Haiyan Miao, Xibin Wang and Deming Jiang. Characteristics of direct injection combustion fuelled by natural gas-hydrogen mixtures using a constant volume vessel, *International journal of hydrogen energy* 33, (2008) 1947-1956.
- [10] P. Ornman, C. Charoenphonphanich, N. Chollacoop and H. Kosaka. Effect of Ethanol Concentration of Gasohol on Lean Flammability Limit in Direct-Injection Stratified Charge Engine, *The 7<sup>th</sup> International Conference on Automotive Engineering (ICAE-7)*, (2011).



**2014 JSAE Annual Congress (Spring)**  
in **PACIFICO YOKOHAMA**

Period : **Wednesday, May 21 to Friday, May 23, 2014**  
Venue : PACIFICO YOKOHAMA  
Sponsor : Society of Automotive Engineers of Japan, Inc.

20145335

## 287-20145335 Effect of Swirl Intensity and Spark Plug Position on Hydrogen Combustion in a Constant Volume Combustion Chamber

Pattanit Nomthongthai <sup>1)</sup> Nuwong Chollacoop <sup>2)</sup> Manida Tongroon <sup>2)</sup> Preechar Karin <sup>1)</sup>

Chinda Charoenphonphanich <sup>3)</sup> Hidenori Kosaka <sup>4)</sup>

*1) International College, King Mongkut's Institute of Technology Ladkrabang  
Chalongkrung Road, Ladkrabang, Bangkok, 10520, Thailand (email: pattanit\_not@gmail.com)*

*2) National Metal and Materials Technology Center, NSTDA*

*Thailand Science Park, Phahonyothin Road, Klong Luang, Pathum Thani, 12120, Thailand*

*3) Department of Mechanical Engineering, King Mongkut's Institute of Technology Ladkrabang  
Chalongkrung Road, Ladkrabang, Bangkok, 10520, Thailand*

*4) Department of Mechanical and Aerospace Systems Engineering, Tokyo Institute of Technology  
O-okayama, Meguro-ku, Tokyo, 152-8550, Japan*

Presented at the JSAE Annual Congress on 5, 22, 2014

**ABSTRACT:** Hydrogen has played a big role in automobile and it is a clean energy that does not produce any pollution. Therefore, this research would like to study the combustion characteristics of dilute Hydrogen-Air mixture in constant volume combustion chamber (CVCC) in wide length of equivalence ratio, swirl intensity from difference initial pressures, chamber temperature and position of spark plug. The results of this study are maximum combustion pressure and combustion delay. Schlieren technics and high speed video camera are used in order to take the video files of swirl intensity and combustion phenomena.

**KEY WORDS:** heat engine, hydrogen, combustion analysis Swirl Intensity, Constant Volume Combustion Chamber (A1)

### 1. INTRODUCTION

Nowadays, fuel prices have been continually increased. Therefore, automotive society has endeavored to improve fuel consumption and thermal efficiency of the engine. In the means time, the clean alternative fuels which result in less emission and global warming effects have been searched. Hydrogen is one of the most interesting candidates to study.

With electrolysis method, hydrogen can be produced from water which covers almost three quarters of the earth. Although cost of electrolysis is still high, it will be decreased in the near future. Hydrogen can be produced via steam reforming process from natural gas, bio-fermentation process from bio mass, bi-photolysis process from algae and etc.

Hydrogen has been used in two means in automotive. One is for fuel-cell vehicles (FCV) and another is for internal combustion engine (ICE) vehicles. However, FCV still has lots of problems due to battery durability and high production cost. Therefore, hydrogen is more proper to apply to ICE vehicles because of trouble-free to manufacture. Also, hydrogen can readily apply in the existing vehicle. Hence, hydrogen has more chance to use widely in the near future.

When hydrogen is used in the internal combustion engines, water is the only product emitted after combustion. Hence, exhaust emissions will be decreased (zero emissions) <sup>(1)</sup>. Properties of hydrogen are high flammability, heating value, and

octane number, which could give rise to increase thermal efficiency. The properties of hydrogen compared with CNG and gasoline are shown in Table 1.

The constant volume combustion chamber (CVCC) is the combustion simulator equipment. The structure is similar to the real engine combustion chamber in case of compression stroke but it does not have the piston movement <sup>(2-3)</sup>. Thus, the volume of the CVCC is constant. Many researchers have investigated in the real engine but it has a lot of parameters that could influence the combustion characteristics. On the other hand, CVCC can be installed with various sensors and equipment, such as ignition, intake, exhaust and temperature control systems that could better control the parameter. Hence, the effects of each parameter can clearly identify.

Hydrogen has high heating value and can ignite in the wide length of equivalence ratio. Therefore, equivalence ratio is one of interesting parameters to study hydrogen combustion. In order to initiate the hydrogen combustion, spark plug is used to ignite the mixture. As the results, its location should affect the combustion characteristics. For real engine application, one cycle can complete with the short period. Hence, the mixing time between fuel and air is relatively short. Consequently, homogeneous mixture can be achieved hardly. Swirl intensity is important parameter to make turbulence inside the combustion chamber to increase chance of reaction between fuel and air.

Thus, the combustion efficiency will be increased. Therefore, the current study has investigated the effects of equivalence ratio, swirl intensity, chamber temperature and the position of spark plug on hydrogen combustion in a constant volume combustion chamber.

Table 1 Properties of hydrogen, CNG and gasoline (4).

Property	Hydrogen	CNG	Gasoline
Density (kg/m <sup>3</sup> )	0.0824	0.72	730
Flammability limits (% in air)	4-75	4.3-15	1.4-7.6
Flammability limits (Ø)	0.1-7.1	0.4-1.6	0.7-4
Auto ignition temp. in air (K)	858	723	550
Flame velocity (m/s)	1.85	0.38	0.42
Adiabatic Flame temp. (K)	2480	2214	2580
Stoichiometric air/fuel ratio	34.48	14.49	14.7
Lower heating value (MJ/kg)	119.7	45.8	44.79
Heat of combustion (MJ/kgair)	3.37	2.9	2.83

2. EXPERIMENTAL PROCEDURE

2.1. CVCC Design

From previous work (10), CVCC was designed based on maximum combustion pressure for safety. The maximum combustion pressure from calculation by using ideal gas law and Otto cycle equation (5-6) is 69 bar. However, over 80 bar of pressure was used in simulation process.

The dimension of CVCC is 70 mm x 100 mm as shown in Fig. 1. The volume of CVCC is equal to 385 cc which similar to one cylinder of sedan gasoline engine car (7-8).

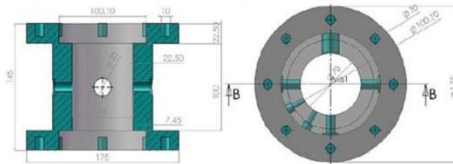


Fig. 1 Dimension of CVCC.

The safety factors of main chamber and lid from simulation program are 12.75 and 7.26, respectively as shown in Fig. 2 and 3. Fig. 4 shows manufactured CVCC.

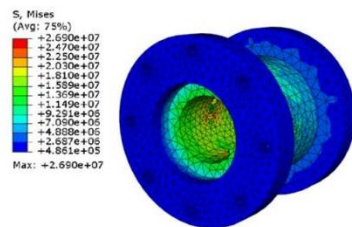


Fig. 2 Simulation result of main chamber.

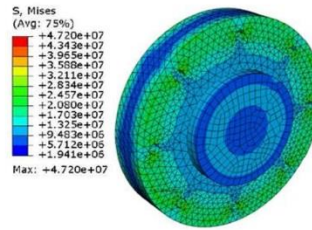


Fig. 3 Simulation result of chamber lid.



Fig. 4 Real CVCC

2.2. Experimental Apparatus

Type The schematic diagram of experimental apparatus for the current study is shown in Fig. 5.

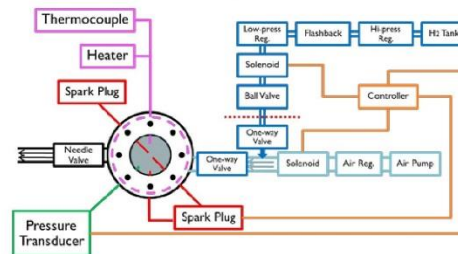


Fig. 5 Experimental schematic diagram of CVCC system.

The procedure to complete the test is described as following:

1. Heating the CVCC to the required temperature by using heater and controller (pink section).
2. Injecting hydrogen into the CVCC (dark blue section)
3. Injecting air into the CVCC to make first stage of premix pressure.
4. Injecting air in high pressure condition (5 bar) to make swirl intensity (light blue section).
5. Igniting mixture of hydrogen – air by using spark plug and ignition coil (red section) controlled by controller (orange section).
6. Collecting combustion pressure data from pressure transducer (green section).
7. Releasing exhaust gas through exhaust valve after combustion finish (black section).

### 2.3. Equivalence Ratio Calculation

This study controlled the pressure of premix mixture before combustion at 5 bar. Partial pressure and real gas equation were used to calculate equivalence ratio as shown below.

Partial pressure equation;

$$P = P_1 + P_2$$

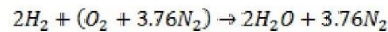
$$x_i = \frac{P_i}{P} = \frac{n_i}{n}$$

$$P_i = x_i \cdot P$$

Real gas equation;

$$PV = ZRT$$

Hydrogen + air chemical equation;



The Z constant or gas compressibility factor of hydrogen and air from thermodynamic table at 105 degree Celsius were used to calculate partial pressure. The result of equivalence ratio calculation by partial pressure method are 0.559, 0.719 and 0.868 while equivalence ratio are 0.3, 0.4 and 0.5 respectively.

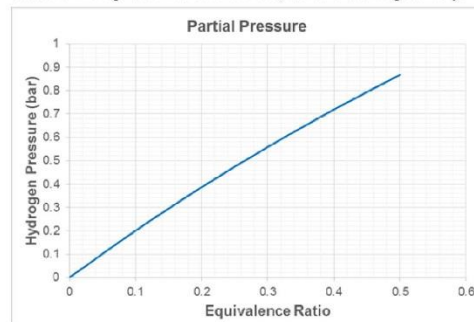


Fig. 6 The result of equivalence ratio with partial pressure calculation.

### 2.4. Swirl Intensity Calibration

The differential intake pressure was used to make swirl intensity<sup>(9)</sup> by varying dP equal to 2, 3 and 4 bar. Air injection duration was calibrated as short as possible that can made initial mixture pressure equal to 5 bar before ignition. The result of air injection duration is 1.8 second.

In the case of high differential pressure, the speed of air inside CVCC is high and also swirl intensity will be higher than those of low differential pressure. High speed video camera (Photron FASTCAM SA3) and Schlieren technic (Fig. 7) were used to capture the motion of mixture inside of CVCC. The high speed video camera will start to capture when intake valve is closed.

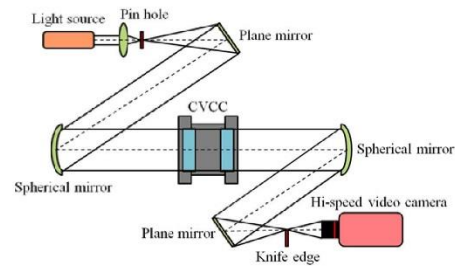


Fig. 7 Schlieren technic diagram.

The computer program (FASTCAM) was used to capture three elements at three positions and calculated the average speed of mixture by measuring the distance of element movement in unit of time as shown in Fig. 8.

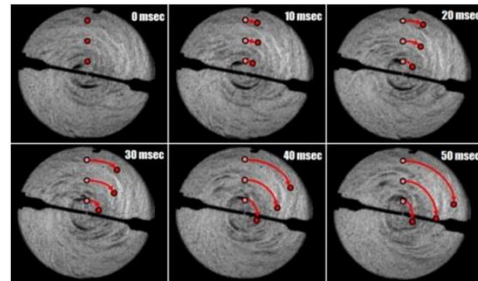


Fig. 8 The program can measure the average speed of swirl intensity by distance of grid pixels in unit of time.

The average speed of swirl intensity of differential pressure at 2, 3 and 4 bar equal to 6.50, 7.54 and 8.10 m/s respectively at 35 msec after intake valve closed<sup>(10)</sup>.

### 2.5. Spark Plug Position

CVCC was designed to install three spark plugs at two locations in order to measure the combustion phenomena. One was located in the center whereas others were installed at the sidewall as shown in Fig. 9.

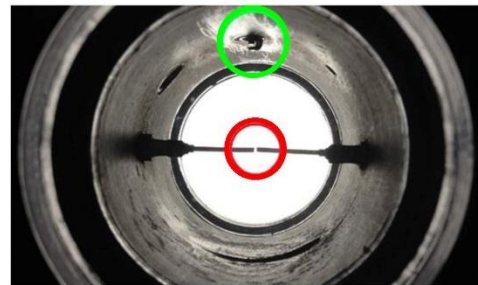


Fig. 9 Position of spark plug. Red circle were used for center ignition and green circle was used for sidewall ignition.

### 3. RESULTS AND DISCUSSION

Maximum combustion pressure shows power output from combustion in unit of bar from start of ignition. High combustion pressure value means high combustion performance and high combustion efficiency.

Combustion delay has been considered in combustion phenomena. This duration called the preparatory phase during ignition has already been admitted into the combustion chamber, but combustion has not yet been commenced<sup>(11)</sup>. This duration was defined as the time between start of ignition and 10 percent of maximum combustion pressure<sup>(12)</sup>.

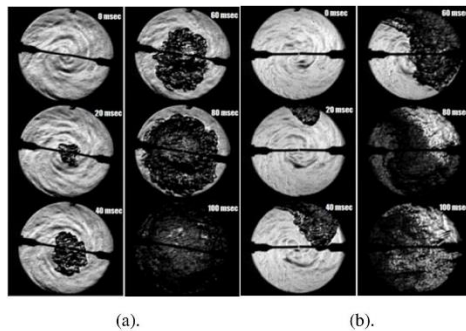


Fig. 10 Combustion phenomena at equivalence ratio equal to 0.3 and swirl intensity at 4 bar with (a). Center ignition and (b). Side ignition.

#### 3.1. Effect of Chamber Temperature

The equivalence ratio at 0.25 was used to investigate the combustion phenomena in case of chamber temperature variation. The chamber temperatures in this study were 75, 85, 95 and 105 degree Celsius.

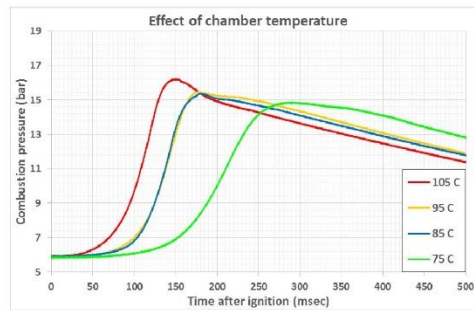


Fig. 11 Effect of premix temperature in order to measure maximum combustion pressure and combustion delay.

Increasing chamber temperature to 75, 85, 95, and 105 degree Celsius resulted in the maximum combustion pressure

14.87, 15.37, 15.48 and 16.21 bar respectively while combustion delay was decreased. The delay times were 145, 101, 95 and 69 msec.

#### 3.2. Effect of Swirl Intensity and Position of Spark Plug

Equivalence ratio was varied to 0.3, 0.4 and 0.5, while swirl intensity was controlled at 6.50, 7.54, and 8.10 m/s, with chamber temperature at 105 degree Celsius. Two positions of spark plug were used to measure the combustion phenomena.

##### 3.2.1. Equivalence Ratio at 0.3

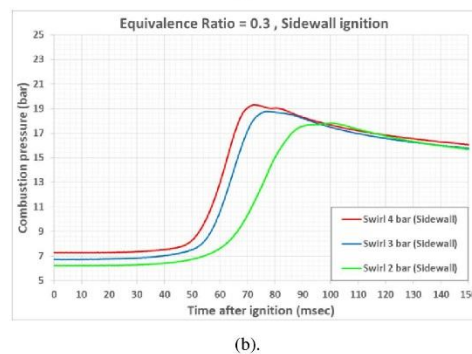
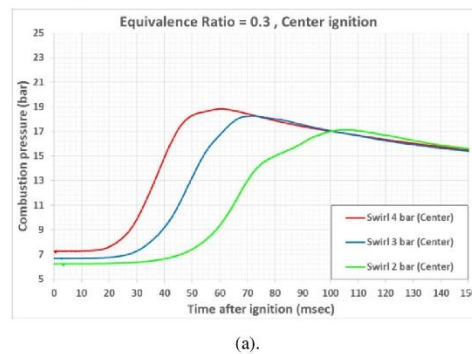


Fig. 12 Effect of swirl intensity and position of spark plug on equivalence ratio at 0.3. (a). Center ignition, (b). Side ignition.

As shown in Fig. 12, when swirl intensity was increased, the maximum combustion pressure were increased while combustion delay were decreased in both cases of spark plug locations.

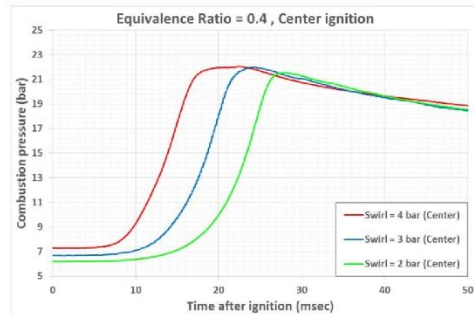
##### Center Ignition

Maximum combustion pressures were 17.14, 18.26 and 18.84 bar and combustion delays were 50, 34 and 29 msec while swirl intensities were 6.50, 7.54 and 8.10 m/s respectively.

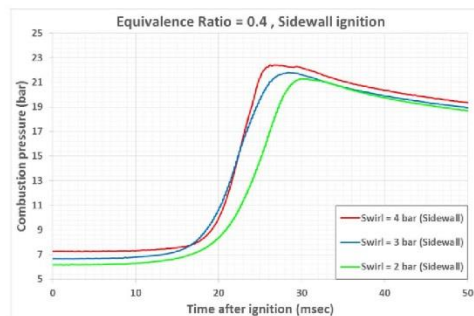
### Sidewall ignition

Maximum combustion pressures were 17.83, 18.79 and 19.30 bar and combustion delays were 58, 53 and 51 msec while swirl intensities were 6.50, 7.54 and 8.10 m/s respectively.

### 3.2.2. Equivalence Ratio at 0.4



(a).



(b).

Fig. 13 Effect of swirl intensity and position of spark plug on equivalence ratio at 0.4. (a). Center ignition, (b). Side ignition.

From Fig. 13, when swirl intensity was increased, the maximum combustion pressures were increased while combustion delays were slight decreased in both cases of spark plug locations.

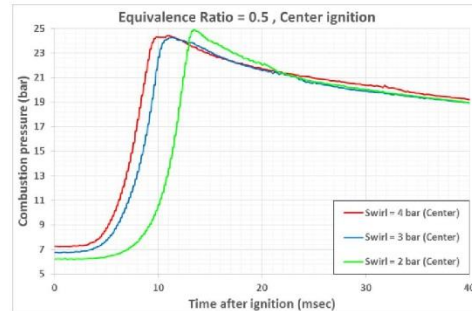
#### Center Ignition

Maximum combustion pressures were 21.54, 22.00 and 22.06 bar and combustion delays were 17, 16 and 10 msec while swirl intensities were 6.50, 7.54 and 8.10 m/s respectively.

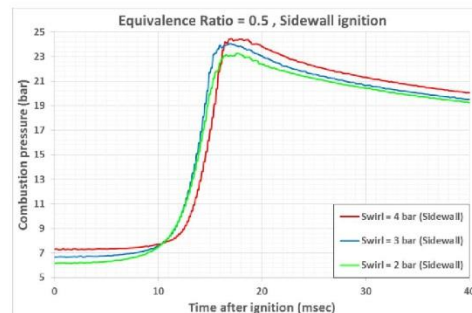
#### Sidewall ignition

Maximum combustion pressures were 21.28, 22.39 and 22.42 bar and combustion delays were 19, 17 and 19 msec while swirl intensities were 6.50, 7.54 and 8.10 m/s respectively.

### 3.2.3. Equivalence Ratio at 0.5



(a).



(b).

Fig. 14 Effect of swirl intensity and position of spark plug on equivalence ratio at 0.5. (a). Center ignition, (b). Side ignition.

From Fig. 14, when swirl intensity was increased, there is no significant different of maximum combustion pressure in case of center ignition. However, maximum combustion pressures were increased in case of sidewall ignition. The swirl intensity has no effect on combustion delay in both cases of spark plug locations

#### Center Ignition

Maximum combustion pressures were 24.89, 24.24 and 24.41 bar and combustion delays were 8, 6 and 5 msec while swirl intensities were 6.50, 7.54 and 8.10 m/s respectively.

#### Sidewall ignition

Maximum combustion pressure rise rates were 23.25, 24.08 and 24.45 bar and combustion delays were 11, 11 and 13 msec while swirl intensities were 6.50, 7.54 and 8.10 m/s respectively.

#### 4. CONCLUSIONS

When increasing the chamber temperature, the maximum combustion pressure was increased while the combustion delay was decreased. The high temperature before combustion acts as catalyst for reaction between hydrogen and oxygen in air. Hence, the combustion will arise faster than low chamber temperature.

Increasing the equivalence ratio means increasing the power input. Therefore the maximum combustion pressure is higher and also combustion delay is shorter when compared with low equivalence ratio.

When the swirl intensity is increased, hydrogen and air can be completely mixed up. Premix mixture is nearly a homogeneous. Therefore, combustion efficiency will be higher than low swirl intensity conditions. However, in case of high equivalence ratio, swirl intensity has no effect because of high amount of hydrogen and high chance of reaction between hydrogen and oxygen.

When changing the ignition position to sidewall position, the combustion delay is longer than center ignition. The combustion flame can fully expand in CVCC faster than sidewall ignition. Therefore, the maximum combustion pressure is slightly lower than center ignition.

#### REFERENCES

- (1) Bohacik, T., De Maria, S. and Saman, W.Y., Constant-Volume Adiabatic Combustion of Stoichiometric Hydrogen-Oxygen Mixtures, WREC 1996, University of South Australia, (1996).
- (2) Tinaut, F.V., Melgar, A., Giménez, B. and Reyes, M., Characterization of The Combustion of Biomass Producer Gas in a Constant Volume Combustion Bomb, *Fuel* 89, (2010) 724-731.
- (3) Dhananjay Kumar Srivastava, Kewal Dharamshi and Avinash Kumar Agarwal., Flame kernel characterization of laser ignition of natural gas-air mixture in a constant volume combustion chamber, *Optic and Lasers in Engineering* 49, (2011) 1201-1209.
- (4) Technical Review of Hydrogen-fueled Internal Combustion Engines, Sandia National Laboratory.
- (5) Pulkrabek, Willard W., *Engineering Fundamentals of the Internal Combustion Engine*, Prentice Hall, New Jersey.
- (6) Turns, Stephen R., *An Introduction to Combustion: Concepts and Applications*, 2<sup>nd</sup> edition, ISBN 0-70-230096-5, McGraw-Hill Series in Mechanical Engineering.
- (7) Dugkhuntod, T., Nomthongthai, P. and Songsaengchan, Y., Ethanol Combustion Characteristics in a Constant-Volume Combustion Chamber (in Thai), Department of Mechanical Engineering, KMITL (2009).
- (8) Ornman, P., Kosaka, H., Chollacoop, N. and Charoenphonphanich, C., Study on Combustion Characteristics of Direct Injection Stratified Charge in Ethanol/Gasoline Blends, The First TSME International Conference on Mechanical Engineering, (2010).
- (9) Ornman, P., Charoenphonphanich, C., Chollacoop, N. and Kosaka, H., Effect of Ethanol Concentration of Gasohol on Lean Flammability Limit in Direct-Injection Stratified Charge Engine, The 7<sup>th</sup> International Conference on Automotive Engineering (ICAE-7), (2011).
- (10) Nomthongthai, P., Tongroon, M., Charoenphonphanich, C., Kosaka, H., et al., Design of Hydrogen Constant Volume Combustion Chamber, TSME International Conference on Mechanical Engineering, (2012).
- (11) Shahabuddin, M., Liaquat, A.M., Masjuki, H.H., Kalam, M.A., et al., Ignition Delay, Combustion and Emission Characteristics of Diesel Engine Fueled with Biodiesel, *Renewable and Sustainable Energy Reviews* 21, (2013) 623-632.
- (12) Lee, K., Lee, C., Jeoung, H., A Study on the Effect of Stratified Mixture Formation on Combustion Characteristics in a Constant Volume Combustion Chamber, *JSME International Journal Series B*, (2009) Vol. 48.

#### ACKNOWLEDGMENTS

The authors are grateful to scholarship support from TAIST Tokyo Tech Program, with special acknowledgement for Automotive Laboratory, KMITL and Bioenergy Laboratory, NSTDA, MTEC, Thailand.

Pathumwan Institute of Technology (Thailand) for their supports in pressure transducer and pressure sensor. Hi-Tech resource (Thailand) company for their helps and supports in high speed video camera.

The authors also thank Thailand Research Fund (TRF) for supports the research scholarship.

# Combustion Characteristics of Hydrogen in Constant Volume Combustion Chamber

Presented by

**Pattanit Nomthongthai<sup>1</sup>**

*27<sup>th</sup> July 2015*

Advisors :

1. Dr. Manida Tongroon<sup>2</sup>
2. Asst. Prof. Dr. Chinda Charoenphonphanich<sup>3</sup> and
3. Prof. Dr. Hidenori Kosaka<sup>4</sup>

<sup>1</sup>TAIST Tokyo Tech Automotive Engineering Program, International College, King Mongkut's Institute of Technology Ladkrabang, Thailand

<sup>2</sup>National Metal and Materials Technology Center (MTEC), NSTDA, Thailand

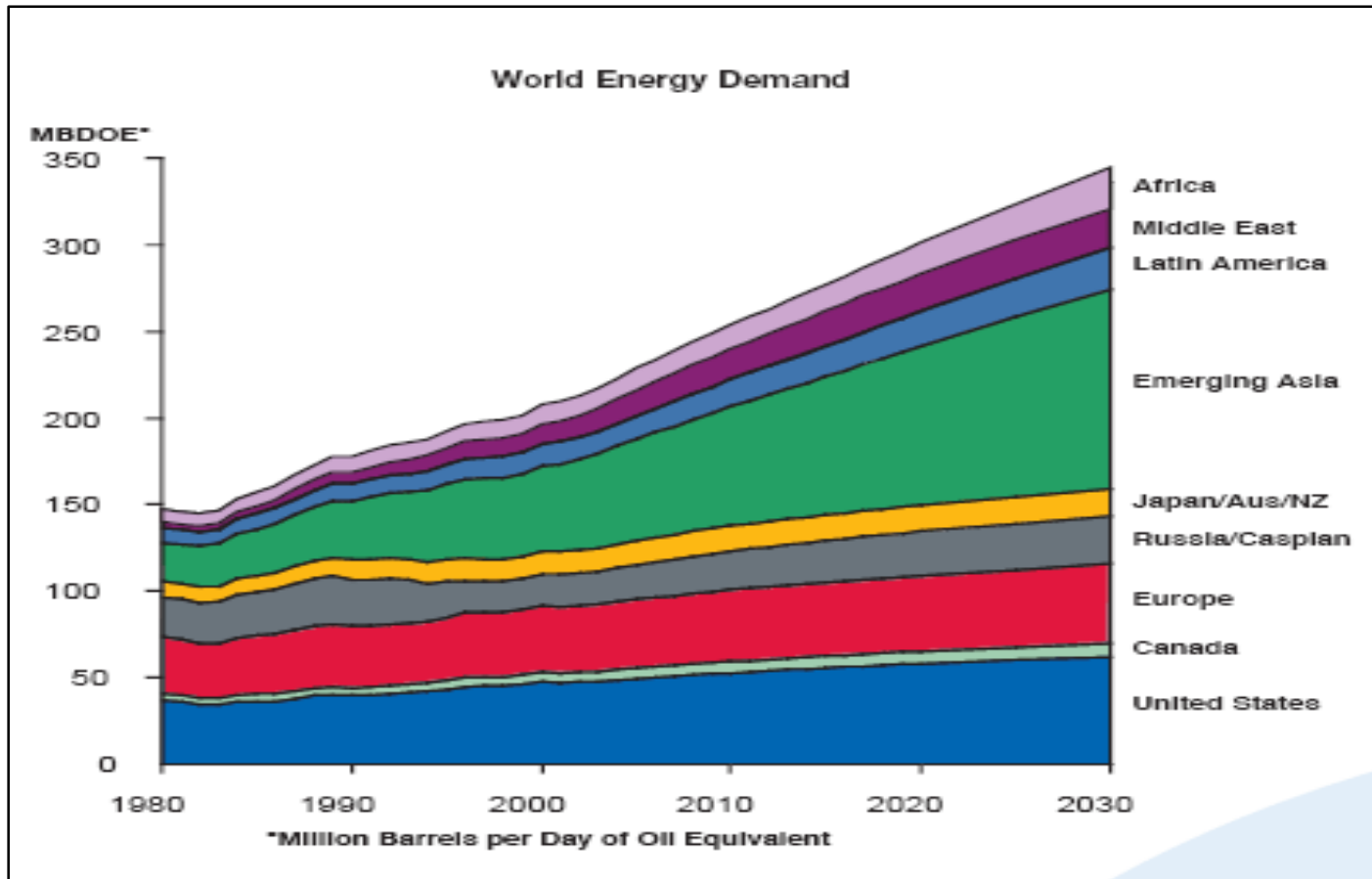
<sup>3</sup>Faculty of Engineering, King Mongkut's Institute of Technology Ladkrabang, Thailand

<sup>4</sup>Department of Mechanical and Control Engineering, Tokyo Institute of Technology, Japan

# Contents

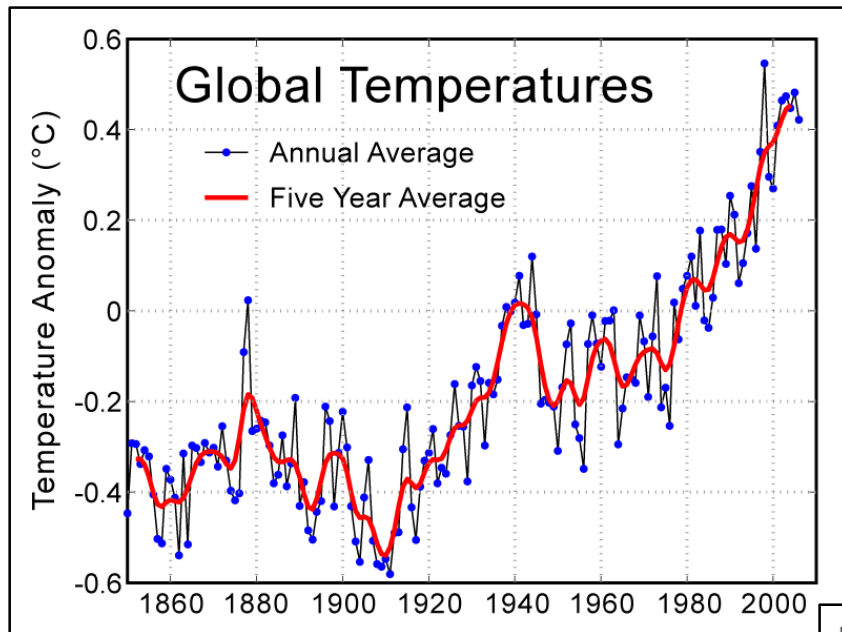
- Introduction
- Literature review
- Objective
- Experimental setup
- Results
- Conclusions

# Introduction



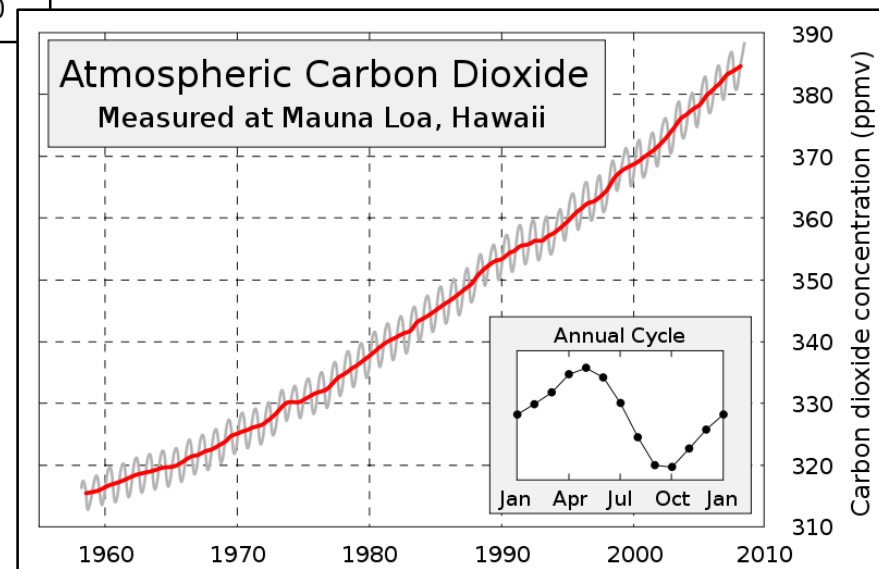
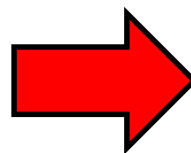
\* Exxon Mobil Corporation

# Introduction



← Increasing of Global temperature

Increasing of CO<sub>2</sub>



# Introduction

## Type of Alternative fuels

- Liquefied Petroleum Gas (LPG)
- Compressed Natural Gas (CNG)
- Liquefied Natural Gas (LNG)
- Methanol
- Ethanol
- Biodiesel
- Electricity
- Hydrogen

# Introduction



Hydrogen is the new alternative fuel to replace the conventional fuel that will be empty in the near future. The combustion product of it is only steam. So, zero emissions can be appear.

# Introduction

Properties	Hydrogen	CNG	Gasoline
Density (kg/m <sup>3</sup> )	0.0824	0.72	730
Flammability limits (volume % in air)	4-75	4.3-15	1.4-7.6
Flammability limits (Ø)	0.1-7.1	0.4-1.6	0.7-4
Autoignition temperature in air (K)	858	723	550
Flame velocity (m/s)	1.85	0.38	0.42
Adiabatic Flame temperature (K)	2480	2214	2580
Stoichiometric air/fuel mass ratio	35.52	14.49	14.7
Lower heating value (MJ/kg)	119.7	45.8	44.79
Heat of combustion (MJ/kg <sub>air</sub> )	3.37	2.9	2.83

\* Technical Review of Hydrogen-fueled Internal Combustion Engines, Sandia National Laboratory

## Benefit of Hydrogen:

- Hi-speed Flame velocity
- Wide range of equivalence ratio for possible combustion  
 (because of small size of hydrogen molecule resulting in more homogenous mixture)
- High Heating value (combustion) and Difficult to Auto ignition  
 (due to strong bonding of hydrogen molecule)
- Low consumption  
 (because of high heating value per unit of mass)

# Contents

- Introduction
- Literature review
- Objective
- Experimental setup
- Results
- Conclusions

# Literature Review

*Energy & Fuels* **2009**, 23, 1431–1436

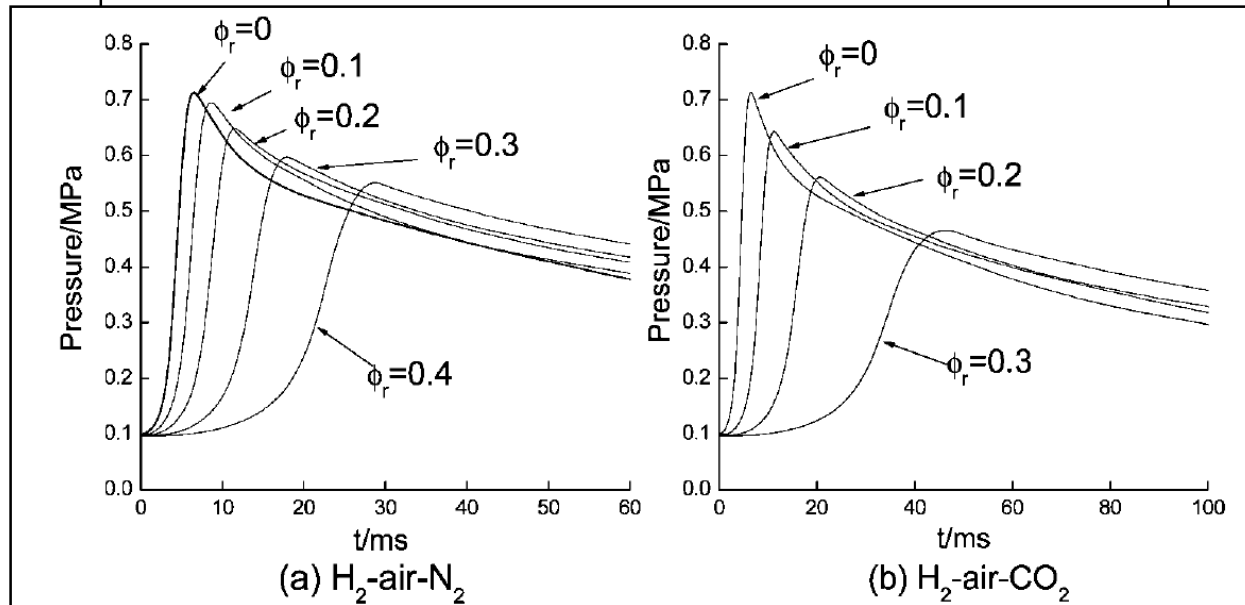
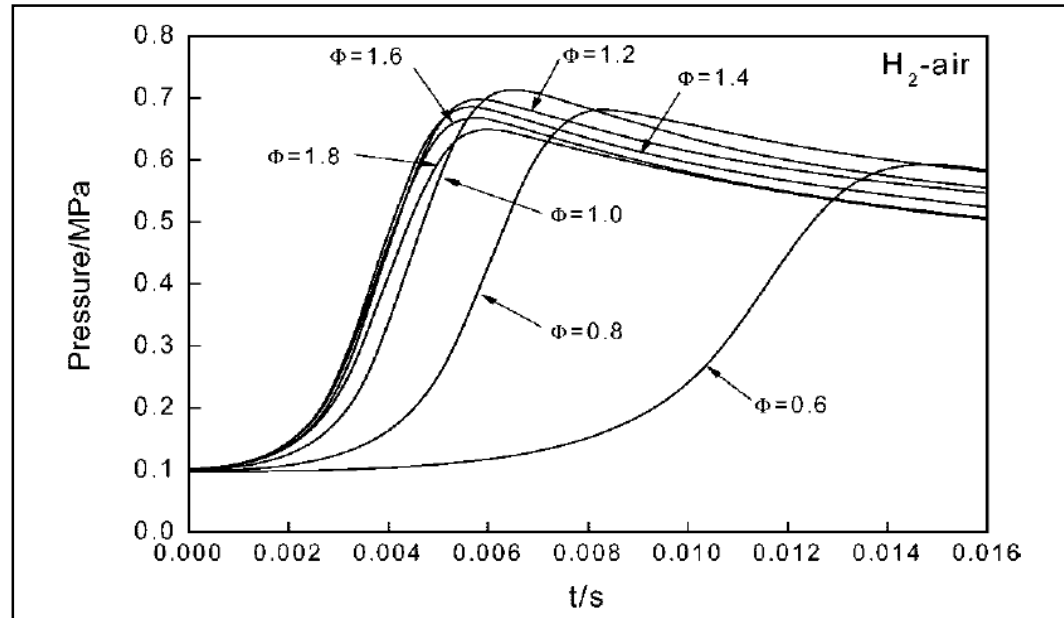
## **Premixed Combustion of Diluted Hydrogen–Air Mixtures in a Constant Volume Bomb**

Haiyan Miao,\* Qian Huang, Erjiang Hu, Zuohua Huang, and Deming Jiang

*State Key Laboratory of Multiphase Flow in Power Engineering, Xi'an Jiaotong University,  
Xi'an 710049, China*

*Received September 17, 2008. Revised Manuscript Received November 9, 2008*

# Literature Review



# Literature Review

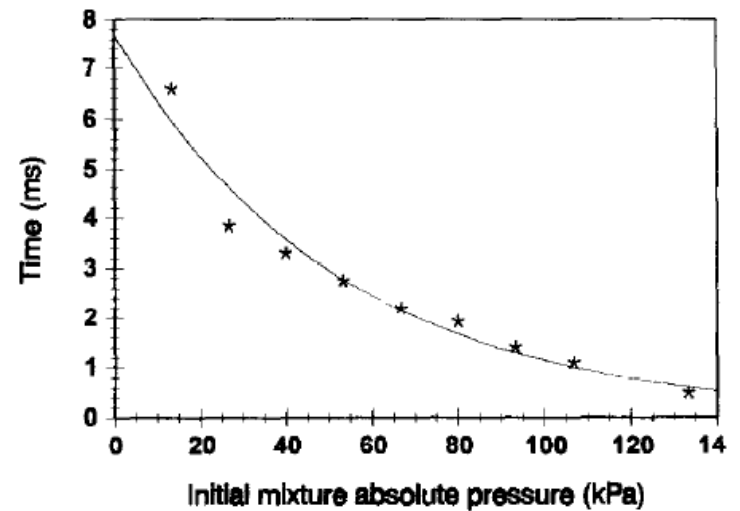
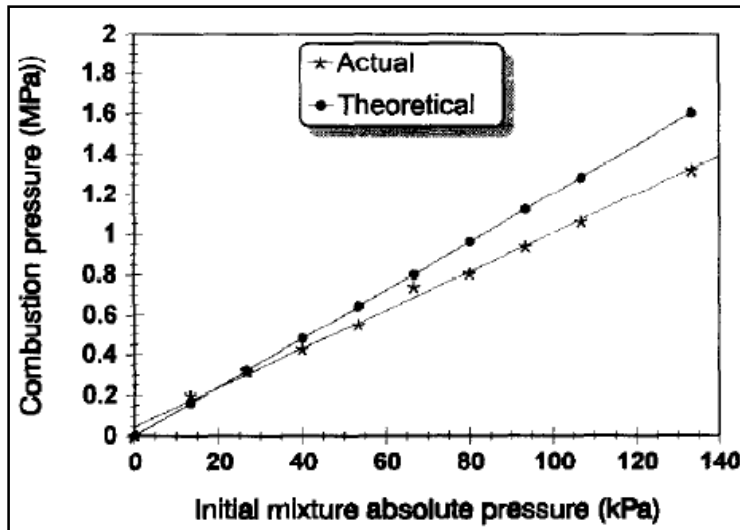
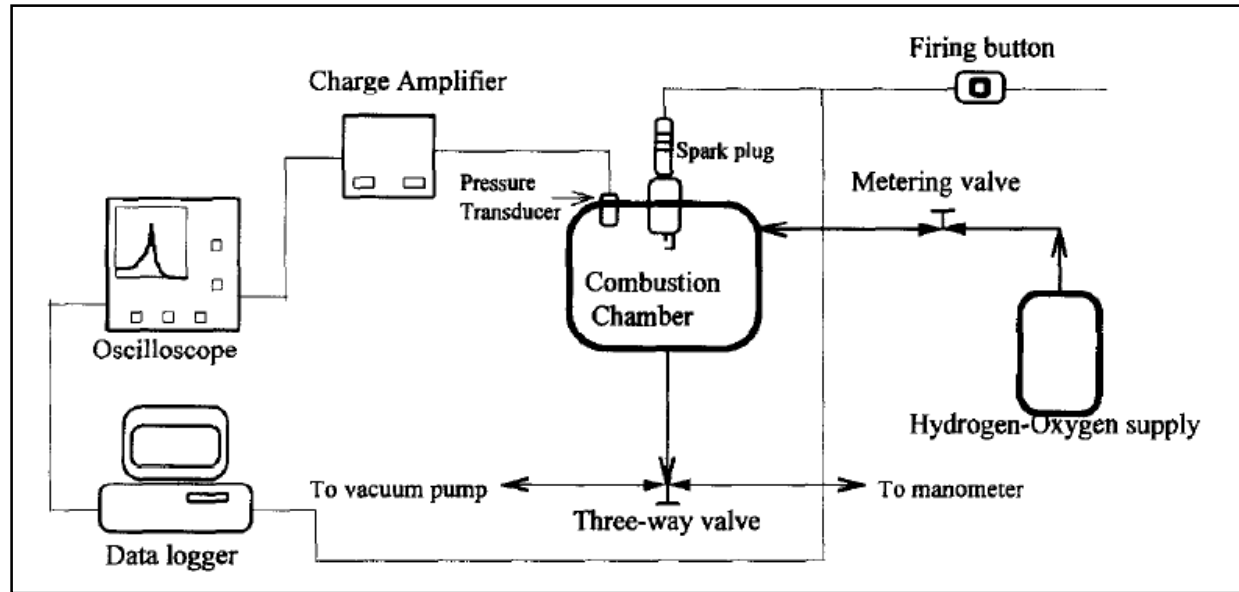
WREC 1996

## **CONSTANT-VOLUME ADIABATIC COMBUSTION OF STOICHIOMETRIC HYDROGEN-OXYGEN MIXTURES**

T. Bohacik, S. De Maria, W. Y. Saman

Energy and Engines Research Group,  
School of Manufacturing and Mechanical Engineering  
University of South Australia,  
South Australia 5095  
Australia

# Literature Review



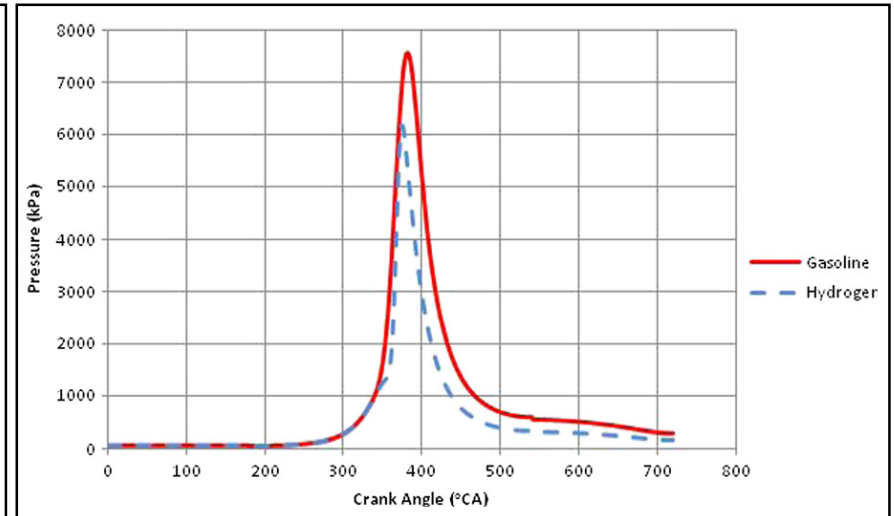
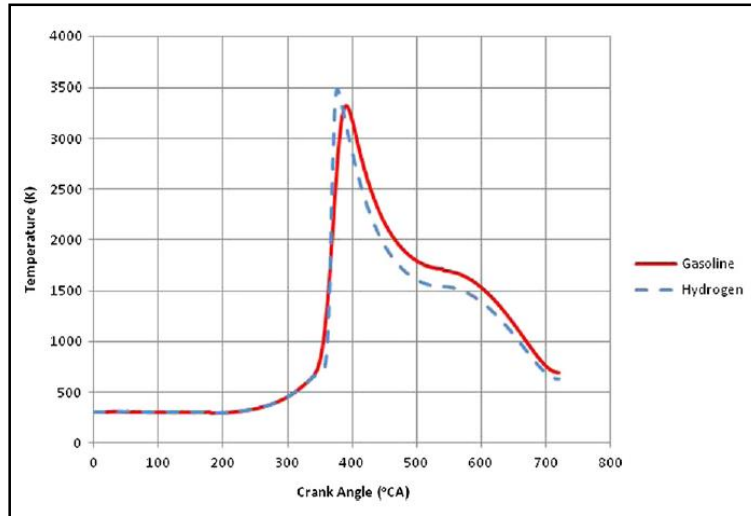
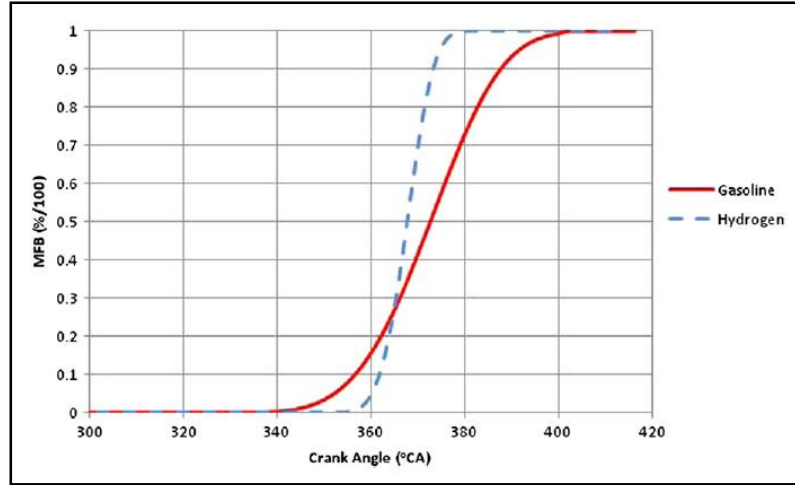
# Literature Review

## **Comparative combustion characteristics of gasoline and hydrogen fuelled ICEs**

*Jonathan Nieminen\**, *Ninochka D'Souza*, *Ibrahim Dincer*

*Faculty of Engineering and Applied Science, University of Ontario Institute of Technology, 2000 Simcoe Street North, Oshawa, ON L1H 7K4, Canada*

# Literature Review

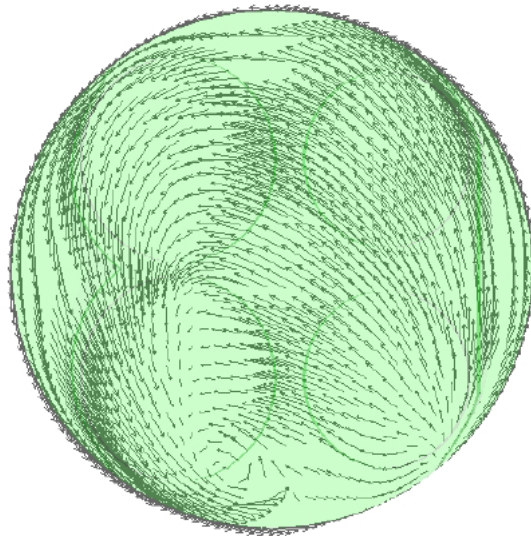


# Literature Review

## **Modeling of Gasoline Direct Injection Mixture Formation Using KIVA-3V: Development of Spray Breakup & Wall Impingement Models and Validation with Optical Engine Planar Laser Induced Fluorescence Measurements.**

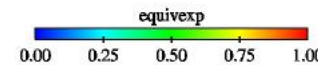
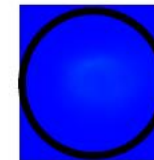
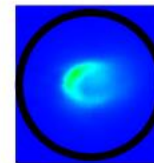
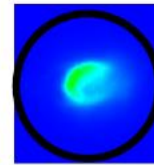
\*B. P. Vanzielegem, C. A. Chryssakis, R. O. Grover, V. Sick, H. G. Im,  
and D. N. Assanis

*W.E. Lay Automotive Laboratory  
Department of Mechanical Engineering, University of Michigan  
1231 Beal Ave., Ann Arbor, MI 48105, U.S.A.*



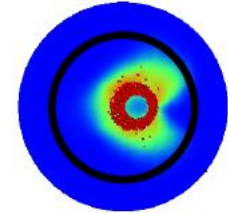
# Literature Review

Experiment

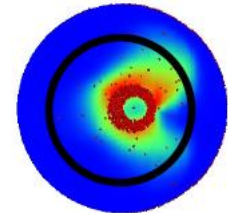


Model  
 Gas & Liquid Phase

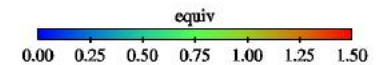
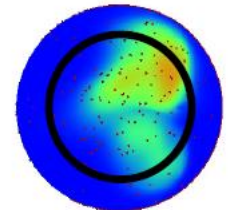
82° CA



88° CA



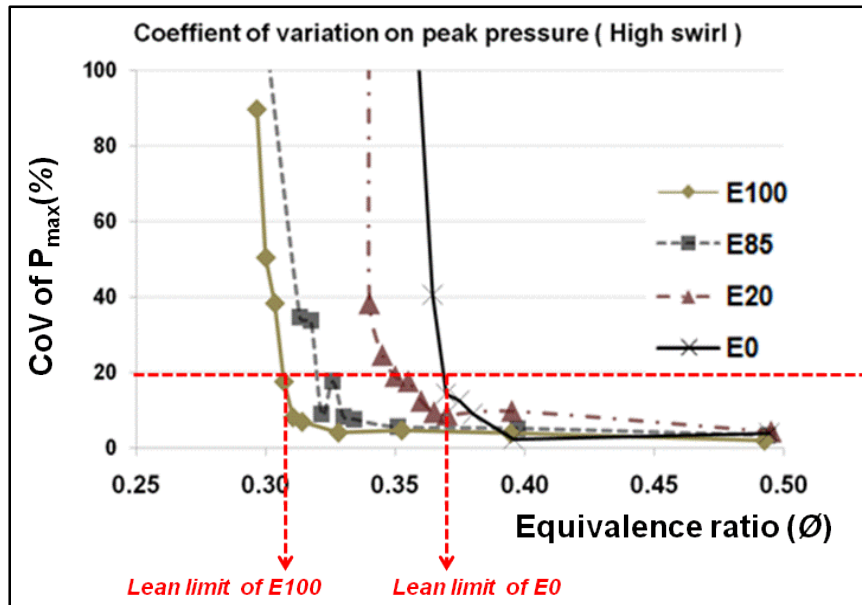
97° CA



# Literature Review

Study of cyclic variations of direct-injection combustion fueled with natural gas hydrogen blends using a constant volume vessel

Jinhua Wang et.al (2008)



The definition of lean limit that use in this study. In this figure, the data of 20 cycles of each condition were collected for investigate the lean limit and maximum acceptable value of CoV was 20%.

# Contents

- Introduction
- Literature review
- **Objective**
- Experimental setup
- Results
- Conclusions

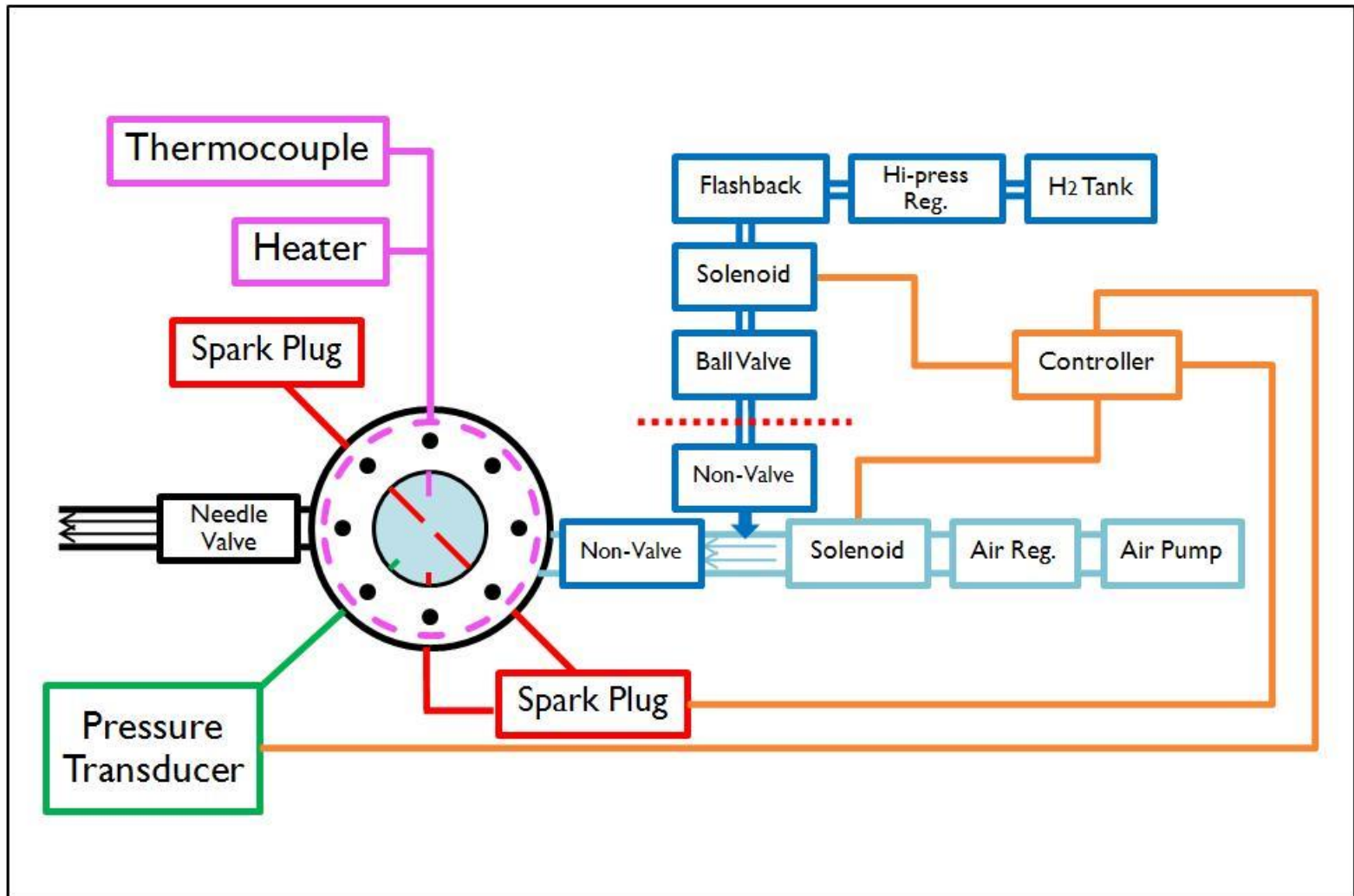
# Objective

- To study and analyze the main parameter that has the effect for hydrogen combustion
- To optimize parameters to get the highest efficiency
- To provide technical combustion information

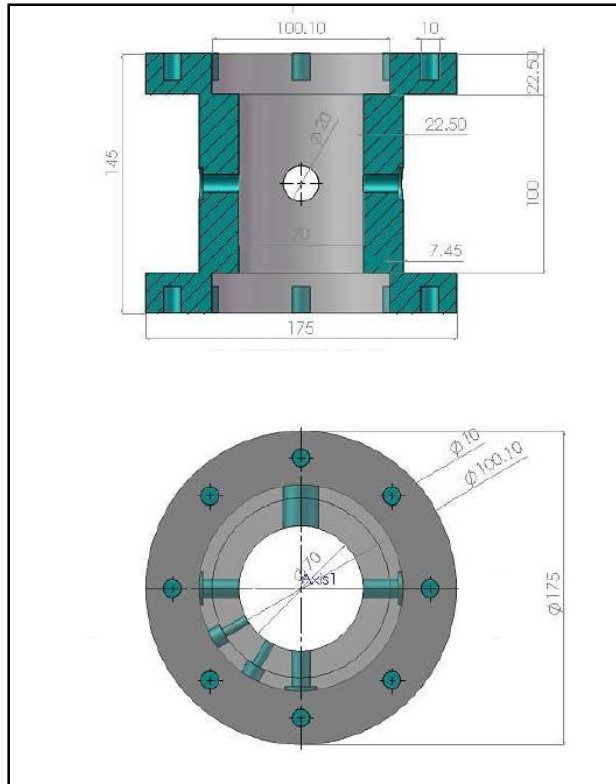
# Contents

- Introduction
- Literature review
- Objective
- **Experimental setup**
- Results
- Conclusions

# Experimental Setup

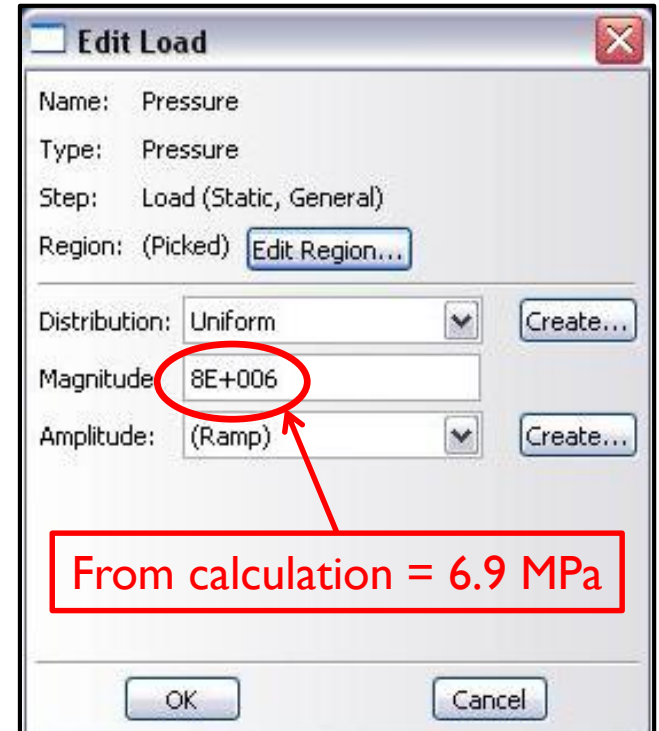
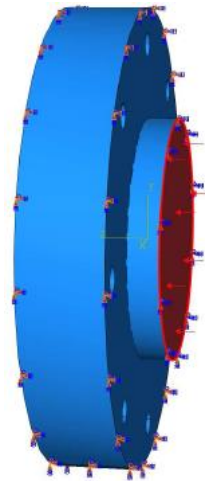
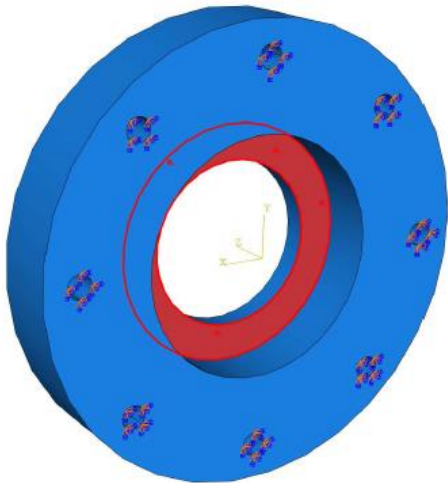
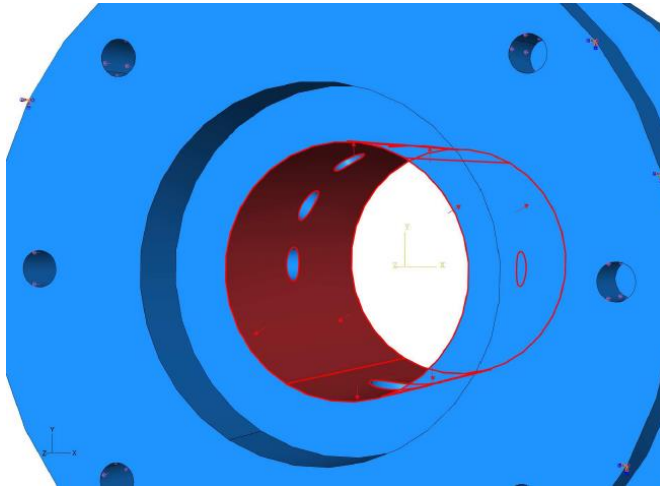


# Experimental Setup (CVCC Design)



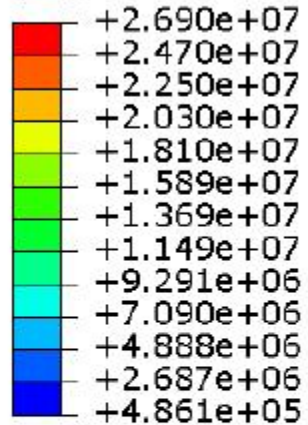
Dimension of CVCC  
 Inner Diameter : 70 mm.  
 Length : 100 mm.  
 Volume : 385 cc.

# Experimental Setup (CVCC Design)

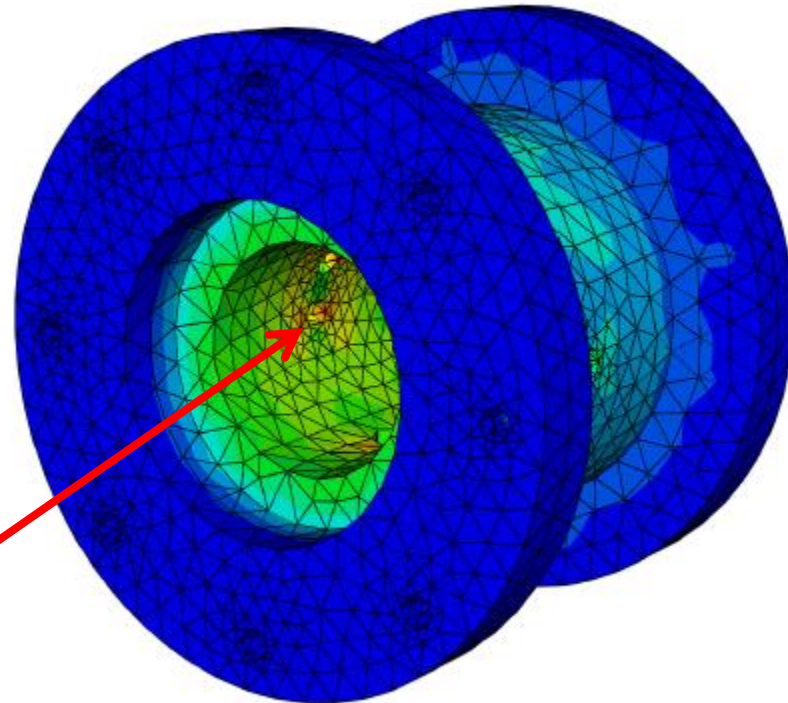


# Experimental Setup (CVCC Design)

S, Mises  
(Avg: 75%)



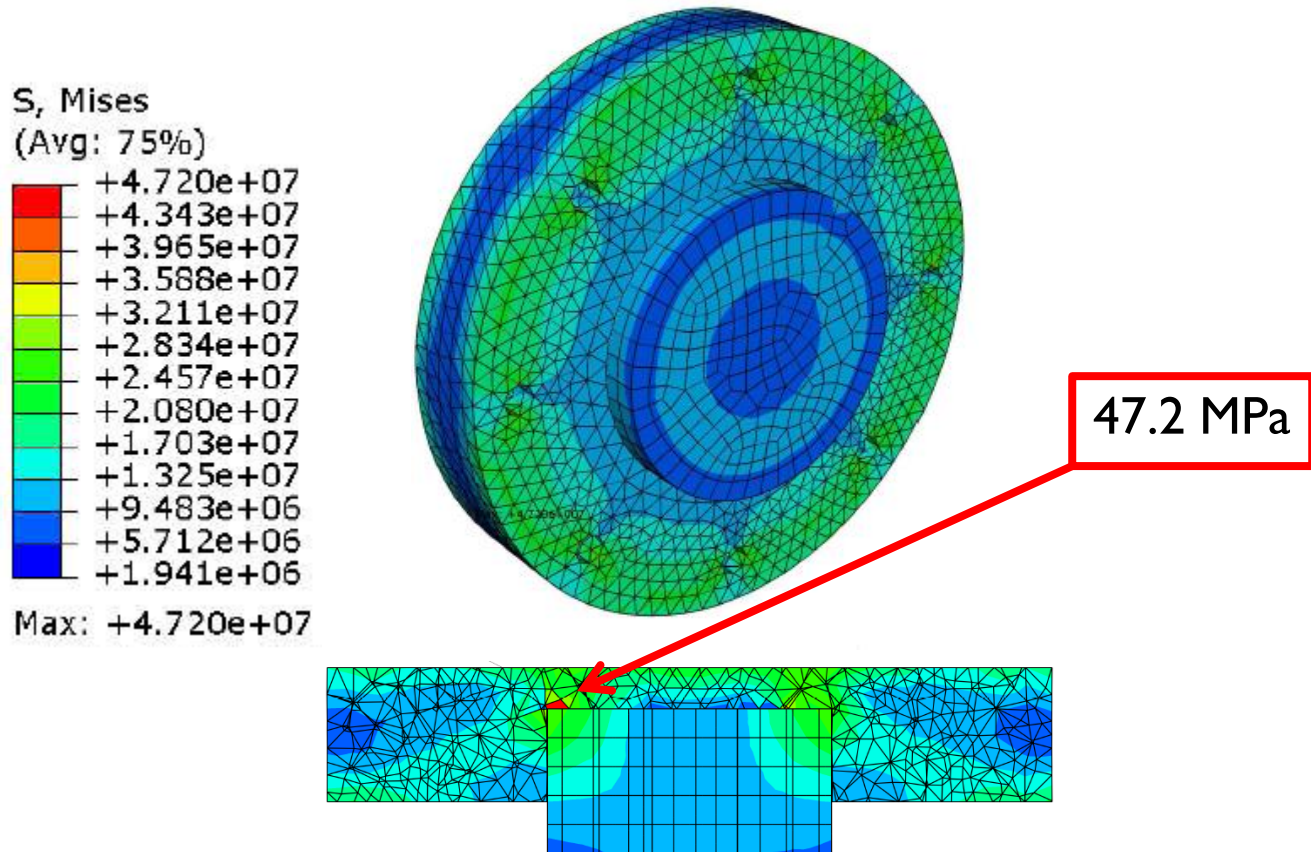
Max: +2.690e+07



26.9 MPa

Maximum Stress : 26.9 MPa , Safety Factor = 8.55

# Experimental Setup (CVCC Design)

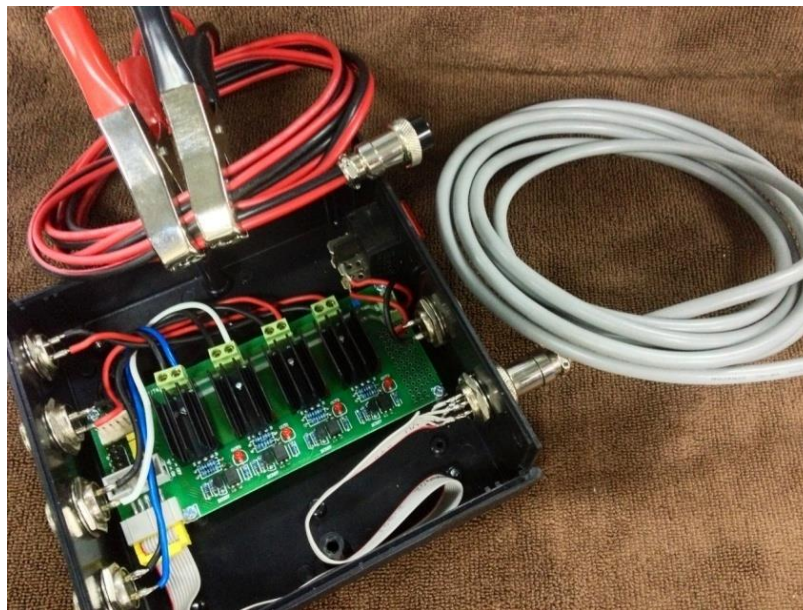


Maximum Stress : 47.2 MPa , Safety Factor is 4.87

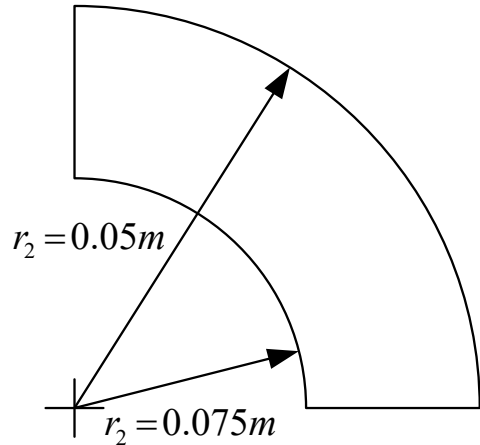
# Experimental Setup (CVCC Design)



# Experimental Setup (Device Design)



# Experimental Setup (Heater Calculation)



$$q_r = \frac{2\pi LK(T_{s2} - T_{,wall})}{\ln(r_2 / r_1)}$$

$$Q = 1300 \text{ w}$$

$$T_{,wall} = 185 \text{ Degree C}$$

# Experimental Setup (Device Design)



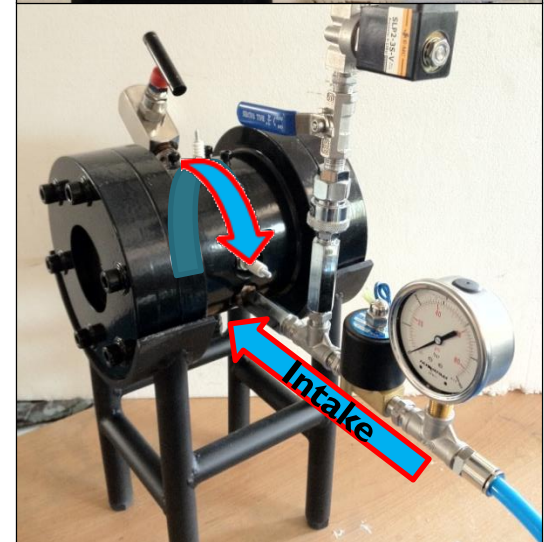
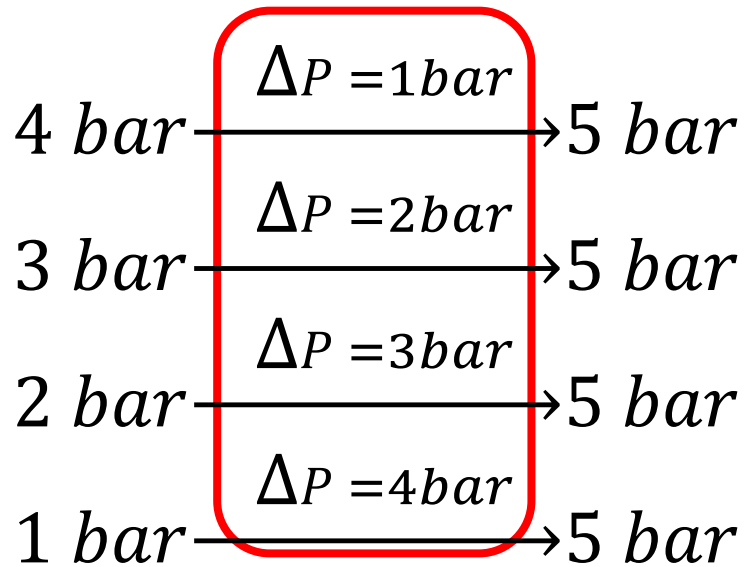
Safety device	F53N*	F53N/H*	RF53N	RF53N/H
Flame arrester <b>FA</b>		X		X
Non-return valve <b>NV</b>		-		X
Temperature sensitive cut-off valve <b>TV</b>		X		X
Weight [g]		181		195
Certification BAM	BAM/ZBA/003/04			
Material	Housing – Stainless steel; Flame arrester – Stainless steel; Seal – Elastomer			
Gases	max. working pressure [bar]			
Acetylene (A)	1,5	-	1,5	-
Natural gas (M)	5,0	12,0	5,0	12,0*
LPG (P)	5,0	8,0	5,0	8,0
Hydrogen (H)	3,0	10,0	3,0	9,0
Ethylene (E)	-	9,0	-	5,0
Oxygen (O)	30,0	-	30,0	-
Compressed air (D)	30,0	-	30,0	-



INDUSTRIAL SCIENTIFIC The Gas Detection People				
Case:	Rugged, water-resistant polycarbonate shell with protective concussion-proof overmold. RFI resistant.			
Dimensions:	3.7 x 2 x 1.1 inches (94 mm x 50.8 mm x 27.9 mm)			
Weight:	3 oz. (85 grams)			
Measuring Ranges:	Gas	Symbol	Range	Increments
	Carbon Monoxide	CO	0-1,500	1 ppm
	Hydrogen Sulfide	H <sub>2</sub> S	0-500 ppm	0.1 ppm
	Oxygen	O <sub>2</sub>	0-30% of volume	0.1%
	Nitrogen Dioxide	NO <sub>2</sub>	0-150 ppm	0.1 ppm
	Sulfur Dioxide	SO <sub>2</sub>	0-150 ppm	0.1 ppm
	Ammonia	NH <sub>3</sub>	0-500 ppm	1 ppm
	Chlorine	Cl <sub>2</sub>	0-100 ppm	0.1 ppm
	Chlorine Dioxide	ClO <sub>2</sub>	0-1 ppm	0.01 ppm
	Phosphine	PH <sub>3</sub>	0-10 ppm	0.01 ppm
	Hydrogen Cyanide	HCN	0-30 ppm	0.1 ppm
	Hydrogen	H <sub>2</sub>	0-2,000 ppm	1 ppm
	CO/H2 Null	CO/H2 Null	0-1,000 ppm	1 ppm

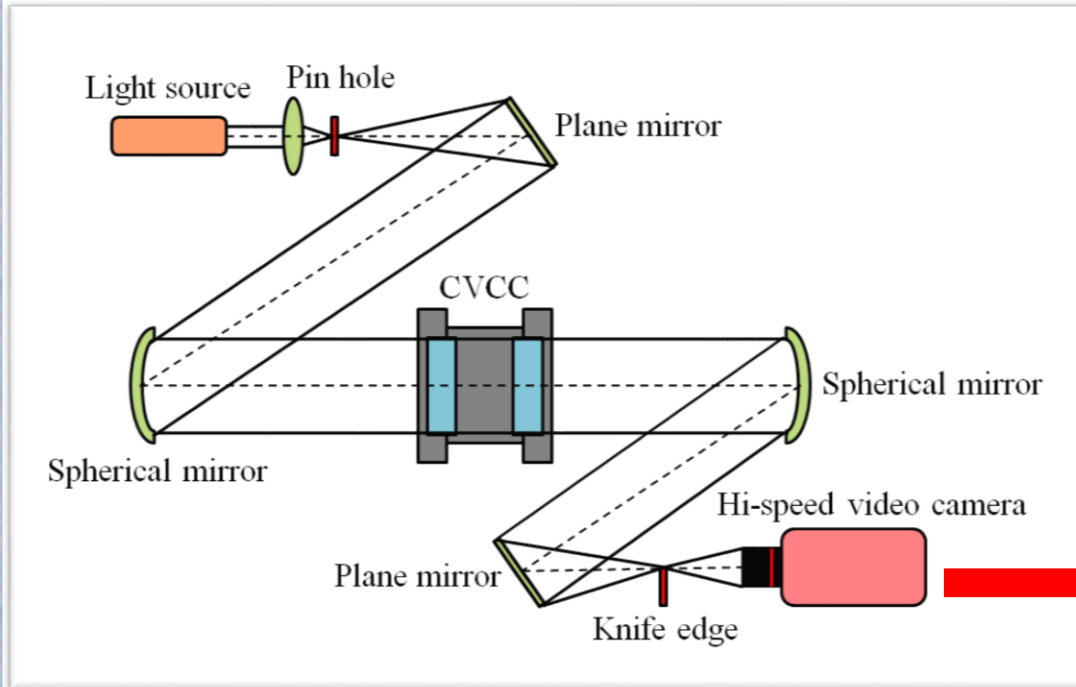
# Experimental Setup (Swirl intensity calibration)

4 Conditions :



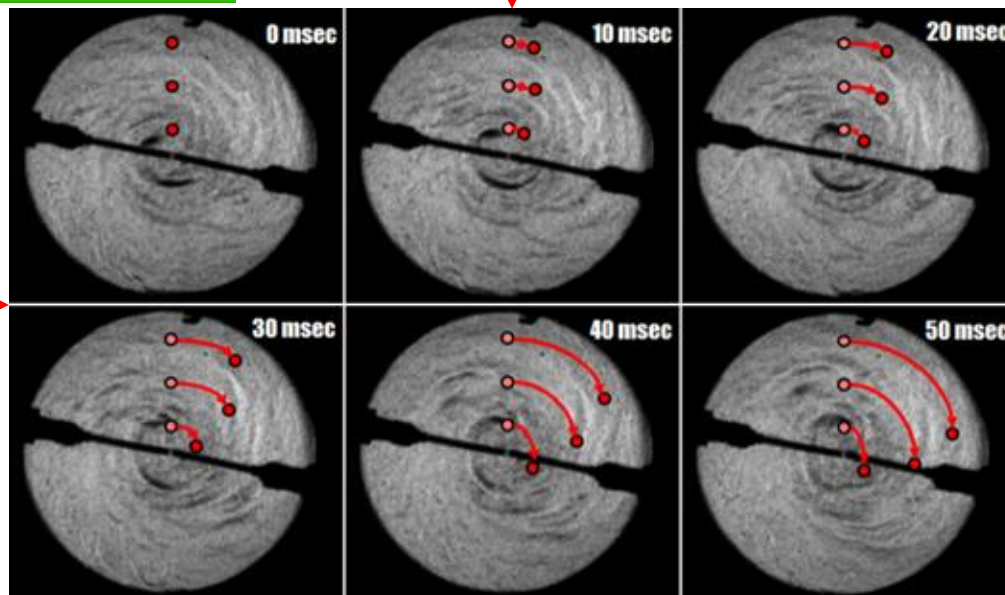
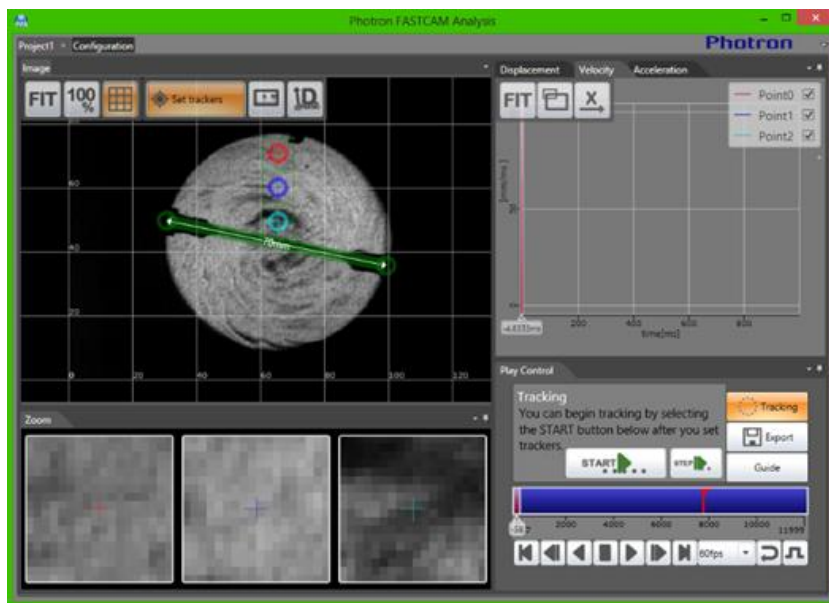
\* Gauge pressure

# Experimental Setup (Swirl intensity calibration)

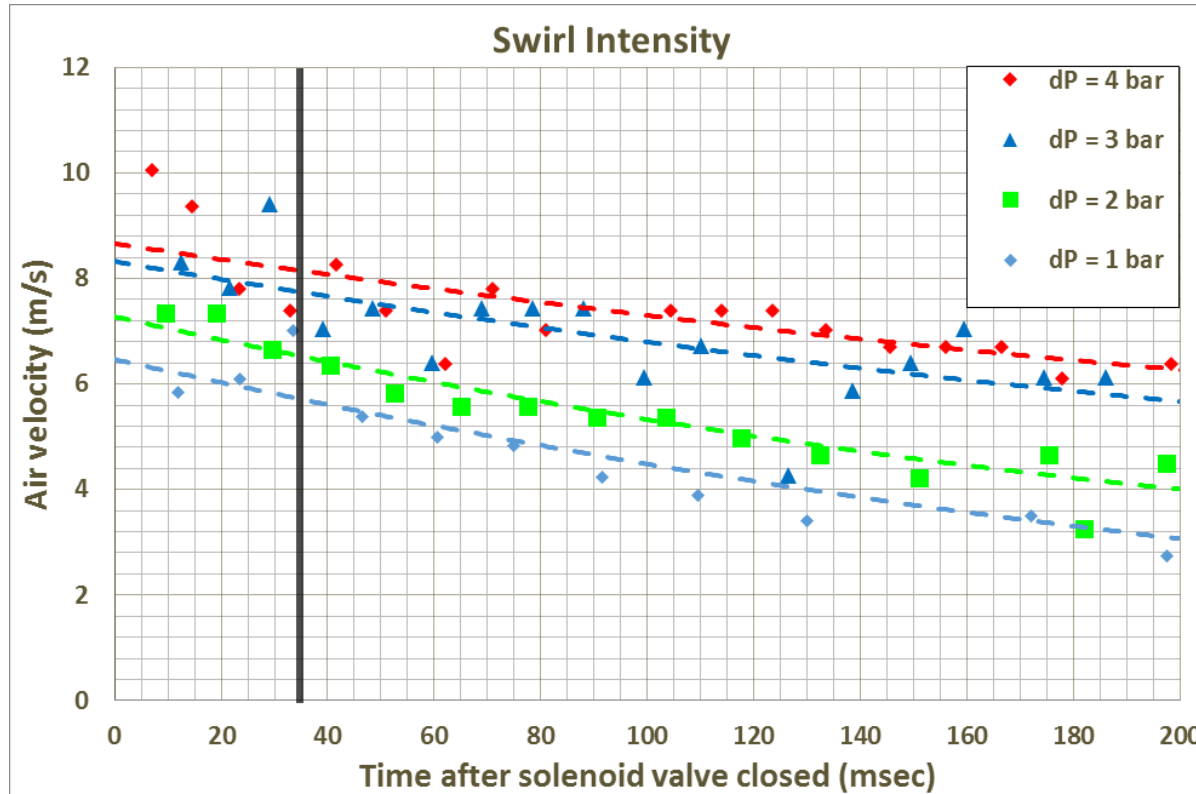


Schlieren technique and Hi-speed video camera

# Experimental Setup (Swirl intensity calibration)



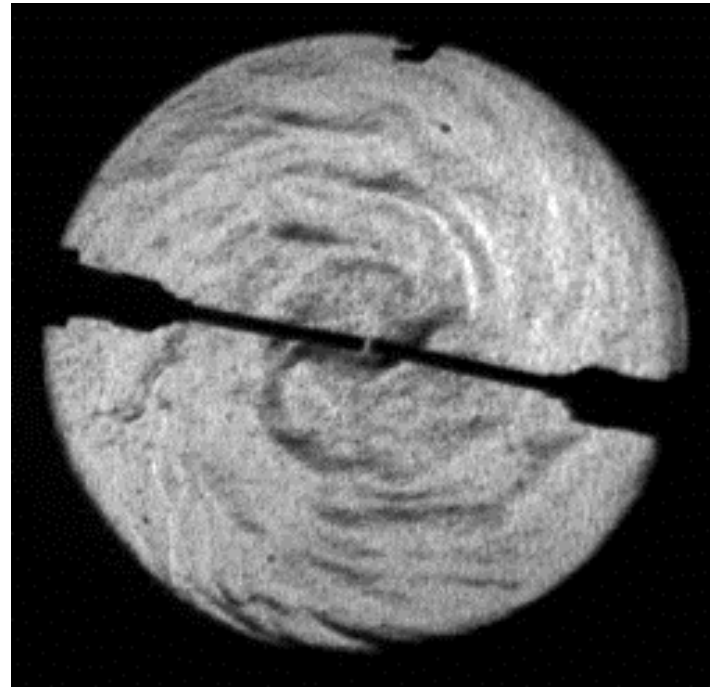
# Experimental Setup (Swirl intensity calibration)



4 bar = 8.10 m/s  
 3 bar = 7.54 m/s  
 2 bar = 6.50 m/s  
 1 bar = 5.73 m/s

\*@ 35 msec

# Experimental Setup (Swirl intensity calibration)



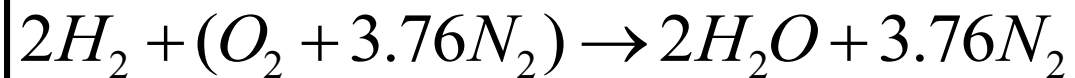
# Experimental Setup (Partial pressure calibration)

Equivalence Ratio Calculation from the Partial Pressure

$$P = P_1 + P_2$$

$$x_i = \frac{P_i}{P} = \frac{n_i}{n}$$

$$P_i = x_i \cdot P$$



# Experimental Setup (Partial pressure calibration)

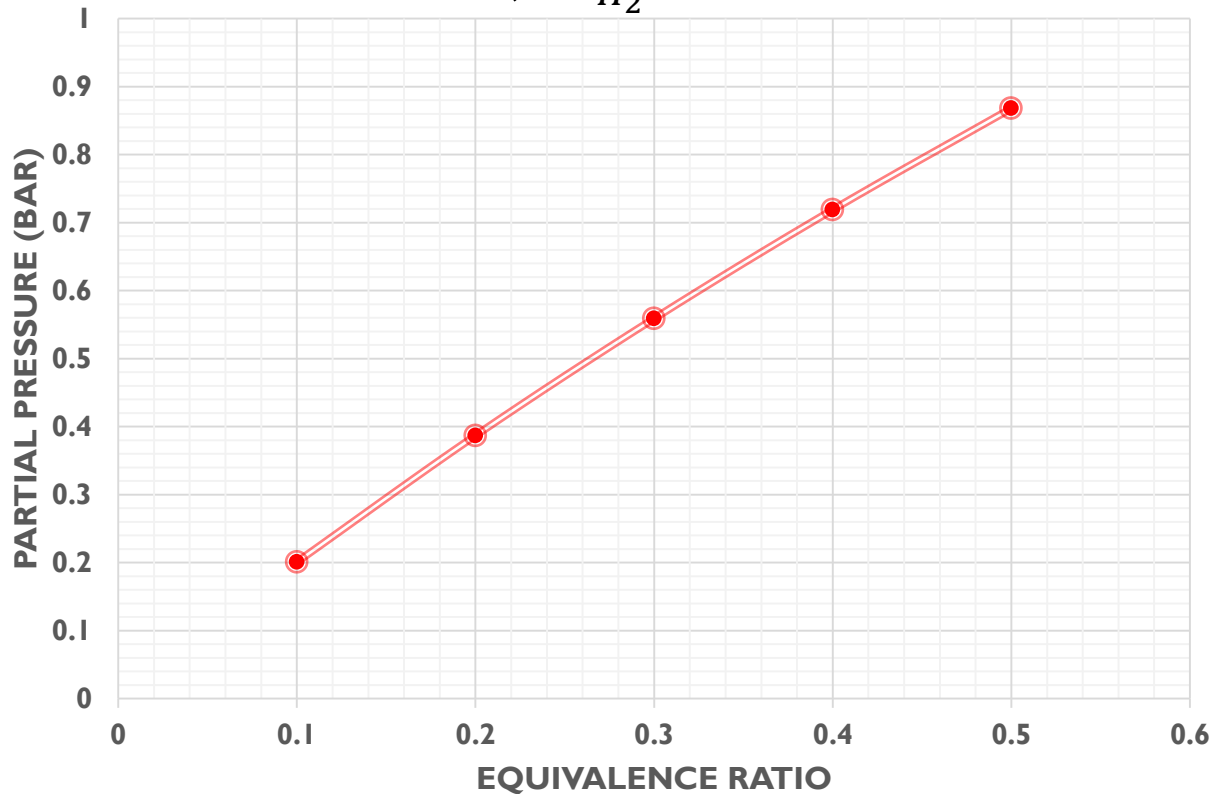
$$\emptyset = 0.1 ; P_{H_2} = 0.201 \text{ bar}$$

$$\emptyset = 0.2 ; P_{H_2} = 0.387 \text{ bar}$$

$$\emptyset = 0.3 ; P_{H_2} = 0.559 \text{ bar}$$

$$\emptyset = 0.4 ; P_{H_2} = 0.719 \text{ bar}$$

$$\emptyset = 0.5 ; P_{H_2} = 0.868 \text{ bar}$$



Initial Pressure = 0.5 MPa

# Experimental Setup (Partial pressure calibration)

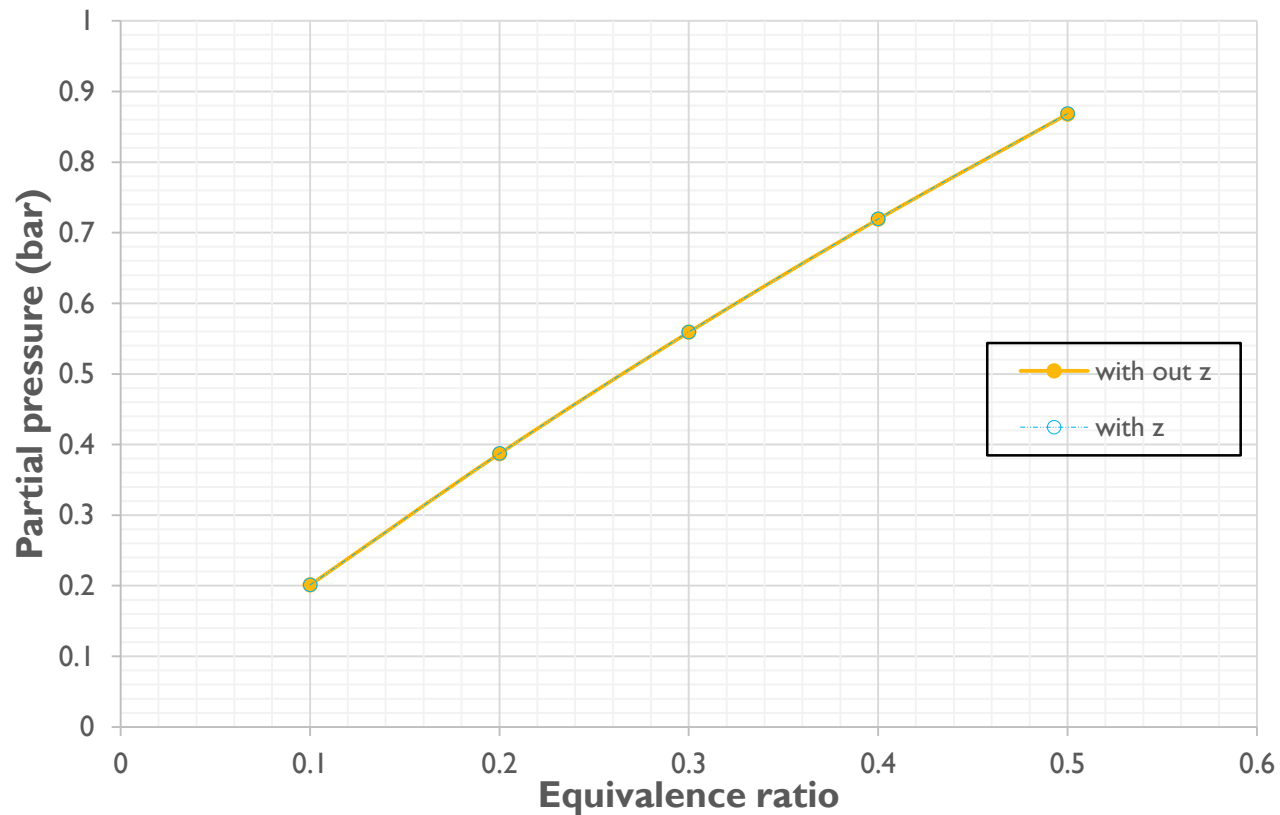
Real gas equation : Compressibility factor

$$Z_{air} @ 5 \text{ bar} = 1.0008$$

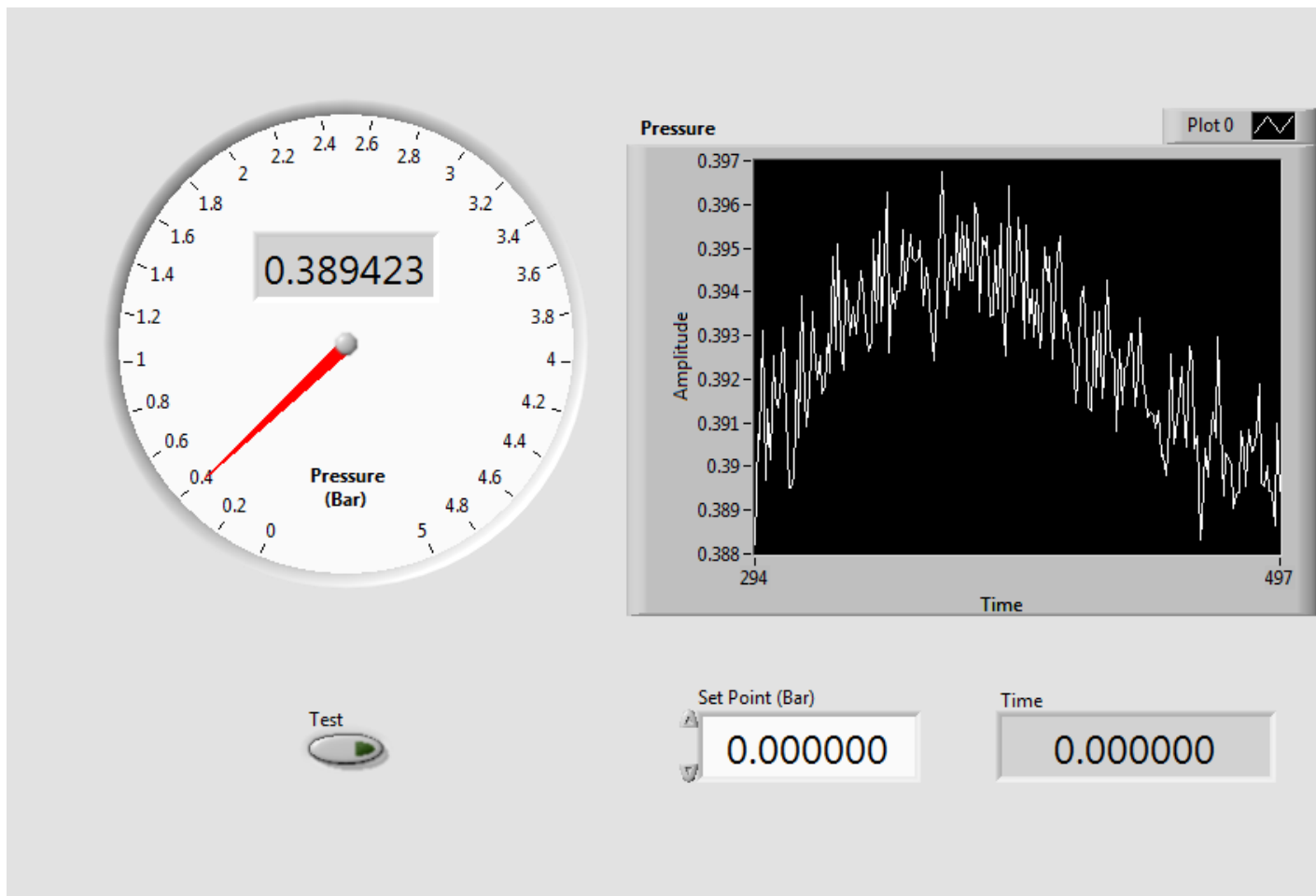
$$\begin{aligned} Z_{H_2} @ 0.201 \text{ bar} &= 1.0005209 \\ Z_{H_2} @ 0.387 \text{ bar} &= 1.0005402 \\ Z_{H_2} @ 0.559 \text{ bar} &= 1.0005623 \\ Z_{H_2} @ 0.719 \text{ bar} &= 1.0005747 \\ Z_{H_2} @ 0.868 \text{ bar} &= 1.0005902 \end{aligned}$$

# Experimental Setup (Partial pressure calibration)

$\emptyset = 0.1 ; P_{H_2} = 0.201 \rightarrow 0.20110 \text{ bar}$   
 $\emptyset = 0.2 ; P_{H_2} = 0.387 \rightarrow 0.38720 \text{ bar}$   
 $\emptyset = 0.3 ; P_{H_2} = 0.559 \rightarrow 0.55931 \text{ bar}$   
 $\emptyset = 0.4 ; P_{H_2} = 0.719 \rightarrow 0.71941 \text{ bar}$   
 $\emptyset = 0.5 ; P_{H_2} = 0.868 \rightarrow 0.86817 \text{ bar}$



# Experimental Setup (Partial pressure calibration)



# Experimental Setup (Partial pressure calibration)

$\emptyset = 0.1$  ;  $t = 118$  ms

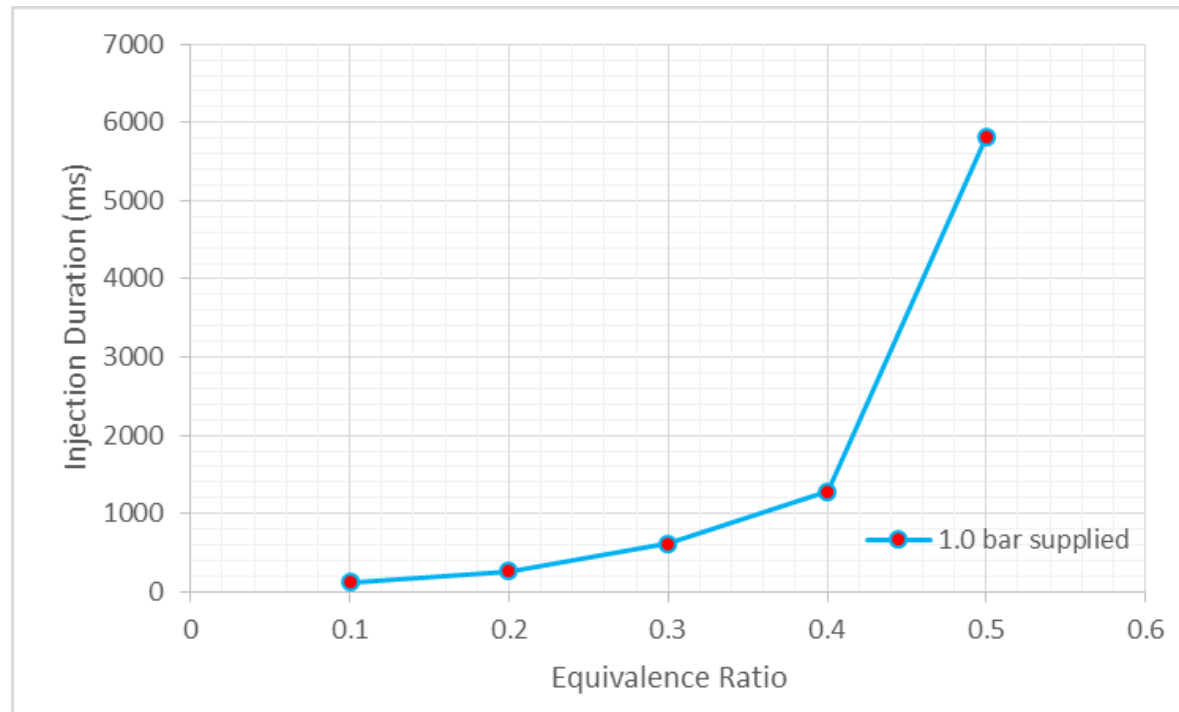
$\emptyset = 0.2$  ;  $t = 266$  ms

$\emptyset = 0.3$  ;  $t = 612$  ms

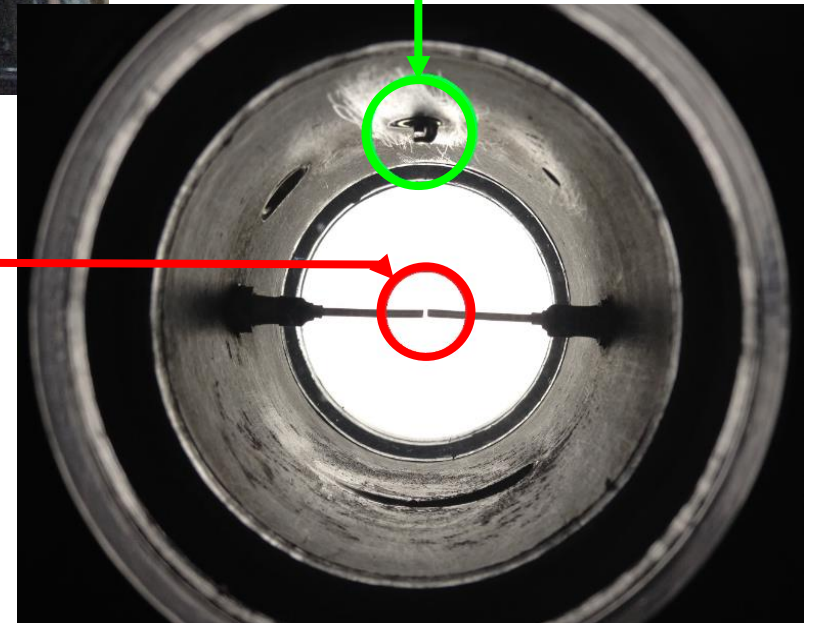
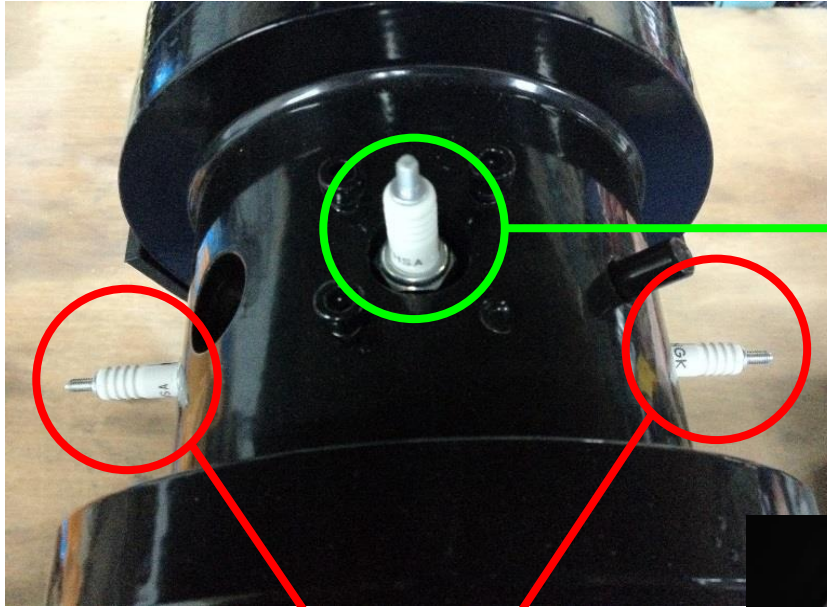
$\emptyset = 0.4$  ;  $t = 1278$  ms

$\emptyset = 0.5$  ;  $t = 5814$  ms

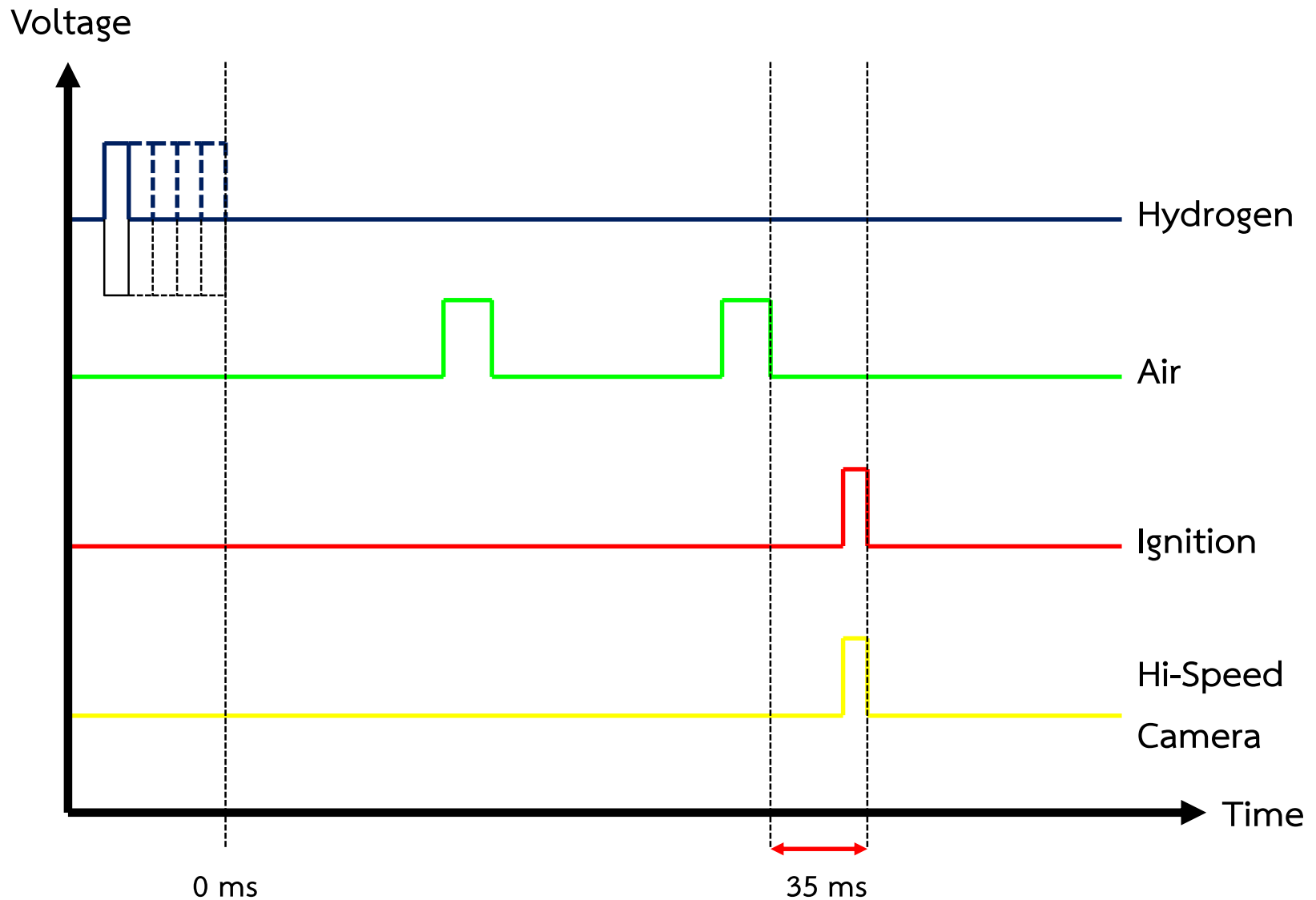
@ 1.0 bar



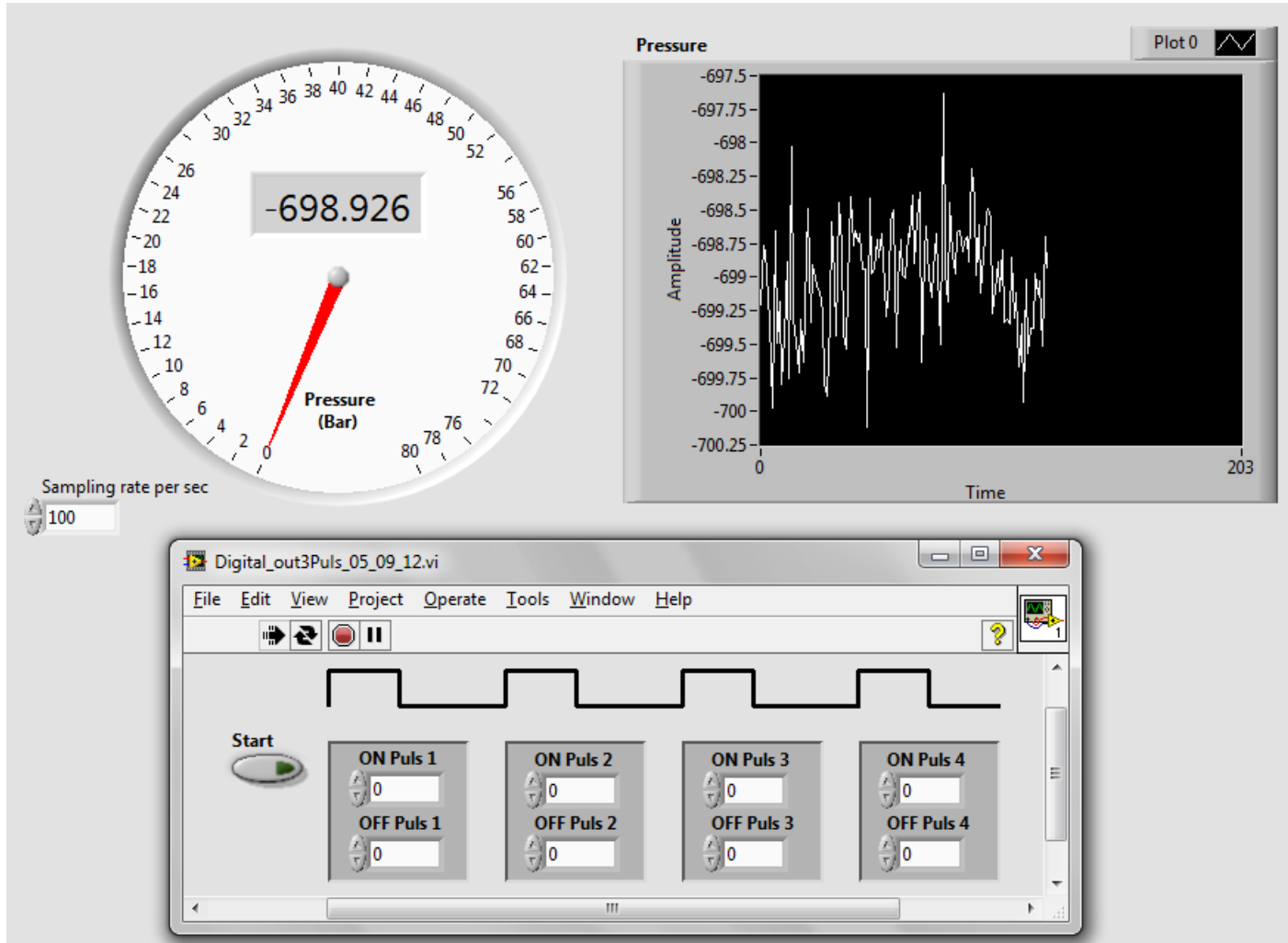
# Experimental Setup (Spark plug positions)



# Experimental Setup (Experimental sequential)



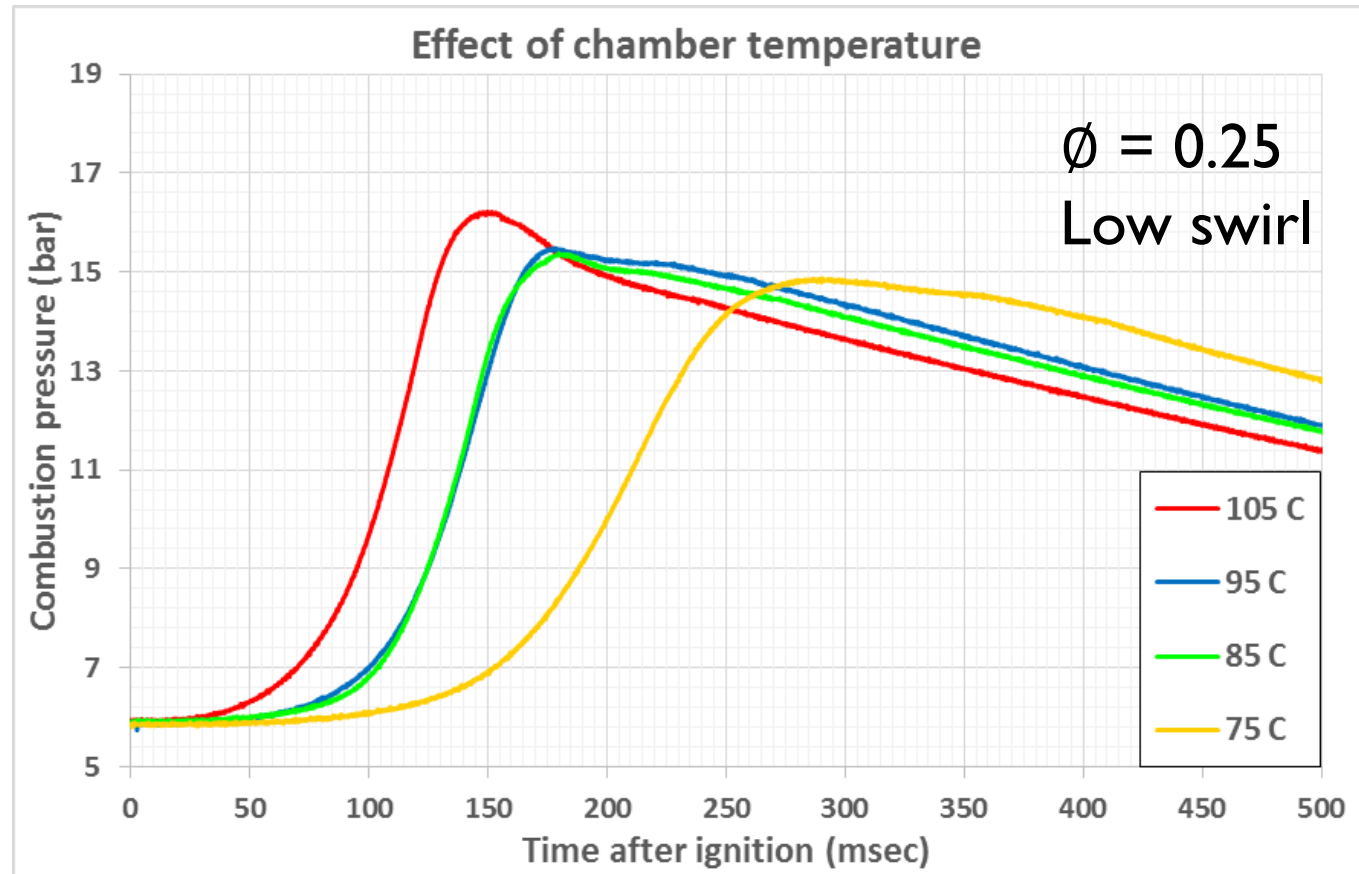
# Experimental Setup (Experimental sequential)



# Contents

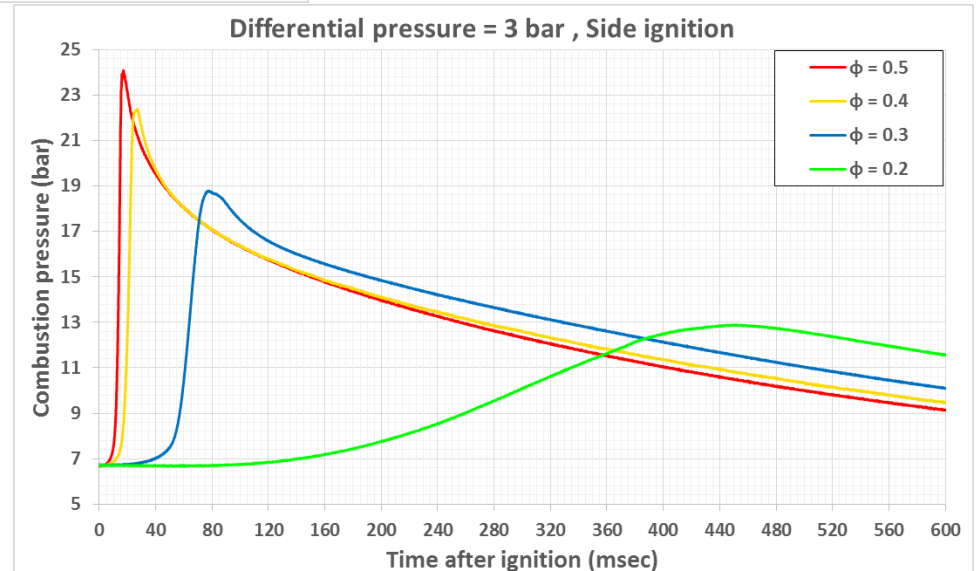
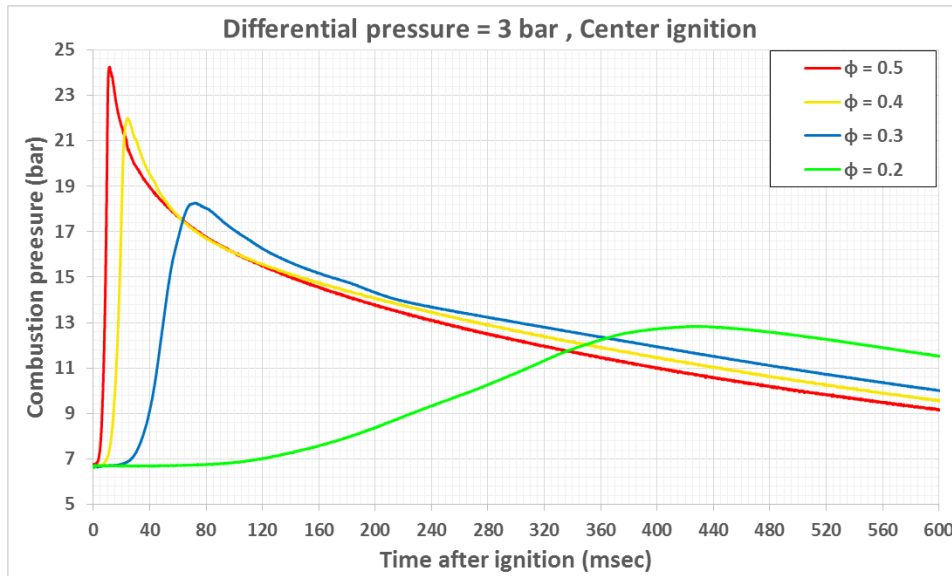
- Introduction
- Literature review
- Objective
- Experimental setup
- **Results**
- Conclusions

# Results (Effect of chamber temperature)

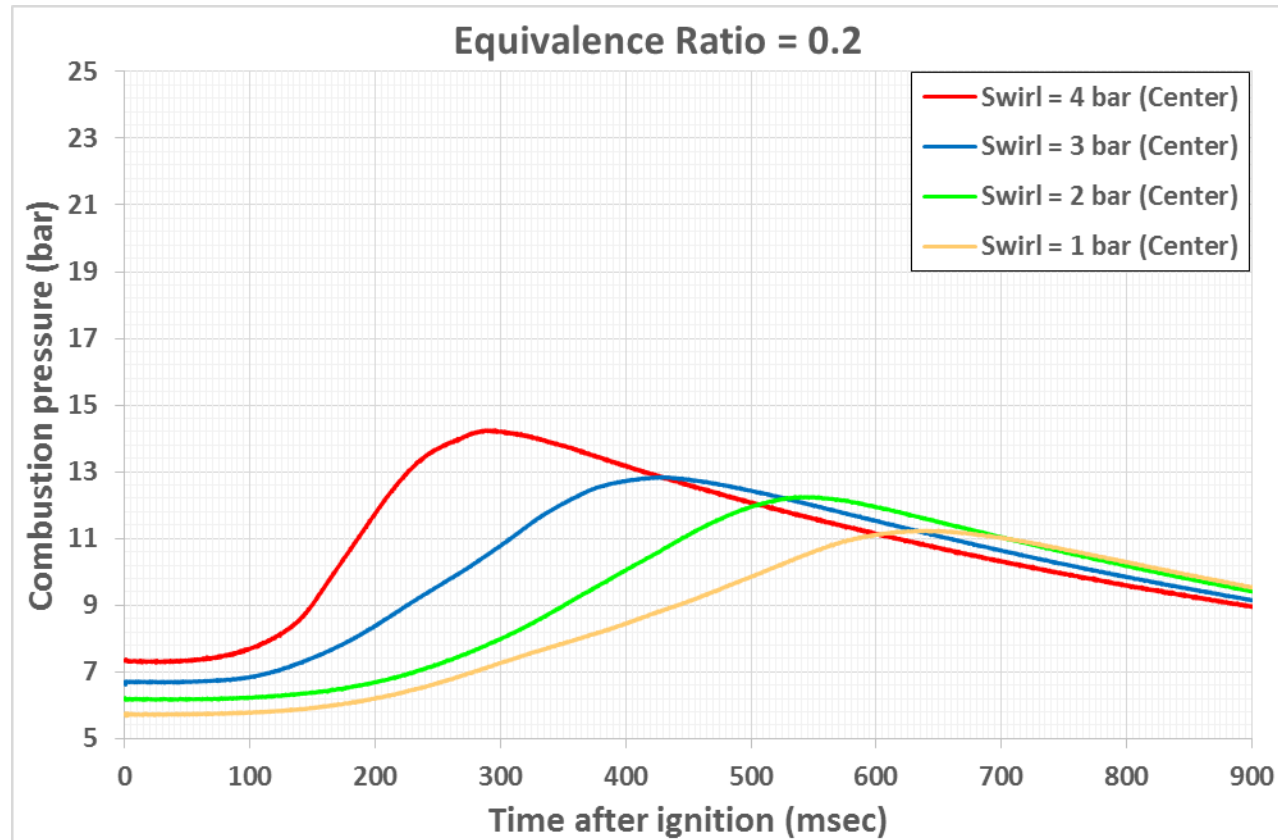


Maximum combustion pressure were 14.87, 15.37, 15.48 and 16.21 bar  
Combustion delay were 144, 100, 95 and 69 msec

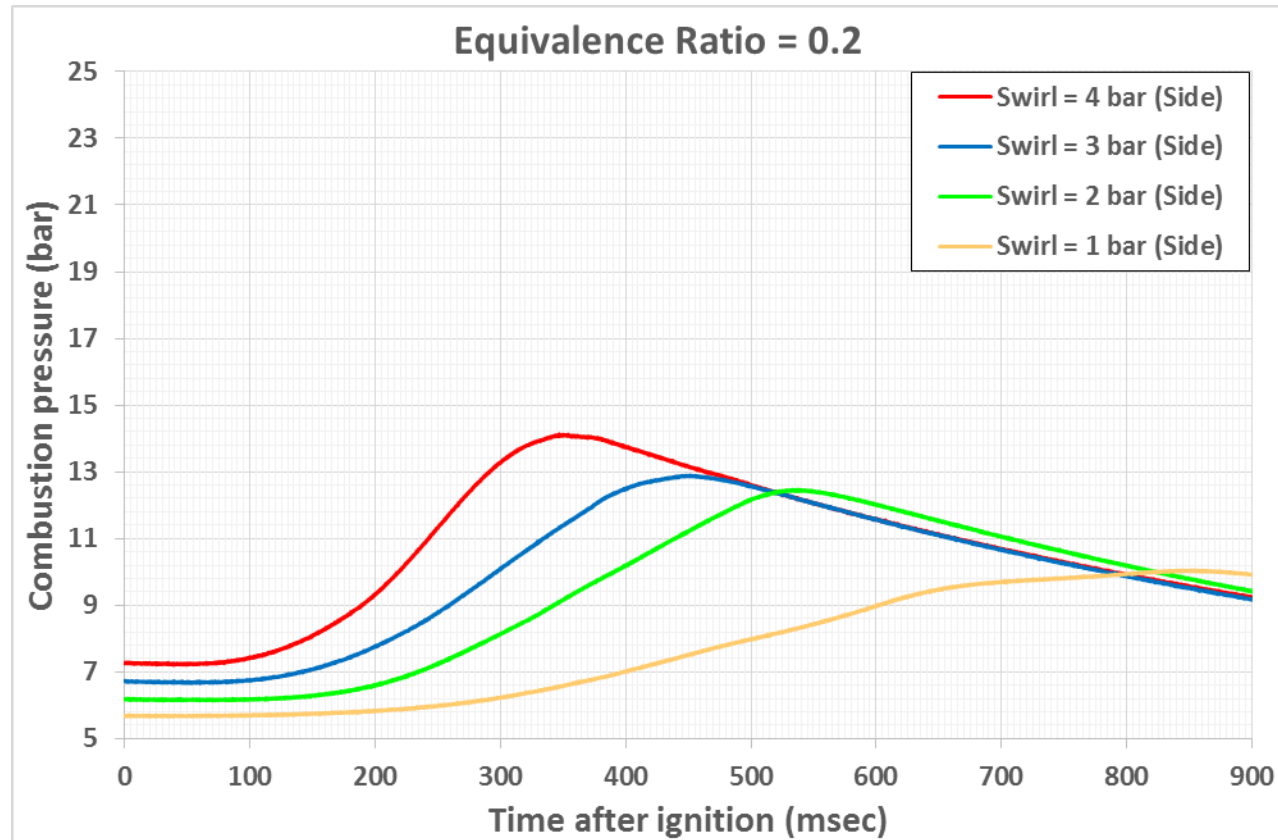
# Results (Effect of equivalence ratio)



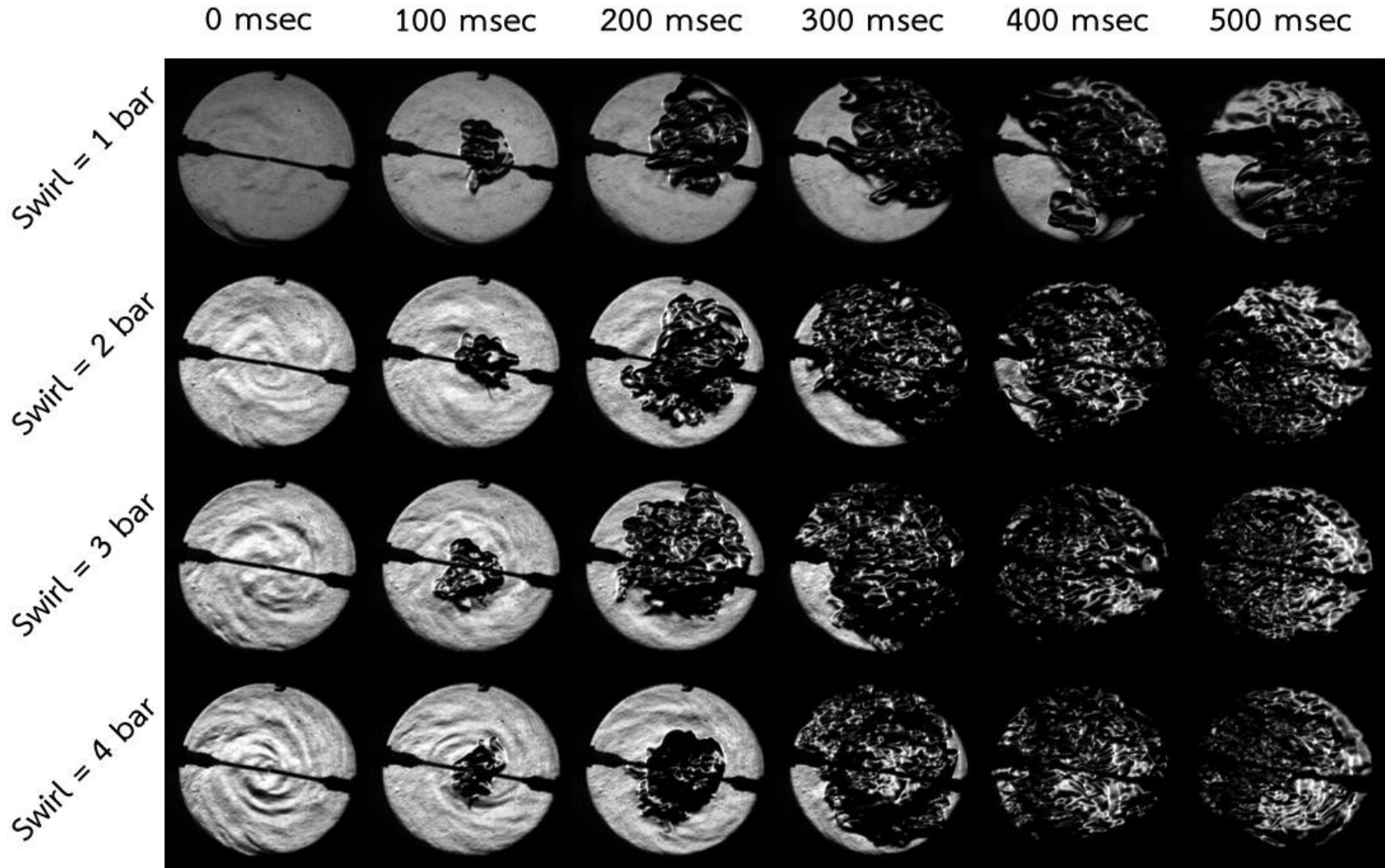
# Results (Effect swirl intensity and spark plug positions)



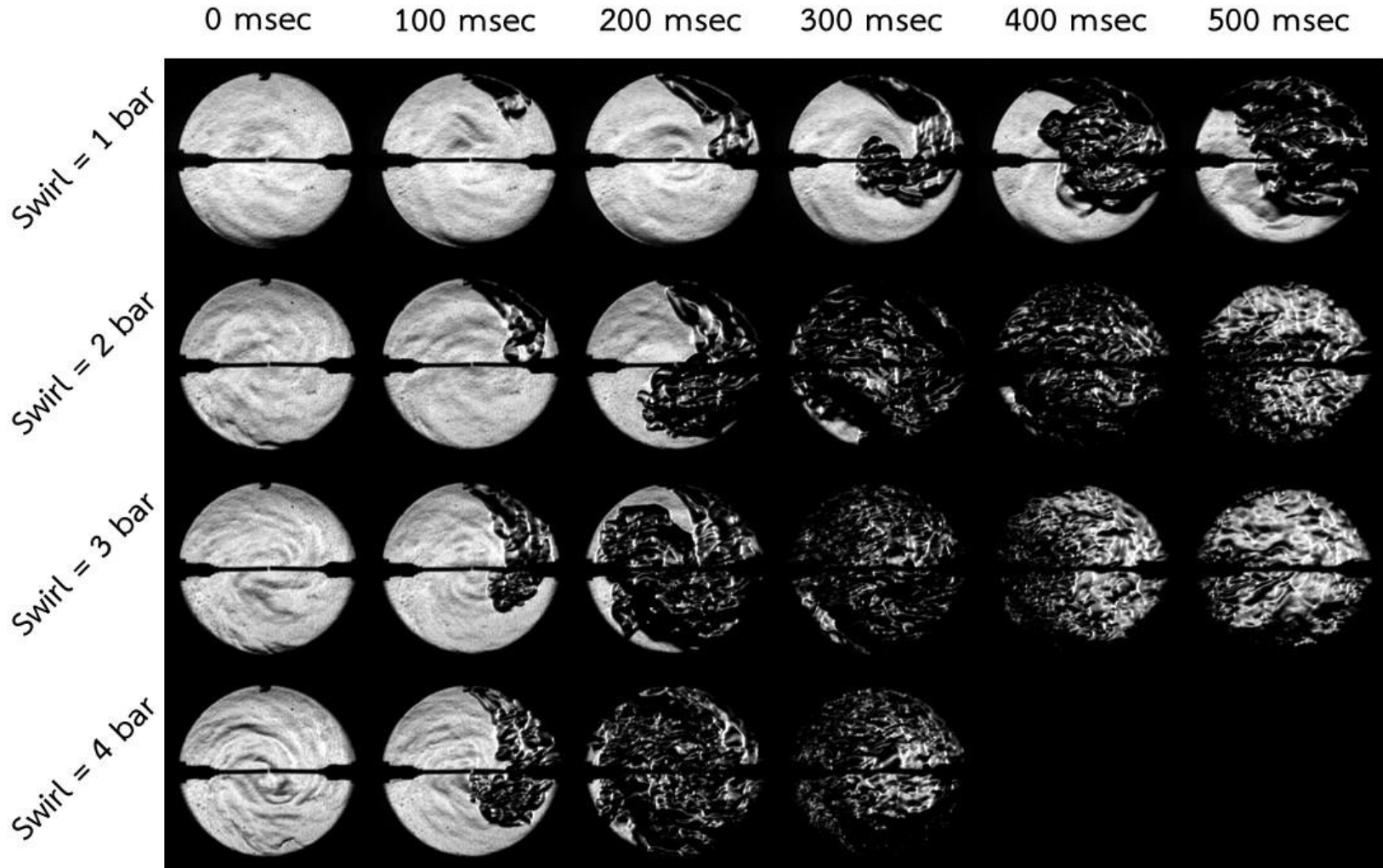
# Results (Effect swirl intensity and spark plug positions)



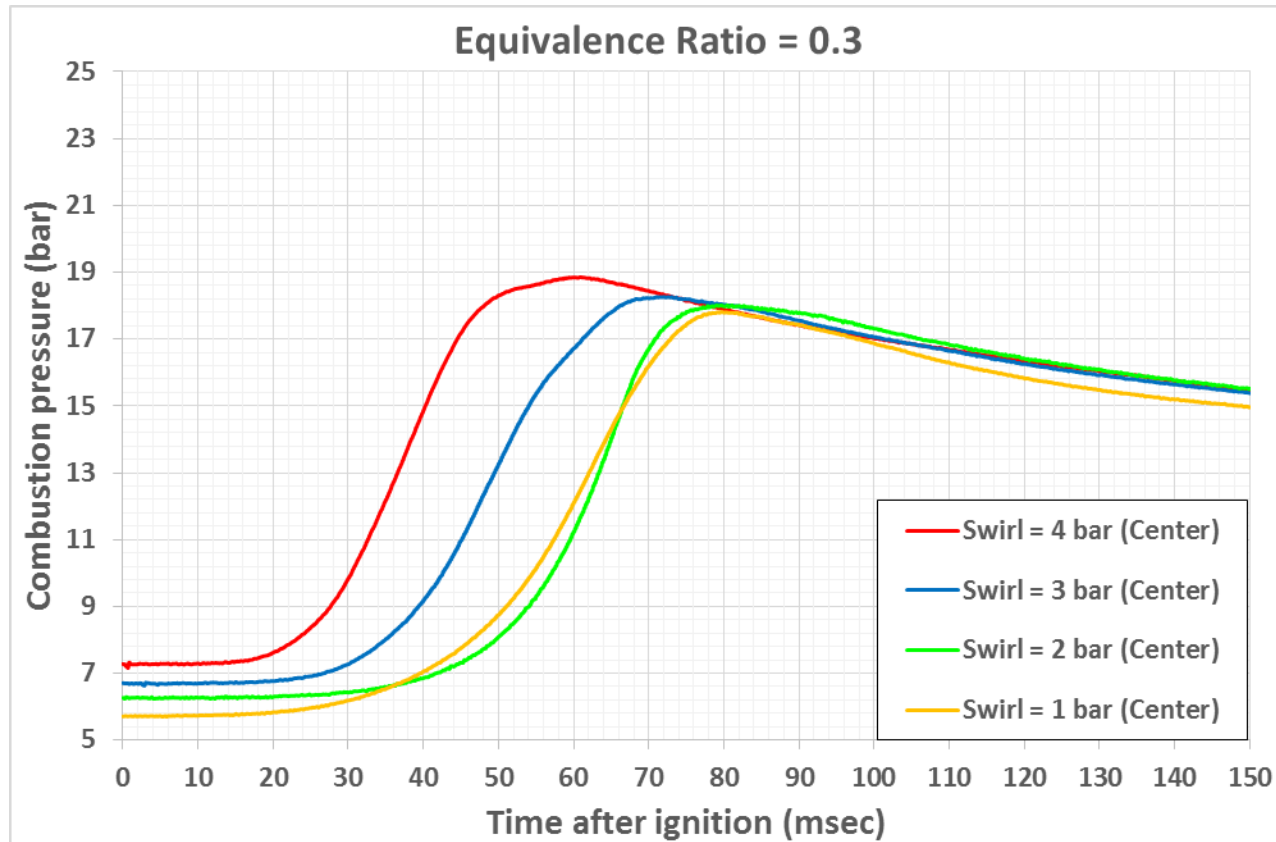
# Results (Effect swirl intensity and spark plug positions)



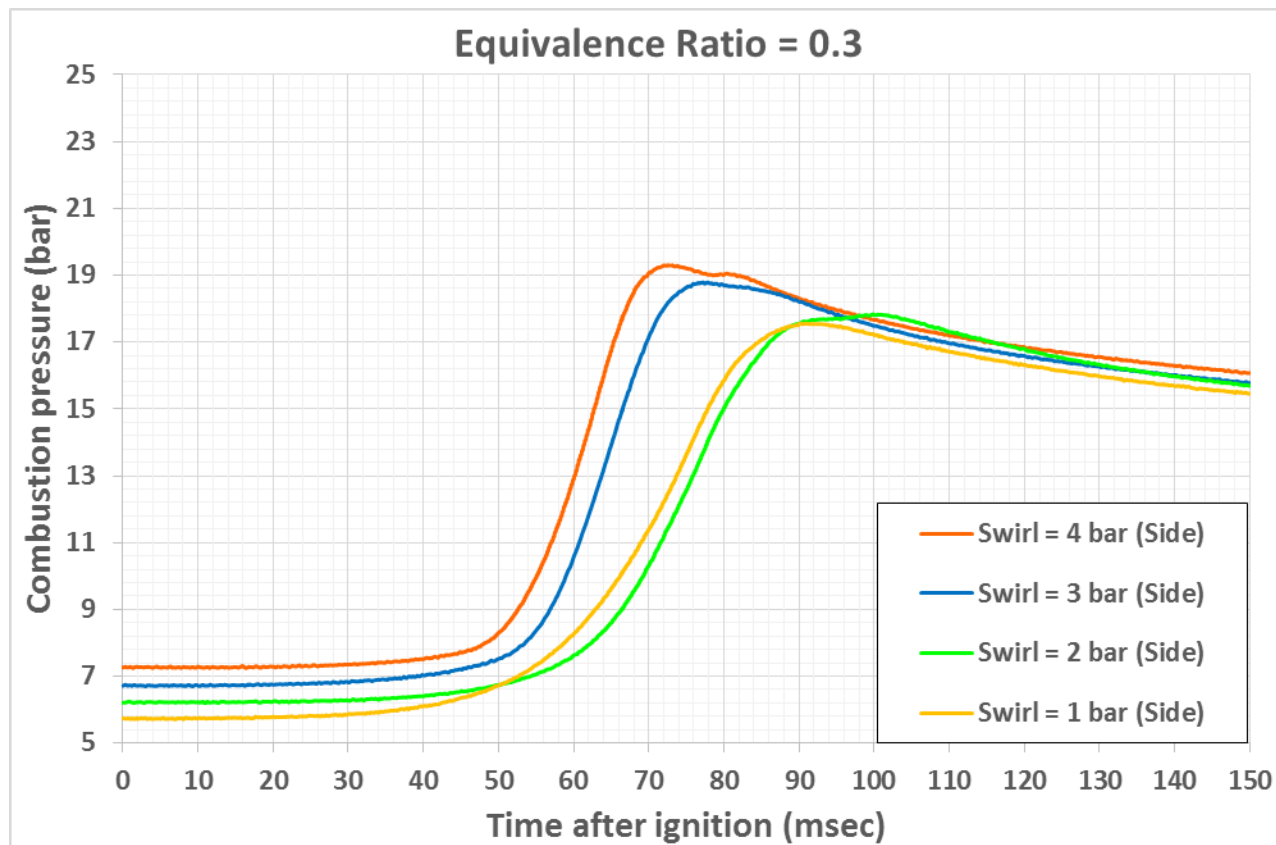
# Results (Effect swirl intensity and spark plug positions)



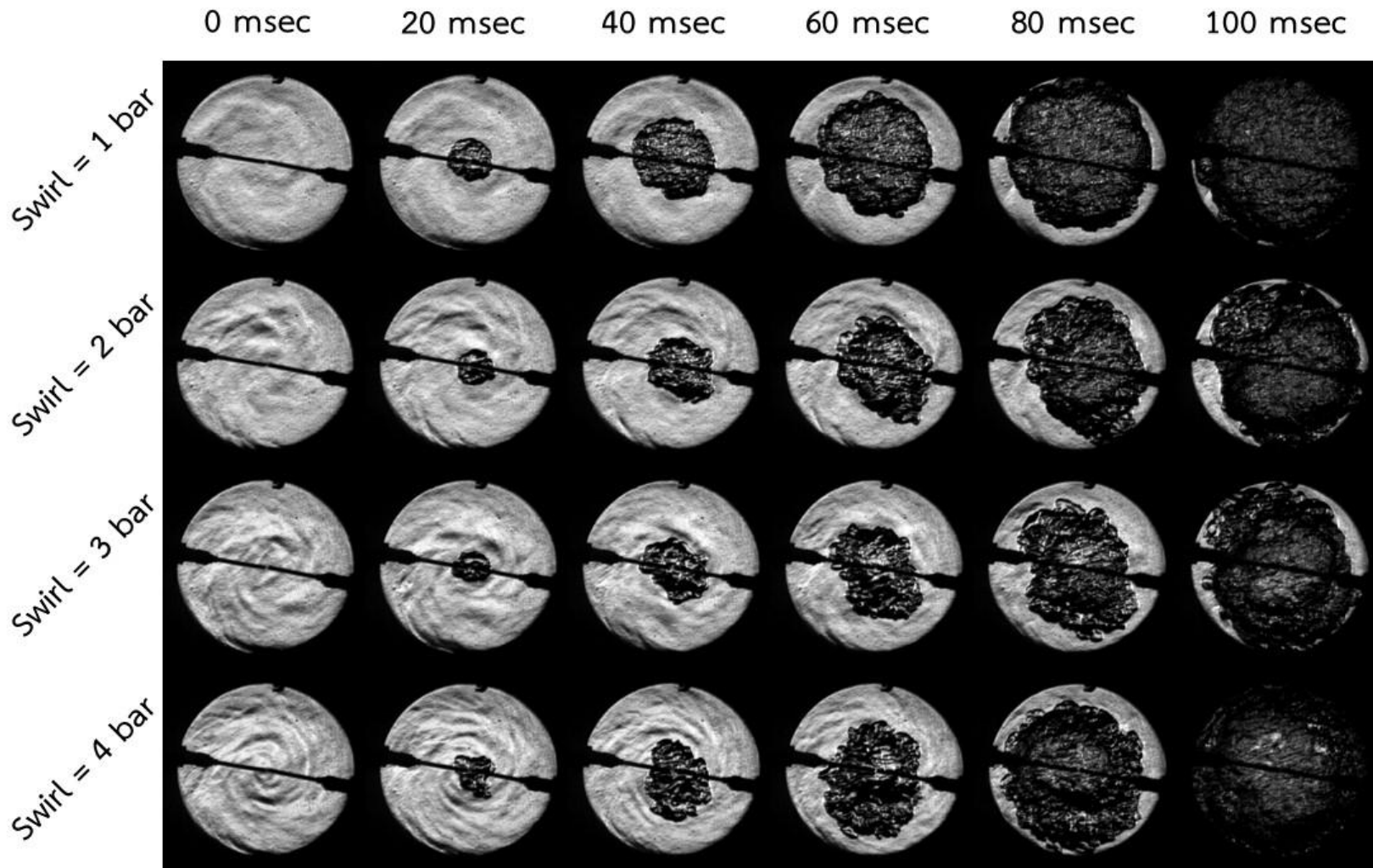
# Results (Effect swirl intensity and spark plug positions)



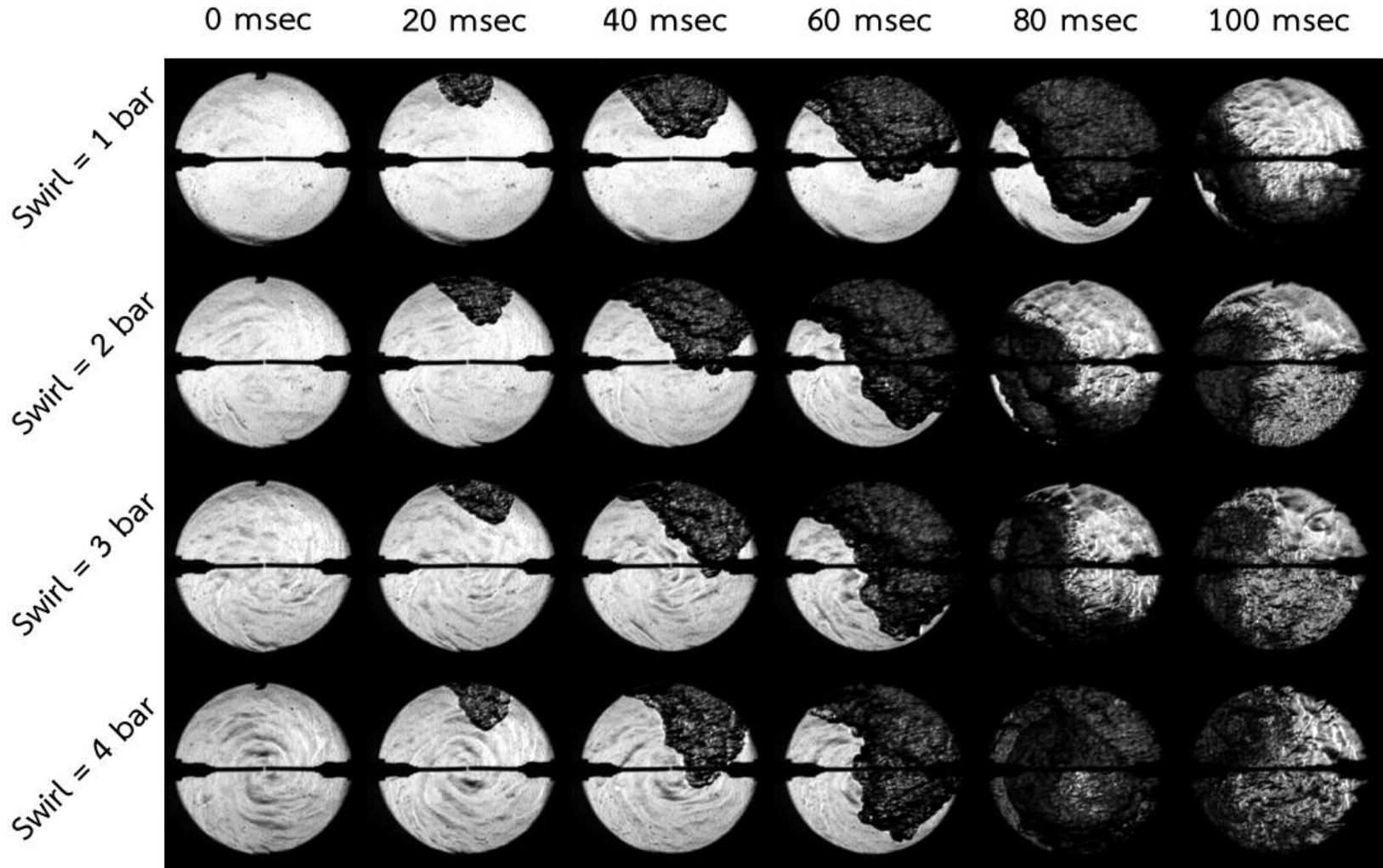
# Results (Effect swirl intensity and spark plug positions)



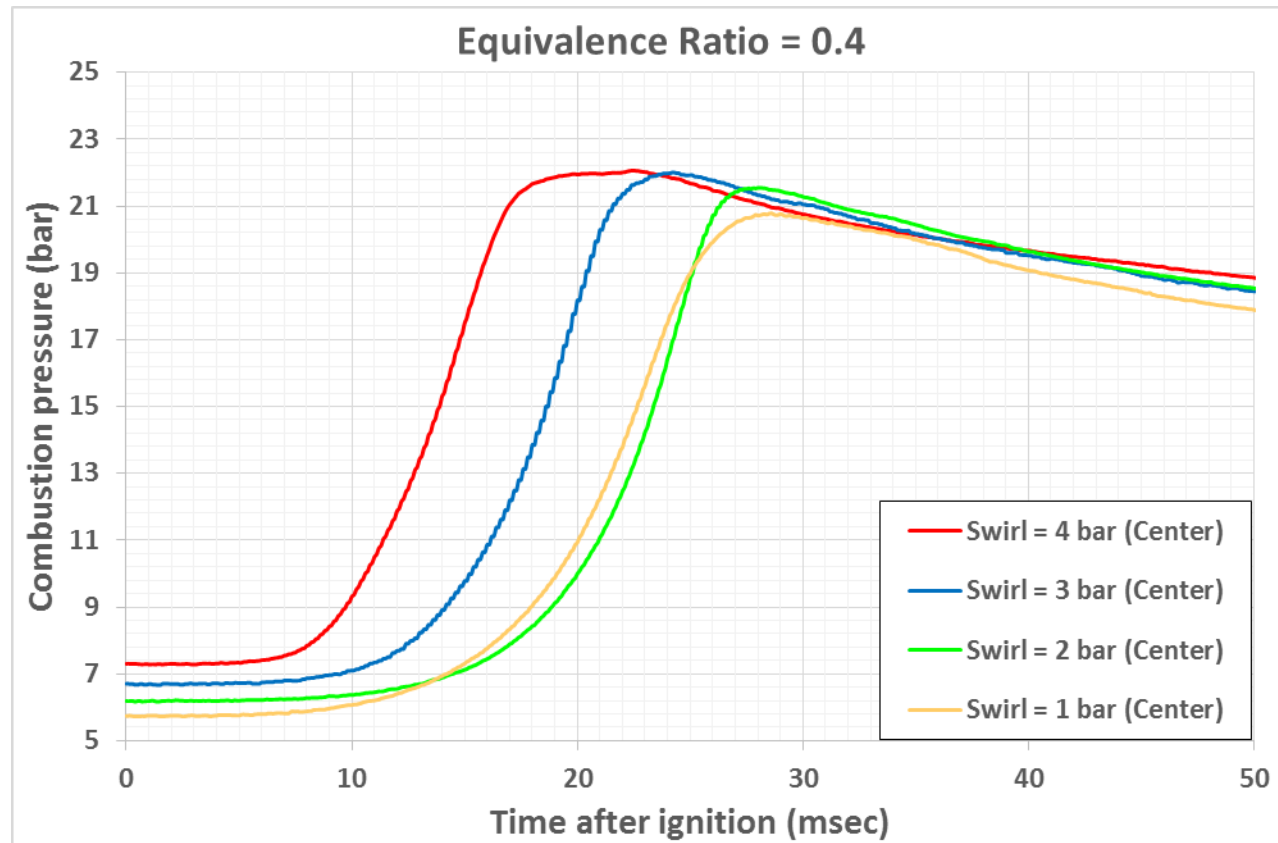
# Results (Effect swirl intensity and spark plug positions)



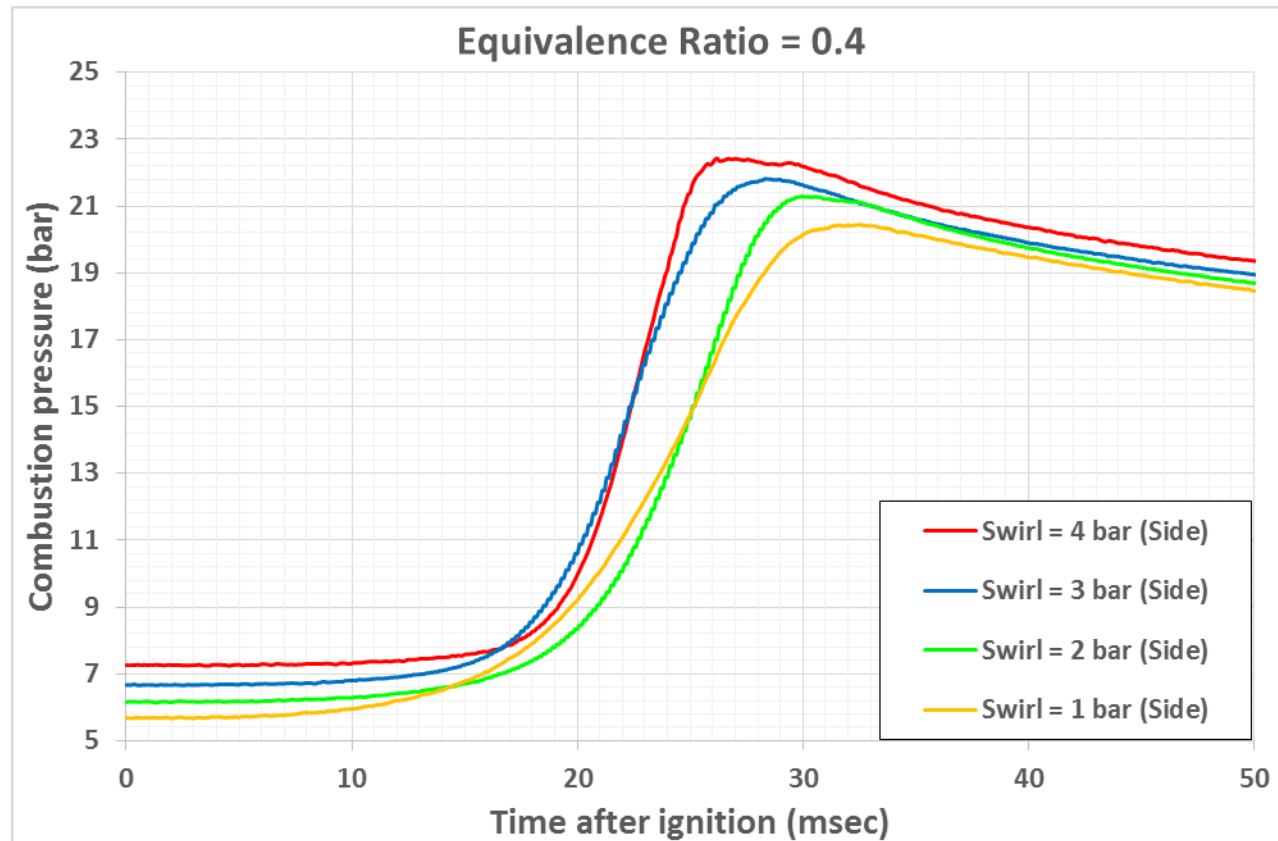
# Results (Effect swirl intensity and spark plug positions)



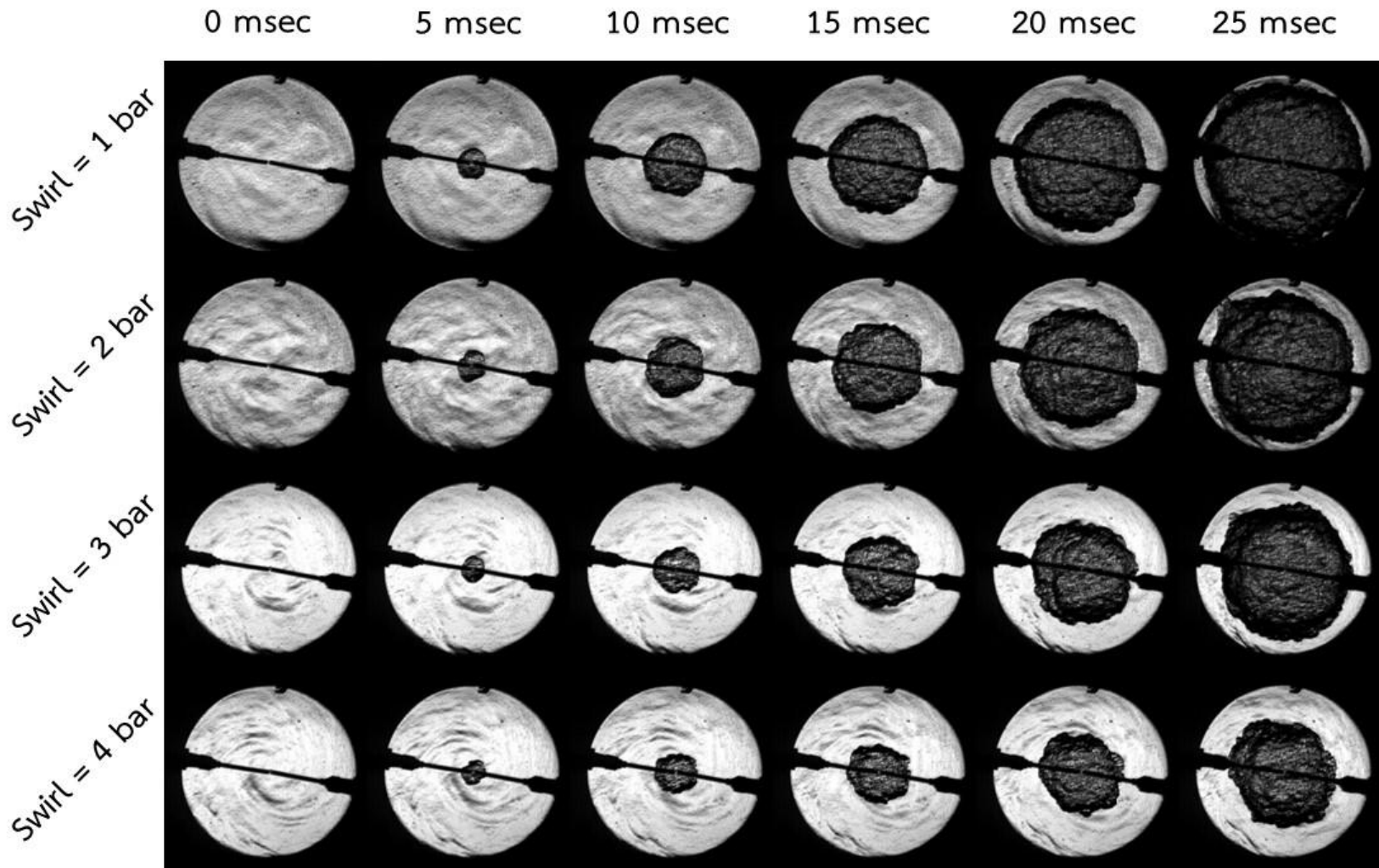
# Results (Effect swirl intensity and spark plug positions)



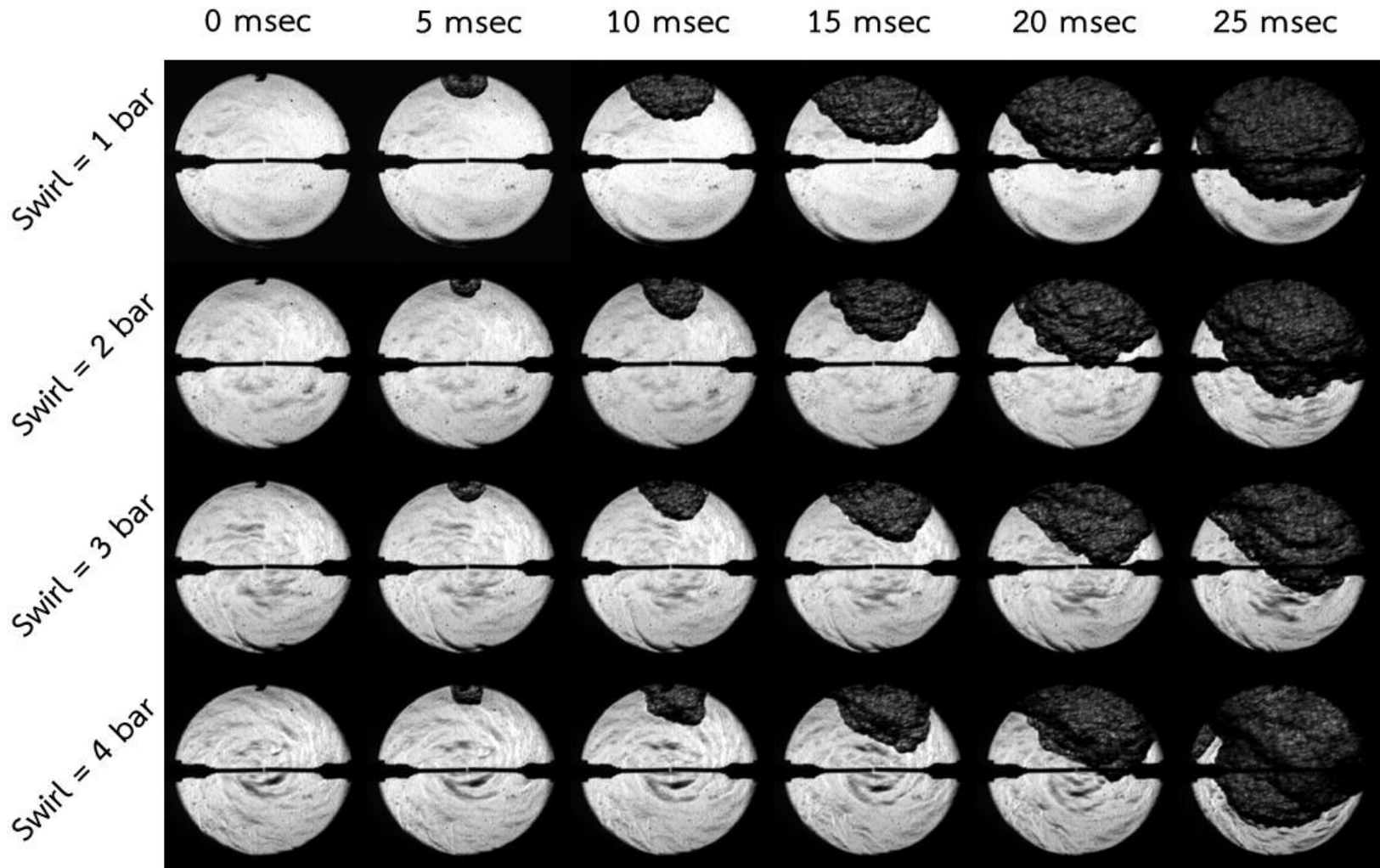
# Results (Effect swirl intensity and spark plug positions)



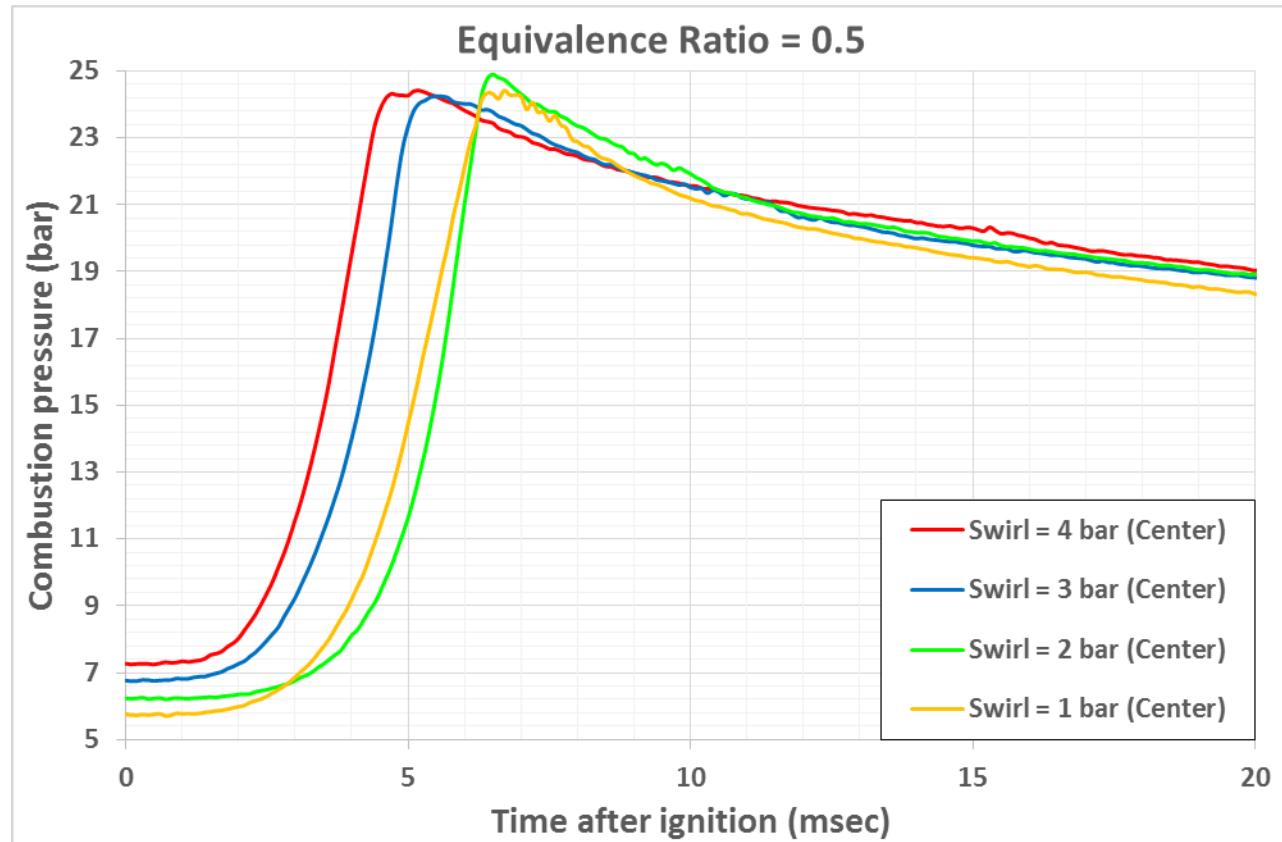
# Results (Effect swirl intensity and spark plug positions)



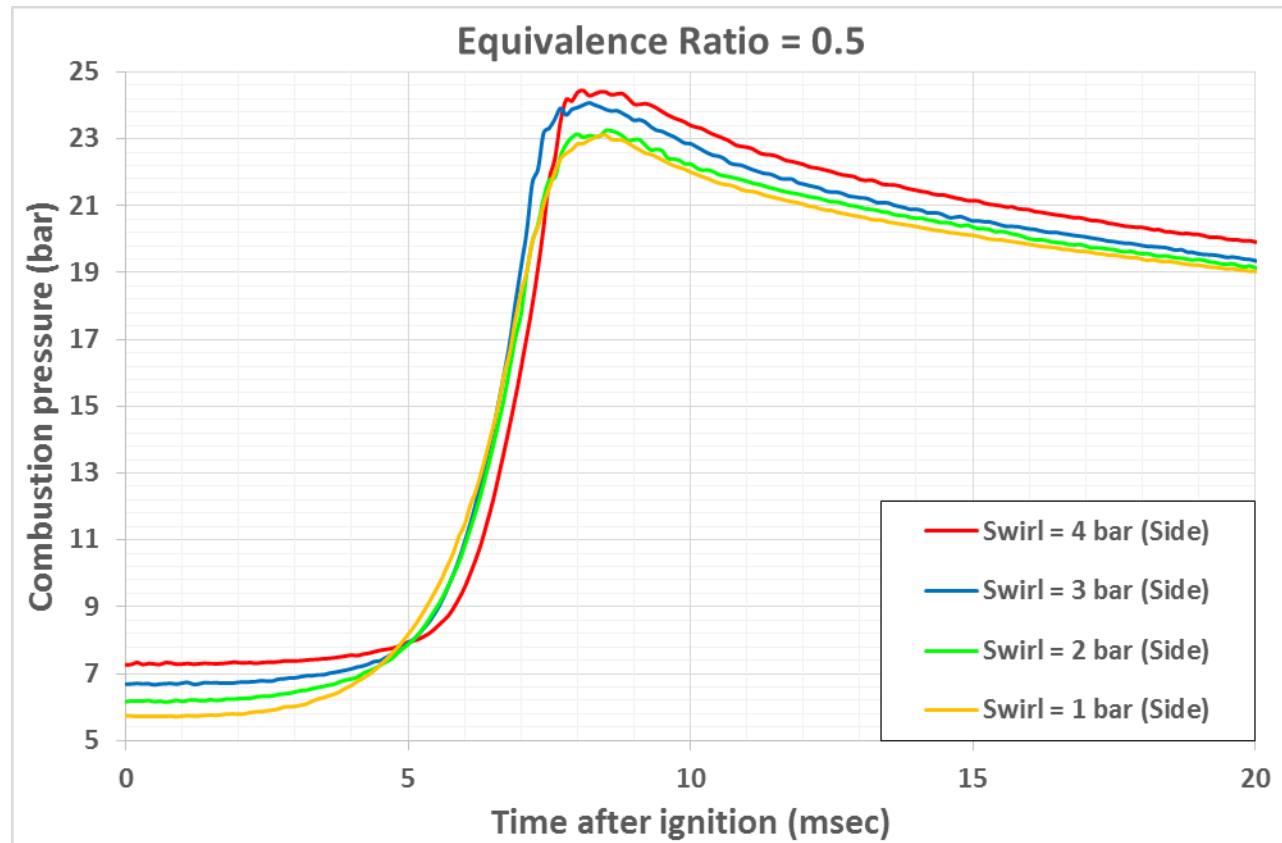
# Results (Effect swirl intensity and spark plug positions)



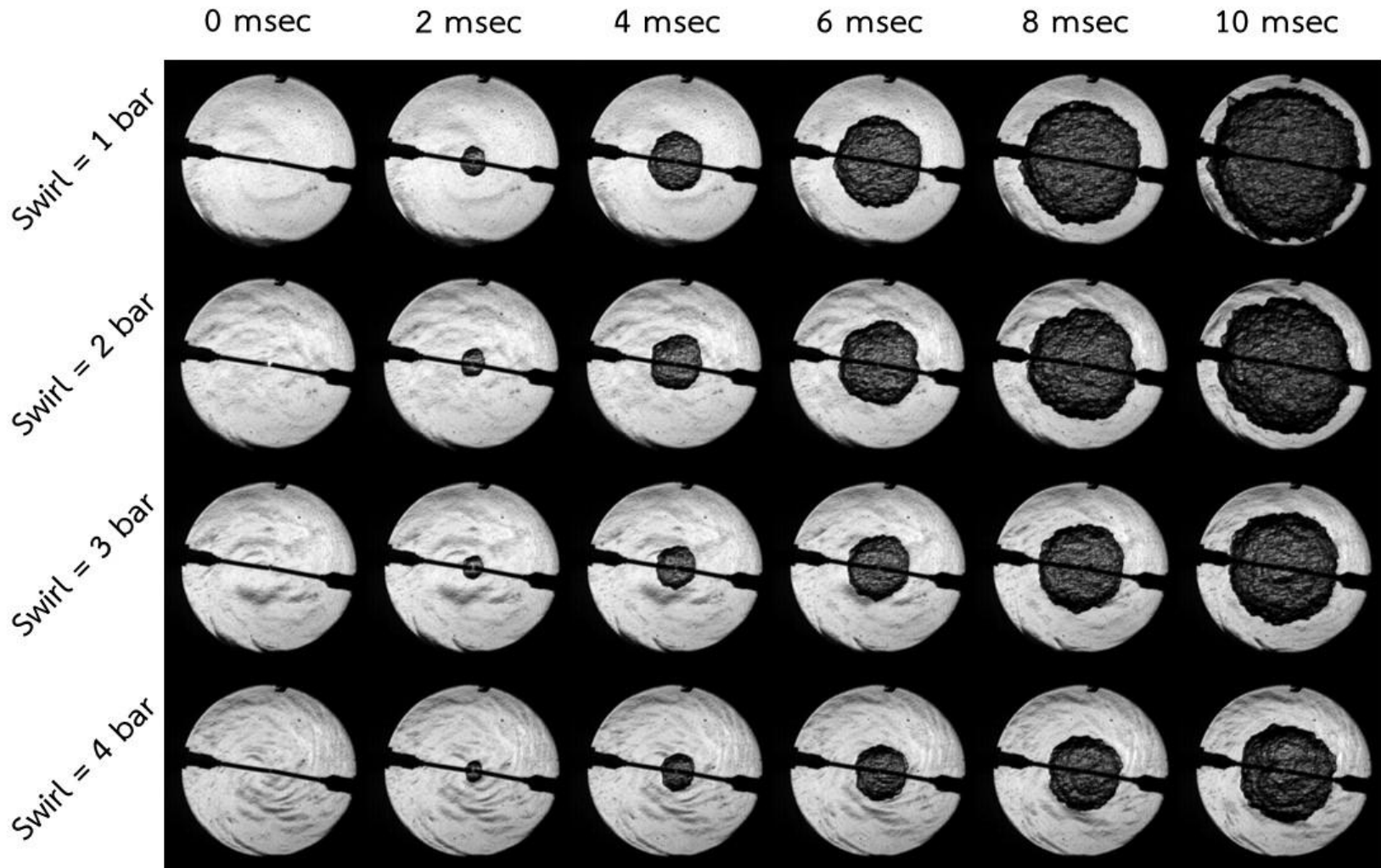
# Results (Effect swirl intensity and spark plug positions)



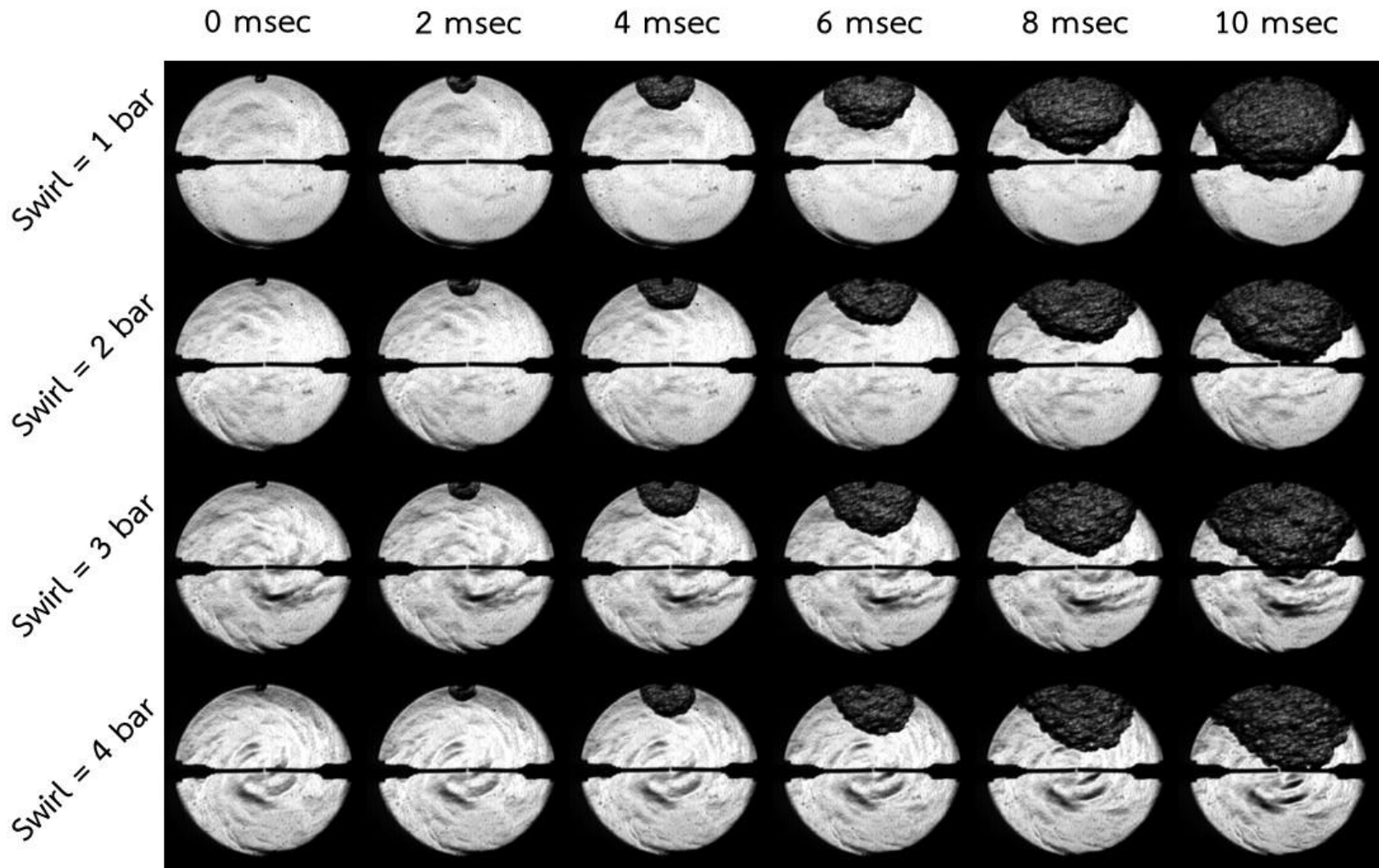
# Results (Effect swirl intensity and spark plug positions)



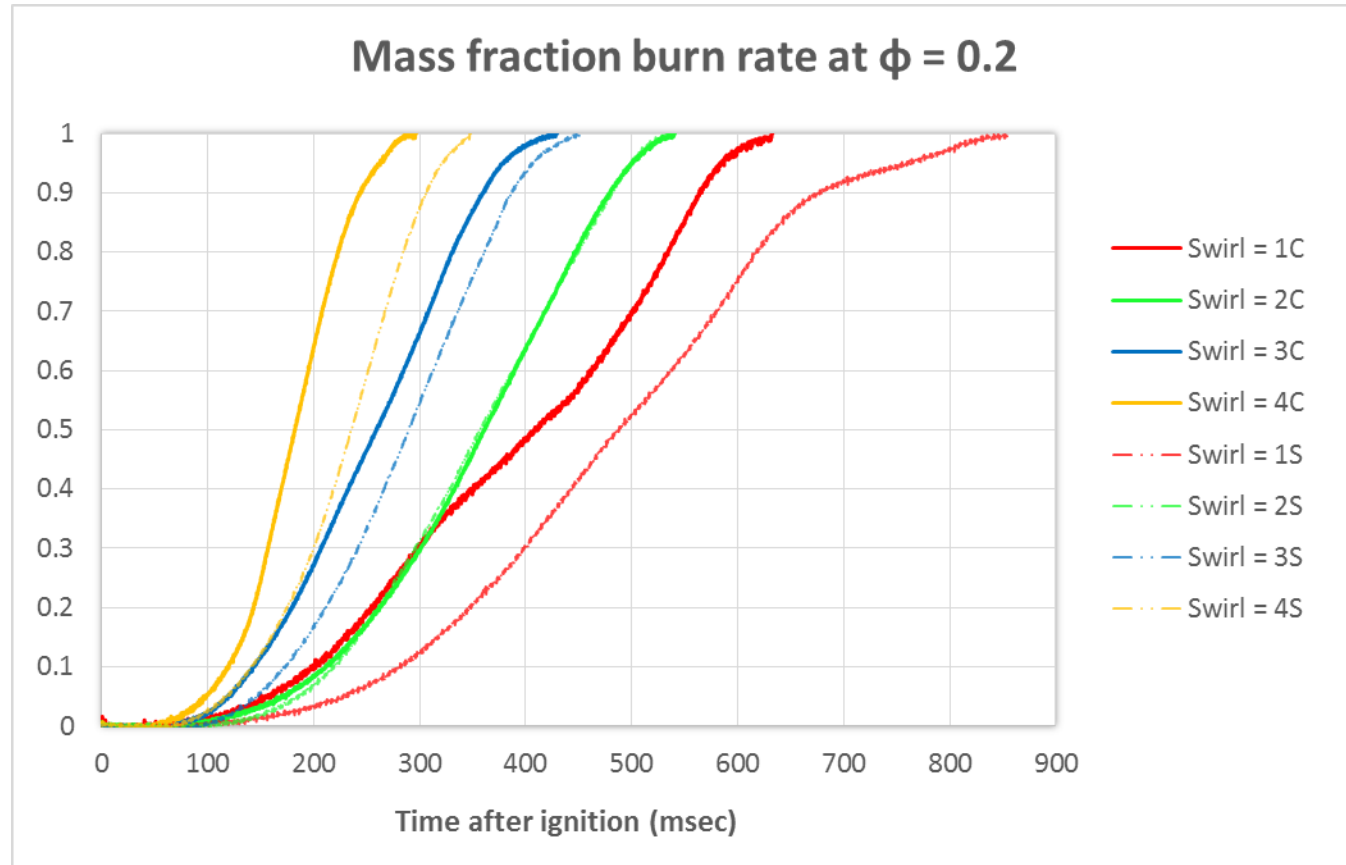
# Results (Effect swirl intensity and spark plug positions)



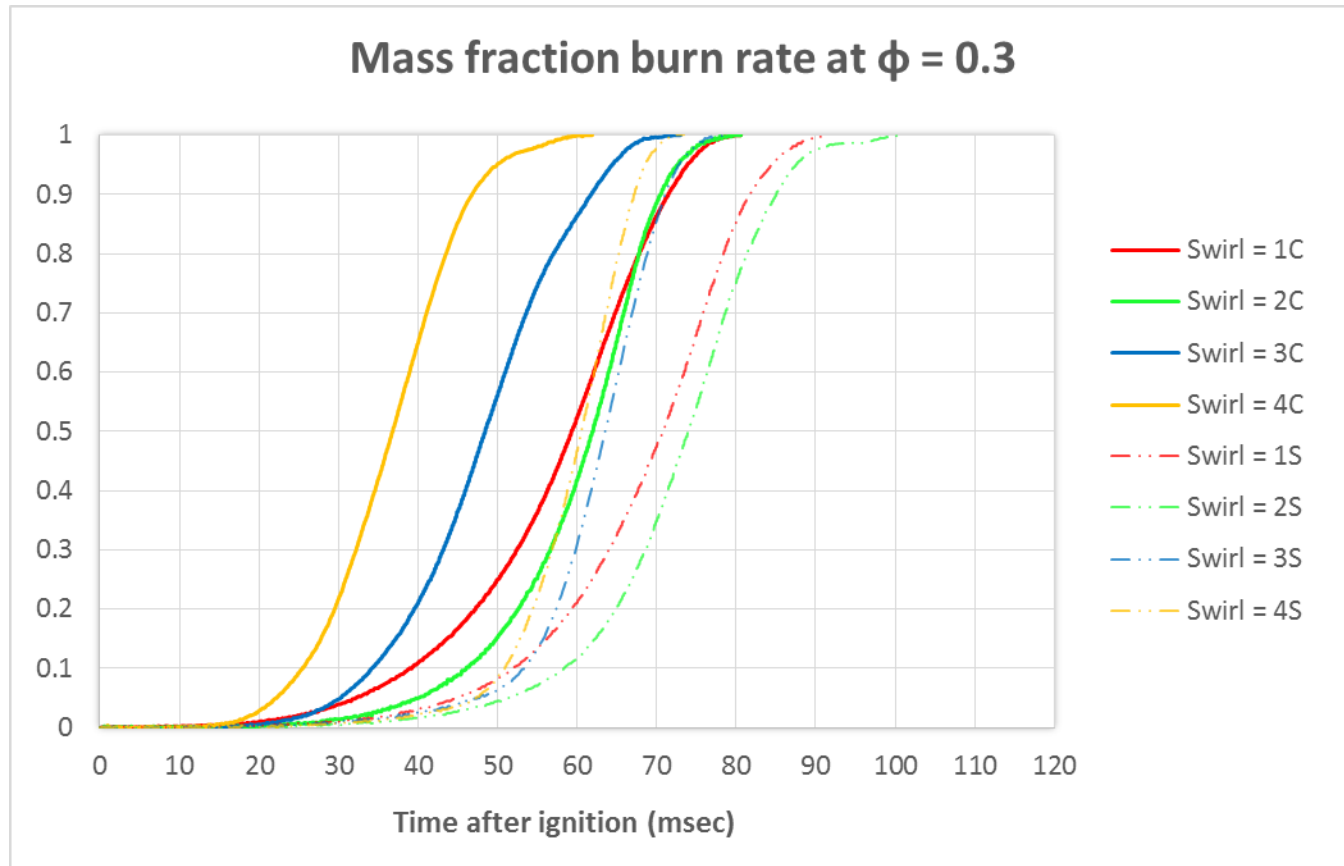
# Results (Effect swirl intensity and spark plug positions)



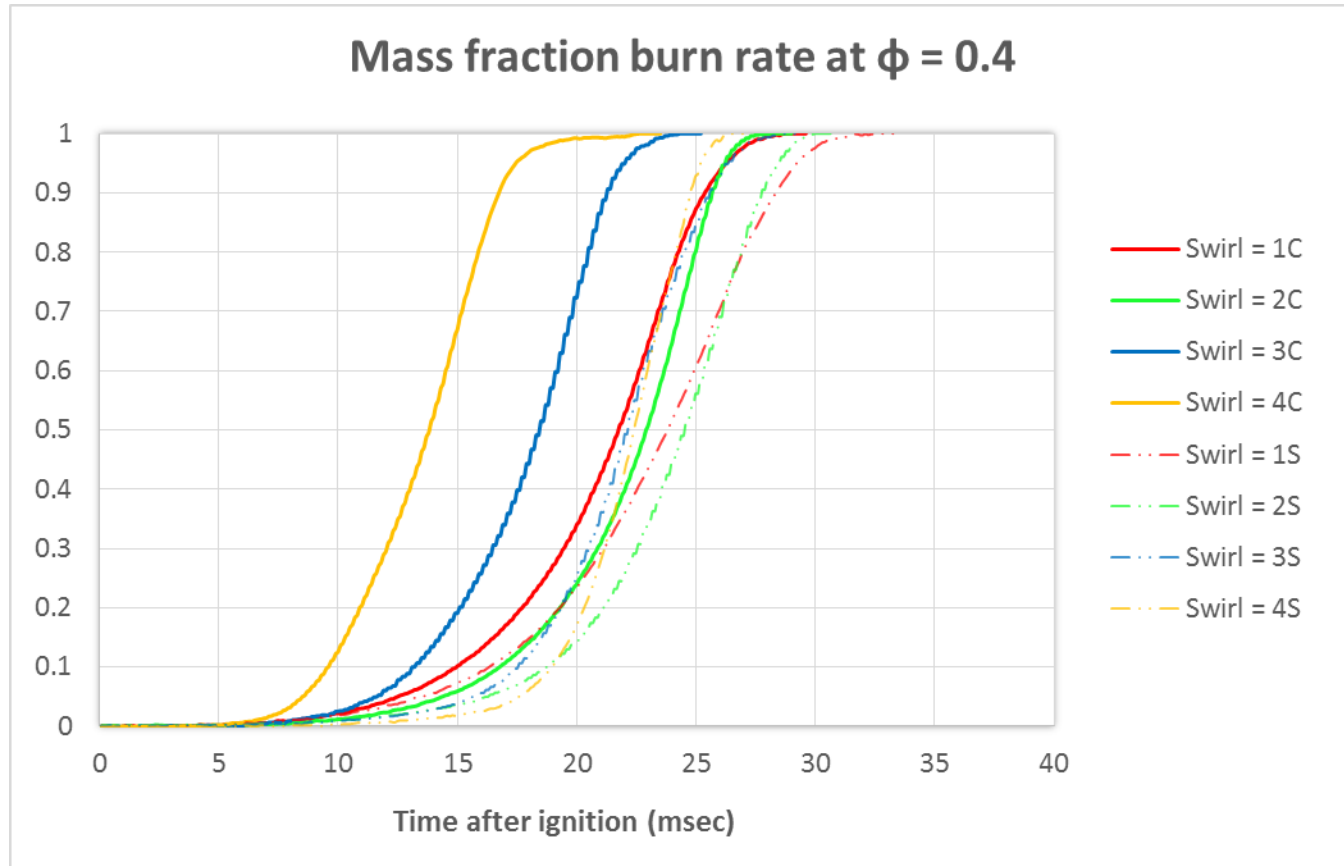
# Results (Mass Fraction Burn Rate)



# Results (Mass Fraction Burn Rate)



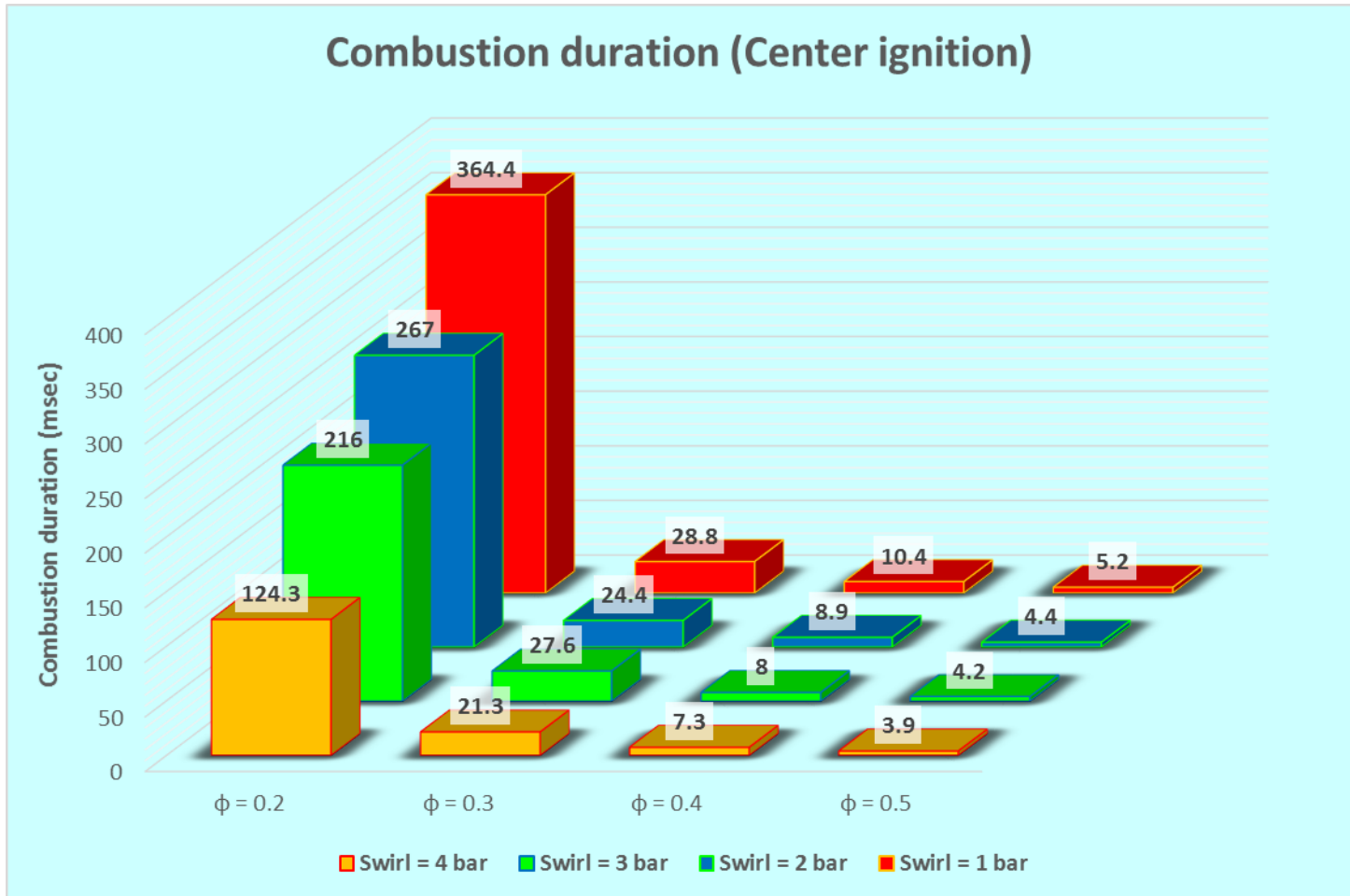
# Results (Mass Fraction Burn Rate)



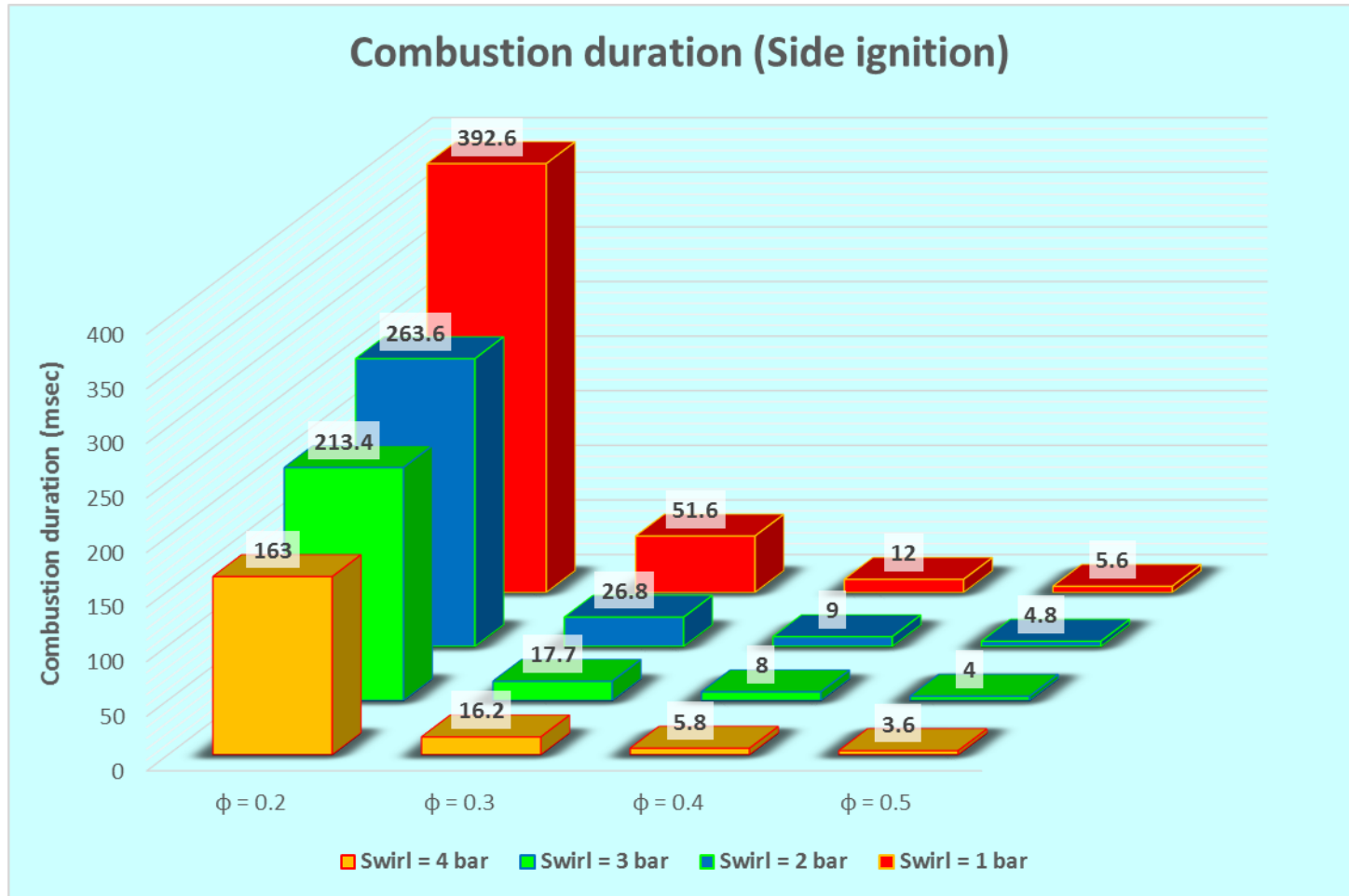
# Results (Mass Fraction Burn Rate)



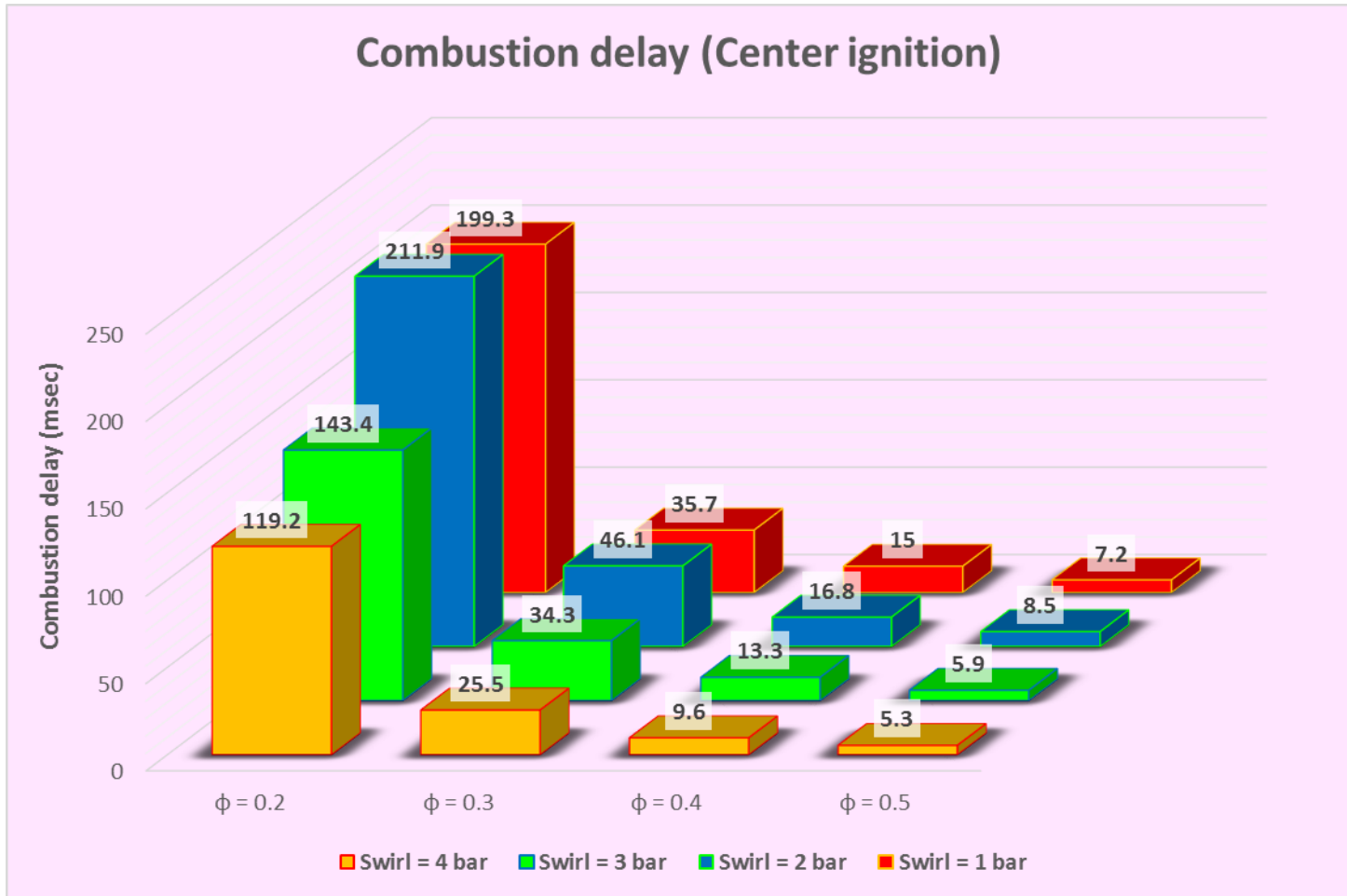
# Results (Combustion Duration)



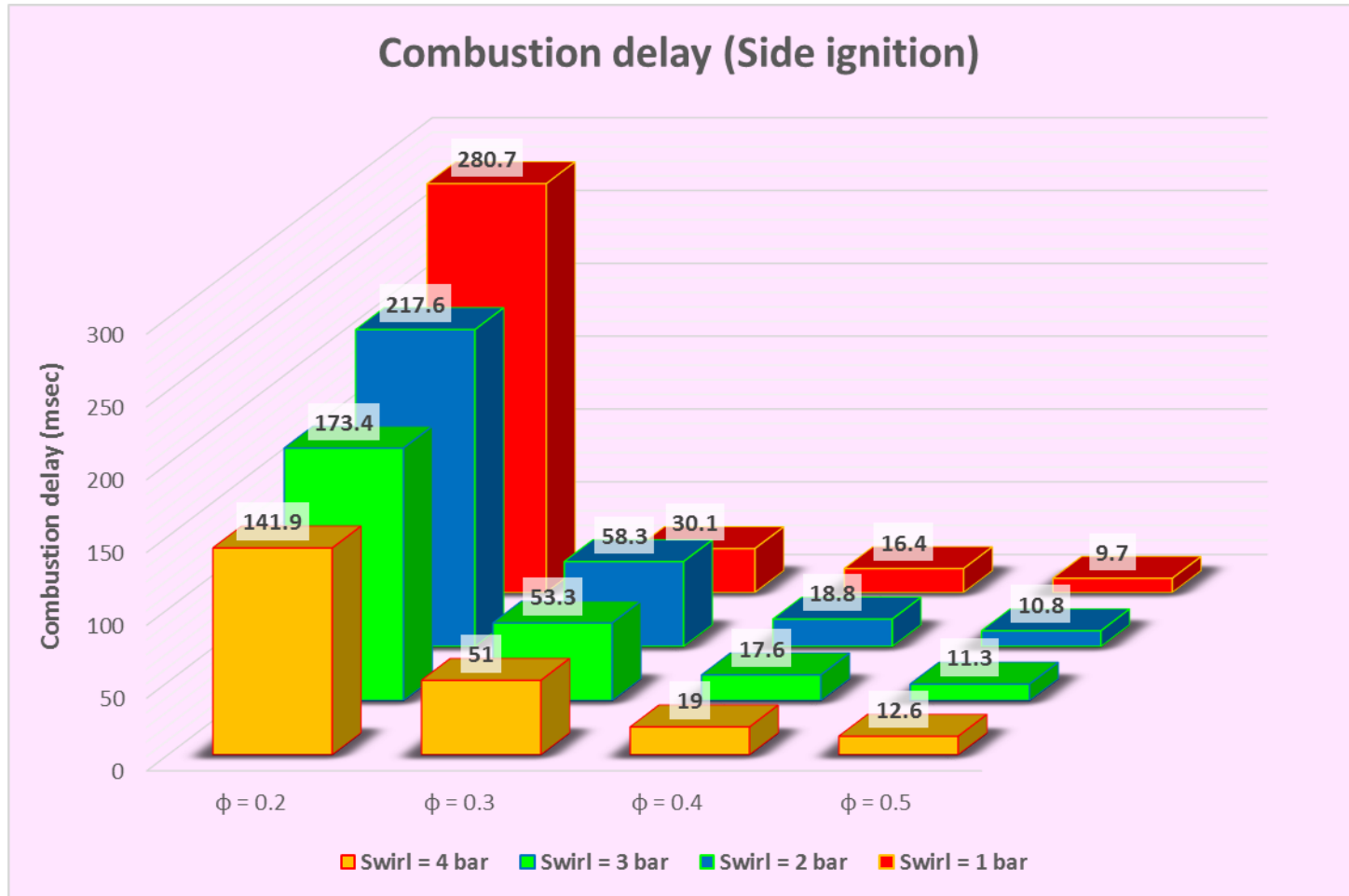
# Results (Combustion Duration)



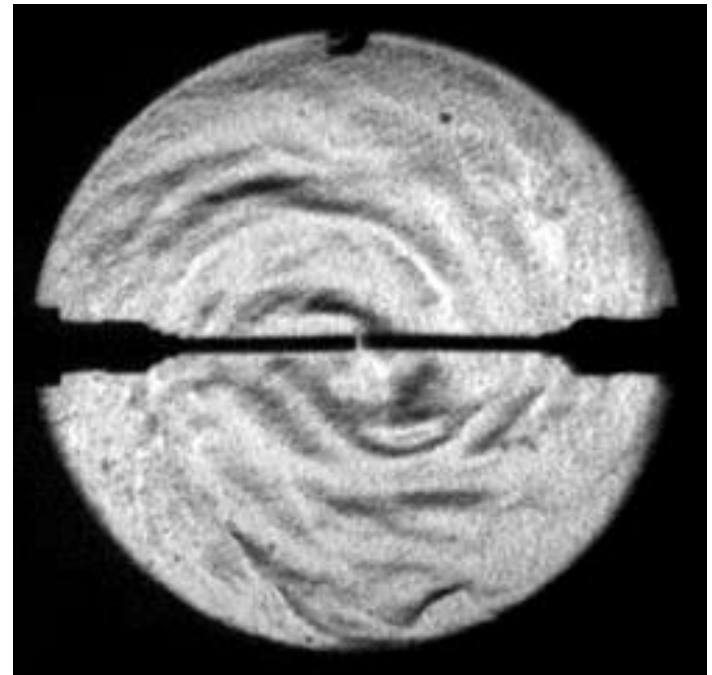
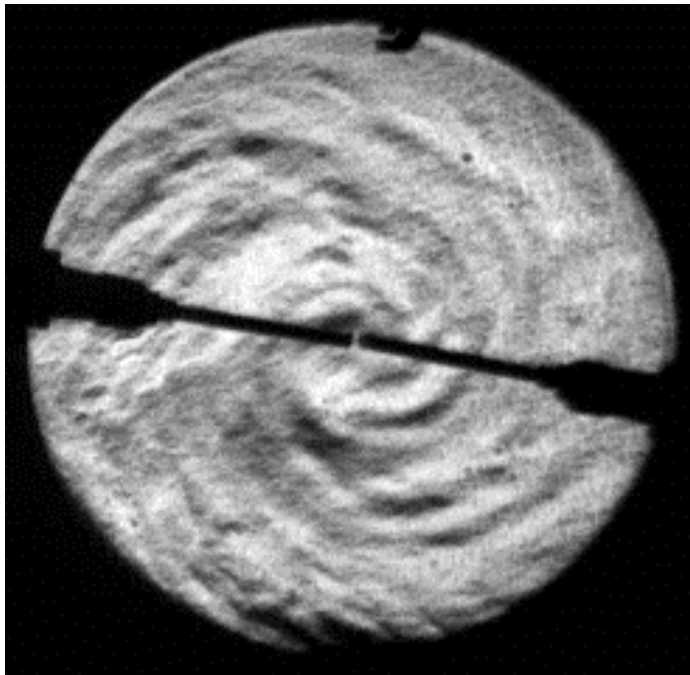
# Results (Combustion Delay)



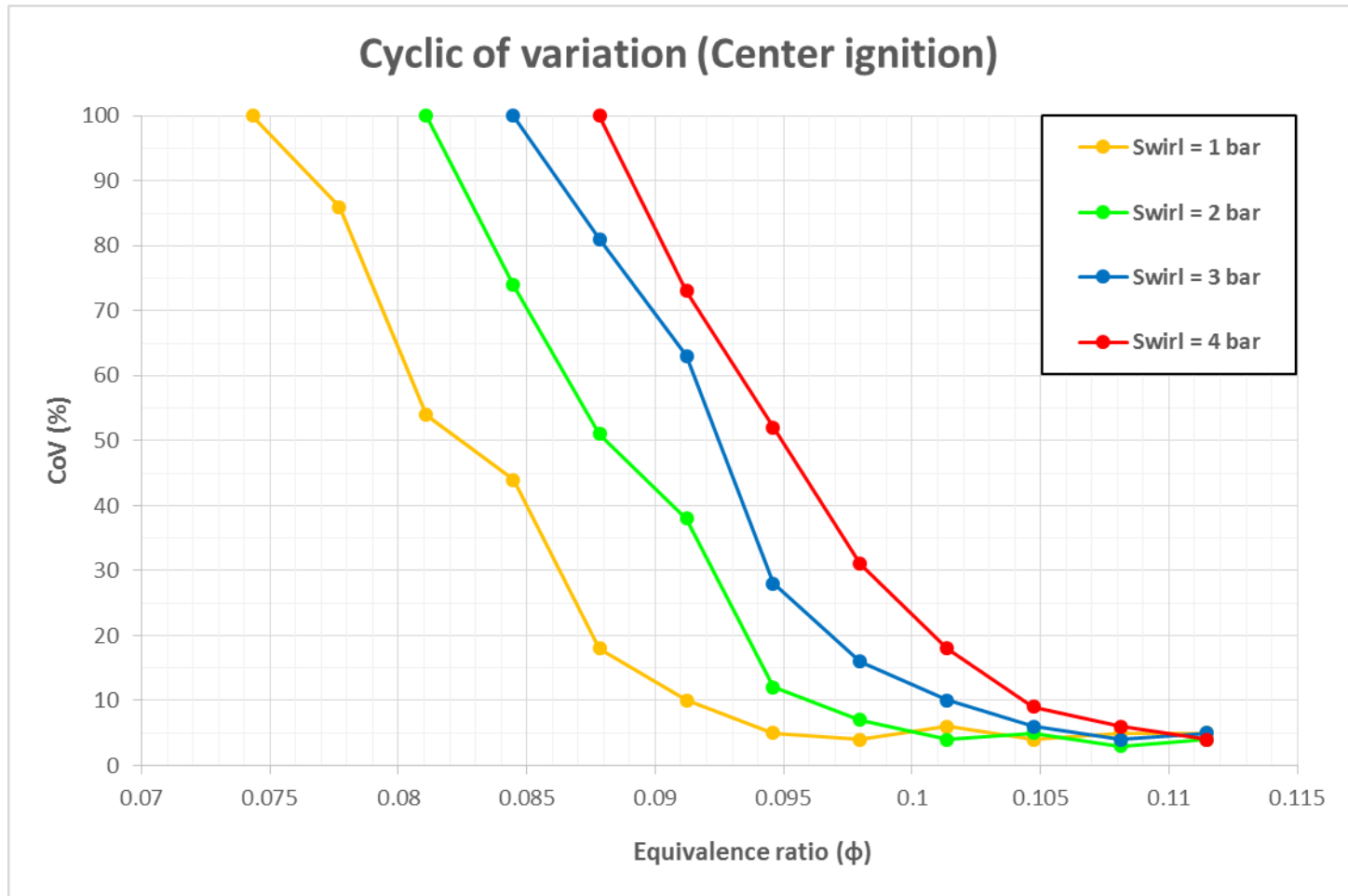
# Results (Combustion Delay)



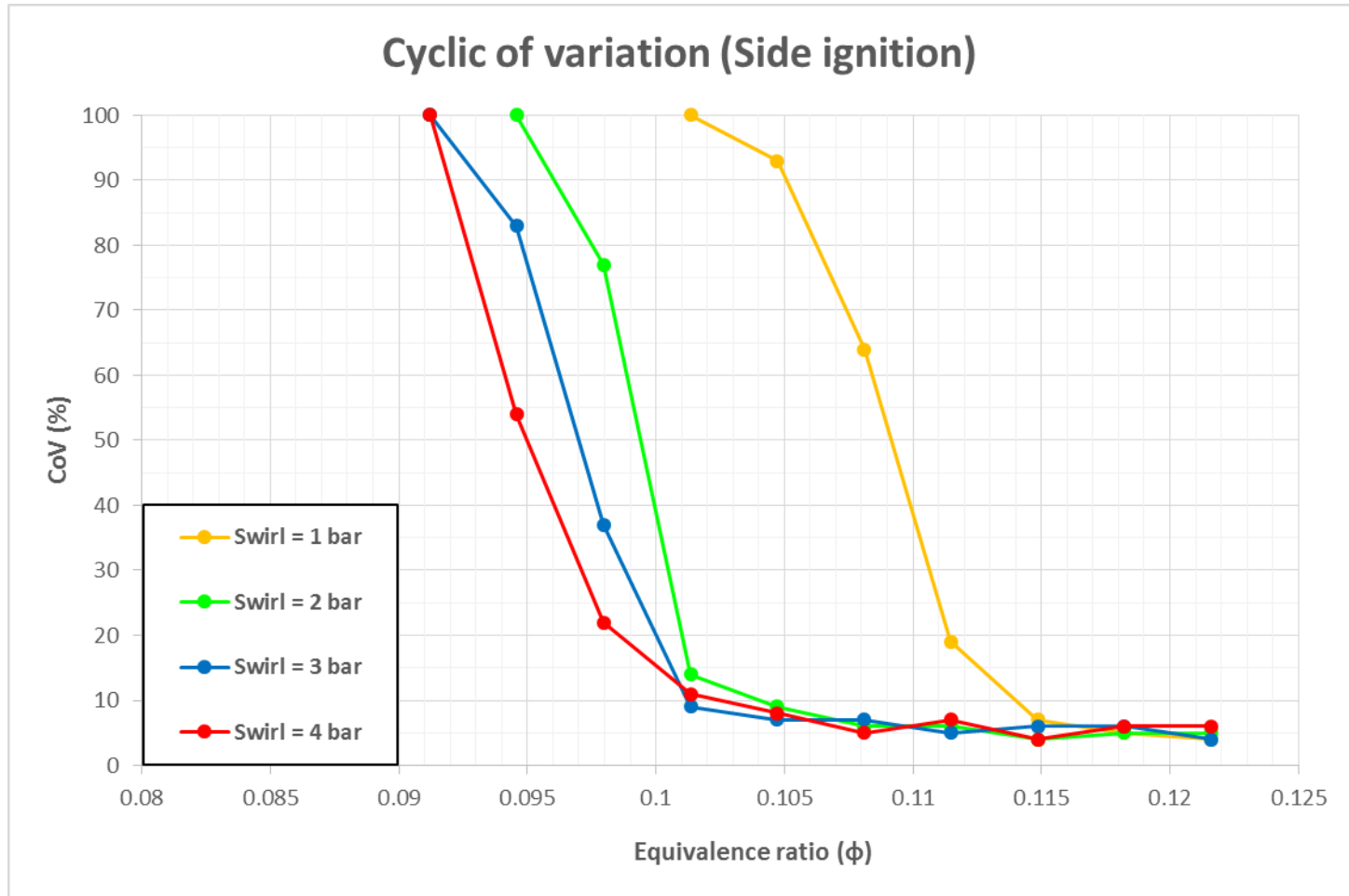
# Results (Combustion Phenomena)



# Results (Cyclic of Variation)



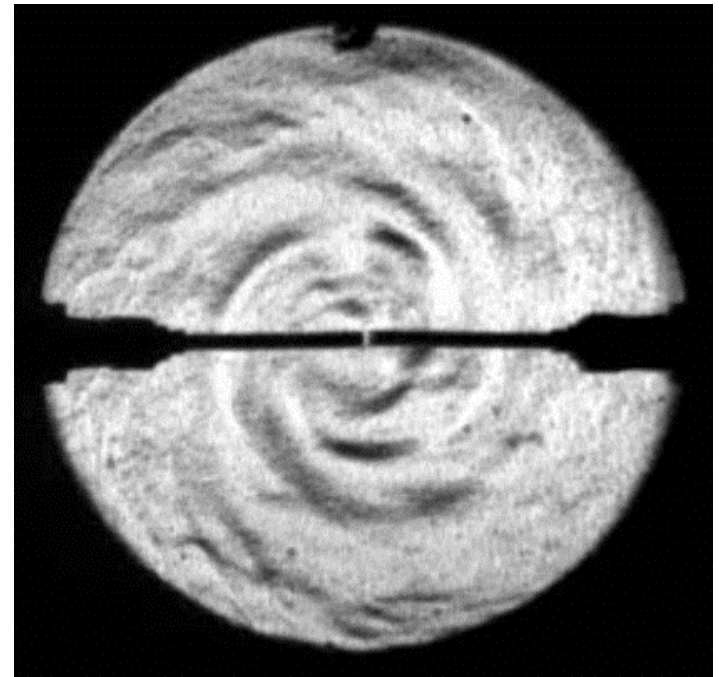
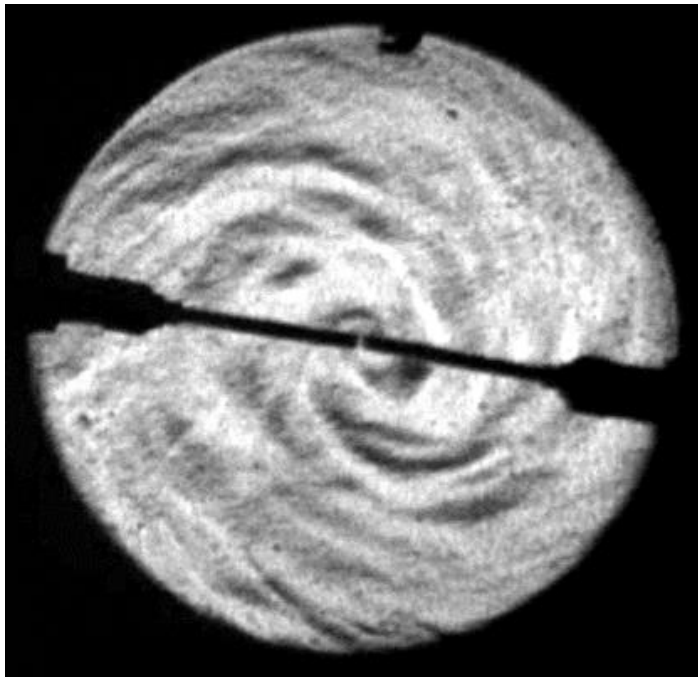
# Results (Cyclic of Variation)



# Results (Lean Burn Limit)



# Results (Lean Burn Limit)



# Contents

- Introduction
- Literature review
- Objective
- Experimental setup
- Results
- **Conclusions**

# Conclusions

- When increasing the chamber temperature, the maximum combustion pressure rise rate was increased while the combustion delay was decreased. The high temperature before combustion acts as catalyst for reaction between hydrogen and oxygen in air. Hence, the combustion will arise faster than low chamber temperature.
- Increasing the equivalence ratio means increasing the power input. Therefore the maximum combustion pressure rise rate is higher and also combustion delay is shorter when compared with low equivalence ratio.

# Conclusions

- In lean conditions such as  $\phi$  0.2 and 0.3, swirl intensity also affected to the hydrogen combustion characteristics. Turbulent flow can increase chance of reaction between hydrogen and air. Thus the combustion efficiency (maximum combustion pressure, combustion duration and combustion delay) was increased.
- When changing the ignition position to sidewall position, the combustion delay is longer than center ignition. Because of the thermal radiation of side wall to atmosphere and also from the flame explosion that in the flame center ignition can expand faster than sidewall ignition.

# Conclusions

- From CoV of lean burn limit investigation results, it found that appropriate equivalence ratio that the mixture can be make the stable combustion (low CoV) even the swirl intensities were changed can be found at  $\phi > 0.087$  for center ignition and  $\phi > 0.098$  for sidewall ignition
- The ignition position directly related to lean burn limit of hydrogen. The result of lean burn limit show the inversion of combustion stability. When changing swirl intensity conditions, amount of air was went to center of combustion chamber by tangential force but hydrogen was went to the outside that because of the density of itself. Therefore center ignition was suitable for low turbulent flow but sidewall ignition with high swirl intensity is become more effective combustion.

Thank you  
for your  
kind attention

## AUTHOR BIOGRAPHY

Author: Mr. Pattanit Nomthongthai

Date of Birth: 7<sup>th</sup> August 1987

Address: 25/25 Moo 19 T.Bangpakong A.Bangpakong, Chachoengsao 24130

Education:

2006 – 2009: Bachelor Degree in Mechanical Engineering,

King Mongkut's Institute of Technology Ladkrabang.

2010 – 2014: Master Degree, Automotive Engineering

(International Program), International College, King Mongkut's Institute of Technology Ladkrabang.

Publications:

- 1) Pattanit Nomthongthai, Piyaboot Ornman, Manida Tongroon, Preecha Karin, Nuwong Chollacoop, Chinda Charoenphonphanich and Hidenori Kosaka, "Design of Hydrogen Constant Volume Combustion Chamber", The 3rd TSME International Conference on Mechanical Engineering, October 24 – October 27, 2012, Dusit Island Resort Hotel, Chiang Rai, THAILAND.
- 2) Pattanit Nomthongthai, Nuwong Chollacoop, Manida Tongroon, Preecha Karin, Chinda Charoenphonphanich and Hidenori Kosaka, "Effect of Swirl Intensity and Spark Plug Position on Hydrogen Combustion in a Constant Volume Combustion Chamber", JSAE Annual Congress (Spring), May 21 – May 23, 2014, Pacifico Yokohama, Yokohama, JAPAN.